MONITORING OF GLULAM STRUCTURES BY THEODOLITE INTERSECTION

by

W F Price, BSc MSc

Thesis submitted to The University of Nottingham
for the degree of Doctor of Philosophy

May 2002

ABSTRACT

The use of glued laminated timber (glulam) in building and construction provides a designer with an attractive, environmentally friendly alternative to steel and concrete. However, along with other engineering materials, glulam is subject to creep and in order to use it efficiently without the risk of unacceptable long-term deflections occurring, a reliable method of estimating creep in glulam is desirable.

With this mind, the Structural Timber Research Unit (STRU) at the University of Brighton embarked, in 1988, on an extensive glulam research programme. Since then, the deflection of prepared glulam specimens has been measured in the laboratory under controlled conditions and in 1992, the programme was broadened to include measurements to determine the behaviour of glulam in full-scale structures.

A number of test sites have been established in a variety of buildings and the method chosen to monitor glulam beams in these is theodolite intersection using a Leica Electronic Coordinate Determination System (ECDS3). Borrowed from industrial and engineering surveying, the use of the theodolite intersection technique to monitor glulam is unique and it has, despite the practical difficulties and size of structure involved, enabled the movement of beams to be monitored with an accuracy of 0.1 mm.

By processing three-dimensional intersection coordinates, vertical deflections

and creep have been determined and results show that the creep response of the glulam beams monitored in full-scale structures can be represented by a seasonally modulated exponential function. This correlates well to results from the laboratory tests and demonstrates that measurements taken in the laboratory can predict the behaviour of glulam in-situ. The creep factors obtained also agree well with the values given for these in *Eurocode 5: Design of Timber Structures*.

CONTENTS

LIST of FIGURES

Chapter 8

Chapter 9

LIST of TABLES

ACKNOWLEDGEMENTS

During the ten years that this thesis has taken to complete on a part-time basis, a considerable amount of help has been given to me by the individuals and organisations listed below. I hope everyone approves of the outcomes presented here as they have all contributed towards to these in some way.

Colin Prior, a personal friend and survey technician in the former Department of Civil Engineering and now School of the Environment at the University of Brighton. He has worked with me throughout the whole of the ten years of the thesis, has taken all the observations with me and without his continued interest and enthusiasm, none of this would have been possible. As he is a graphic artist as well as technician, he also prepared all of the line drawings included in the thesis. I owe him more than I can ever repay and if I am awarded a PhD for this work, Colin should get the 'D' at least!

Peter Gardiner, Head of the former Department of Civil Engineering and now School of the Environment at the University of Brighton. Back in 1992, Peter encouraged me to register and start work on my PhD. He has always shown a personal interest in the monitoring I have been carrying out over the years.

The **Church Authorities** at **Wokingham Baptist Church,** in particular **David** and **Joan Nixon,** for allowing monitoring to take place in the church extension since 1993 and before them **Alistair Watson,** the architect responsible for designing and building the extension in 1992.

Adur District Council for allowing access to Wadurs Pool at Shoreham and all the pool staff who have, since 1993, providing supervision outside normal working hours for me whilst I have been on site taking measurements.

The **South Downs Health Authority** and **staff at the Moulsecoomb Health Centre, Brighton** for making it possible to take measurements here since 1994. A tribute is paid to **Michael Blee,** the architect for the Centre who was a great advocate of glulam and supported this work. Michael died in 1998.

The Church Warden, **Nigel Sarjudeen** at **Bishop Hannington Church, Hove** for giving permission to use the church from 1995 onwards.

A special mention is made of **Barry Hilson,** former head of STRU, who had the foresight to initiate research at Brighton into glulam and who made the work described here possible by obtaining the necessary funding. Sadly, Barry died in 1999, only two years after his retirement.

Other members of STRU at Brighton who I would like to thank for the advice they have given and numerous questions they have answered are **Geoff Taylor, Peter Rodd** and **Hashim Abdul-Wahab.** A special mention is given to **Dave Pope,** for providing continued technical support from the beginning for the work completed here and for reviewing several chapters in the thesis.

Another person who has made a considerable input to this thesis is **Patrick Warren,** the Engineering Librarian at the University of Brighton. Patrick is thanked for tirelessly ordering and seeking out all the references mentioned.

Mike Grist, formerly of Leica Geosystems, has provided technical support for ECDS3 and also on a personal basis since the start of this project. Thanks are also due to **Leica Geosystems** directly for providing information and for allowing publication of many of the figures in the thesis. **Stephen Kyle** was of great assistance in the preparation of the mathematics presented in this thesis and his input here is acknowledged.

When a professional-looking photograph is encountered in the thesis, it is very likely that **Bob Seago**, the University of Brighton photgrapher took it. Bob has had an input to this project from its onset. Without the help of **Paul Kerr** of the Reprographics Section at the University of Brighton, much of the photocopying would not have been done on time or so well.

Last and definitely not least in any sense, I would like to thank **Martin Smith** and **Alan Dodson** at the University of Nottingham for their extremely able and well-directed supervision throughout and for their hospitality over the years.

Finally, many thanks are due to **Teresa, John** and others, who did not make any direct contribution towards this thesis, but had to live with or put it with me whilst the write-up was in progress.

Apologies to anyone else who I have forgotten to include here.

Bill Price

April 2002

1

INTRODUCTION

The origin of this thesis lies in a personal interest the author has had in three-dimensional coordinate measuring and monitoring since the late 1980s. This resulted in the development, in 1989, of a portable non-contact coordinate measuring system called ARCS (Analytical Remote Coordination System) which was completed whilst the author was a member of the academic staff at Portsmouth Polytechnic (now Portsmouth University). ARCS was a theodolite intersection system and comprised two Kern E2 electronic theodolites, a Husky Hunter field computer and software developed in-house (Ashworth, 1989). One of the applications of ARCS included monitoring surveys carried out in the Mary Rose Dock in Portsmouth Harbour (Price and Ashworth, 1990a and 1990b). At the same time ARCS was developed, a general overview of theodolite based coordinate measuring systems was published (Price, 1989) with a later update (Price, 1995).

Following a move to Brighton Polytechnic (now the University of Brighton) in 1990, the author subsequently joined the Structural Timber Research Unit (STRU) in the Civil Engineering Department. STRU has an international reputation for timber research and had embarked, in 1988, on a research project to assess the long-term behaviour of a timber construction product known as glulam (glued laminated timber). This work included some theoretical analyses

and glulam sections of varying size were being tested in different environments but under laboratory conditions. It was hoped that this work would have some input to *Eurocode 5: Design of Timber Structures* (British Standards Institution, 1994).

In wood mechanics, there has always been a debate as to how measurements taken in the laboratory in order to assess the behaviour of wood and glulam relate to the behaviour of these when they are part of a structure. Consequently, during early 1992, STRU decided that the glulam project needed spatial data relating to the behaviour of glulam in-situ in full-scale structures as well as the data from laboratory tests. When combined with the laboratory data it was hoped that the question of there being any correlation between laboratory and full-scale measurements could be answered and a better understanding of glulam would result.

The data required by STRU to define the long-term behaviour of glulam both in-situ and in the laboratory is a measurement of the deflection of glulam under sustained load. Based on the experience gained from testing glulam in the laboratory, it was estimated by STRU that deflections had to be determined with an accuracy approaching 0.1 mm to model the long-term response of glulam adequately. For any full-sized structure, one of the most important decisions to be made was which measurement method to use to measure beam deflections to the accuracy required. At this point the author was consulted, various alternatives were suggested and STRU decided to proceed with a programme to monitor glulam in some full-scale structures.

1.1 Aims and objectives

Based on the requirements of STRU, the aims and objectives of this thesis are as follows:

Aim 1: To implement a measurement system for recording the deflections of in-situ glulam beams in full-size structures to a specified accuracy.

Objectives

- to establish a specification for the measurements
- to investigate the choice, availability and suitability of instrumentation for measurement of deflection in large-scale structures
- to establish a measurement procedure and to comment on its performance
- to assess the accuracy obtained from the chosen measurement system

Aim 2: To demonstrate that the measurements of the deflection of glulam beams taken at each site by surveying methods can produce results that are of value in timber research.

Objectives

- to devise a method of converting survey data into beam deflections
- to model the beam deflections obtained and to compare these model(s) with those proposed by others engaged in timber research
- to discuss the correlation between laboratory and full-scale measurements
- to determine the relationship of the results obtained with Eurocode 5

1.2 Methodology

In order to fulfil the aims, the proposed method of working is as follows:

- establish with STRU the measurement requirements
- undertake an analysis of potential measurement techniques
- identify a number of suitable sites where long-term (several years) monitoring can be undertaken - these are to be chosen to give a variety of conditions (structural and environmental)
- design and implement measurement strategies at the various test sites
- undertake an analysis of the measurements to assess the accuracy and suitability of the results for future use in wood mechanics

1.3 Thesis overview

The research undertaken by STRU to investigate the behaviour of glulam is outlined in Chapter 2 which also describes the manufacture of glulam. A discussion of the significance of Eurocode 5 in the design of structures using glulam is also included together with reasons for the work undertaken in this thesis.

Chapter 3 discusses research methods used for the measurement of deflection of glulam under laboratory conditions. It soon became evident that these methods were unsuitable for the measurement of full-scale structures and that one based on survey techniques would be better. Consequently, a discussion of

the survey methods available for high precision close range monitoring in 1992 is in chapter 3 together with an assessment of their suitability for the glulam project. Based on this, it was decided that a Leica ECDS3 (Electronic Coordinate Determination System version 3) theodolite intersection system was the best option for the in-situ measurements. This was purchased and monitoring of some glulam structures started in November 1992.

Having decided that theodolite intersection was the most appropriate method, chapter 4 presents a view of the mathematics of this. It is not claimed that all of the material presented in this chapter is new but it does present the complete theoretical basis, especially for intersection calculations, in the order in which they developed and were implemented in the first intersection systems through to the latest.

A brief history of commercially available theodolite intersection systems is given at the start of chapter 5 which leads into the development of ECDS to the version used here, ECDS3. The main part of this chapter is a detailed description of the use of ECDS3 at the glulam sites monitored which reveals a number of practical issues relating to the use of the system software. Further details of the practical nature of the on-site measurements taken with ECDS3 are given in an initial report by Price (1994) followed by updates (Price, 1995a and 1995b). Chapter 6 describes each of the monitored sites at length and gives full details of the way in which the system was set up at each of these. This gives an insight into some of the difficulties experienced when attempting to monitor large-scale structures with precise surveying equipment.

Without any doubt, assessing the accuracy of coordinates obtained from any monitoring system is very difficult because of the large number of variables usually involved. Rather than attempt an assessment of the theoretical accuracy, a different approach has been tried in Chapter 7 and the question of the accuracy of the measurement system has been investigated from a practical point of view. It is the experience of others, together with some laboratory-based tests carried out at Brighton, that has been used to appraise the accuracy that has been obtained at the glulam sites. Although an unorthodox means of confirming the accuracy obtained, it is considered to be the most appropriate in this case.

Since this project began in November 1992, monitoring has continued to date (March 2002), a continuous period of almost ten years at one site and a unique set of data relating to glulam in-situ has been accumulated. During the period of this thesis, this data has been analysed by Taylor, Price and Pope (1996) and by Abdul-Wahab, *et al.*, 1998. The extensive data processing carried out by the author is described in chapter 8 and shows that the behaviour of glulam in-situ can be expressed as an exponential function: this is one of the two most widely used mathematical models for describing the long-term deflections of glulam.

To complete the thesis, a question was asked – if the project were to start today, what method would be chosen to monitor the deflection of glulam beams? Chapter 9 is, in a sense, a continuation of chapter 3, in which the various options available for high precision close range measurement in 2002 are discussed.

2

THE STRUCTURAL TIMBER RESEARCH UNIT AND GLULAM

Much of the work completed in this thesis was undertaken on behalf of the Structural Timber Research Unit (STRU) of the University of Brighton.

STRU was formed by Brighton Polytechnic in 1964 and to date has completed many research and development projects. Funding for these has come from a variety of sources including the former Science and Engineering Research Council (SERC) and its successor, the Engineering and Physical Science Research Council (EPSRC).

2.1 Scope of work completed by STRU

The objectives of STRU throughout its existence have been

- to promote the use of timber as an engineering material through fundamental research
- to provide a consultative service for industry in the development of new timber engineering products
- to promote timber engineering education in undergraduate and continual professional development courses

The work of the Unit covers the routine testing of components, product

development for industry and investigations into existing structures but the major contribution has always been in fundamental research. The principal programmes that STRU has covered include

- the structural applications of fibreboards
- mechanical jointing systems for timber
- the development of new beam systems
- numerical modelling of timber structures

and

- the behaviour of glued laminated timber

part of which is the subject of this thesis.

The glued laminated timber (glulam) research started in 1985 when a post-doctoral research fellowship was awarded to STRU by the SERC and this was completed by Dr P.J. Pellicane of Colorado State University. The results from the fellowship included a comparison of the UK glulam industry with those of other countries and the development of a linear elastic finite interval numerical model to enable the deflection profile of a glulam beam with non-uniform laminate properties to be calculated (see Pellicane & Hilson, 1985 and Pellicane, Hilson & Smith, 1986).

In 1986, the head of STRU at the time, Professor Barry Hilson, accompanied five industrialists on a tour of glulam manufacturing plants in West Germany,

Switzerland and Holland which was sponsored by the Department of Trade & Industry. Following publication of the report of the findings of the tour, the Glued Laminated Timber Association (GLTA) was formed with STRU playing an active part in its work.

Some of the main projects included in the glulam programme have been

Project 1: The effect of non-uniform laminate properties on the optimisation of glulam (1986-1989), SERC and Timber Research and Development Association (TRADA) funding. This project involved the development of a linear elastic finite element model for glulam, which modelled the glue lines as well as the timber, and this was used to examine the effect of glue and timber properties on the stress distribution within glulam beams. Additional studies included an examination of the economic advantages of laminate upgrading by defect removal and finger jointing and a correlation of non-destructive parameters with ultimate tensile strength for finger joints (see Whale, Hilson & Rodd, 1989 and Hilson, Whale & Rodd, 1990).

Project 2: Moment resistant connections in glulam (1987-1992), National Advisory Body for Higher Education (NAB) funding. The main section of work in this project was to use the fundamental knowledge acquired in the first project to make a study of full-sized moment resisting connections in corner joints for glulam frameworks where theoretical moment rotation characteristics were compared with those obtained from full-scale tests. Other practical aspects were covered, such as on-site injection procedures, as well as load duration and moisture cycling effects (see Rodd, 1994 and Rodd & Pope,

1994).

Project 3: The effect of fluctuating moisture conditions upon the creep behaviour of glulam beams (1988-1995 with NAB, Polytechnic Central Funding Council (PCFC), the Building Research Establishment (BRE) and Leica funding but has continued to 2002 with STRU funds). The first part of this project ran from 1988 to 1992 with NAB funding and was concerned with measurements taken of the long-term deflections of prepared glulam specimens under laboratory and external conditions. The second phase of the project from 1992 also aimed to measure the long-term displacement of glulam beams but as well as continuing the laboratory programme, the original project was broadened to include measurements taken to determine the behaviour of glulam in-situ. This work was funded for the period 1992 to 1995 by the PCFC, the BRE and Leica but has continued with STRU funds to date. It is the second phase of this project from 1992 onwards that this thesis is concerned with.

2.2 Glulam

Glulam is an engineered laminated structural component which is fabricated by bonding together accurately planed laminations, normally of whitewood or redwood timber, with their grain in the longitudinal direction of the member. This produces an attractive constructional material that is made from timber produced in properly managed softwood forests which represents a renewable resource. The benefits of using glulam as an alternative to steel and concrete in construction are its appearance as a natural wood product and it can be made in almost any size to suit the load requirements and design of any structure.

According the Glued Laminated Timber Association (GLTA, 2002), glulam has a good strength to weight ratio, an unlimited service life provided the moisture content is not excessive for prolonged periods and a high fire and chemical resistance.

The manufacturing process for glulam starts with the timber being prepared in laminations which are normally 45 mm thick for straight beams but can be as small as 16 mm for curved beams. Although a wide range of sizes are available, standard straight glulam sections vary typically from 65 mm wide x 315 mm deep with seven 45 mm laminations to 115 mm x 495 mm with 11 laminations. Since the moisture content of the laminations must be controlled during manufacture, they are kiln-dried to a moisture content specified in *BS EN 386: 1995 Glued laminated timber – Performance requirements and minimum production requirements*.

In production, the length of glulam members normally exceeds the length of commercially available solid timber and it has to be finger jointed (see figure 2.1) to make laminations of the required length. In a normal section, these

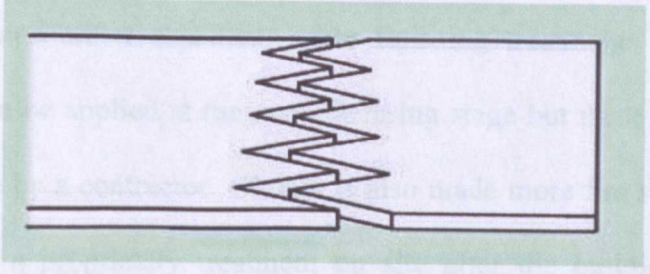

Figure 2.1 *Finger joint in timber (GLTA, 2002)*

finger joints will occur randomly and they are guaranteed to be as strong as the

timber itself in accordance with *BS EN 385: 1995 Finger jointed structural timber – Performance requirements and minimum production requirements.*

Once prepared, the requisite number of laminations are assembled for a section, an adhesive mix is applied to the faces of the laminations under carefully controlled conditions and these are then placed in mechanical or hydraulic jigs and pressure is applied. Adhesives used in glulam bonding are selected in accordance with *BS EN 301: 1992 Adhesives, phenolic and aminoplastic, for load-bearing timber structures: classification and performance characteristics.* The most widely used adhesive is phenol-resorcinol-formaldehyde (PRF) which is recommended as an assembly adhesive for severe environments (Desch and Dinwoodie, 1996).

Once glued, glulam members are trimmed to size and planed to a clean finish to remove any glue squeezed out in the jigs and to remove any appearance defects. Glulam is normally supplied to site with one coat of treatment, such as a water repellent, to protect against any moisture pick-up during construction. When a preservative is to be applied to a section, this is normally done before the water repellent which itself will have fungicidal additives. As well as preservatives and water repellent, other finishing treatments (for example, varnishing) can be applied at the manufacturing stage but these are very often applied on site by a contractor. Glulam is also made more fire resistant by the application of a proprietary treatment on site after the building is dry and watertight.

The normal timber used to manufacture glulam is European whitewood because of its clear, bright appearance, the small knot sizes and its glueing properties. Glulam can be made to almost any size and the members can be straight with spans of more than 50 m or they can be curved to suit any structural requirement. However, the cost and difficulty of producing curved sections increases with tighter curves and the minimum radius that can be made with 45 mm laminations is 6 m and with 16 mm laminations, a 2 m radius is possible (GLTA, 2002). The size, length and shape of glulam sections are only limited by the capacity of manufacturing plants and by restrictions governing the transportation of the beams to site.

Recent advances in wood products include Fibre Reinforced Plastic (FiRP) glulam (Pooley, 1996). This looks very similar to conventional glulam but a thin layer of reinforcement plastic is added to the laminates to increase the load-bearing capacity of a section. Different types of FiRP reinforcement are available including carbon and fibre-glass fibre, which are embedded in a plastic film. These are supplied in rolls of various widths, they are cut to the length of a section, cleaned and then glued in between the laminations.

2.3 Creep in timber and glulam

Along with many other engineering materials, glulam is subject to a phenomenon known as creep and a classic example often given of this is the behaviour of a wooden shelf when loaded with books. There will be an initial deflection of the shelf as the books are placed on it, but this will increase

gradually with time. This is creep behaviour and is defined as the additional deflection that has occurred with time after the initial elastic deflection took place when the books were first placed on the shelf. Another everyday example of creep behaviour can be seen on the roofs of very old buildings where the ridge has a pronounced sag.

Although in the example given, the wood shelf can be considered to be an elastic material when the initial load is applied, this is only going to be the case for short periods and does not apply to real-life structures where time becomes an important variable. According to Dinwoodie (1989), in real-life circumstances timber should be treated as a viscoelastic material since its behaviour is neither elastic nor truly plastic, but rather a combination of these. Viscoelasticity infers that the behaviour of a material is time dependent as at any instant in time under load its performance will be a function of its past. The application of stress to a viscoelastic material such as timber usually results, as already described, in an instantaneous elastic deformation, followed by a period of increasing deformation with sustained load, in other words creep.

The magnitude of creep deformation in wood is not only influenced by the time under load and the level of the applied stress but also on the moisture content of the wood (or the relative humidity of the environment the wood is placed in). Creep will be greater at higher levels of stress and it will increase faster if the moisture content changes during the time under load (Desch & Dinwoodie, 1996 and Dinwoodie, 2000). The type of creep behaviour under changing moisture content has been given the title 'mechano-sorptive' behaviour

(attributed to Grossman, 1976) and this is an extremely complex phenomenon that has been the subject of much research (Morlier, 1994).

The use of solid timber for the construction of large and multi-storey buildings has always been limited because of the inherent variability of wood, the limited sizes available, the risk of decay and the problem of creep which can produce relatively high deflection levels over long periods of several years.

The introduction of glulam, with its environmental attractions and architectural possibilities, enhanced the use of timber in construction by reducing the effects of the variability of wood and by greatly increasing the size and length of section that can be utilised. It is also possible to minimise the risk of decay in glulam by coating with preservatives but the possibility of progressively increased deflections due to creep under long-term loading and changing moisture content still remains.

2.4 Code provisions for creep in timber

The British Standards Institution have published a set of structural Eurocodes that serve as reference documents for the design of building and civil engineering works. These include separate codes for concrete, steel and aluminium structures, for geotechnics and also include Eurocode 5 (British Standards Institution, 1994), which deals exclusively with the design of timber structures. In this, detailed rules are given to ensure that timber structures are designed and constructed such that they will remain fit for the use for which they are required for the intended life of the structure. These objectives are met

by the choice of suitable construction materials, by appropriate design and detailing and by specifying procedures for the construction and eventual use of the structure.

In Eurocode 5, it is stated that the deformation of a structure which results from the effects of loading and moisture should remain within appropriate limits. These are known Serviceability Limit States and the final deformation of a structural element should be calculated using equation 4.1b from the code

$$\mu_{fin} = \mu_{inst}\,(1 + k_{def}) \qquad 2.1$$

where

μ_{fin} = final long-term deformation (or deflection)

μ_{inst} = instantaneous or initial elastic deflection

$$k_{def} = \text{creep factor} = \frac{\text{creep deflection over stated period}}{\text{initial elastic deflection}}$$

This can be written

$$\mu_{fin} = \mu_{inst} + \text{creep deflection over stated period} \qquad 2.2$$

Values of the modulus of elasticity for different materials are given in Eurocode 5 and initial elastic deflections can be calculated using these. Creep levels (or k_{def} values) in all forms of timber are known to depend on the load duration and moisture environment of the timber or glulam that vary with time.

Using the definition given for k_{def}, a value of 1.0 indicates a creep deflection equal to the initial elastic deflection and this value is sometimes used as a 'rule of thumb' in estimating long-term creep. However, in order to utilise glulam efficiently without the risk of unacceptable long-term deflections occurring, a more reliable method of estimating creep at the design stage of a structure is desirable.

There has been much debate as to what appropriate creep allowances should be and values of k_{def} for glulam and solid timber that take into account the increase in deflection with time due to creep, as recommended by Eurocode 5, are shown in table 2.1 for different load durations and Service Class of building.

Load duration category	**Service class**		
	1	**2**	**3**
Permanent	0.60	0.80	2.00
Long-term	0.50	0.50	1.50
Medium-term	0.25	0.25	0.75
Short-term	0.00	0.00	0.30

Table 2.1 *Values of k_{def} for solid timber and glulam (table 4.1 in Eurocode 5)*

In table 2.1, load durations are classified as (see Eurocode 5, table 3.1.6)

Permanent more than 10 years (> 3600 days)

Long-term 6 months to 10 years (180-3600 days)

Medium-term 1 week to 6 months (7-180 days)

Short-term less than 1 week (0-7 days)

Service Classes are defined as follows (see Eurocode 5, section 3.1.5)

Class 1 is characterised by a moisture content in the materials corresponding to a temperature of 20°C and relative humidity of the surrounding air exceeding 65% for a few weeks only per year (average moisture content in softwoods not exceeding 12%).

Class 2 is similarly defined except that a maximum relative humidity of 85% applies (average moisture content in softwoods not exceeding 20%).

Class 3 refers to conditions leading to higher moisture contents than Service Class 2.

Service Classes 1 and 2 are broadly classified as buildings that are internal heated and internal unheated though it is likely that the moisture content in buildings which are intermittently heated in winter could rise above 12%. Eurocode 5 indicates that many external covered structures would fall into Service Class 2 with some structures exceptionally falling into the Service Class 3 category.

A design procedure for any given structure would involve calculating an initial elastic deflection and then a long-term deflection based on one of the k_{def} values given in table 2.1. Having done this, the long-term value obtained is checked where Eurocode 5 further recommends that the final deflection for a simply supported beam of length L resulting from the effect of all load conditions should be limited to $L/500$. As well as this, designers can also use BS 5268 (British Standards Institution, 1996) which recommends that the deflection in timber members should not exceed 0.003 of the span. Other conditions apply to this somewhat simplified description of a design procedure

but it is evident that creep and k_{def} values play an important part in this and that an improved knowledge of these can only improve the reliability of structural design with timber and glulam components.

It is worth noting that the k_{def} values in Eurocode 5 are only guidelines and that other values can be used if more reliable data is available for a specific material and design. Thelandersson (1994a) states that the accurate prediction of long-term deflections of glulam is very important from a practical point of view and should have the same level of priority as prediction of failure in timber. Accordingly, a better knowledge of creep in timber is required.

2.5 Measuring the long-term deflection of glulam beams

Up to the 1980s, there was little known about the creep behaviour of glulam and its effect on the performance and serviceability of timber and little experimental data was available on the magnitude of creep in structural glulam. In order to provide this information, STRU embarked on glulam *Project 3: The effect of fluctuating moisture conditions upon the creep behaviour of glulam beams.* It was hoped that the results obtained from this project would advance knowledge of the behaviour of glulam in the medium and long-term and the data gathered could also be used to verify the creep factors recommended by Eurocode 5.

As previously stated, Project 3 started in 1988 and the first phase involved the long-term measurement of the moisture content and creep displacement of solid

and glulam sections under laboratory conditions paying particular attention to

- section size
- surface coatings
- stress level
- relative humidity (moisture content) changes

in the glulam.

This work has been described in detail by Taylor, West and Hilson (1991), by Taylor and Pope (1994) and by Abdul-Wahab, *et al.*, 1998 and a summary is given here.

A total of 60 beams, 2 m in length are being subjected to four point bending at 1.72 m span using special double vertical rigs on permanent loan from the Building Research Establishment. These have a pulley system with a 5:1 mechanical advantage to apply the required loads and are used to save laboratory space as shown in figure 2.2. These sections are divided into three groups that are exposed to three different environments: constant humidity and variable humidity both at a constant temperature of 20°C and an external environment, as shown in figure 2.3. The specimens tested in the rigs vary in section size from 100 x 30 mm up to 190 x 70 mm and have different bending stresses applied. Some of the samples have been given two coats of a proprietary yacht varnish.

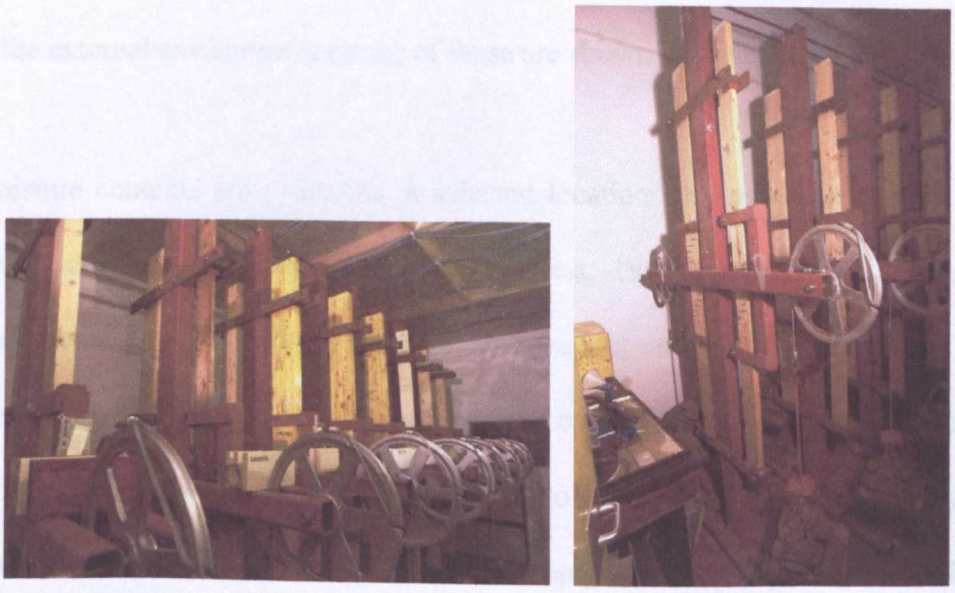

Figure 2.2 *Vertical test rigs at Brighton*

Figure 2.3 *External but covered test environment at Brighton*

In addition to the 60 vertical rigs, five unvarnished beams of section 265 x 90 mm are also being monitored as simply supported beams over a span of 7.7 m in the external environment (some of these are shown in figure 2.3).

Moisture contents are measured at selected locations in the sections using an electrical resistance method (Taylor and West, 1990). In order to ensure a proper contact with the laminations in each section, measurements are taken by connecting the resistance meter leads to pairs of permanently installed sheathed stainless steel pins (see figure 2.4), driven to various depths. In the external environment, readings of the moisture content, temperature and relative humidity of the glulam sections are taken at regular intervals by hand.

In the controlled humidity environments, a computer-based data-logging system is now used in which each pair of pins is scanned for measurement and recording of moisture content at selected times (Pope and Taylor, 1994). Temperature and relative humidity transmitters are also incorporated to record these environmental conditions.

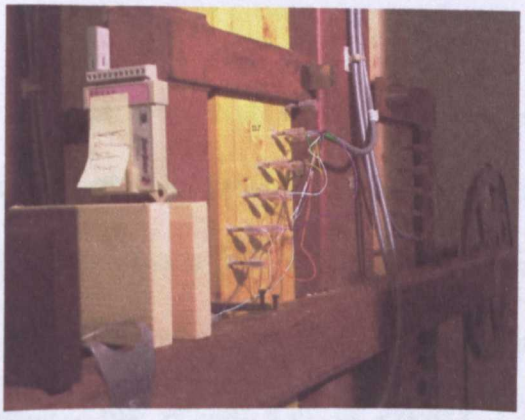

Figure 2.4 *Moisture reading pins*

Creep deflections are obtained by hand using a simple digital caliper system shown in figure 2.5, which minimises the effects of distortion of the sections.

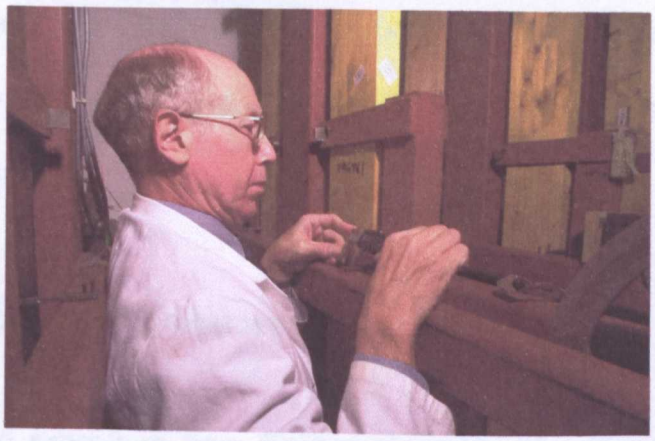

Figure 2.5 *Measurement of deflection*

The second phase of Project 3 commenced in 1992 and is still in operation. The aim of this research is to continue the laboratory measurements started in 1988 that have the specific objective of determining the effect of size, surface treatment and environment on the creep behaviour of glulam beams in the laboratory. To this end, all the creep rigs, environmentally controlled rooms, data acquisition systems and computer hardware in place in 1992 have continued operating for a continuous period of 10 years to date from then.

However, because there is little experimental information available on the magnitude of creep in glulam structures, designers and researchers are uncertain as to whether the results from creep measurements taken on glulam specimens in the laboratory would be the same as for glulam in 'real' structures. Consequently, the second aim of *Project 3* is to measure the deflections and environmental conditions of glulam structures from the time of

their construction for as long as possible.

In 1992, funding for this work was obtained from the BRE (£33 000), the PCFC (£33 000) and Leica (£6000). The sum allocated for the purchase of equipment for the measurement of the behaviour of glulam in-situ was of the order of £45 000.

2.6 Specifications for the measurement of creep

Having gained experience from theoretical studies and from the laboratory trials, some specifications and conditions for the monitoring of any full-scale glulam structures were established by STRU. Although no formal contract was agreed to define these with the author in early 1992, the monitoring was to adhere to the following guidelines:

- Only vertical movement was to be monitored in medium to large glulam sections. In this context, medium was expected to be about 50 mm width x 150mm depth and large anything up to 150 mm width x 500 mm depth. The length of any section was not specified but it was expected that the longer the section, the more it would deflect under long-term load. If it was possible to take three-dimensional measurements of the glulam sections, this might be advantageous, but was not essential.

- It was desirable to monitor the behaviour of glulam in a variety of environments. The critical factors affecting the behaviour of glulam are the temperature and humidity of the rooms and buildings in which it is

placed and the age of the structure. In addition, different types of structure (simply supported, symmetrical or complex) give rise to different glulam responses and the monitoring programme should try to account for all of these.

- The rooms to be monitored should also vary in size and use. This condition really combines the first two conditions in that the buildings selected for monitoring should have a variety of different glulam sections and lengths, together with different working environments.

- The accuracy required for the measurement of vertical deflections was to be 0.25 mm at the 95% confidence level, which would mean a standard error of about 0.1 mm depending on whether one, two or three dimensional monitoring is analysed. In simple terms and for close range measurements up to say, 25 m , an accuracy of 0.25 mm represents a proportional error of 1 in 100 000.

- Monitoring over a long period was required. This would be at least five years in the first instance and depending on site conditions, could well extend beyond this.

- In any building, measurements were required frequently (say once a week) at the start of monitoring and it was expected that they might only be needed monthly on a long-term basis.

- The funding available to purchase equipment for this part of the project was of the order of £45 000 (see section 2.5).

2.7 First sites to be monitored

At the start of this work, structures comprising simply supported beams with large spans would have been ideal for measurement but in the summer of 1992, only two sites were identified as being suitable for monitoring. A brief description of these is included here as they form the basis of the discussion concerning the choice of the measurement method used to measure creep (given in chapter 3).

The first 'site' chosen was the top floor of an extension to be built at Wokingham Baptist Church in Berkshire. A feature of this room was to be an exposed glulam roof which would measure approximately 16 m x 8 m in plan when finished and would comprise a number of rafters of varying section, length and pitch. Figure 2.6 shows the interior of the completed second floor of the extension during monitoring (a detailed description of Wokingham is given in section 6.1).

Figure 2.6 *Glulam roof being monitored at Wokingham Baptist Church*

The Church Authorities and the architect for the project were contacted to seek permission to carry out the monitoring work and both agreed to this. After a visit to Wokingham and studying the plans of the proposed extension, it was decided that it was only necessary to monitor a selection of rafters of different size to obtain enough data to represent how the full roof might behave. With building work due to commence in September 1992, monitoring was planned to start soon after this in order to try and measure the behaviour of the roof frame both before and after it was initially loaded.

The advantage of using this site was that it offered the chance to monitor a selection of large section glulam beams of varying length in a room that would not be used at all times and would therefore only be heated intermittently. This would expose the glulam beams to a higher than normal variation in temperature and humidity. When complete, all of the roof would also be accessible but using a ladder for the highest beams. The main drawbacks of the site were its location some 70 miles from Brighton (a journey of up to about two hours depending on traffic) and the complicated nature of the roof (which would make it difficult to analyse).

At Shoreham in West Sussex, a second site was to become available later in the year in December. Again, an exposed glulam roof frame could be monitored, but compared to Wokingham, this was a simpler but larger structure that covers a 25 m x 10 m swimming pool. Figure 2.7 is a photograph of the pool whilst under construction and this shows the symmetrical layout forming a double pitched roof with large rafters each spanning approximately 6 m in plan and

rising to about 6 m above the pool side. A full description of the site is given in section 6.2.

Figure 2.7 *Roof over swimming pool to be monitored at Shoreham*

At the time monitoring was being proposed for Wokingham, the site at Shoreham was only at the planning stage and a detailed measurement scheme could not be devised but one similar to that to be used at Wokingham was envisaged. However, this site was of great interest to the glulam project as it offered the chance to study glulam in a controlled environment and it would have other advantages if it was added to the monitoring programme of its proximity to Brighton (only eight miles from the University) and a simpler structure for future analysis.

Permission to carry out monitoring at this site was sought from Adur District Council who were both client and architect for the pool and they agreed to this.

Based on the specifications and the conditions at each site, a choice had to be made regarding which measurement system to adopt for monitoring the long-

term deflections of these structures. The various methods available at the time (1992) are reviewed in the following chapter.

3

CHOICE OF MEASUREMENT SYSTEM

At the time of the start of work on this thesis, COST 508 (1992) lists 54 university laboratories and technical centres in the European Union engaged in wood mechanics research during 1992. Of these, nearly all were investigating creep in wood and wood products. If North American and Pacific institutions were added, it is evident that a considerable amount of research in wood mechanics was being carried out at the time and this still continues today. However, only a small number of institutions, including the University of Brighton, are investigating creep in glulam.

3.1 Methods used to measure creep

According to Le Govic (1994a), any creep test carried out on wooden structural components (such as glulam) should concern itself with the following.

- *The specimen and material it is made from.* For the sites at Wokingham, Shoreham and elsewhere the test specimens are the glulam beams in-situ and details of these are given in section 2.7 and chapter 6.

- *The mechanical test and load history.* When monitoring full-scale structures, it is not possible to subject glulam beams and structural elements to some sort of mechanical test, as is possible with laboratory tests. However, the maximum bending displacement due to loading of

in-situ glulam beams has been obtained by measuring the mid-span deflection of each beam (see Taylor, Price and Pope, 1996). As regards the actual load applied, Le Govic states that these should be as similar as possible to those expected in practice, they should be constant and they should be applied for as long as possible to obtain the best results. All of these conditions are met for the beams at the various sites but the loading varies throughout the construction period for each new building monitored. This has been recorded and referenced to the creep measurements discussed in chapter 8.

- *Climatic conditions*. For most experiments to determine creep, the test specimens are placed in climatic or conditioning chambers to control humidity and temperature. The climatic conditions are either kept constant or are cycled. For monitoring in real buildings, no control of environmental conditions is possible but it is essential to record the temperature and relative humidity at each site and to do this, data loggers have been permanently installed. When each site is visited, further readings of temperature and relative humidity are taken with a reference meter so that the data logger output can be calibrated. It is also necessary to measure the moisture content in the beams and this is done using stainless steel pins and a resistance meter (see Taylor and West, 1990 and Pope and Taylor, 1994).

- *Deflection measurements*. Le Govic stipulates that the equipment used for this should be able to record the early part of creep, it should be stable for a long period of time and it should be capable of measuring a

relative deformation.

It is the latter of these (deflection measurements) and their analysis that is the main subject of this thesis.

Many examples can be given of the different methods adopted for taking deflection measurements and those given below are restricted to glulam sections only. In chronological order and by decade, the first example is Sasaki and Maku (1963) who give details of a laboratory test rig with deflections measured by observing a piano wire against a scale. Madsen and Barrett (1976) measured creep using vertical test rigs similar to those used by STRU (see figure 2.2) where deflection is obtained with dial gauges. Vertical rigs have also been used for creep tests by the Building Research Establishment (BRE) since 1974. Srpcic (1988) also uses dial gauges and a fixed laboratory test rig to measure creep. Into the 1990s, Rouger, *et al.,* (1990) use a combination of optical sights and displacement transducers to measure deflections to test glulam sections but again under laboratory conditions. Martensson (1991) describes a number of laboratory-based test methods where deflections are measured using transducers, extensometers and strain gauges. A number of other methods is also given by Morlier (1994).

The common thread through all of these is that the creep behaviour of timber and glulam is assessed by using specially prepared sections mounted in a fixed laboratory test rig of some sort. The rigs themselves are often placed in a climatic chamber where the specimens can be exposed to a controlled environment. Measurement of deflection for these is carried out on relatively

small sections which can usually be recorded directly.

In the late 1980s, some researchers started investigating creep in covered outdoor facilities so exposing the test samples to an uncontrolled temperature and relative humidity regime but protecting them from rain and direct sunlight. For glulam, the work of Badstube, *et al.,* (1989) and Andriamitantsoa (1991) are good examples of this together with the later work of Toratti & Morlier (1995), Dill-Langer, *et al.,* (1996) and Ranta-Maunus, *et al.,* (1996). However, as with indoor testing, these experiments have been done under 'laboratory' conditions using prepared test specimens and deflections are measured by a combination of optical sights/transducer (Toratti & Morlier), dial gauge (Badstube), transducer (Andriamitantsoa, Dill-Langer) and manually (Ranta-Maunus).

As described in section 2.5, similar tests to those given above have also been carried out from 1988 by the University of Brighton both in the laboratory and outdoors under cover. No individual or organisation known to the author had, up to 1992, reported a project for recording deflections and creep in timber or glulam sections located in full-scale buildings instead of in the laboratory. Consequently, the decision was made by STRU at this time to implement a programme to determine creep in a number of buildings both during and after construction.

The means by which measurements could be taken for STRU with a sub-millimetre accuracy in full-scale structures had to be chosen and the first two sites at Wokingham and Shoreham would involve measuring deflections on a

large scale compared to the laboratory and often at inaccessible points (see section 2.7). How to monitor these structures using such equipment as dial gauges could not be envisaged and, for aesthetic reasons, attaching transducers or other devices permanently to glulam beams was not possible.

In this case, an alternative to all the laboratory based methods in current use for measuring deflections of glulam beams was required and it was decided that an indirect method of measurement should be used, such as one of those developed for high precision monitoring in surveying.

As an addendum to this section it noted here, that in 1996, two researchers at the University of Florence published the results of tests carried out to determine the creep occurring in composite concrete and glulam beams (Capretti and Ceccotti, 1996). These tests included some short and long-term experiments carried out on prepared beams in an outdoor environment but also included measurements taken in a 'real' full-size building following construction. Inside this building, three 10 m composite beams were monitored during the period 1991-1996 but the authors give no details as to how the beam deflections were measured.

3.2 Choosing the equipment best suited to the glulam project

A number of different methods for monitoring the glulam roof frames were considered at the start of this project and a description and assessment of the suitability of these is given in the following sections. An overview of some of the methods available at the time is also given by Aeschlimann (1988), Teskey

(1988), Fondelli (1990), Katowski (1990), Shortis & Fraser (1991), Anon (1992), Milne, *et al.*, (1992) and Moore (1992).

When selecting the most suitable method for a monitoring scheme, there can be a tendency to choose a measurement system based solely on the quality of the instruments to be used. Whilst this is important, the emphasis for the glulam project focussed not only on the suitability of various instruments and systems as regards their cost and accuracy, but also on the complete measuring process. This approach to establishing a measurement system is advocated by Stanek (1993). In this, the instruments and associated computer hardware/software are as important as how well they would be expected to cope with site conditions, with long-term use and with the personnel expected to use them. In addition, the sub-millimetre accuracy required for the measurement of creep and deflection in glulam is paramount, and this is dependent on many factors of which instruments are only a part.

Traditionally, the measuring techniques and instrumentation used for monitoring and close range measurement have been classified into two groups according to the professionals who use the equipment. These are (Chrzanowski, *et al.*, 1993)

- *geodetic surveys* which include conventional land surveying, close range photogrammetry and some special techniques such as interferometry, hydrostatic levelling and others
- *geotechnical/structural measurements* using electrolevels,

inclinometers, strain gauges, extensometers and so on

Geodetic surveys give global information on the behaviour of the object monitored, they are labour intensive and require skilled operators but can take absolute measurements with reference to stable points. On the other hand, geotechnical measurements have been used to obtain very localised relative information regarding deformation and deflections within the object monitored but they are easier to adapt for automatic and continuous monitoring and once installed, require infrequent checks.

However, due to advances made in measurement technology over the last twenty years or so, the differences between the two measurement categories and their main applications are not so obvious as before. For example, modern digital levels with an accuracy of 0.1 mm over distances greater than 20 m may provide a better accuracy for tilt determination than electrolevels and precision electromagnetic distance measurement also over short ranges may serve as extensometers in relative deformation surveys. New developments in three-dimensional coordinate measuring systems with electronic theodolites and by using photogrammetry may provide relative positioning in real-time with a high accuracy (better than 0.1 mm) over several metres.

With the recent advances in both geodetic and geotechnical instrumentation, it is now possible to achieve almost any resolution and precision, full automation and real-time data processing. The list of different types of instruments available is considerable and this creates a number of problems when designing a monitoring scheme: what instruments to choose, where to locate them and how to combine them into one integrated monitoring scheme. Some of these

issues are examined in the following sections.

Levelling

Taking note of the specifications given for the glulam monitoring given in section 2.6, the first method investigated for taking measurements of the vertical deflections expected in glulam rafters at the Wokingham and Shoreham sites was levelling. With an accuracy requirement for detecting vertical movement of 0.1 mm, optical (or spirit) levelling could have been carried out using either a precise optical level fitted with a parallel plate micrometer or a digital level such as the Wild NA3000.

The method that was proposed for assessing movement in the glulam roof frames was to target selected rafters at a regular spacing and to measure vertical deflections at these discrete points (see chapter 6). If levelling were to be carried out, all of the targeted points would have to be fitted with some form of mechanical device to ensure that a levelling staff could be held on them in exactly the same place each time a reading is taken. A solution to this would be to install something similar to the levelling station developed by the Building Research Establishment (BRE) and originally described by Cheney (1973). This consists of a stainless steel socket (see figure 3.1) and a number of these would have to be permanently fixed into the glulam rafters. During a measurement, a stainless steel plug would be inserted into the socket and this would ensure that the other end of the plug, which is spherical, accepted a levelling staff in the same position each time the levelling station was used. The spherical plug in the levelling station can be positioned radially with a repeated

accuracy of 0.03 mm (Cheney, 1980). Further examples of levelling stations currently available are given by Cook (2001).

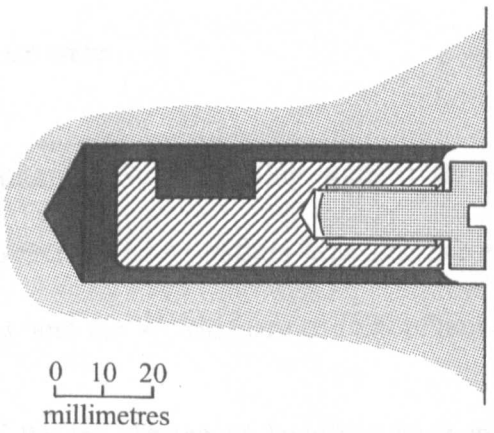

Figure 3.1 *Cross section of a BRE levelling station (Cheney, 1973)*

The advantages of levelling were considered to be

- the method is well known and does not require any specialist knowledge other than conventional levelling
- an accuracy of 0.1 mm was possible for measuring vertical displacements
- it was inexpensive compared to other methods (for example a theodolite intersection system or photogrammetry)
- measurements could be taken fairly quickly with minimum contact on the glulam rafters
- data processing and recording would be straightforward and would be in electronic form with a digital level
- the equipment would not be bulky or heavy and could be transported to

site quite easily

Despite these advantages, some serious disadvantages for levelling were envisaged. These were

- installation of BRE levelling stations or similar mechanical devices along several glulam rafters was not permitted by the architect and client at both the Wokingham and Shoreham sites
- even if the installation of levelling stations or something similar was possible, the problem of taking reliable and accurate readings to elevated points (probably with an inverted staff) remained
- monitoring at Shoreham would be impossible as most of the targets to be accessed would eventually be above water
- levelling can only provide positional information in the vertical direction and three-dimensional data may have been required for analysis

Despite the simplicity of levelling and the low costs involved, it was rejected as a measurement method for the glulam monitoring project because of uncertainties about the accuracies that could achieved with some staff readings, the limited data output (only vertical movements can be recorded) and its inability to be used at Shoreham.

Trigonometrical heighting

This technique for determining heights (or *Z*-coordinates) would involve the measurement of vertical (or zenith) angles between points and has some advantages over levelling. The most significant of these is that it could be used to determine the heights of inaccessible points on the glulam roof frames such as those at higher elevations and especially those points that would eventually be over the pool at Shoreham.

A method proposed by Teskey (1989) states that accuracies of 1 in 100 000 can be achieved for trigonometrical heighting at close ranges. However, this involves taking measurements of zenith angles to the points to be heighted from a network of reference points with precisely known three-dimensional coordinates. At Wokingham and Shoreham, it was decided at an early stage that it was not possible to install fixed reference points and observe from these to the glulam roof frames. Consequently, it was not possible to use this method for determining *Z*-coordinates. Teskey (1992) again proposes trigonometrical heighting as a precise method for determining *Z*-coordinates but in this case, a 'free station' approach is adopted which is essentially a theodolite intersection system.

Theodolite intersection systems

A typical theodolite intersection system comprises two or more electronic theodolites linked directly to a computer which has appropriate software to compute *XYZ* coordinates of points intersected on the object being measured.

For the glulam project and because of anticipated financial constraints, a two-theodolite system was under consideration in which, after an initial set up procedure to orientate the theodolites is completed, the two observers were required to identify passive target points on glulam beams and to sight these manually. The horizontal and vertical angles to each point observed would then be digitally recorded and transmitted to the system computer for the on-line computation of the coordinates of the target sighted. Following this, the coordinates would be processed off site to give the required vertical deflections.

The development of theodolite intersection systems to the point they were being considered for use in the glulam project is discussed by Allan (1988), Price (1989), Kennie (1990) and Grist (1991).

The advantages of using a theodolite intersection system for the glulam project were assessed as follows

- the accuracy requirement could be achieved
- once the object is targeted, a theodolite intersection system would be capable of taking remote, non-contact measurements to any point and the equipment could be used at more than one site
- three-dimensional measurements could be made to any point (elevated or over water) on both roofs at Wokingham and Shoreham at close range

- the cost of a system would be within budget for the project
- the author was familiar with the technology of theodolite intersection systems

The disadvantages were seen to be

- compared to other close range monitoring systems, the rate of data capture is not fast and relies on at least two operators to take observations
- although portable, transporting the equipment and setting up on site would be time consuming
- the quoted accuracy of 1 in 100 000 (Leica, 1993a) could only be realised in good geometric conditions and there was some doubt about how this would affect the measurement of vertical deflections

Despite some of the disadvantages, this method of measurement was thought to be the most likely for monitoring the glulam roof frames but others were considered.

Automated theodolite intersection systems

Further developments in theodolite intersection systems gave rise to automated versions of these in the late 1980s. The use of a theodolite can be improved, especially in response time, by automating the observation of targets and most attempts at automation at the time concentrated on driving the theodolite to

approximate target positions and then using digital image processing techniques to sight the target exactly. The benefits of automation are to reduce the chance of human error occurring, an improvement in the consistency of the pointing accuracy and faster data acquisition.

The automation process required stepping motors to be built into a theodolite with the facility for data input (for target location) and data output (of precise measurement of horizontal and vertical angles to targets). Instruments such as the Leica TM Series and Kern E2SE are examples of motorised theodolites available in the early 1990s and both of these would accept either *XYZ* coordinates or horizontal and vertical angles as their input. The motors would drive the telescope to approximate target positions according to the input data and automatic target location was carried out using a charge coupled device (CCD) built into the optics of the telescope. The digital images produced in the field of view of the telescope were used to refine a pointing so that the theodolite reticule was automatically centred exactly on a target.

Two examples of automated theodolite intersection systems available in 1992 were the Kern SPACE system (Roberts & Moffitt, 1987 and Gottwald, 1988) which was available from 1987 and the Wild ATMS system which first appeared in 1988. The SPACE system is shown in figure 3.2.

When setting up these systems, the theodolites have to be mutually referenced (through a bundle adjustment procedure, see section 4.3), scale has to be established and targets defining a coordinate system have to observed. This is

similar to the procedure required in manual theodolite intersection systems. However, the measurement to points of interest is quite different, as the theodolites are driven to each target in turn, the reading is taken automatically and the whole process could be overseen by one operator regardless of the number of theodolites in use thereby significantly reducing observation time.

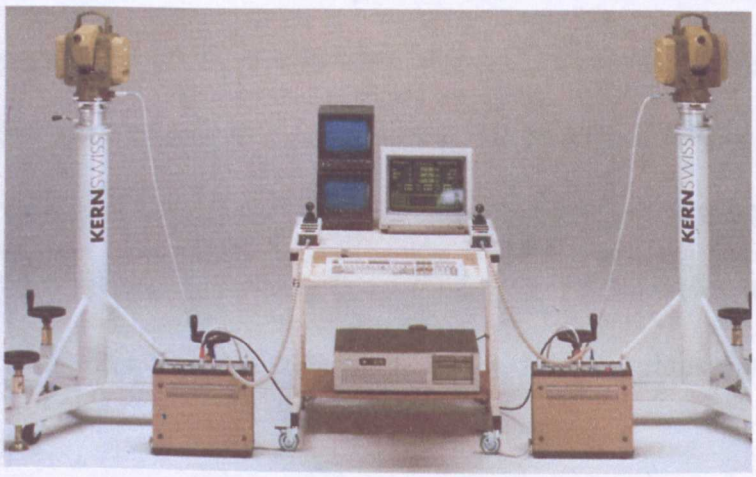

Figure 3.2 *Kern SPACE measuring system (courtesy Leica Geosystems)*

Although perfectly acceptable as a measurement solution, automated theodolite intersection systems were rejected because of costs. For example, the Kern SPACE system was sold for £150 000 in 1992 and at three times the budget allowed this made the choice not to use it fairly straightforward. The measurement to a relatively small number of targets in a research setting was, perhaps, not the best application for automated systems which are more suited to production line environments where measurements are repetitive and at predictable locations.

Polar methods

As an alternative to a theodolite intersection system, monitoring of the glulam

structures at Wokingham and Shoreham could have been carried out using a system deriving coordinates from polar (or bearing and distance) measurements.

Compared to intersection, polar methods are not so dependent on intersection geometry and only one observer is required to take measurements. As with any monitoring system, it is only viable when electronic surveying instruments are used together with electronic data recording, all interfaced with a computer processing real-time coordinates. The Japanese company Sokkia marketed their MONMOS polar measuring system in 1992 (Sokkia, 1992a) which was clearly of interest at the time and was seriously considered for the glulam project (see figure 3.3).

The system derives its name form ***MON***o ***MO***bile 3-D ***S***tation and it was designed specifically for three-dimensional measurement in the shipbuilding industry (Sokkia, 1992b). In its first version, MONMOS had two main components: the NET2 total station and the SDR4B control terminal. The NET2 was described as a high precision total station capable of measuring angles with a precision of 2″ and distances with a precision of (1 mm + 2 ppm). The SDR4B controlled the operation of the MONMOS system and it also stored the data generated by the NET2. This data could, of course, be transferred to a computer for further analysis. Some reflective targets were developed by Sokkia that could be used as an alternative to corner-cube prisms for distance measurement. The principle on which MONMOS is based and its use is described by Uren (1992) and Whitted (1993).

Figure 3.3 *Sokkia MONMOS system (courtesy Sokkia)*

With a quoted accuracy of (1 mm + 2 ppm) for distance measurements, the accuracy expected for *XYZ* coordinates from MONMOS was assumed to be at about the 1 mm level at short ranges. However, Uren quotes the RMS error of coordinates measured by MONMOS to be ± 0.4 mm at ranges of up to 30 m. It is not clear how this figure was derived which seems to be over optimistic. Whitted claims a standard error of 0.2 mm for measurement of *XYZ* coordinates with MONMOS but only at very short ranges within a 7.5 m square with the

angles of incidence to the targets restricted.

In summary, the advantages of using MONMOS to monitor glulam were assessed as

- only one instrument and one operator would be required to take measurements
- the NET2 could be set up at wide variety of points (subject to the type of target used – see MONMOS disadvantages) and no complex setting up routine was required
- the results obtained would not be dependent on the geometry of intersections
- the cost of the system was within the budget for the project

The disadvantages were

- the accuracy obtainable was limited by the distance measuring capability of the NET2 which was 1 mm at close range
- it is not possible to check the measurements because there is no redundancy in polar observations taken from a single position
- the method relied on taking distance measurements to targets marked with special reflecting tape - if any measurements were taken at acute angles of incidence to the tape, this would reduce the range of the NET2 and might introduce unwanted errors into the distance

measurements

- the long-term performance of the targets (special reflecting tape) in a harsh environment such as the swimming pool at Shoreham was unknown and these could not be replaced once installed

Although a possible solution for the glulam measurements, MONMOS was not thought to be suitable as it did not meet an accuracy requirement of 0.1 mm for coordinate determination. A subsequent paper published confirmed this decision and it was claimed by Tor (1993) that 'MONMOS was an effective way for measuring deformations in the *X*, *Y* and *Z* directions if precisions of ± 1 mm and distances of less than 100 m are acceptable'. In his paper, Tor also states that the precision of *Z*-coordinates obtained from MONMOS is about two times worse than [that obtained for] *X* and *Y* coordinates.

The Wild APS (Automatic Polar System) has been available from Leica since 1990 (Wild Leitz, 1990). This is an automatic polar measuring system designed specifically for non-contact monitoring, the two main components of which

Figure 3.4 *Wild APS system (courtesy Leica Geosystems)*

were (in 1992) a Wild TM3000 motorised theodolite fitted with a distance measuring unit (shown in figure 3.4).

As with MONMOS, the accuracy attainable at short ranges with APS was dependent on distance measurement to about 1 mm and this, together with costs well in excess of the budget, meant that APS was never seriously considered for monitoring at Wokingham or Shoreham.

Laser monitoring systems

In 1992, another of the industrial surveying methods available for optical close range measurement was to use a laser tracker. Instruments of this type consist of a motorised laser interferometer combined with angle encoders which produce the equivalent of a short range total station with a very precise distance measuring capability. If it were possible to use such an instrument at Wokingham or Shoreham it would overcome the accuracy limitations of close range polar measurements taken with a conventional total station.

The Kern SMART 310 shown in figure 3.5 was an example of a single beam laser based tracker system available in 1989 which was modified and produced by Leica in 1990. This was a non-contact measuring system in which the laser interferometer automatically followed a moving target whilst measuring and recording horizontal and vertical displacement angles as well as distances. From these polar measurements, three-dimensional coordinates could be derived to an accuracy of 20 ppm and the system could record hundreds of three-dimensional positions every second at target speeds of up to 2 ms^{-1} with a

range of 25 m (Leica, 1992a). For all this to be possible, a reflecting prism had to be attached to the target point being monitored. As might be expected with advanced technology of this type, the complete measurement procedure was controlled on-line by a computer and software which produced the required coordinates with error analysis.

Figure 3.5 *Leica SMART 310 (courtesy Leica Geosystems)*

Although the SMART 310 certainly met the accuracy requirement for the glulam project and it had the advantages of being mobile whilst taking non-contact measurements, the disadvantages were costs (which were well beyond the project budget) and the targeting arrangements that required some form of retro-reflector to be placed at each point to be measured (not reflecting tape). This would, of course, be impossible at Shoreham. Some of the system features such as the high tracking speed and a fast data acquisition rate were not needed in this case and it was evident that the most appropriate applications for the SMART 310 (and other similar laser trackers) were in dynamic measurements rather than those required for monitoring structures on a periodic basis.

The most widespread applications for laser trackers have been in such areas as robot calibration where the reflector is mounted on the moving robot arm and in machine control where the system tracks and records the movements of cutting tools, especially in milling machines.

Close range photogrammetric systems

Photogrammetry is a very wide-ranging subject with a considerable amount of published material associated with it and no attempt is made here to cover all aspects of its application to close range measurement. Instead, some background is given to indicate the development of close range industrial photogrammetry up to the early 1990s to coincide with the start of the glulam project.

It is well known that the majority of maps for engineering and other purposes are made from aerial photographs and decades of research and development have been pursued to improve the equipment and methods used for this. Since aerial (or topographic) photogrammetry has been the dominant form of photogrammetry, there has been a tendency to describe anything that uses different techniques as non-topographic photogrammetry. The terms close range and terrestrial photogrammetry have also been used alongside non-topographic but close range photogrammetry indicates surveys where photographs have been taken having object to camera distances of up to about 300 m.

Although the origins of close range photogrammetry can be traced back to the

nineteenth century, it was not until the 1960s and 1970s that non-topographic applications of photogrammetry became common. The most popular use at this time was for architectural and heritage recording but engineering and industrial applications were also being identified (see Karara, ed., 1979 and Atkinson, 1980).

Shortis and Fraser (1991) trace the development of the early period of modern close range photogrammetry from the 1970s. Initially, metric cameras were used and the techniques employed were essentially the use of simple stereopairs together with conventional stereoplotters or stereocomparators. To some extent, this was aerial photogrammetry adapted to a terrestrial situation. Unfortunately, this has a limited accuracy in close range photogrammetry as it usually involves taking photographs of objects with considerable variations in camera to object distances and with convergent camera axes. It was these restrictions that led to the development of multistation convergent photogrammetry employing bundle triangulation (or a bundle adjustment) and this was seen as the way forward for close range photogrammetry from the early 1980s (Granshaw, 1980 and Brown, 1982). Consequently, the reason for the increasing popularity of close range photogrammetry through the 1980s was the development of computer programs capable of calculating bundle adjustments and at the same time, advances made in computer hardware. The ability to implement adjustment programs on fast computers made it possible to use a variety of different cameras, but semi-metric in particular.

The third reason for the increased use of close range photogrammetry in

industrial measurement was the introduction of the automated image measurement comparator. These do not require trained or skilled operators to use them and they are considerably faster when taking measurements compared to manual comparators. This helped reduce the turn-around time of close range photogrammetry to a level far more acceptable to industry.

So, the situation with regard to close range photogrammetry in the early 1990s was that of a measurement process considerably more advanced than a decade earlier (Fraser, 1988) and capable of very high accuracies (Fraser, 1992). As well as this, commercially produced systems were much easier to use than their earlier counterparts.

In 1992, digital photogrammetric systems and real-time processing of images had been introduced. However, these were very much in their infancy and the use of a digital photogrammetric measurement system was assumed to be too specialist for the glulam project. Instead, an 'off the shelf' close range film-based system using semi-metric cameras, bundle adjustment software and an automated comparator was the only one under consideration.

For the glulam measurements at Wokingham and Shoreham, close range photogrammetry was seen to have the following advantages

- photogrammetry is capable of taking remote, non-contact measurements
- the cameras and associated equipment could be taken to any structure
- data recording could be rapid so that the length of time spent on site

could be kept to a minimum

- photographs provide a permanent record of each survey which could be re-measured at any time

- an accuracy of 1 in 100 000 was possible with an appropriate system

The disadvantages were assessed as

- the cost of commercially available close range photogrammetric systems was beyond the budget available for the project

- the technology was unknown to the author and those expected to use whatever system might be chosen

Contrary to the latter of these, it was claimed at the time that most close range photogrammetric systems were capable of being used by 'non-specialists' after a short training course. Whilst this may have been true, it was considered something of a risky policy to embark on a major research measurement programme without any experience of the methods to be used.

Regarding costs, measurements at Wokingham and Shoreham did not require the coordination of more than about 80 targets at most (often as few as 10) and photogrammetry only becomes cost effective when large numbers of points are to be measured (Brown, 1989).

An alternative to buying a close range photogrammetric system was the possibility of paying a photogrammetric specialist to do the measurements at

each site. Although this was considered, it was eventually discounted for the following reasons. First, costs were estimated assuming several sets of measurements had to be taken each year at several sites, for at least five years. Without any doubt, these would have consumed the budget for the project very quickly and with hindsight, the total budget for the project would have been spent on photogrammetric surveys at the Wokingham site alone, where 55 full surveys have been completed to date (February 2002). The second objection to using a photogrammetric specialist were concerns over loss of control over the project which would effectively be handed over to a third party and doubts about the continuity and consistency of measurements were raised.

Although it was a strong contender, the final decision was to reject close range photogrammetry as the method to be used for monitoring the glulam structures because it was too expensive.

Electrolevels and other methods

In the 1970s, electrolevels were considered for monitoring on many geotechnical and structural applications but it was felt that the standard of manufacture was not sufficiently consistent or accurate. Throughout the 1980s, electrolevel system research was carried out by the Building Research Establishment in the UK and in the 1990s, due to improvements in manufacture and readout equipment, it gained a far greater acceptance for structural monitoring.

The installation of electrolevels at each of the sites chosen to be monitored

would have, in many respects, been the ideal measurement solution for the glulam project. The accuracy they are capable of would have easily met the 0.1 mm required for vertical displacement and, compared to the optical methods available, a further advantage was that readings could be taken completely automatically and stored in data loggers wired directly to an array of interconnected electrolevels. When convenient, data could be downloaded from the loggers by a relatively unskilled operator and, after the initial installation was complete, little survey knowledge would be required to use the system.

In addition, it was possible to integrate the whole measuring and monitoring process at each site and the environmental data required, such as temperature and humidity, could have been recorded and stored by the same loggers. Taking automation to its extreme, a fully automated computer-controlled system could have been installed where data could be stored, processed and transferred all without operator intervention.

Electrolevel systems capable of all the above were available from such organisations as the Building Research Establishment in 1992 (Institution of Civil Engineers, 1990 and Building Research Establishment, 1992) and some commercial companies, for example JB Developments at Edenbridge in Kent (Winney, 1992), also offered these at the time.

Unfortunately, it became apparent at an early stage when assessing electrolevels that it would not be possible to use them. The reason for this is amply demonstrated in figure 3.6 which shows the size of electrolevels and

their associated recording equipment.

Figure 3.6 *Electrolevel system (courtesy Monitoring Systems Ltd)*
Top right: Data collector/computer
Main picture: Logging equipment and junction box
Bottom left: 2 m electrolevel beams and cabling

Recalling the objections raised by client and architect at the Wokingham and Shoreham sites where concerns were raised over the installation of somewhat smaller levelling stations and even targets, it was quite obvious that permission to install electrolevel monitoring systems would not be given because of the permanent visual impact they would have at each site. Discussions with the architect at Wokingham and Adur District Council confirmed this.

Consequently, the use of electrolevels was not possible as a measurement method for the glulam project.

Additional methods for close range monitoring that were investigated for the glulam project included water levelling systems (described by Feistauer, *et al.*, 1988), the installation of equipment such as linear variable differential transformers (LVDTs) (described by Collins, 1989 and Kopczynski, 1992) or the installation of wire extensometers and inclinometers (described by Ding, *et al.*,2000). All were rejected as either being impractical (water levelling systems and extensometers) or it was assumed that permission to install the apparatus would not be given (installation of LVDTs, and other electromechanical/electronic sensors). Many of these systems of measurement were also not vandal proof and if installed in a public area, their security would have been a cause for concern.

3.3 Summary

Taking account of the descriptions of the various methods used for close range monitoring given in this chapter, theodolite intersection carried out manually was chosen as the measurement system for the glulam project. Although not ideal in some respects (labour intensive, rate of data capture slow and more equipment to transport compared to other methods), its ability to match the accuracy required within the budget allowed was the decisive factor. As well as this, measurements could be taken to unobtrusive passive targets which had the approval of both the client and architect at Wokingham and Shoreham.

The inevitable question that followed was the choice of system to be used and how it would be implemented at a number of different sites. An 'in-house' system was not developed because of the need to start measurements as soon as possible and only one system was available commercially at the time in the UK: the Electronic Coordinate Determination System (ECDS) from Leica. This met all specifications and cost and was purchased by STRU for the glulam project in the autumn of 1992.

In section 2.1, it was noted that Leica provided some of the financial support for the monitoring carried out in *Project 3*. The author would like to state that this was offered after ECDS3 had been purchased on the basis that Leica was keen to support new research and to gain experience from a non-industrial use of ECDS3.

4

THE MATHEMATICS OF THEODOLITE INTERSECTION

In the previous chapter, the use of a theodolite intersection system for the measurement of deflection and creep in a variety of glulam structures was proposed. The system chosen to do this was the Electronic Coordinate Determination System (ECDS) version 3 marketed by Leica.

At close range, a theodolite intersection system such as ECDS3 is capable of determining the three-dimensional coordinates of a point to a high degree of accuracy. Coordinates are determined in a three-dimensional intersection from at least two theodolites where the unknown coordinates are calculated from observed horizontal and vertical angles. The results obtained can be calculated in any coordinate system, whether this is local and related to the theodolite positions or defined by the object being measured.

This chapter describes the procedures that can be used to set up a theodolite intersection system and gives details of some of the methods used to calculate spatial intersections. The intention here is to provide a personal interpretation and understanding of the processes involved and how these have developed in modern theodolite intersection systems and not to attempt to explain the mathematics in full. Different versions of this have already been published by many authors including Kyle (1988), El-Gohary (1989), Bingley (1990) and Bayly (1991) with more recent contributions from Zhang, *et al.*, (1997) and

Zou, *et al.*, (2001) but some new material is presented here.

4.1 Coordinate systems

For close range surveys, it is usual to define the positions of theodolites, control points and intersected points in a right-handed cartesian coordinate system as shown in figure 4.1. On this, a point P has coordinates x, y and z measured along each axis.

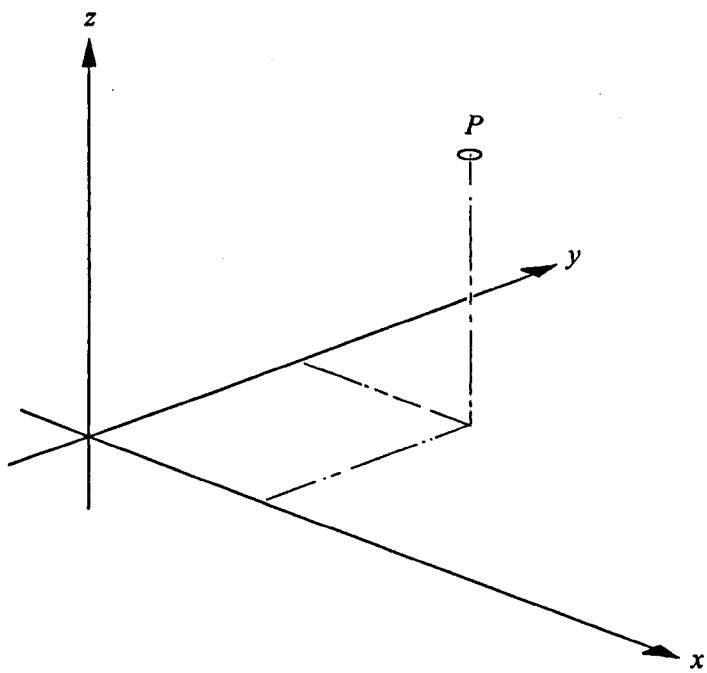

Figure 4.1 *Right-handed cartesian coordinate system*

Two types of cartesian coordinate system are used with theodolite intersection systems: a local or object system.

Local coordinate system

In its simplest form, the origin is defined to coincide with the axes of one of the

theodolites used for measuring intersection angles with the z-axis defined as coincident with the vertical axis of the theodolite. For a single baseline where two theodolites are used as in figure 4.2, theodolite A (the reference theodolite) will have coordinates ($x_A = 0, y_A = 0, z_A = 0$) and the plane containing the z and x-axes will pass through theodolite B at the other end of the baseline which will have coordinates (x_B, $y_B = 0$, z_B).

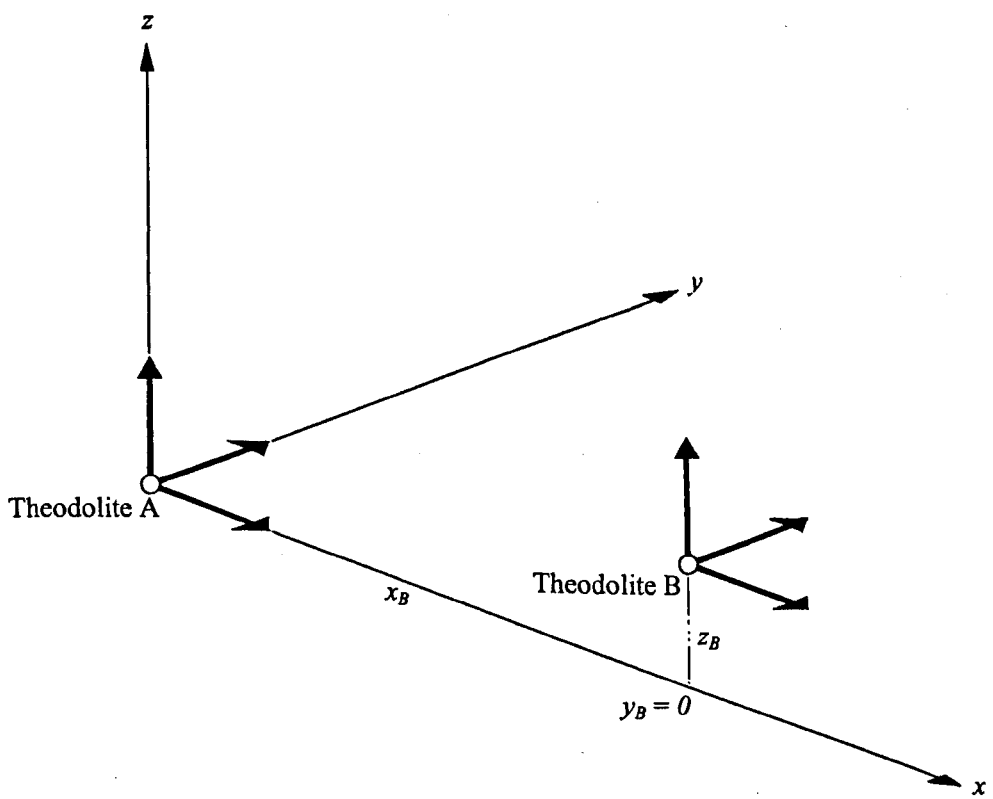

Figure 4.2 *Local coordinate system for single baseline*

Establishing a local system is usually arbitrary and it is positioned through placement of the first theodolite and will therefore, for the same repeated survey, vary slightly from one set-up to the next.

A local coordinate system is often used where periodic measurement of relative dimensions is required. This is the case for the determination of the

displacement of the glulam structures so far described and all surveys carried out as part of the work in this thesis have been based on local coordinate systems.

The benefits of a local coordinate system are its simplicity, especially for *z*-coordinates which are in the same direction for levelled theodolites (the direction of gravity) and that the quality of results obtained from a survey are based on the sighting accuracy for horizontal and vertical angles. In addition, a local system allows the theodolites to be orientated without knowing anything about the object to be measured, a situation ideally suited to the glulam structures.

The limitations of setting up a local coordinate system are that the results obtained cannot be compared directly to the coordinates defined for a part or the whole object. This situation can be rectified by transforming local coordinates into an object-based coordinate system. This might be done, for example, when measuring a large object where it is necessary to perform several surveys in separate local systems and then transform all of these into a single object coordinate system. To transform coordinates from a local to an object system requires at least three control points with coordinates known in both the object and local systems to be available so that transformation parameters can be determined. No such transformations have been carried out for this project.

Object coordinate system

This is defined by known coordinates on the part (or object) to be measured. Figure 4.3 shows a cube representing the part and a set of axes defining an object coordinate system.

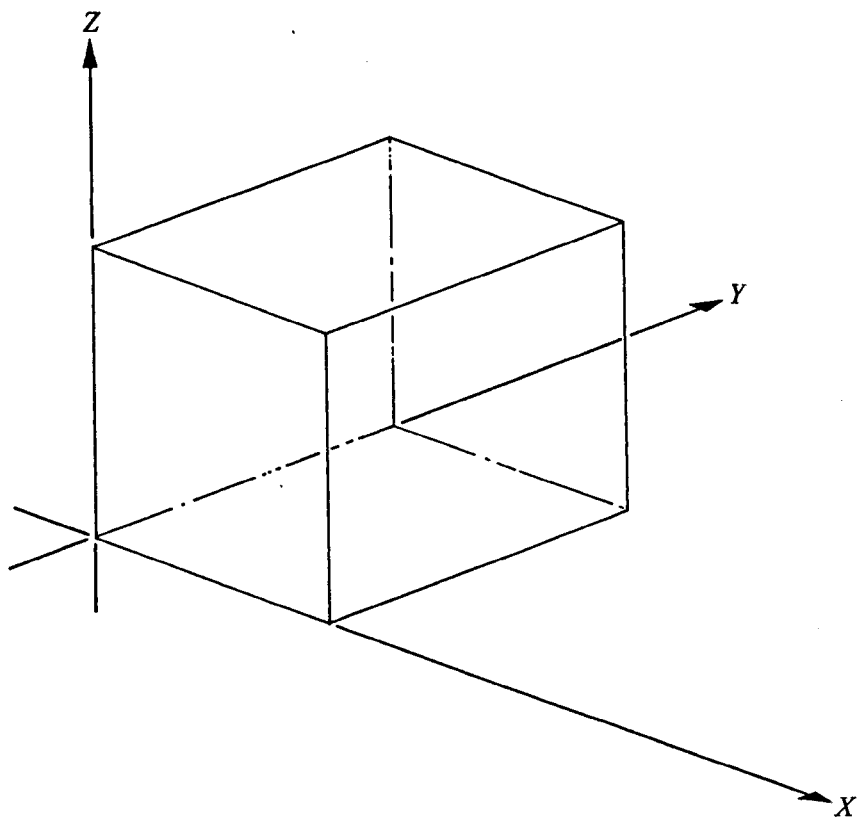

Figure 4.3 *Object coordinate system*

If a theodolite intersection system is set up to measure object coordinates, the results obtained can be compared directly with coordinates specified on the object without further processing: in a manufacturing process, this would be the normal requirement. An object system is established by knowing values of the coordinates of enough control points based in the object system so that the orientation of the theodolites can be determined from them.

When monitoring the displacement of a structure, working with object coordinate systems would allow absolute monitoring to be carried out. At each site selected for monitoring in this project, it was not possible to install or define points that could be used to establish an object coordinate system over any period of time.

4.2 Setting up a theodolite intersection system

Setting up and using any theodolite intersection system will always involve two separate stages.

First, it is necessary to determine the position and orientation of all the theodolites used in the measurement system. For a *local coordinate system*, this can be done with respect to one of the theodolites which will then define the origin. For an *object coordinate system*, this can be done with respect to a series of control points of known coordinates.

Second, once the theodolite positions and orientations have been established, the coordinates of targeted points are found by intersection.

The first methods used for orientating a theodolite intersection system involved known control points in an object coordinate system. Two methods were used to do this: in the most straightforward case, the theodolites were levelled and centred over control points whose coordinates were known and the orientation was defined by the bearings along the baselines between the control points or by assuming known directions along these baselines. For close range work, this

is a scaled down version of traditional intersection, a technique familiar to all surveyors and engineers. In the second method, the theodolites were set up in any convenient position and were orientated by resection but over smaller distances than for normal survey work.

It was natural to expect that these first attempts to set up a theodolite intersection system would be based on conventional survey methods but they have serious accuracy limitations because of the need to centre the theodolites or the reliance on how well control points have been coordinated.

For close range and industrial applications, a better method of setting up a theodolite intersection system is to designate the centre of one of the theodolites as the origin of a coordinate system (see figure 4.2) in which the *z*-axis is coincident with the vertical axis of the theodolite. If this is the case and two theodolites are used along a single baseline, it is conventional to define the *x*-axis of the coordinate system as coinciding with a horizontal line in the vertical plane containing the baseline between the theodolites. In other words, a local coordinate system is usually adopted. Establishing this involves the following: orientation of the theodolites, determining the distances between the theodolites and determining the height difference between the theodolites.

One of the first methods used for orientation of the theodolites was known as collimation and this is the process of bringing the lines of sight of a pair of theodolites, or their axes of collimation, into coincidence. This is achieved, at a particular theodolite, by observing the reticule of another theodolite with the

telescope focusing rings at various settings. The procedure for doing this is quite involved, not to say tedious, and can take quite a long time and considerable skill to do satisfactorily. Great care is needed with this as the accuracy of any subsequent measurements depends heavily on the procedure. An indication of the steps involved in collimating is given by Ashworth (1989). Once collimation has been carried out, the horizontal circle readings at each theodolite can be recorded or, for a single baseline involving only two theodolites, the horizontal circle readings can be zeroed when the two telescopes are mutually pointed towards each other along the x-axis (or baseline) between the theodolites.

As an orientation procedure, collimation has some drawbacks. First, there must be a clear line of sight between the theodolites and the instruments cannot be positioned close to each other at less than their minimum focusing distance. Second, there must be good lighting conditions for viewing the reticule images. Third, it becomes very difficult to see the reticules when the baseline is longer than about 20 m. Where more than two theodolites are to be orientated, the process has to be repeated several times with an inevitable increase in the time taken.

Determining the horizontal baseline distances D between the various theodolites of an intersection system can be done by direct measurement but this is not recommended if a reliable sub-millimetre accuracy is required. The usual method for determining D between a pair of theodolites is to use a calibrated scale bar, the length of which is known to a high degree of accuracy

(see Appendix A).

The procedure for determining D starts with this being estimated by some means as d with there being no need to measure d accurately. If a measurement system consists of two theodolites only, the theodolite at the origin of the local coordinate system (theodolite A) will have ($x_A = 0$, $y_A = 0$, $z_A = 0$) as coordinates. The approximate coordinates of theodolite B can be determined using the estimated base length d where $x_B = 0$, $y_B = d$ and $z_B = (h_B - h_A) = \Delta h$ = the height difference between the two theodolites. This can be obtained from

$$\Delta h = \frac{d(\tan\beta_{AB} - \tan\beta_{BA})}{2} \qquad 4.1$$

where β_{AB} and β_{BA} are the vertical angles between the theodolites observed when they are collimated and where $\beta_{AB} = -\beta_{BA}$ within a suitable tolerance.

Observations are then made to the targets at the ends of the scale bar and provisional coordinates for the scale bar can be computed. Using these, it is possible to compute the length of the scale bar and obtain this as, say, b. However, because this has a known calibrated length B, the proportion of b to B will be the same as the proportion of the assumed base length d to the actual base length D from which we obtain

$$\frac{b}{B} = \frac{d}{D} \qquad \text{or} \qquad D = d\frac{B}{b} \qquad 4.2$$

Using this value of D as a better estimate for the baseline length, the procedure is repeated to give another value for the scale bar length which in turn will yield another estimate for the baseline length. The procedure is repeated until the estimated and actual values for D are within a specified tolerance. It is good practice to move the scale bar to a different position for each iteration in this process.

Following collimation and baseline determination, the final stage in setting up the system by this method requires the height difference between the collimation axes of the theodolites to be determined. Equation 4.1 could be used for this (using D instead of d) but other methods by which this can be done are discussed in section 4.4.

As described above, the main problem associated with setting up a theodolite intersection system is the collimation process which is very difficult and takes a long time to perform, especially for more than two theodolites. In addition, determining the baseline lengths can also be time consuming if several iterations are required to achieve a satisfactory value for this.

For the glulam project, adoption of a theodolite intersection system based on the collimation process would not be ideal because of the length of time taken to orientate the system. Fortunately, in later systems such as ECDS3, the problems of collimation and baseline determination have been overcome using a bundle adjustment technique which enables the coordinates of the axial centres of each theodolite and the orientations of their axes to be determined

much quicker than by collimation and with respect to whatever coordinate system is adopted.

4.3 The bundle adjustment

The bundle adjustment is a well-known technique that has been used in analytical photogrammetry for some time. Used successfully in engineering and industrial applications of photogrammetry, the technique is used to determine camera positions and orientations in multi-station photogrammetry. For close range theodolite intersection, the camera is replaced by a theodolite and the adjustment is carried out by measuring the horizontal and vertical angles to a number of targeted points (called bundle points), the coordinates of which do not have to be known. Having sighted these, the bundle adjustment software then calculates the position and orientation of each theodolite and, as a useful by-product, the coordinates of the bundle points. The significance of this is that no mutual pointing of theodolite telescopes is necessary thus avoiding the collimation process.

The method is not restricted to two theodolites and most commercial systems, including ECDS3, allow up to eight to be used. Since the technique relies on common bundle points being sighted and does not require mutual theodolite pointings, intervisibility between theodolites is not required and they can be placed close to each other if required. In certain industrial applications where space is restricted, this is advantageous. As well as this, multiple theodolite set-ups enhance the accuracy to which points can be subsequently coordinated because multiple intersections can be observed and adjusted.

A bundle adjustment can be used to set up local as well as object coordinate systems. In a *local coordinate system*, it is usual that none of the bundle points will have known coordinates whereas in an *object coordinate system*, some of the bundle points sighted must have known coordinates. However, it is not necessary that all of the bundle points have known object coordinates provided the minimum number for a successful bundle are known. In fact, any combination of known/unknown points can be used for setting up an object coordinate system.

This section discusses some of the methods used by ECDS3 to adapt the bundle adjustment method to theodolite observations. No attempt is made to cover all possible aspects of a bundle adjustment as this is well beyond the scope of this thesis.

Theodolite coordinate system

A theodolite has two axes about which rotation is possible: the vertical axis around which horizontal angles are measured and the trunnion axis around which vertical (or zenith) angles are measured. These two axes, and the line of sight (or collimation axis) of the theodolite all intersect at the centre of the theodolite and this is the point to which all measurements of angle are referred.

These axes define a cartesian coordinate system called the theodolite coordinate system. This will be a local coordinate system and the origin of this is the centre of the theodolite. The x-axis is defined along the zero mark of the horizontal circle, the y-axis is defined along the 270° mark and the z-axis is

defined to be perpendicular to the x and y axes as shown in figure 4.4.

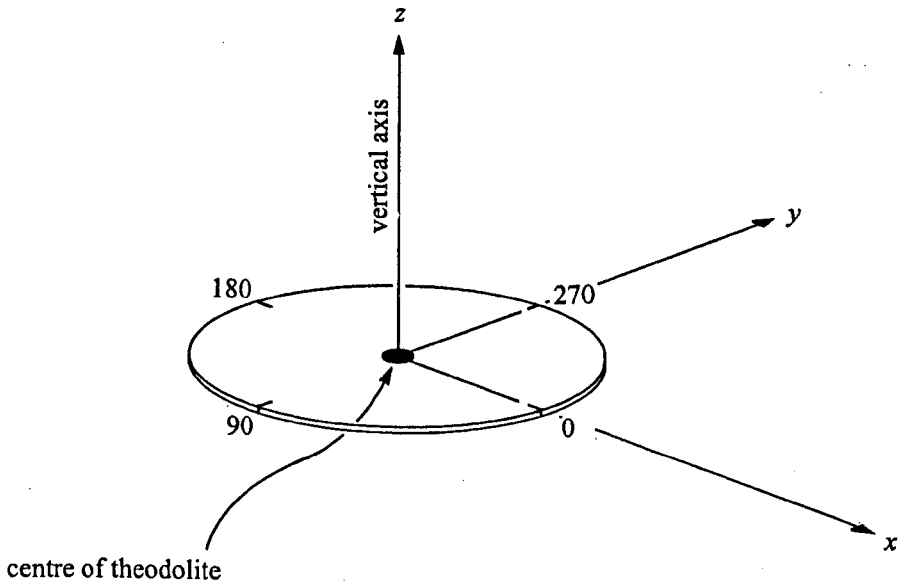

Figure 4.4 *Theodolite coordinate system*

When the theodolite is turned and set at different inclinations, the theodolite coordinate system described does not move. Once the theodolite has been levelled (to set the vertical or z-axis) and the horizontal circle has been zeroed (to set the x-axis) the theodolite coordinate system is fixed relative to any other coordinate system.

Conversion between theodolite and object coordinate systems

For any theodolite intersection system, coordinates are usually required in a different system (usually called the object system) and the orientation of a theodolite coordinate system $x\ y\ z$ relative to an object coordinate system $X\ Y\ Z$ has to be derived. These two coordinate systems are at different scales and, as illustrated in figure 4.5, they are not parallel and their origins do not coincide.

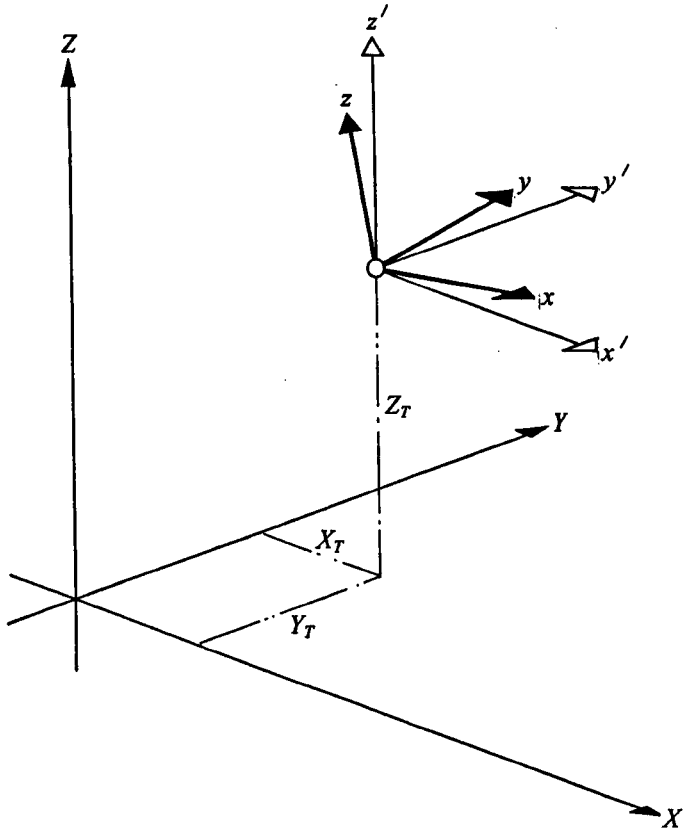

Figure 4.5 *Theodolite and object coordinate systems*

The necessary transformation equations between the two systems can be expressed in terms of seven independent parameters: three rotation angles omega (ω), phi (ϕ) and kappa (κ); a scale factor λ and three translation parameters X_T, Y_T and Z_T. The rotations are the angles through which each axis in the $x\ y\ z$ theodolite system must be rotated in turn to $x'\ y'\ z'$ to make them parallel with the $X\ Y\ Z$ object system. It is conventional that ω is a rotation about the x-axis, ϕ a rotation about the once rotated y-axis and κ a rotation about the twice rotated z-axis of the theodolite coordinate system all of which are required to align it with the object system but taken in the order ω-ϕ-κ. In the development of rotational formulae, it is customary to consider the three rotations taking place so as to convert from the $x'\ y'\ z'$ system to the $x\ y\ z$ system. The rotations are represented mathematically by a rotation matrix **M** in

which the elements are derived as a series of two-dimensional rotations in appropriate planes where

$$\mathbf{M} = \begin{bmatrix} m_{11} & m_{12} & m_{13} \\ m_{21} & m_{22} & m_{23} \\ m_{31} & m_{32} & m_{33} \end{bmatrix} \qquad 4.3$$

The elements of this matrix are derived in many textbooks where the version given by Wolf and Dewitt (2000) is a good example. The elements are

$$m_{11} = \cos\phi\cos\kappa$$

$$m_{12} = \sin\omega\sin\phi\cos\kappa + \cos\omega\sin\kappa$$

$$m_{13} = -\cos\omega\sin\phi\cos\kappa + \sin\omega\sin\kappa$$

$$m_{21} = -\cos\phi\sin\kappa$$

$$m_{22} = -\sin\omega\sin\phi\sin\kappa + \cos\omega\cos\kappa$$

$$m_{23} = \cos\omega\sin\phi\sin\kappa + \sin\omega\cos\kappa$$

$$m_{31} = \sin\phi$$

$$m_{32} = -\sin\omega\cos\phi$$

$$m_{33} = \cos\omega\cos\phi$$

This links the original theodolite coordinate system $x\ y\ z$ with its equivalent rotated parallel to the object system $x'\ y'\ z'$ as

$$\mathbf{x} = \mathbf{M}\ \mathbf{x}' \qquad 4.4$$

where

$$\mathbf{x} = \begin{bmatrix} x \\ y \\ z \end{bmatrix} \quad \text{and} \quad \mathbf{x'} = \begin{bmatrix} x' \\ y' \\ z' \end{bmatrix}$$

The rotation matrix **M** is an orthogonal matrix which has the property that its inverse is equal to its transpose or

$$\mathbf{M}^{-1} = \mathbf{M}^{\mathrm{T}} \tag{4.5}$$

Using this, any vector in the theodolite coordinate system $x\ y\ z$ can be rotated or transformed to be parallel to the object system $x'\ y'\ z'$ by multiplying it by $\mathbf{M}^{\mathrm{T}}$ where

$$\mathbf{x'} = \mathbf{M}^{-1}\mathbf{x} = \mathbf{M}^{\mathrm{T}}\mathbf{x} \tag{4.6}$$

or

$$\begin{bmatrix} x' \\ y' \\ z' \end{bmatrix} = \begin{bmatrix} m_{11} & m_{21} & m_{31} \\ m_{12} & m_{22} & m_{32} \\ m_{13} & m_{23} & m_{33} \end{bmatrix} \begin{bmatrix} x \\ y \\ z \end{bmatrix} \tag{4.7}$$

Accounting for translation also

$$\begin{bmatrix} X \\ Y \\ Z \end{bmatrix} = \begin{bmatrix} m_{11} & m_{21} & m_{31} \\ m_{12} & m_{22} & m_{32} \\ m_{13} & m_{23} & m_{33} \end{bmatrix} \begin{bmatrix} x \\ y \\ z \end{bmatrix} + \begin{bmatrix} X_T \\ Y_T \\ Z_T \end{bmatrix} \tag{4.8}$$

where

$\begin{bmatrix} X \\ Y \\ Z \end{bmatrix}$ = the coordinates of any point in the object coordinate system

$\begin{bmatrix} X_T \\ Y_T \\ Z_T \end{bmatrix}$ = the coordinates of the centre of the theodolite expressed in the object coordinate system

If a scale change λ occurs between the theodolite and object coordinate systems, this can be applied to the theodolite coordinates as

$$\begin{bmatrix} X \\ Y \\ Z \end{bmatrix} = \lambda \begin{bmatrix} m_{11} & m_{21} & m_{31} \\ m_{12} & m_{22} & m_{32} \\ m_{13} & m_{23} & m_{33} \end{bmatrix} \begin{bmatrix} x \\ y \\ z \end{bmatrix} + \begin{bmatrix} X_T \\ Y_T \\ Z_T \end{bmatrix} \qquad 4.9$$

or in full matrix notation

$$\mathbf{X} = \lambda \mathbf{M}^{\mathrm{T}} \mathbf{x} + \mathbf{X}_{\mathrm{T}} \qquad 4.10$$

This set of equations defines a seven-parameter transformation where the parameters are X_T, Y_T, Z_T, ω, ϕ, κ and λ.

For each theodolite in an intersection system, these parameters have to be derived by some means so that the orientation of each theodolite relative to the object or nominated coordinate system is known.

Photo coordinates

As already stated, a photogrammetric approach is used to solve for unknown parameters in a theodolite orientation procedure. The usual method for doing this is to generate fictitious (or pseudo) photo coordinates for each observation taken by a theodolite to a bundle point. The reason for creating photo coordinates and adopting the photogrammetric solution is that it allows photogrammetric bundle adjustment procedures to input theodolite observations and then solve for all of the unknown theodolite orientation parameters as if they were camera orientations. This procedure is really a matter of convenience as it applies existing, but well-established techniques to a new problem. What is required, however, is a special computer program to convert measured horizontal and vertical angles into their equivalent photo coordinates.

The derivation of photo coordinates from theodolite observations and how these are related to orientation parameters is considered below.

As shown in figure 4.6, observed horizontal and vertical angles are referenced in a right-handed theodolite coordinate system as h = the observed horizontal angle which is zero at the x-axis and increases in a clockwise direction and v = the observed vertical angle in a plane perpendicular to the vertical axis and which increases towards the zenith.

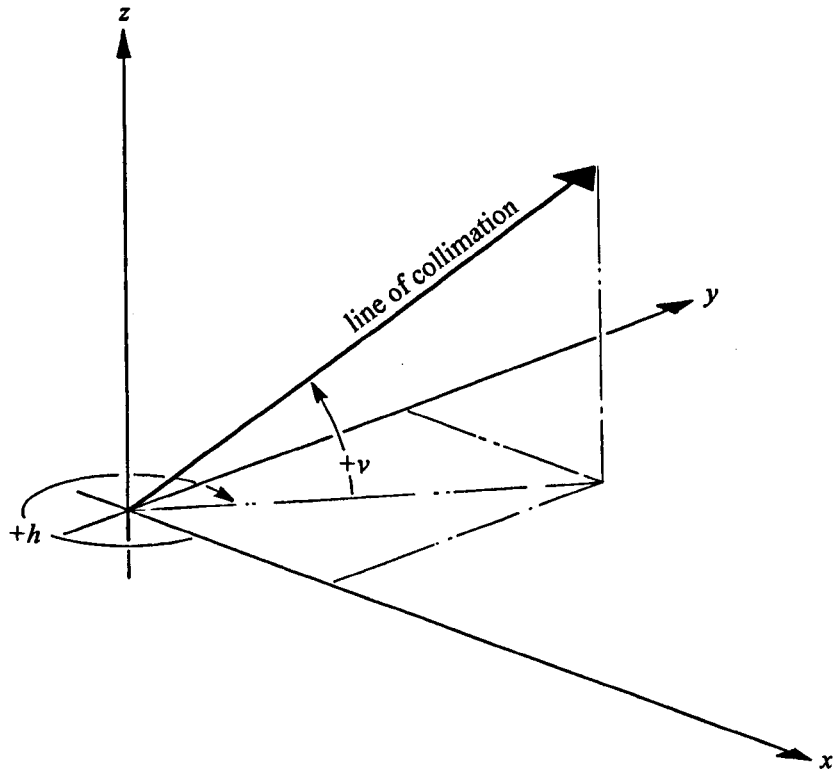

Figure 4.6 *Observed angles in theodolite coordinate system*

Figure 4.7 shows a virtual photo plane at principal distance f along the y-axis defining, in this case, photo coordinates x and z. For the pointing shown, these are related to the observed horizontal and vertical angles by (Obidowski & Chapman, 1993 and Zhang, *et al.*, 1997)

$$x = f\tan(h-270) \qquad 4.11$$

$$z = f\frac{\tan v}{\cos(h-270))} \qquad 4.12$$

In these equations, f is an arbitrary adopted focal length of the fictitious camera and it is convenient to select f = 206.265 mm so that 1 μm on the photo corresponds to 1 second of arc in angle (Zou, *et al.*, 2001).

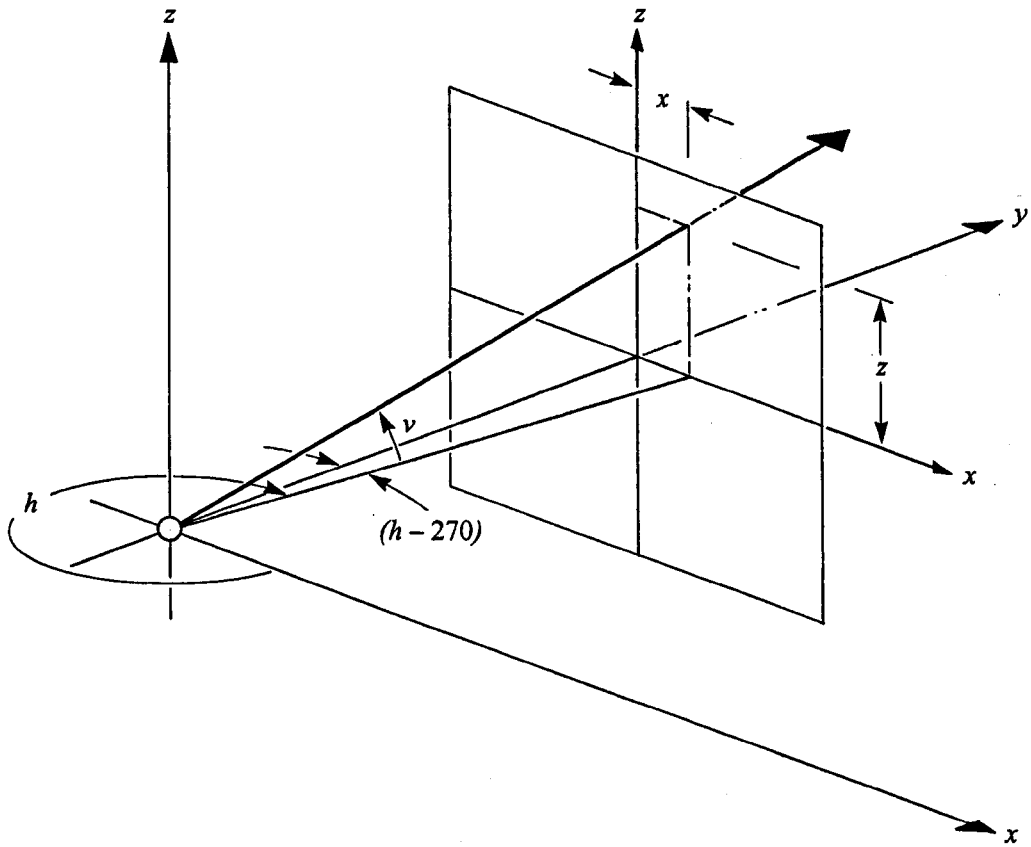

Figure 4.7 *Photo coordinates*

For a single baseline two theodolite set up, similar expressions can be developed for the second theodolite when it measures horizontal and vertical angles to the same bundle point.

Since x and z are derived quantities, they should be accompanied in a bundle adjustment by a covariance matrix that accounts for the propagation of errors from the observed angles to the derived photo coordinates. If errors in h and v are uncorrelated and have covariances σ_h^2 and σ_v^2, the covariance matrix Σ of the photo coordinates x and z derived from h and v will be given by (Brown, 1985)

$$\Sigma = \begin{bmatrix} \sigma_x^2 & \sigma_{xz} \\ \sigma_{xz} & \sigma_z^2 \end{bmatrix} = \mathbf{J}\,\Sigma_0\,\mathbf{J}^T \qquad 4.13$$

where

$$\mathbf{J} = \begin{bmatrix} \frac{\partial x}{\partial h} & \frac{\partial x}{\partial v} \\ \frac{\partial z}{\partial h} & \frac{\partial z}{\partial v} \end{bmatrix} \quad \text{and} \quad \Sigma_0 = \begin{bmatrix} \sigma_h^2 & 0 \\ 0 & \sigma_v^2 \end{bmatrix}$$

Collinearity equations

In figure 4.8, **v** is a vector along the line of sight from theodolite *T* to a bundle point *P* defining fictitious photo coordinates and

$$\mathbf{v} = \begin{bmatrix} x' \\ f' \\ z' \end{bmatrix} = \mathbf{M}^T \begin{bmatrix} x \\ f \\ z \end{bmatrix} \qquad 4.14$$

where **M** is the rotational matrix and x', f' and z' are the fictitious photo coordinates rotated so that they are parallel to the object coordinate system.

The vector **V** in figure 4.8 is the full length vector along the line of sight from theodolite *T* to bundle point *P*. **V** can be expressed in terms of the object coordinates of point *P* ($X\ Y\ Z$) and the object coordinates of the theodolite *T* ($X_T\ Y_T\ Z_T$) as

$$\mathbf{V} = \begin{bmatrix} X - X_T \\ Y - Y_T \\ Z - Z_T \end{bmatrix} \qquad 4.15$$

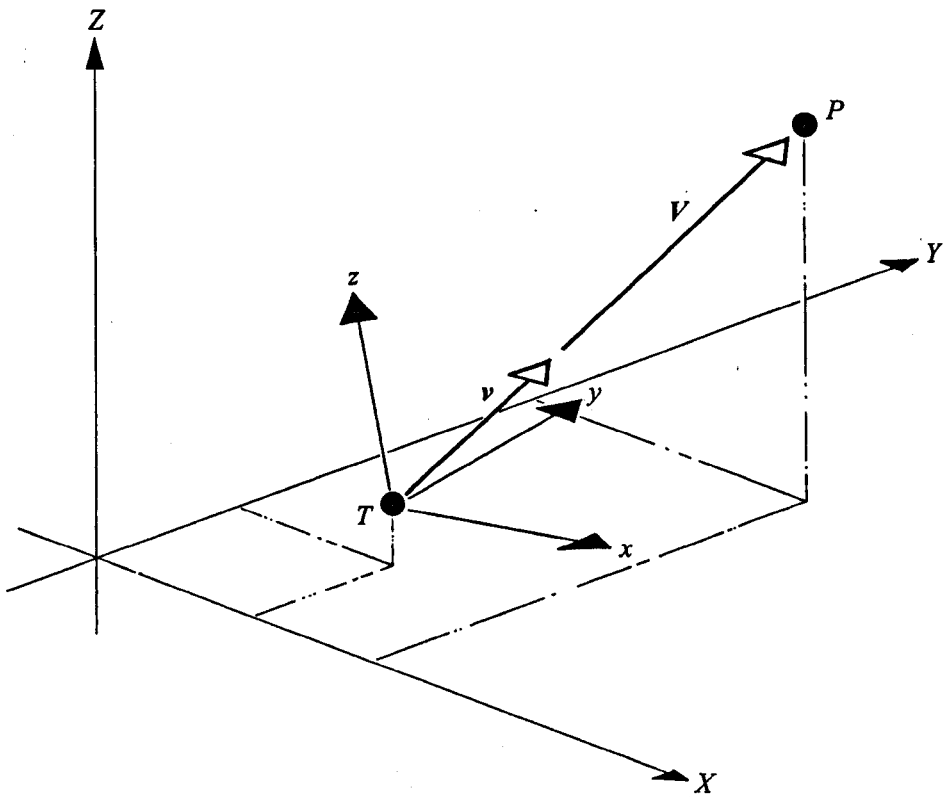

Figure 4.8 *Collinearity of two vectors*

Since vectors **v** and **V** are pointing in the same direction, the relationship between them is given by the collinearity equation

$$\mathbf{V} = \lambda\, \mathbf{v} \qquad 4.16$$

where the components of both vectors are described in terms of an object system and λ is a scale factor.

This gives

$$\begin{bmatrix} X-X_T \\ Y-Y_T \\ Z-Z_T \end{bmatrix} = \lambda \mathbf{M}^{\mathrm{T}} \begin{bmatrix} x \\ f \\ z \end{bmatrix} \qquad 4.17$$

and

$$\begin{bmatrix} x \\ f \\ z \end{bmatrix} = \frac{1}{\lambda}\mathbf{M}\begin{bmatrix} X-X_T \\ Y-Y_T \\ Z-Z_T \end{bmatrix} = \frac{1}{\lambda}\begin{bmatrix} m_{11} & m_{12} & m_{13} \\ m_{21} & m_{22} & m_{23} \\ m_{31} & m_{32} & m_{33} \end{bmatrix}\begin{bmatrix} X-X_T \\ Y-Y_T \\ Z-Z_T \end{bmatrix} \qquad 4.18$$

or

$$x = \frac{1}{\lambda}\left[m_{11}(X-X_T)+m_{12}(Y-Y_T)+m_{13}(Z-Z_T)\right] \qquad 4.19a$$

$$f = \frac{1}{\lambda}\left[m_{21}(X-X_T)+m_{22}(Y-Y_T)+m_{23}(Z-Z_T)\right] \qquad 4.19b$$

$$z = \frac{1}{\lambda}\left[m_{31}(X-X_T)+m_{32}(Y-Y_T)+m_{33}(Z-Z_T)\right] \qquad 4.19c$$

Dividing equations 4.19a and 4.19c by 4.19b gives

$$x = f\,\frac{m_{11}(X-X_T)+m_{12}(Y-Y_T)+m_{13}(Z-Z_T)}{m_{21}(X-X_T)+m_{22}(Y-Y_T)+m_{23}(Z-Z_T)} \qquad 4.20a$$

$$z = f\,\frac{m_{31}(X-X_T)+m_{32}(Y-Y_T)+m_{33}(Z-Z_T)}{m_{21}(X-X_T)+m_{22}(Y-Y_T)+m_{23}(Z-Z_T)} \qquad 4.20b$$

Equations 4.20 are a version of the well-known photogrammetric collinearity equations which in this case link observed horizontal and vertical angles through equations 4.11 and 4.12 to the coordinates of a bundle point and a

series of unknowns defining the orientation of the theodolite. It is the unknowns defining the orientation of the theodolite that need to be determined by a bundle adjustment.

In deriving the collinearity equations, x and z photo coordinates have been used. In practice, an observation could lie in a number of different photo planes and in the case of ECDS3, each observation is assigned to a photo plane according to the magnitudes of the horizontal and vertical angles. This gives rise to a different set of collinearity equations for each observation for the software to process. The way in which ECDS3 derives these has not been made available to the author.

In a two theodolite set-up, 12 unknowns are involved in defining the orientation of the theodolites and these are

For theodolite A: ω_A, ϕ_A, κ_A, X_{TA}, Y_{TA}, Z_{TA}

For theodolite B: ω_B, ϕ_B, κ_B, X_{TB}, Y_{TB}, Z_{TB}

Each bundle point sighted by the two theodolites produces four collinearity equations: two from each theodolite (equations 4.20a and 4.20b) but introduces three additional unknowns – the coordinates of the bundle point itself. Therefore, each point sighted in a bundle adjustment adds one more equation than the number of unknowns it introduces.

In a local coordinate system, theodolite A is taken to be the datum for the coordinate system and ω_A, ϕ_A, κ_A, X_{TA}, Y_{TA}, Z_{TA} are all equal to zero which

removes six of the unknown orientation parameters. All that is needed is to sight six points to determine the parameters. However, it is usual that a scale bar is sighted as part of the bundle adjustment procedure and these are counted as two bundle points but provide a scale constraint equal to the known length of the scale bar. This reduces the minimum number of points to be sighted to orientate two theodolites in a local coordinate system to five. This number can vary for an object system depending on the number of control points available.

In practice, more points than the minimum are observed to create redundancy to improve the solution for the unknown orientation parameters and to provide a better chance for detecting observational errors in the bundle point observations.

Solution of the collinearity equations

The methods used to solve a series of collinearity equations are described in full by Wong (1980) and by Mikhail, *et al.,* (2001) and a detailed analysis of the solution is not considered here. Instead, what follows is a general description of the solution but with emphasis on some of the techniques used by ECDS3.

A bundle adjustment is formed and solved in the following way in the ECDS3 system (see section 5.6 also).

- Each observed horizontal and vertical angle taken to a bundle point is used to derive fictitious photo coordinates as the 'observations' or

image coordinates that form a pair of collinearity equations. This is performed by the ECDS3 *Pre-Process* program which also computes the covariance matrices for the photo coordinates.

- The collinearity equations are linearized and observation equations are formed from these. This requires initial estimates for ω, ϕ, κ, X_T, Y_T, Z_T, X, Y and Z to be obtained for each theodolite and bundle point. Values for deriving these estimates are determined in the ECDS3 *Angle Capture* program.

- A unified least squares adjustment technique is used and the normal equations are formed with all unknowns (theodolite parameters and bundle point coordinates) being treated as observations with *a priori* variances. The *a priori* covariance matrices for the fictitious photo coordinates are also used in the formation of the normal equations.

- The normal equations are solved by least squares to produce a set of corrections to the initial estimates for the theodolite orientation parameters and bundle point coordinates. The new estimates for the theodolite orientation parameters and bundle point coordinates give rise to new normal equations which are solved to produce another set of corrections. The process of correction/solution is repeated until the estimates and new values are within a specified tolerance, at which point the solution has assumed to converge. The final values for the theodolite orientation parameters and bundle point coordinates are now known. This is performed by the ECDS3 *Bundle Adjustment* program.

Initial estimates for ω, ϕ, κ, X_T, Y_T, Z_T, X, Y and Z in a local coordinate system are obtained from measurements in the *Angle Capture* program by ECDS3 as follows.

First, theodolite A (the theodolite assumed to be at the origin of the local coordinate system) is pointed along the positive x-axis of the local coordinate system. This can be a completely arbitrary setting and the x-axis direction could be chosen, for example, such that all y-coordinates will be positive or that the x-axis is parallel to some feature to be measured.

However, if only two theodolites are used, it is usual to take the x-axis as the direction from theodolite A to theodolite B. So, in this case, the telescope of theodolite A is pointed towards theodolite B. It is not necessary to do this exactly or to some precise point on theodolite B, it is sufficient to point in the general direction of the instrument only. Again, in a two theodolite set-up, the telescope of theodolite B is also pointed in the general direction of the x-axis along the baseline between theodolites A and B extended.

In a multiple set-up, all the other theodolites will have their telescopes aligned approximately parallel with that of the theodolite designated to be at the origin of the local coordinate system (the reference theodolite).

As soon as this is done the system software sets, at each theodolite, the horizontal circles to zero. This establishes the approximate direction of each x-axis at each theodolite to be set at zero gon and each y-axis at 300 gon. Since

the theodolites are levelled, the z-axes will also be nearly parallel.

ECDS3 now assumes that ω, ϕ and κ are zero at each theodolite. It must be remembered however, that these are treated as observations in the least squares adjustment and, except for the theodolite at the origin (the reference theodolite), these change from zero as the bundle adjustment passes through its various iterations.

The next step in the orientation process is to estimate the position of each theodolite used relative to the reference theodolite. This is achieved by pointing each theodolite in turn at the reference theodolite and by estimating the distance between them. Again, this need not be done exactly and the pointing can be in the general direction of the reference theodolite and the distance can be guessed (by pacing for example). However, the better the estimate of the distance, the sooner the bundle adjustment will converge. With modern fast computers, though, this is not important. This procedure provides estimates for X_T, Y_T and Z_T, the translation coordinates of each theodolite relative to the reference theodolite.

The final step in the bundle adjustment procedure is to sight all the bundle points required. The angles observed here, together with the approximate orientation data already gathered enable approximate coordinates X, Y and Z to be computed for each bundle point.

4.4 Spatial intersection

Following orientation, horizontal and vertical angles are measured from the known theodolite positions to targeted points whose coordinates are required.

The fundamental problem with the computation of an observed intersection is that the exact orientation of the theodolites is not known and this, combined with pointing/observation errors, creates a situation where the two vectors (one from each theodolite) usually do not intersect. Questions arising from this are what is the best geometric estimate of the point of intersection and what is the quality of the results obtained?

Early versions of theodolite intersection systems computed an intersection by combining the calculation of a conventional intersection in the horizontal plane with separate calculations of height in what is known as a two-dimensional plus one dimensional model ($2D + 1D$ model).

2D + 1D intersection model

Figure 4.9 shows the intersection of a point P by two theodolites A and B. The calculation of the horizontal coordinates of P (x_P, y_P) proceeds as follows.

With D as the horizontal baseline length between the two theodolites we have

$$\frac{D_{AP}}{\sin\theta_B} = \frac{D_{BP}}{\sin\theta_A} = \frac{D}{\sin\{180-(\theta_A+\theta_B)\}} = \frac{D}{\sin(\theta_A+\theta_B)} \qquad 4.21$$

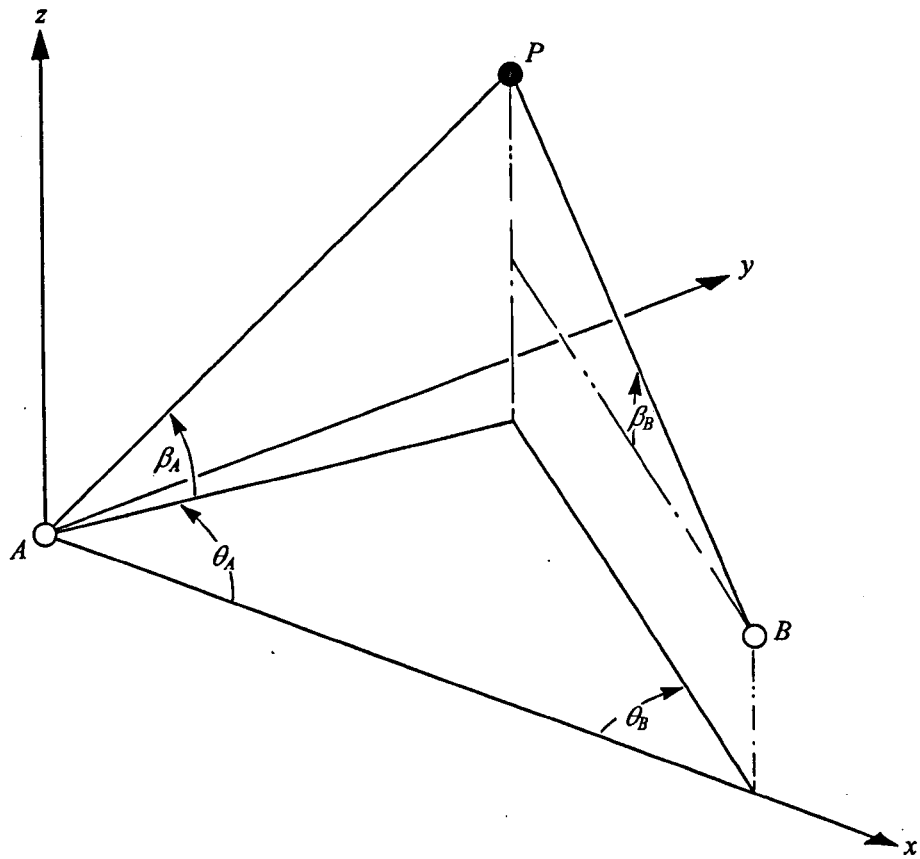

Figure 4.9 *Theodolite intersection*

where

D_{AP} = horizontal distance from theodolite A to target point P

D_{BP} = horizontal distance from theodolite B to target point P

θ_A = horizontal angle observed at theodolite A to target point P

θ_B = horizontal angle observed at theodolite B to target point P

This gives

$$D_{AP} = D\frac{\sin\theta_B}{\sin(\theta_A + \theta_B)} \qquad 4.22$$

The x-coordinate of P is

$$x_P = D_{AP}\cos\theta_A = D\frac{\sin\theta_B\cos\theta_A}{\sin(\theta_A+\theta_B)} \qquad 4.23$$

The y-coordinate of P is

$$y_P = D_{AP}\sin\theta_A = D\frac{\sin\theta_B\sin\theta_A}{\sin(\theta_A+\theta_B)} \qquad 4.24$$

The z-coordinate of P is

$$z_P = \frac{z_A + z_B}{2} \qquad 4.25$$

where

z_A = the z-coordinate of P calculated from theodolite A

z_B = the z-coordinate of P calculated from theodolite B

The z-coordinate calculated from theodolite A is

$$z_A = (x_P^2 + y_P^2)^{1/2}\tan\beta_A \qquad 4.26$$

where

β_A = vertical angle observed from theodolite A to target point P

The z-coordinate calculated from theodolite B is

$$z_B = \{(D - x_P)^2 + y_P^2\}^{1/2} \tan \beta_B + (h_B - h_A) \qquad 4.27$$

where

β_B = vertical angle observed from theodolite B to target point P

h_A = the height of the centre of theodolite A

h_B = the height of the centre of theodolite B

In the case where $(h_B - h_A)$ is not known, this can be found by calculating z_A, setting $z_A = z_B$ and solving equation 4.27 for $(h_B - h_A)$. This procedure can be repeated at a number of target positions to improve the value of $(h_B - h_A)$.

For each pair of horizontal and vertical angles taken from any instrument, it is possible to compute two vertical coordinates z_A and z_B. If the system set-up was perfect and there were no observational errors present, the two z-coordinates would be equal. As this can only happen by chance, the difference between these can be used as a guide to the reliability of the observations (to detect gross errors) and the accuracy of the observations (when the two values are within a specified tolerance). Once they are accepted, it is usual to take the mean value of the two z-coordinates as the final value.

This method of computing an intersection, although widely used in surveying and initially by theodolite intersection systems has the disadvantages, especially for the high precisions required in metrology and industrial engineering, that it is based on a $2D + 1D$ mathematical model and it does not enable the true accuracy of an intersection to be determined.

Various approaches to computing spatial intersections have been published and that proposed by Cooper (1986) was one of the first to deal with spatial intersection in terms of vectors in a three-dimensional model.

Figure 4.10 is similar to figure 4.9 and shows the intersection of point P from two collimated theodolites A and B where the horizontal angle θ_A and vertical

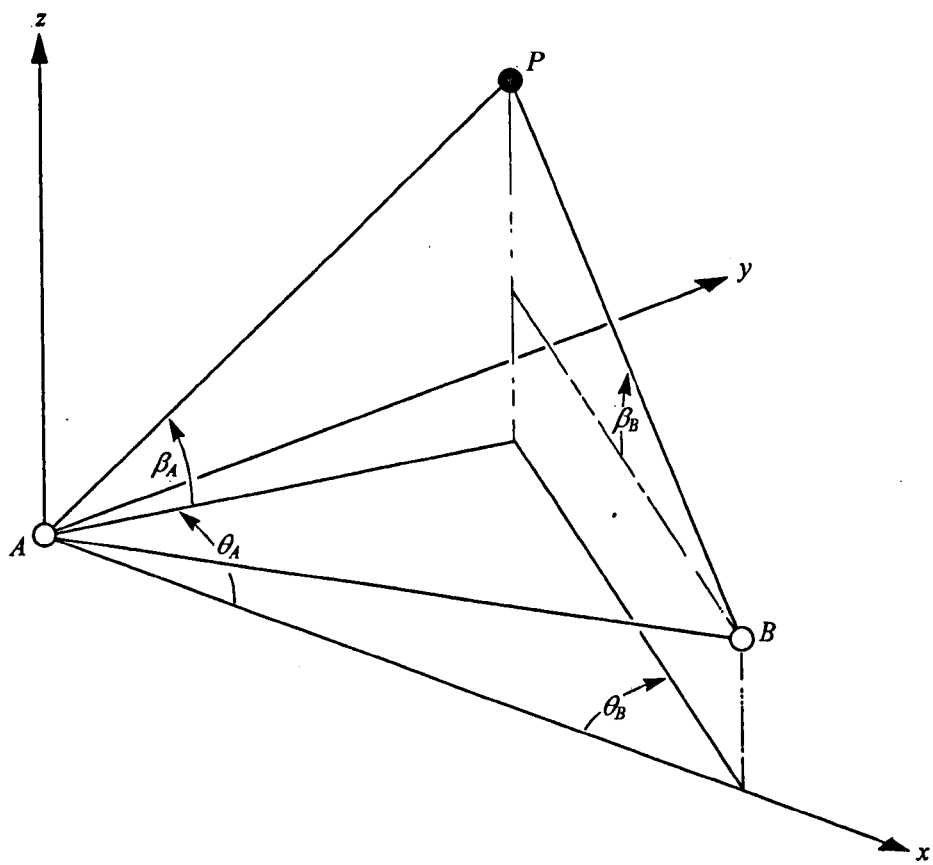

Figure 4.10 *Intersection in a local coordinate system*

angle β_A are observed at A and the horizontal angle θ_B and vertical angle β_B are observed at B.

As shown, these angles are referenced to a local coordinate system which has

its origin at A, the x-axis along the line in the vertical plane from A to B, the z-axis vertically upwards and the y-axis orthogonal to these. In the local coordinate system so established, the coordinates of A are (0, 0, 0) and those of B are $(x_B, 0, z_B)$ where x_B is the horizontal distance from A to B and z_B is the height difference between A and B.

In figure 4.11, the direction of the line of sight from A to P is represented by a unit vector **p** and that from B to P by a unit vector **q**. The length of the baseline and its direction is represented by vector **b**. The components of these vectors are

$$\mathbf{b} = \begin{bmatrix} b_x \\ b_y \\ b_z \end{bmatrix} = \begin{bmatrix} x_B \\ 0 \\ z_B \end{bmatrix} \qquad 4.28$$

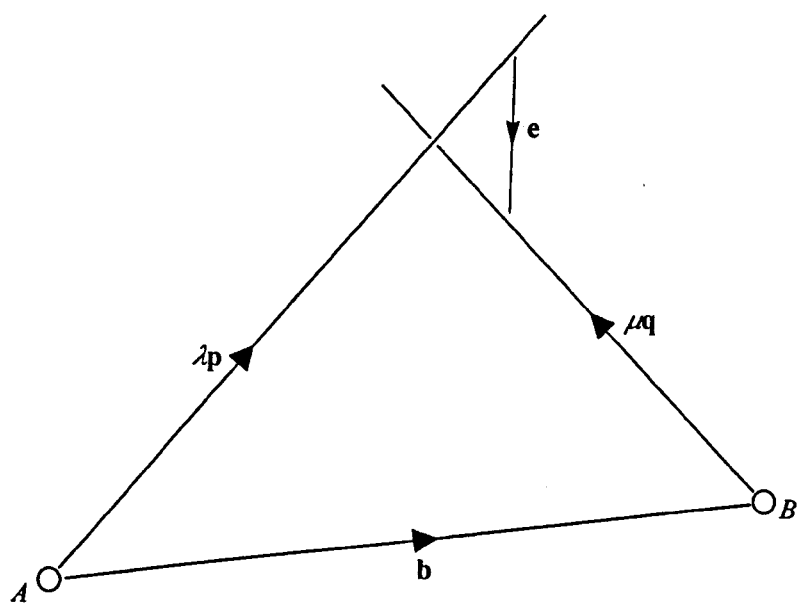

Figure 4.11 *Vector representation of spatial intersection*

$$\mathbf{p} = \begin{bmatrix} p_x \\ p_y \\ p_z \end{bmatrix} = \begin{bmatrix} \cos\theta_A \cos\beta_A \\ \sin\theta_A \cos\beta_A \\ \sin\beta_A \end{bmatrix} \qquad 4.29$$

$$\mathbf{q} = \begin{bmatrix} q_x \\ q_y \\ q_z \end{bmatrix} = \begin{bmatrix} -\cos\theta_B \cos\beta_B \\ \sin\theta_B \cos\beta_B \\ \sin\beta_B \end{bmatrix} \qquad 4.30$$

In practice, it is usual to expect that the vectors observed from A and B will not intersect and this is written in vector notation as (again with reference to figure 4.11 following an anticlockwise direction)

$$\mathbf{e} = -\lambda\mathbf{p} + \mathbf{b} + \mu\mathbf{q} \qquad 4.31$$

where

$\mathbf{e}$ = an error or residual vector from a point on $\lambda\mathbf{p}$ to a point on $\mu\mathbf{q}$

$$= \begin{bmatrix} e_x \\ e_y \\ e_z \end{bmatrix}$$

$\lambda\mathbf{p}$ = the vector observed from A to P

$\mu\mathbf{q}$ = the vector observed from B to P

λ and μ are scalars

As λ and μ change, the length and direction of $\mathbf{e}$ will also change.

Combining equations 4.28 to 4.31 with $\mathbf{e}$ gives

$$\begin{bmatrix} e_x \\ e_y \\ e_z \end{bmatrix} = -\lambda \begin{bmatrix} p_x \\ p_y \\ p_z \end{bmatrix} + \begin{bmatrix} b_x \\ b_y \\ b_z \end{bmatrix} + \mu \begin{bmatrix} q_x \\ q_y \\ q_z \end{bmatrix} \qquad 4.32$$

or

$$\begin{aligned} e_x &= -\lambda p_x + b_x + \mu q_x \\ e_y &= -\lambda p_y + b_y + \mu q_y \\ e_z &= -\lambda p_z + b_z + \mu q_z \end{aligned} \qquad 4.33$$

The length of **e** is given by

$$e = (e_x^2 + e_y^2 + e_z^2)^{1/2} \qquad 4.34$$

and if this is to be a minimum

$$\frac{\partial}{\partial \lambda}(e_x^2 + e_y^2 + e_z^2) = 0 \qquad \text{and} \qquad \frac{\partial}{\partial \mu}(e_x^2 + e_y^2 + e_z^2) = 0$$

Substituting the values for e_x, e_y and e_z from 4.33 and differentiating gives the following linear simultaneous equations for λ and μ

$$\begin{bmatrix} p_x^2 + p_y^2 + p_z^2 & -(p_x q_x + p_y q_y + p_z q_z) \\ -(p_x q_x + p_y q_y + p_z q_z) & q_x^2 + q_y^2 + q_z^2 \end{bmatrix} \begin{bmatrix} \lambda \\ \mu \end{bmatrix}$$

$$= \begin{bmatrix} b_x p_x + b_y p_y + b_z p_z \\ -(b_x q_x + b_y q_y + b_z q_z) \end{bmatrix} \qquad 4.35$$

In terms of scalar (dot) products

$$p_x^2 + p_y^2 + p_z^2 = \mathbf{p}.\mathbf{p} = 1 \qquad 4.36a$$

$$q_x^2 + q_y^2 + q_z^2 = \mathbf{q}.\mathbf{q} = 1 \qquad 4.36b$$

since **p** and **q** are unit vectors

$$\begin{aligned} (p_x q_x + p_y q_y + p_z q_z) &= \mathbf{p}.\mathbf{q} \\ (b_x p_x + b_y q_y + b_z q_z) &= \mathbf{b}.\mathbf{p} \\ (b_x q_x + b_y q_y + b_z q_z) &= \mathbf{b}.\mathbf{q} \end{aligned} \qquad 4.37$$

and equations 4.35 become

$$\begin{bmatrix} 1 & -\mathbf{p}.\mathbf{q} \\ -\mathbf{p}.\mathbf{q} & 1 \end{bmatrix} \begin{bmatrix} \lambda \\ \mu \end{bmatrix} = \begin{bmatrix} \mathbf{b}.\mathbf{p} \\ -\mathbf{b}.\mathbf{q} \end{bmatrix} \qquad 4.38$$

and

$$\begin{bmatrix} \lambda \\ \mu \end{bmatrix} = \begin{bmatrix} 1 & -\mathbf{p}.\mathbf{q} \\ -\mathbf{p}.\mathbf{q} & 1 \end{bmatrix}^{-1} \begin{bmatrix} \mathbf{b}.\mathbf{p} \\ -\mathbf{b}.\mathbf{q} \end{bmatrix} \qquad 4.39$$

The inverse is given by

$$\begin{bmatrix} 1 & -\mathbf{p.q} \\ -\mathbf{p.q} & 1 \end{bmatrix}^{-1} = \frac{1}{\Delta}\begin{bmatrix} 1 & \mathbf{p.q} \\ \mathbf{p.q} & 1 \end{bmatrix} \qquad 4.40$$

where Δ is the determinant given by

$$\Delta = 1 - (\mathbf{p.q})^2 \qquad 4.41$$

These equations cannot be solved if

- $\mathbf{b.p} = \mathbf{b.q} = 0$ which would mean that **p** and **q** are perpendicular to **b**
- $\Delta = 0$ which will only occur if $\mathbf{p.q} = 1$ which would mean that p and q are parallel

In practice, it is very unlikely that these conditions would arise and the values of λ_0 and μ_0 for a minimum value of *e* are obtained from

$$\begin{bmatrix} \lambda_0 \\ \mu_0 \end{bmatrix} = \frac{1}{\Delta}\begin{bmatrix} 1 & \mathbf{p.q} \\ \mathbf{p.q} & 1 \end{bmatrix}\begin{bmatrix} \mathbf{b.p} \\ -\mathbf{b.q} \end{bmatrix} \qquad 4.42$$

These values are then used to define the position of *P* at the mid-point of **e** where *P* has a position vector **r** from *A* of

$$\mathbf{r} = \lambda_0\mathbf{p} + \frac{\mathbf{e}}{2} = \lambda_0\mathbf{p} + \frac{1}{2}(-\lambda_0\mathbf{p} + \mathbf{b} + \mu_0\mathbf{q}) = \frac{1}{2}(\lambda_0\mathbf{p} + \mathbf{b} + \mu_0\mathbf{q}) \qquad 4.43$$

When solving a spatial intersection in this way, **b**, **p** and **q** are first computed from equations 4.29 to 4.30 , λ_0 and μ_0 are then computed from equations 4.42 and these are then used to compute **r** and the position of P. The values of **b**, **p** and **q** can also be substituted into equation 4.31 to determine the components e_x, e_y and e_z of the error vector **e**. These values will give an indication of the accuracy of the position of point P in three dimensions.

Although this procedure gives what might be considered a better answer for the position of P and its error components, like the traditional approach it has been compared to it is still not, in a true mathematical sense, a rigorous method for solving intersections. However, it does attempt to solve the problem of spatial intersection in three dimensions simultaneously using vectors to represent the observed horizontal and vertical angles. Cooper does state that it is a least squares method in the sense that $(e_x^2 + e_y^2 + e_z^2)$ is minimised. Although never widely adopted, this method for solving spatial intersections bridges the gap between the $(2D + 1D)$ and $3D$ models.

Formal 3D model

Following the $(2D + 1D)$ and semi-rigorous version of a $3D$ model so far developed, one of the rigorous methods used in a number of theodolite intersection systems for the computation of a spatial intersection is given in this section. There are several ways in which a $3D$ intersection model can be presented and no claim is made here that this is the definitive version. For simplicity, an intersection with only one baseline and two theodolites is

considered.

Figure 4.12 is a variation of figures 4.9 and 4.10 and shows P as the intersected point with A and B representing the centres of the theodolites that have known positions in a local xyz coordinate system of

$$\mathbf{A} = \begin{bmatrix} x_A \\ y_A \\ z_A \end{bmatrix} \qquad \mathbf{B} = \begin{bmatrix} x_B \\ y_B \\ z_B \end{bmatrix} \tag{4.44}$$

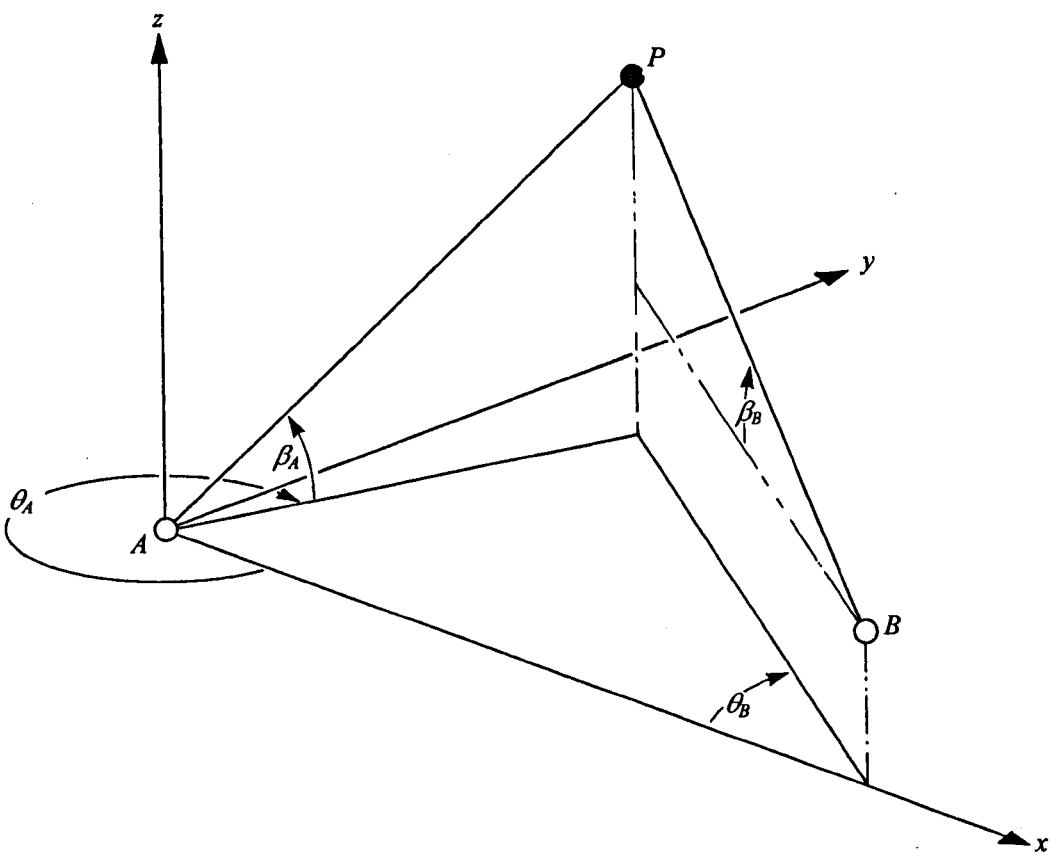

Figure 4.12 *Spatial intersection in the xyz system*

The observed horizontal angles are θ_A and θ_B but these are now considered positive in a clockwise direction and are measured together with the vertical angles β_A and β_B. All of these observations are recorded assuming that both

theodolites are collimated and orientated in the *xyz* coordinate system. The observed angles can be used to define direction cosines for the unit vectors from each theodolite to point *P* as

From *A*	From *B*	
$l_1 = \cos(360 - \theta_A)\cos\beta_A$	$l_2 = -\cos\theta_B \cos\beta_B$	
$m_1 = \sin(360 - \theta_A)\cos\beta_A$	$m_2 = \sin\theta_B \cos\beta_B$	4.45
$n_1 = \sin\beta_A$	$n_2 = \sin\beta_B$	

These can be used to compute the coordinates of the target point *P* using

$x_P = x_A + l_1 s_A$	$x_P = x_B + l_2 s_B$	
$y_P = y_A + m_1 s_A$	$y_P = y_B + m_2 s_B$	4.46
$z_P = z_A + n_1 s_A$	$z_P = z_B + n_2 s_B$	

where

s_A = the slope distance from *A* to point *P* (unknown)

s_B = the slope distance from *B* to point *P* (unknown)

To use equations 4.46, the values of s_A and s_B must be determined. If the lines (or vectors) from *A* and *B* intersect, the coordinates for *P* will be unique and

$$x_A + l_1 s_A = x_B + l_2 s_B \qquad 4.47$$

or

$$(x_B - x_A) = l_1 s_A - l_2 s_B \qquad 4.48$$

which gives

$$s_A = \frac{(x_B - x_A) + l_2 s_B}{l_1} \qquad 4.49$$

Substituting the expression for s_A into equation 4.46 for y_P gives

$$y_A + m_1\left[\frac{(x_B - x_A) + l_2 s_B}{l_1}\right] = y_B + m_2 s_B \qquad 4.50$$

or

$$(y_A - y_B) + m_1\left[\frac{(x_B - x_A) + l_2 s_B}{l_1}\right] = m_2 s_B \qquad 4.51$$

Multiplying each term by l_1 gives

$$(y_A - y_B) l_1 + m_1[(x_B - x_A) + l_2 s_B] = m_2 s_B l_1 \qquad 4.52$$

and

$$(y_A - y_B) l_1 + (x_B - x_A) m_1 = s_B[m_2 l_1 - m_1 l_2] \qquad 4.53$$

This gives s_B as

$$s_B = \frac{(y_A - y_B)l_1 + (x_B - x_A)m_1}{(m_2 l_1 - m_1 l_2)} \qquad 4.54$$

Similarly

$$s_A = \frac{(y_A - y_B)l_2 + (x_B - x_A)m_2}{(m_2 l_1 - m_1 l_2)} \qquad 4.55$$

The direction cosines can be computed from the observed angles using equations 4.45 and values for s_A and s_B can be computed from these and the known coordinates for A and B using equations 4.54 and 4.55. These in turn can be substituted into equations 4.46 to obtain the coordinates of point P.

As it is expected that the two vectors will not intersect, the coordinates of P have to be determined by a different method. Allan (1988) suggests the following which is based on a two theodolite system.

In figure 4.13, observations are taken from theodolites located at A and B in order to fix the coordinates of the target point P where the vector AP_1 is observed from A and the vector BP_2 is observed from B. The vector P_1P_2 is the common normal to the vectors observed from A and B and

- point P_1 is at the foot of the perpendicular on the vector observed from A to the target point P
- point P_2 is at the foot of the perpendicular on the vector observed from B to the target point P

- the target point P is assumed to be the mid-point of P_1P_2

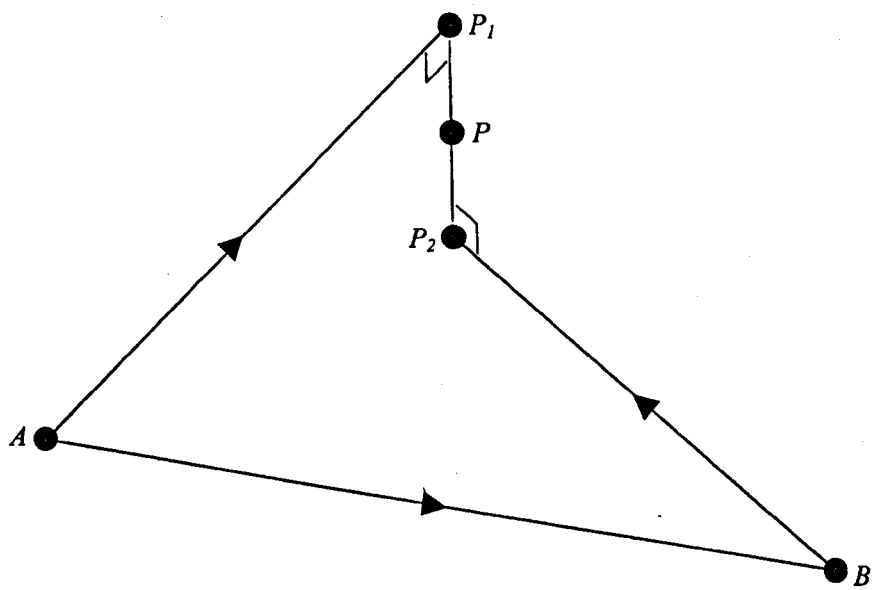

Figure 4.13 *Vector spatial intersection*

The direction cosines defining the vectors observed along AP_1 and BP_2 are

For AP_1	For BP_2	
$l_1 = \cos(360 - \theta_A)\cos\beta_A$	$l_2 = -\cos\theta_B \cos\beta_B$	
$m_1 = \sin(360 - \theta_A)\cos\beta_A$	$m_2 = \sin\theta_B \cos\beta_B$	4.56
$n_1 = \sin\beta_A$	$n_2 = \sin\beta_B$	

The lengths of these vectors are

$AP_1 = s_A$	$BP_2 = s_B$	4.57

and it is these distances that are to be found to define the coordinates of point P.

The positions of P_1 and P_2 are given by

$$\begin{aligned} x_{P1} &= x_A + s_A l_1 & x_{P2} &= x_A + s_B l_2 \\ y_{P1} &= y_A + s_A m_1 & y_{P2} &= y_B + s_B m_2 \\ z_{P1} &= z_A + s_A n_1 & z_{P2} &= z_B + s_B n_2 \end{aligned} \qquad 4.58$$

or

$$\mathbf{P}_1 = \mathbf{A} + s_A [l_1 \quad m_1 \quad n_1]^t \qquad \mathbf{P}_2 = \mathbf{B} + s_B [l_2 \quad m_2 \quad n_2]^t \qquad 4.59$$

where

$$\mathbf{P}_1 = \begin{bmatrix} x_{P1} \\ y_{P1} \\ z_{P1} \end{bmatrix} \quad \mathbf{A} = \begin{bmatrix} x_A \\ y_A \\ z_A \end{bmatrix} \quad \mathbf{P}_2 = \begin{bmatrix} x_{P2} \\ y_{P2} \\ z_{P2} \end{bmatrix} \quad \mathbf{B} = \begin{bmatrix} x_B \\ y_B \\ z_B \end{bmatrix} \qquad 4.60$$

Denoting

$$\mathbf{a} = [l_1 \quad m_1 \quad n_1]^t \qquad \mathbf{b} = [l_2 \quad m_2 \quad n_2]^t \qquad 4.61$$

equations 4.59 give

$$\mathbf{P}_2 - \mathbf{P}_1 = [\mathbf{B} + s_B \mathbf{b}] - [\mathbf{A} + s_A \mathbf{a}] \qquad 4.62$$

$$= \mathbf{A} - \mathbf{B} + s_B \mathbf{b} - s_A \mathbf{a} \qquad 4.63$$

The vector (dot) product of direction cosines **a** with all the terms in equation

4.63 gives

$$(\mathbf{P}_2 - \mathbf{P}_1).\mathbf{a} = (\mathbf{B} - \mathbf{A}).\mathbf{a} + s_B\mathbf{b}.\mathbf{a} - s_A\mathbf{a}.\mathbf{a} \qquad 4.64$$

Since the vectors P_1P_2 and **a** are perpendicular

$$(\mathbf{P}_2 - \mathbf{P}_1).\mathbf{a} = 0 \qquad 4.65$$

and

$$0 = (\mathbf{B} - \mathbf{A}).\mathbf{a} + s_B\mathbf{b}.\mathbf{a} - s_A\mathbf{a}.\mathbf{a} \qquad 4.66$$

By definition $\mathbf{a}.\mathbf{a} = 1$ since the direction cosines refer to a unit vector and

$$s_A = (\mathbf{B} - \mathbf{A}).\mathbf{a} + s_B\mathbf{b}.\mathbf{a} \qquad 4.67$$

By inspection of figure 4.13 and considering vectors in an anticlockwise direction

$$P_1P_2 = -AP_1 + AB + BP_2 \qquad 4.68$$

or

$$(\mathbf{P}_2 - \mathbf{P}_1) = (\mathbf{B} - \mathbf{A}) + s_B\mathbf{b} - s_A\mathbf{a} \qquad 4.69$$

The vector products of **b** with all of the terms in equation 4.63 are

$$(\mathbf{P}_2 - \mathbf{P}_1).\mathbf{b} = (\mathbf{B} - \mathbf{A}).\mathbf{b} + s_B \mathbf{b}.\mathbf{b} - s_A \mathbf{a}.\mathbf{b} \qquad 4.70$$

since $(\mathbf{P}_2 - \mathbf{P}_1)$ and $\mathbf{b}$ are perpendicular and $\mathbf{b}.\mathbf{b} = 1$

$$0 = (\mathbf{B} - \mathbf{A}).\mathbf{b} + s_B - s_A \mathbf{a}.\mathbf{b} \qquad 4.71$$

and

$$s_B = -(\mathbf{B} - \mathbf{A}).\mathbf{b} + s_A \mathbf{a}.\mathbf{b} \qquad 4.72$$

Substituting this into equation 4.67 gives

$$s_A = (\mathbf{B} - \mathbf{A}).\mathbf{a} + \{-(\mathbf{B} - \mathbf{A}).\mathbf{b} + s_A \mathbf{a}.\mathbf{b}\}\mathbf{b}.\mathbf{a} \qquad 4.73$$

$$= (\mathbf{B} - \mathbf{A}).\mathbf{a} - (\mathbf{B} - \mathbf{A}).\mathbf{b}\,\mathbf{b}.\mathbf{a} + s_A \mathbf{a}.\mathbf{b}\,\mathbf{b}.\mathbf{a} \qquad 4.74$$

$$s_A - s_A \mathbf{a}.\mathbf{b}\,\mathbf{b}.\mathbf{a} = (\mathbf{B} - \mathbf{A}).\mathbf{a} - (\mathbf{B} - \mathbf{A}).\mathbf{b}\,\mathbf{b}.\mathbf{a} \qquad 4.75$$

$$s_A = \frac{(\mathbf{B} - \mathbf{A}).\mathbf{a} - (\mathbf{B} - \mathbf{A}).\mathbf{b}\,\mathbf{b}.\mathbf{a}}{1 - \mathbf{a}.\mathbf{b}\,\mathbf{b}.\mathbf{a}} \qquad 4.76$$

By definition, the vector products of **a** and **b** are

$$\mathbf{a}.\mathbf{b} = \mathbf{b}.\mathbf{a} = l_1 l_2 + m_1 m_2 + n_1 n_2 = \cos\delta \qquad 4.77$$

where δ is the angle between the vectors **a** and **b** which can be evaluated from

equation 4.56 using the observed angles.

Equation 4.75 can be re-written

$$s_A = \frac{(\mathbf{B}-\mathbf{A}).\mathbf{a} - (\mathbf{B}-\mathbf{A}).\mathbf{b}\,\mathbf{b}.\mathbf{a}}{1-\cos^2\delta} \qquad 4.78$$

$$= \frac{(\mathbf{B}-\mathbf{A}).\mathbf{a} - (\mathbf{B}-\mathbf{A}).\mathbf{b}\,\mathbf{b}.\mathbf{a}}{\sin^2\delta} \qquad 4.79$$

In this expression

$$(\mathbf{B}-\mathbf{A}).\mathbf{a} = (x_B - x_A)l_1 + (y_B - y_A)m_1 + (z_B - z_A)n_1 = \mathbf{p} \qquad 4.80$$

which is a known quantity

$$(\mathbf{B}-\mathbf{A}).\mathbf{b} = (x_B - x_A)l_2 + (y_B - y_A)m_2 + (z_B - z_A)n_2 = \mathbf{q} \qquad 4.81$$

which is also a known quantity.

This gives

$$s_A = \frac{\mathbf{p}-\mathbf{q}\,\mathbf{b}.\mathbf{a}}{\sin^2\delta} = \frac{\mathbf{p}-\mathbf{q}\cos\delta}{\sin^2\delta} \qquad 4.82$$

By a similar process

$$s_B = \frac{\mathbf{p}\cos\delta - \mathbf{q}}{\sin^2\delta} \qquad 4.83$$

Using the direction cosines defined in equation 4.56 and the distances s_A and s_B from equations 4.82 and 4.83, the coordinates of P_1 and P_2 can be calculated using equations 4.58.

The mean of the two sets give the position of point P as

$$x_P = \frac{x_A + s_A l_1 + x_B + s_B l_2}{2}$$

$$y_P = \frac{y_A + s_A m_1 + y_B + s_B m_2}{2} \qquad 4.84$$

$$z_P = \frac{z_A + s_A n_1 + z_B + s_B n_2}{2}$$

These coordinates are only considered to be preliminary as it is likely that in any intersection survey a multiple theodolite set-up is possible and that a redundancy exists in the intersection. This is solved by the method of least squares to give adjusted coordinates and some form of assessment of the accuracy of these coordinates. A full treatment of the least squares adjustment for the equations developed so far for a spatial intersection is given by Bingley (1990) and is outlined by Allan (1988).

ECDS3 intersection model

After a bundle adjustment has been carried out, the absolute position and orientation of each theodolite in an ECDS3 set-up are determined and the *XYZ*

object coordinates at the centre of each theodolite together with their rotations ω, ϕ and κ are known.

The horizontal and vertical angles observed to a target point will define, for a given theodolite, the direction of the line of sight in the local theodolite coordinate system and since the rotations are known, it is possible to compute the direction of the line of sight in the object coordinate system. When two or more theodolites are used to intersect a point this defines more lines of sight which will, in general, not intersect at the point observed.

Where only two theodolites are used, it is shown in the previous section that the position of the intersected point is assumed to be at the mid-point of the common normal to the two lines of sight. Since the common normal lies along the shortest distance between the two lines of sight, the mid-point is a point whose distance from both observed lines of sight is a minimum. When observations are taken from more than two theodolites to a target point, the intersection is defined as the point whose distance from each line of sight is also a minimum. ECDS3 uses the method of least squares to solve these intersections.

The intersection of a point P from two theodolites A and B is shown in figure 4.14. The direction cosines for any instrument i in the object coordinate system can be expressed as

$$\begin{bmatrix} l_i \\ m_i \\ n_i \end{bmatrix} = \mathbf{M}^{\mathrm{T}}{}_i \begin{bmatrix} \cos\theta_i \cos\beta_i \\ \sin\theta_i \cos\beta_i \\ \sin\beta_i \end{bmatrix} \qquad 4.85$$

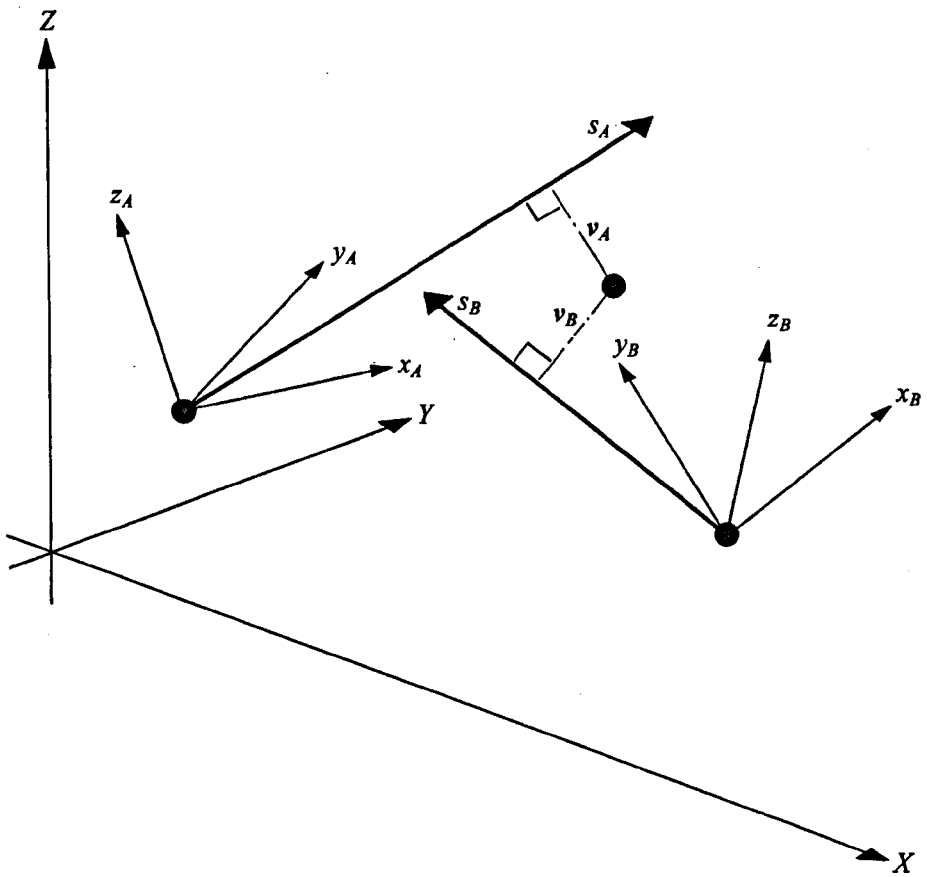

Figure 4.14 *ECDS3 two-theodolite intersection*

where

$\mathbf{M}^{\mathrm{T}}{}_i$ = the rotation matrix for instrument i obtained from a bundle adjustment (see equation 4.3)

θ_i = the horizontal angle observed at instrument i (positive is taken to be clockwise from the local x-axis)

β_i = the vertical angle observed at instrument i

For each theodolite, the vector along the line of sight is given by

$$s_i \begin{bmatrix} l_i \\ m_i \\ n_i \end{bmatrix} = \begin{bmatrix} X_P - X_i \\ Y_P - Y_i \\ Z_P - Z_i \end{bmatrix} + \begin{bmatrix} v_{X_i} \\ v_{Y_i} \\ v_{Z_i} \end{bmatrix} \qquad 4.86$$

where

s_i = the slope distance from instrument i to the foot of the residual offset vector

$\begin{bmatrix} X_P \\ Y_P \\ Z_P \end{bmatrix}$ = the coordinates of the intersected point P in the object system

$\begin{bmatrix} X_i \\ Y_i \\ Z_i \end{bmatrix}$ = the position of instrument i in the object coordinate system

$\begin{bmatrix} v_{X_i} \\ v_{Y_i} \\ v_{Z_i} \end{bmatrix}$ = the components of the residual offset vector $\mathbf{v}_i$

The residual offset vector $\mathbf{v}_i$ represents the minimum distance from each line of sight to the intersected point.

These equations are reduced to two by dividing through by l_i, m_i or n_i. The largest of these is chosen by ECDS3 and three possibilities exist. For the case where n_i is the largest

$$\frac{l_i}{n_i} = \frac{X_P - X_i + v_{X_i}}{Z_P - Z_i + v_{Z_i}} \qquad 4.87a$$

$$\frac{m_i}{n_i} = \frac{Y_P - Y_i + v_{Y_i}}{Z_P - Z_i + v_{Z_i}} \qquad 4.87b$$

These can be written

$$+n_i v_{X_i} + 0.v_{Y_i} - l_i v_{Z_i} + n_i X_P + 0.Y_P - l_i Z_P = n_i X_i + 0.Y_i - l_i Z_i \qquad 4.88a$$

$$+0.v_{X_i} + n_i v_{Y_i} - m_i v_{Z_i} 0.X_P + n_i Y_P - m_i Z_P = 0.X_i + n_i Y_i - m_i Z_i \qquad 4.88b$$

For theodolite A in figure 4.14

$$+n_A v_{X_A} + 0.v_{Y_A} - l_A v_{Z_A} + n_A X_P + 0.Y_P - l_A Z_P = n_A X_A + 0.Y_A - l_A Z_A \qquad 4.89a$$

$$+0.v_{X_A} + n_A v_{Y_A} - m_A v_{Z_A} 0.X_P + n_A Y_P - m_A Z_P = 0.X_A + n_A Y_A - m_A Z_A \qquad 4.89b$$

and for theodolite B in figure 4.14

$$+n_B v_{X_B} + 0.v_{Y_B} - l_B v_{Z_B} + n_B X_P + 0.Y_P - l_B Z_P = n_B X_B + 0.Y_B - l_B Z_B \qquad 4.90a$$

$$+0.v_{X_B} + n_B v_{Y_B} - m_B v_{Z_B} 0.X_P + n_B Y_P - m_B Z_P = 0.X_B + n_B Y_B - m_B Z_B \qquad 4.90b$$

For the two theodolite intersection shown these represent four observation equations and combining them gives

$$\begin{bmatrix} n_A & 0 & -l_A & 0 & 0 & 0 \\ 0 & n_A & -m_A & 0 & 0 & 0 \\ 0 & 0 & 0 & n_B & 0 & -l_B \\ 0 & 0 & 0 & 0 & n_B & -m_B \end{bmatrix} \begin{bmatrix} v_{X_A} \\ v_{Y_A} \\ v_{Z_A} \\ v_{X_B} \\ v_{Y_B} \\ v_{Z_B} \end{bmatrix} + \begin{bmatrix} n_A & 0 & -l_A \\ 0 & n_A & -m_A \\ n_B & 0 & -l_B \\ 0 & n_B & -m_B \end{bmatrix} \begin{bmatrix} X_P \\ Y_P \\ Z_P \end{bmatrix}$$

$$= \begin{bmatrix} n_A X_A - l_A Z_A \\ n_A Y_A - m_A Z_A \\ n_B X_B - l_B Z_B \\ n_B Y_B - m_B Z_B \end{bmatrix} \qquad 4.91$$

or

$$\mathbf{A}\,\mathbf{v} + \mathbf{B}\,\Delta = \mathbf{f} \qquad 4.92$$

where

A = a 4 x 6 rectangular coefficient matrix computed from observed horizontal and vertical angles

$$= \begin{bmatrix} n_A & 0 & -l_A & 0 & 0 & 0 \\ 0 & n_A & -m_A & 0 & 0 & 0 \\ 0 & 0 & 0 & n_B & 0 & -l_B \\ 0 & 0 & 0 & 0 & n_B & -m_B \end{bmatrix}$$

B = a 4 x 3 rectangular coefficient matrix also computed from observed angles

$$= \begin{bmatrix} n_A & 0 & -l_A \\ 0 & n_A & -m_A \\ n_B & 0 & -l_B \\ 0 & n_B & -m_B \end{bmatrix}$$

v = a 6 x 1 matrix representing the residual vectors $\mathbf{v}_A$ and $\mathbf{v}_B$

$$= \begin{bmatrix} v_{X_A} \\ v_{Y_A} \\ v_{Z_A} \\ v_{X_B} \\ v_{Y_B} \\ v_{Z_B} \end{bmatrix}$$

Δ = a 3 x 1 matrix of the coordinates of the unknown point *P*

$$= \begin{bmatrix} X_P \\ Y_P \\ Z_P \end{bmatrix}$$

f = a 4 x 1 matrix of constants derived from the observed angles and coordinates of the theodolites

$$= \begin{bmatrix} n_A X_A - l_A Z_A \\ n_A Y_A - m_A Z_A \\ n_B X_B - l_B Z_B \\ n_B Y_B - m_B Z_B \end{bmatrix}$$

The redundancy *r* in this set of equations is given by the number of rows in the **A** and **B** matrices (denoted by $c = 4$ in this case to represent the four observation equations) minus the number of unknown parameters in the Δ matrix ($u = 3$ for any intersection) so that $r = c - u = 4 - 3 = 1$. This is to be expected since all that is required to compute a unique three-dimensional intersection of two lines (vectors) is the horizontal and vertical angles of one line and the horizontal angle of the other. The second vertical angle introduces

the redundancy into the solution.

As the number of theodolites used in the measurement process increases, the value of c increases by 2 for each theodolite at which a horizontal and vertical angle are observed to the point P. This in turn increases the redundancy of the solution.

The solution to equations of the form $\mathbf{A}\,\mathbf{v} + \mathbf{B}\,\Delta = \mathbf{f}$ in equation 4.92 is given in many textbooks such as Mikhail (1976) and Mikhail & Gracie (1981) and follows recognised procedures.

The solution is given by

$$\Delta = \mathbf{N}^{-1}\,\mathbf{t} \qquad 4.93$$

where

$$\mathbf{N} = \mathbf{B}^{t}(\mathbf{A}\,\mathbf{Q}\,\mathbf{A}^{t})^{-1}\,\mathbf{B} \qquad 4.94$$

$$\mathbf{t} = \mathbf{B}^{t}(\mathbf{A}\,\mathbf{Q}\,\mathbf{A}^{t})^{-1}\,\mathbf{f} \qquad 4.95$$

The solution requires the cofactor matrix $\mathbf{Q}$ of the offset residual vectors $\mathbf{v}_i$ to be known. ECDS3 assumes the components of these vectors to be uncorrelated and $\mathbf{Q}$ will therefore be a diagonal matrix.

If the covariance matrix Σ for the offset residual components is

$$\Sigma = diag \{\sigma^2_{v_{X_A}} \quad \sigma^2_{v_{Y_A}} \quad \sigma^2_{v_{Z_A}} \quad \dots \} \qquad 4.96$$

where

$\sigma^2_{v_{X_A}}$ = the variance of residual component v_{X_A}

$\sigma^2_{v_{Y_A}}$ = the variance of residual component v_{Y_A}

$\sigma^2_{v_{Z_A}}$ = the variance of residual component v_{Z_A}

and so on

Q will be given by

$$\mathbf{Q} = diag \{Q_1 \quad Q_2 \quad Q_3 \quad \dots \} \qquad 4.97$$

where

$$Q_1 = \frac{\sigma^2_{v_{X_A}}}{\sigma^2_0} \qquad Q_2 = \frac{\sigma^2_{v_{Y_A}}}{\sigma^2_0} \qquad Q_3 = \frac{\sigma^2_{v_{Z_A}}}{\sigma^2_0} \qquad \dots \qquad 4.98$$

and

σ^2_0 = the reference variance for the offset residual components

When an intersection is computed by ECDS3 it displays a set of errors together

with the coordinates of the intersected point. The errors displayed are

- The X, Y and Z (object system) components of the sighting errors of the intersection. These are displayed in root mean square (or *RMS*) format as *PeX*, *PeY* and *PeZ*. The formulae used to compute these are

$$PeX = RMS_X = \sqrt{\frac{\sum_{i=1}^{n} v_{X_i}^2}{n}} \qquad 4.99a$$

$$PeY = RMS_Y = \sqrt{\frac{\sum_{i=1}^{n} v_{Y_i}^2}{n}} \qquad 4.99b$$

$$PeZ = RMS_Z = \sqrt{\frac{\sum_{i=1}^{n} v_{Z_i}^2}{n}} \qquad 4.99c$$

where n = the number of theodolites used

- The total *RMS* error which is defined as

$$RMS = \sqrt{\frac{\sum_{i=1}^{n} v_i^2}{n}} \qquad 4.100$$

In these equations, the residual components v_{X_i}, v_{Y_i} and v_{Z_i} are obtained from the least squares solution using

$$\mathbf{v} = \mathbf{Q}\mathbf{A}^t\left(\mathbf{A}\mathbf{Q}\mathbf{A}^t\right)^{-1}\left(\mathbf{f} - \mathbf{B}\Delta\right) \qquad 4.101$$

In equation 4.100, the length of any individual offset residual vector v_i is given by

$$v_i = \sqrt{v_{X_i}^2 + v_{Y_i}^2 + v_{Z_i}^2} \qquad 4.102$$

This method of presenting errors in positional information does give the operators of an ECDS3 system a good indication if a gross error has occurred (for example, if the wrong target has been sighted by an observer) and does give a clear indication if some sort of tolerance is exceeded in determining the coordinates of the target point. All of this is discussed further in section 5.6 (under Online Measurement).

However, the approach adopted does seem to ignore the fact that some useful data is available for presenting the standard error of the coordinates of the intersected point. These can be obtained from the least squares solution as

$$\sigma_{X_p} = \sqrt{\mathbf{N}_{1,1}^{-1}} \qquad \sigma_{Y_p} = \sqrt{\mathbf{N}_{2,2}^{-1}} \qquad \sigma_{Z_p} = \sqrt{\mathbf{N}_{3,3}^{-1}} \qquad 4.103$$

where $\mathbf{N}_{1,1}^{-1}$, $\mathbf{N}_{2,2}^{-1}$ and $\mathbf{N}_{3,3}^{-1}$ are the diagonal terms of the $\mathbf{N}^{-1}$ matrix.

In addition to displaying *RMS* values, ECDS3 also displays quantities called *SX*, *SY* and *SZ* alongside *PeX*, *PeY* and *PeZ*. The *S*-values give some indication of the measuring accuracy expected for a particular ECDS3 set-up and are a function of the geometry of the intersection and assumed *a priori* standard errors of $\pm 1''$ for all measured horizontal and vertical angles. Consequently, the

S-values are not a function of the actual sighting errors and they do not give any information as to the errors in the coordinates of the intersected point. The *S*-values do, however, provide some useful practical information when using ECDS3. This is discussed further in section 5.6 (under Online Measurement).

The computation of the *S*-values is done as a conventional error propagation considering the case where the lines of sight intersect and a full description is given by Bingley (1990).

4.5 Concluding remarks

Taking account of the two methods described for determining the attitude of the theodolites, the bundle adjustment is considered to be the most flexible and convenient. Nowadays, this is easily implemented on a computer using off-the-shelf software. Of the methods given for the computation of an intersection, it is suggested that there is probably little difference between the results that these might produce in practice. However, the so-called rigorous and ECDS3 versions would be preferred as these provide a full three-dimensional and statistical analysis for intersection coordinates.

5

THE DEVELOPMENT AND OPERATION OF ECDS3

The original idea for using coordinates determined by theodolite intersection in dimensional control is attributed to the aerospace industry. In aircraft manufacture, the coordinates of small components of up to about a metre in size are usually obtained by using coordinate measuring machines. However, when larger objects have to be measured, problems often encountered are the limited size of coordinate measuring machines and their portability. In such situations, techniques based on surveying and photogrammetry have been found to offer a considerable advantage for measurement of coordinates since the equipment is mobile and can be taken to the object to be measured. In fact, surveying systems can be said to be portable coordinate measuring machines the size of which can be varied to suit any object. In North America, theodolite intersection systems have had some success in penetrating the market normally dominated by coordinate measuring machines and hundreds of these have been purchased by the aerospace industry.

Woodward (1986) gives an interesting comparison of coordinate measuring machines and coordinate measuring systems from an industrial perspective and Fraser (1989) discusses the current status of optical three-dimensional techniques in the aerospace industry at about the time theodolite intersection was adopted by the University of Brighton for measuring deflections in full-scale structures.

5.1 The era of theodolite intersection

The first commercially produced system for measuring coordinates based on surveying techniques was produced in the United States by Keuffel and Esser in the 1970s when they introduced their Analytical Industrial Measuring System (AIMS) (Keuffel & Esser, 1981 and Vyner & Hanold, 1982). Many North American aerospace companies have purchased various versions of AIMS which was marketed by the Cubic Precision Division of the Cubic Corporation in 1992, but in the United States only (Hooper, 1987).

In addition to Keuffel and Esser, Hewlett Packard (HP) also developed a theodolite intersection system in 1980 which gave rise to a technique called digital theodolite coordinate determination, and this was based on the HP3820A digital theodolite (Johnson, 1980).

Following the success of Keuffel and Esser and Hewlett Packard in North America, the survey companies Wild and Kern have dominated the European theodolite intersection market since this was first identified. In 1982, Wild produced the RMS2000 (Remote Measuring System 2000) and in 1983, Kern produced the first Electronic Coordinate Determination System (ECDS1). Both of these on-line systems consisted of up to four theodolites linked directly to a computer in which horizontal and vertical readings from each theodolite were electronically generated and transmitted to the computer, which had appropriate software to compute *XYZ* coordinates.

Because of limitations imposed by the collimation process for orientation and by the computation technique used for intersections, the number of theodolites that RMS2000 and ECDS1 could use was restricted and they were replaced by ECDS2 in 1986 and the Wild TMS (Theodolite Measuring System), in the United States only, in 1988. Both of these allowed up to 8 theodolites to be used but the orientation was now carried out using a bundle adjustment.

As well as manually operated systems, the Kern System for Positioning and Automated Coordinate Evaluation (SPACE) became available in 1987 (see section 3.2) and the Wild Automated Theodolite Measuring System (ATMS) in 1988. These were the first automated systems produced for coordinate measurement by theodolite intersection.

As a result of the domination of Wild and Kern in the theodolite intersection market it is not surprising that very few of these systems have been manufactured. However, it is worth noting that a number of universities, survey and other organisations have developed their own 'in-house' versions by compiling their own software for use with a variety of theodolites.

5.2 The evolution of ECDS

ECDS1 was introduced by Kern & Co Ltd of Aarau in Switzerland in 1983 and this is described by Kern (1984), Lardelli (1985) and Grist (1986).

The original version of ECDS used two Kern E1 or E2 theodolites and the computer and other hardware for the system fitted into a specially designed and

purpose-built trolley that enabled it to be moved from one location to another (see figure 5.1). This emphasised the portability of the system for industrial applications and has always been a feature of ECDS.

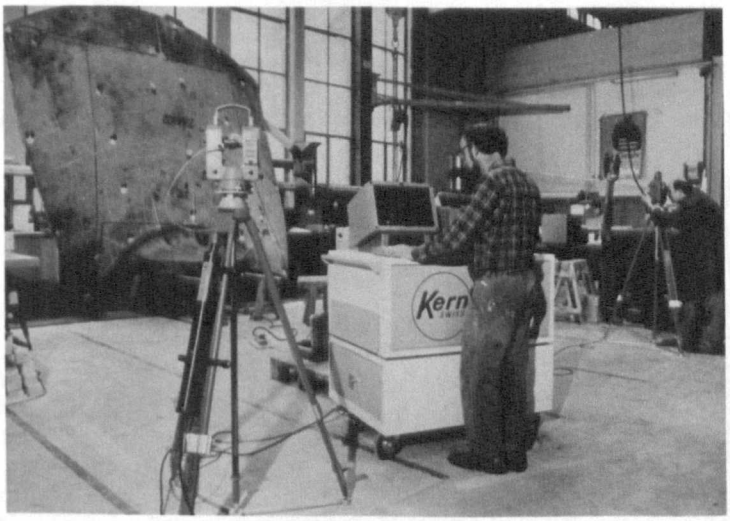

Figure 5.1 *ECDS1 on the factory floor (courtesy Leica Geosystems)*

The software was developed to operate on a DEC (Digital Equipment Corporation) micro PDP-11 or Hewlett Packard HP85 computer and this was accessed through a series of modular programs. When orientated, the two theodolites were set such that when their lines of sight were collimated to each other, both had horizontal angle readings of zero. This established a baseline between the two theodolites from which all horizontal angles were subsequently measured. To complete the system orientation, two ends of a scale bar were sighted and the software would then determine the spatial relationship of the two theodolites, as discussed in chapter 4.

For each intersection, angles were continuously transmitted by the theodolites to the DEC PDP-11 which then computed, via a $2D + 1D$ model (see section

4.4), the corresponding real-time *X*, *Y* and *Z* coordinate values of the target point sighted together with their d*Z* value, which was half the difference of the two *Z*-coordinates obtained from each theodolite. The d*Z* value was a very useful feature and provided instant feedback on the quality of an intersection.

The limitations of ECDS1 were that it would only operate with two theodolites, it relied on a collimation process to orientate the theodolites and the software would only run on the DEC PDP-11or HP85.

5.3 ECDS2

Kern launched this version of ECDS in 1986 but the system was marketed by Wild Leitz following their takeover of Kern in 1988. The following section is summarised from publications attributed to Freeman (1987), Kern (1987) and Lardelli (1988).

ECDS2 incorporated the Kern E2 and Kern E2-I electronic theodolites for angle measurement and up to eight of these could be connected to the system. Because of this, the accuracy of ECDS2 was potentially much better than before since it was possible to sight targets with as many theodolites as possible and to compute a multiple rather than a single intersection. Also, the E2-I had a 42x magnification panfocal telescope compared to the 32x of the E2.

Although the software for ECDS2 also ran on the DEC PDP-11, a significant difference between ECDS1 and ECDS2 was that a separate MS-DOS version of the programs was produced. This allowed the user a choice of computer

rather than having to accept the DEC PDP-11 and any computer that was IBM compatible at the time could be chosen as the system computer.

The third and again significant difference from ECDS1 to ECDS2 was the method used to orientate the theodolites. The new orientation method used a functional model in the form of a bundle adjustment which allowed the relative positions of all the theodolites to be defined. This setting up procedure avoided the need for collimating the theodolites and allowed them to be set up very close to each other if this was required.

When Kern Instruments were absorbed by Wild Heerbrugg in September 1988, the two companies carried on marketing their own products separately. However, following the merger, both Wild and Kern's industrial metrology marketing and product support services were transferred to E. Leitz (Instruments) at Luton. In August 1989 all three companies, Wild, Kern and E. Leitz combined and began operating under the name of Wild Leitz UK Ltd from new premises in Milton Keynes. Further change occurred in September 1989 when Wild Leitz merged with Cambridge Instruments Company plc and became Leica in 1990. Throughout this somewhat turbulent period, ECDS2 continued to be sold as a Kern product.

5.4 ECDS3

Leica released version 3.10 of ECDS3 in March 1992 but Kern theodolites and literature were still in use and this was very much a continuation of ECDS1 and 2. However, later in 1992, version 3.20 of ECDS appeared with a Leica label,

the Kern image was now very much in the background and although their theodolites could still be used, the preferred instruments were now the Wild T2002 and the Wild T3000. A similar system has also been in use in North America under the name of the ManCAT (Manual Computer Aided Theodolite) system and this also has been available since the early 1990s (Leica, 1992b).

Compared to ECDS2, setting up and using ECDS3 is much the same with measurements possible using up to eight theodolites, with a bundle adjustment orientation procedure and with improved software running under MS-DOS (Leica, 1993b). Version 3.21 was released in 1994 and this contained minor improvements and corrections to the theodolite communications and software. This thesis covers a period when version 3.20 of ECDS3 was first used in September 1992 but refers primarily to version 3.21 which has been in use since April 1994.

5.5 ECDS3 at Brighton

The main components of ECDS3 (and any theodolite intersection system) are at least two electronic theodolites together with computer hardware and software. Peripheral components such as theodolite tripods or stands, targets and a scale bar are also required. All of these are briefly described in the following sections with reference to the system purchased by the University of Brighton.

Electronic theodolites

The theodolite chosen by the University of Brighton for ECDS3 is the Wild T2002. A full technical description of this theodolite in its original version, the Wild THEOMAT T2000 is given by Katowski and Saltzmann (1983) and the T2002/T3000 are described in technical data by Leica (1994).

The main difference between the T2002 and the T3000 is the telescope as shown in figure 5.2. The T3000 has a panfocal telescope which, at close and medium ranges of up to 20 m, decreases the magnification and increases the field of view and brightness of images. This, it is claimed by Leica, enables targets to be sighted more quickly and accurately. When focussed to infinity, the standard eyepiece of the T3000 has a magnification of 42x compared to the 32x magnification of the T2002.

Figure 5.2 *T2002 (left) and T3000 (right) electronic theodolites*

In all other respects, the two theodolites are the same, especially their stated accuracy of 0.5″ for both horizontal and vertical readings, notwithstanding the improvement for sightings expected with the panfocal telescope of the T3000. Both instruments have a dual-axis liquid compensator with a setting accuracy of 0.1″. The decision to purchase T2002s was based on a consideration of costs where the extra money required for the T3000 was not justified given that the accuracy would not improve dramatically.

The T2002s supplied to the University of Brighton were fitted with industrial reticules as shown in figure 5.3. Leica recommended these for observing circular targets as it was expected that these would be used. With hindsight, the choice of industrial reticule was appropriate, as the concentric pattern on these has often helped with the intersection of circular targets, especially those with acute sighting angles that appear elliptical in the field of view of the telescope.

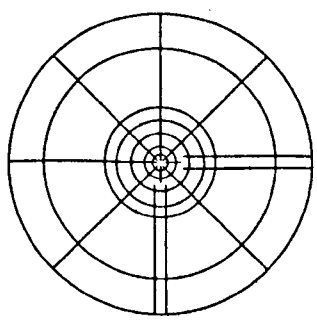

Figure 5.3 *Industrial reticule of T2002*

Computer hardware and software

The first computer supplied by Leica for ECDS3 was a Compaq Deskpro 386s/20. This has a full size console with separate 15 inch monitor and is a

standard office/home computer, something not really designed for frequent moving and for use on construction sites. Although it was used without any serious difficulties, the transportation of the Compaq was awkward and its use was not suitable for the rugged conditions experienced on site. For these reasons, the Compaq was replaced with a Toshiba T6600C power portable in 1994. In its latest version, ECDS3 can be used with any computer but laptops would be the preferred option provided the interfaces and their connections can be properly installed and they can withstand site conditions.

Other items of computer hardware supplied with ECDS3 are the GIF11 interface, interface box and Hostess board. All of these provide the necessary communications and connections between the theodolites and computer. The remaining item of computer hardware is the ECDS3 copy protection plug which must be attached to the printer port LPT1 of the system computer otherwise the ECDS3 software will not run. Great care has to be taken not to forget this when travelling to sites as it is quite small compared to all the other ECDS3 components.

The ECDS3 software is described in section 5.6.

Peripheral components

In addition to the theodolites and computer, theodolite stands or tripods, a scale bar and targets are required components in a theodolite intersection system.

The choice of platform for the T2002s was *conventional tripod, industrial tripod* and *industrial stand*. At first, stands were supplied by Leica as part of the ECDS3 package and although these provided extremely stable observing platforms, they have proved to be very difficult to transport, especially around the construction sites where ECDS3 was first used. In some cases, conventional tripods have been used, but these are not stable for periods greater than about 30 minutes. At all sites where ECDS3 is currently in operation, industrial tripods are now used. A description and discussion of these various platforms is given in section 7.1.

A *scale bar* of some sort is vital for a theodolite intersection system. The University of Brighton has two of these: one is used to set up ECDS3 and the other is used for checking purposes. These are made of carbon fibre to reduce temperature effects and have a target at each end as shown in figure 5.4.

Figure 5.4 *1 m scale bar*

When the bar is calibrated, the length between the targets is measured with a laser interferometer to a tolerance of ± 0.002 mm by Leica under laboratory

conditions and the length confirmed in a test certificate (see Appendix A). The optimum length for a scale bar is for it to be about the same length as the size of the object to be measured but this is nearly always impractical and the 1 m scale bar shown is the most commonly used.

The selection of the most appropriate *targets* for a theodolite intersection system is also of vital importance. The choice of these for the glulam monitoring schemes is discussed at length in section 6.1.

5.6 Using the ECDS3 software

ECDS3 software is a collection of independent programs linked together by a menu system. The organisation of these is shown in figure 5.5 and a full description of each program can be found in the program reference section of the ECDS3 user manual (Leica, 1993c). Based on this, an outline of each program used when monitoring the glulam structures is given below and some of the practical issues arising from this for the glulam project are discussed.

Main Menu

When performing a measurement task with ECDS3, the first screen display obtained when the program is run is the *Main Menu* shown in figure 5.6 which lists all the programs available in version 3.21. These are all called top level menus.

MAIN MENU	PROJECT DEFINITION	Job description File names Orientation parameters
	SYSTEM ORIENTATION	Control editor Angle capture Pre-process Bundle adjustment Local Post transform Manual orientation Simulation
	ONLINE MEASUREMENT	
	SPECIAL FUNCTIONS	Lines Planes Circle Ellipse Sphere Cylinder Parabola File compare Recapitulate
	TEXT FILE EDITOR	
	USER PROGRAMS	MS-DOS shell
	SETUP PARAMETERS	Units and tolerance Hardware and display Sensor configuration

Figure 5.5 *Configuration of ECDS3 programs*

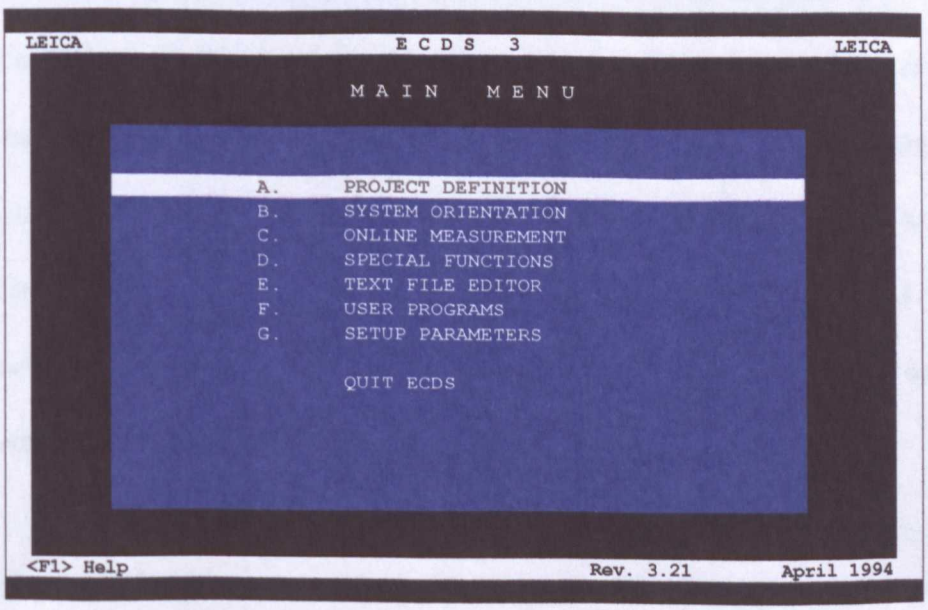

Figure 5.6 *ECDS3 Main Menu program screen*

Setup Parameters

At the start of any glulam survey, the first top level menu usually chosen is *Setup Parameters* and the programs in this group are shown in figure 5.7. All of these are accessed to check that the entries from the previous survey are still the same before any measurements are taken. Of course, the information in these programs seldom changes from survey to survey but a quick check is always done for peace of mind. Lines *A* to *G* of the *Units and Tolerance* program of figure 5.8 are self-explanatory and the entries for *RMS* errors in lines *H* to *L* have been chosen arbitrarily. These tolerances do not represent any theoretical assessment of the errors expected for any ECDS set up and are simply values beyond which the display of ECDS3 changes colour and issues a warning to alert the operators that a pointing error or bundle adjustment has exceeded the specified tolerance. The values of 0.1 mm and 0.05 mm have proved to be realistic and obtainable in practice for all work carried out and in the cases where these *RMS* tolerances have been exceeded, a poor sighting has usually been found and corrected. The only entry in the *Hardware and Display* screen of figure 5.9 ever changed has been the scale bar length on line *A*. The *Sensor Configuration* menu shown in figure 5.10 lists the two T2002s as the sensors (theodolites) used and the recording buttons are set to active.

Project Definition

After the Setup Parameters have been checked, *Project Definition* is selected from the main menu and each of the programs listed in figure 5.11 is run in

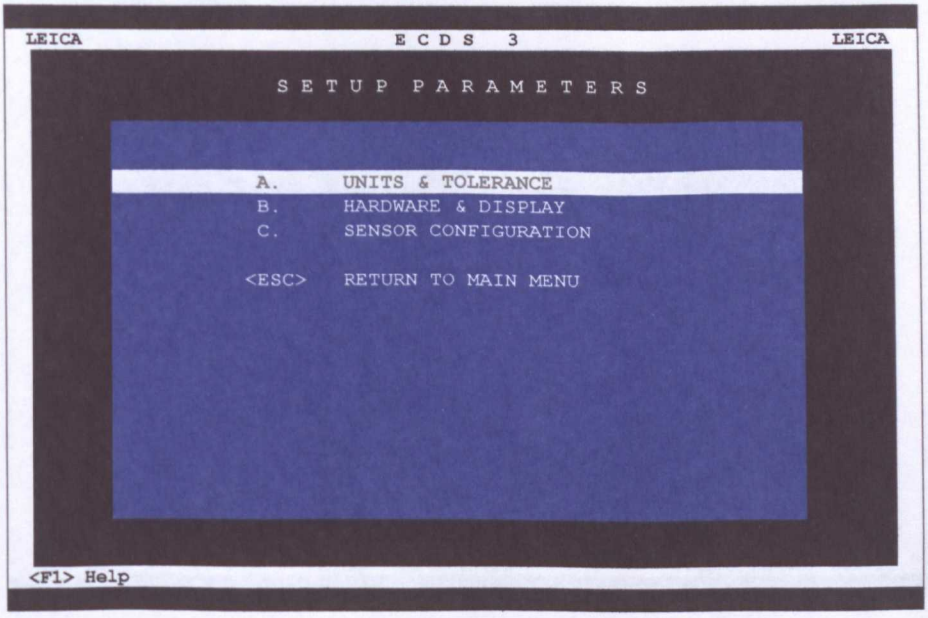

Figure 5.7 *ECDS3 Setup Parameters menu*

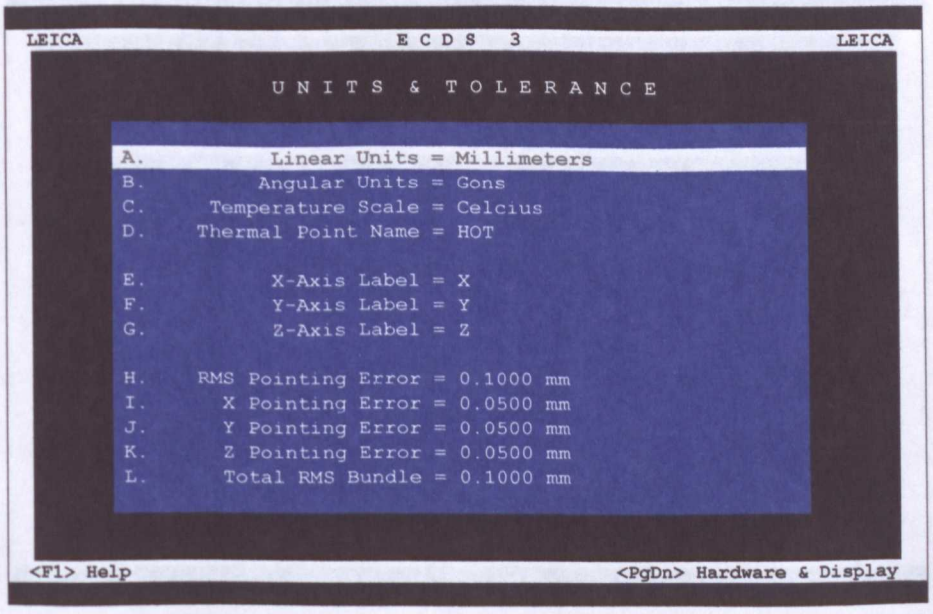

Figure 5.8 *Units and tolerance settings used in glulam project*

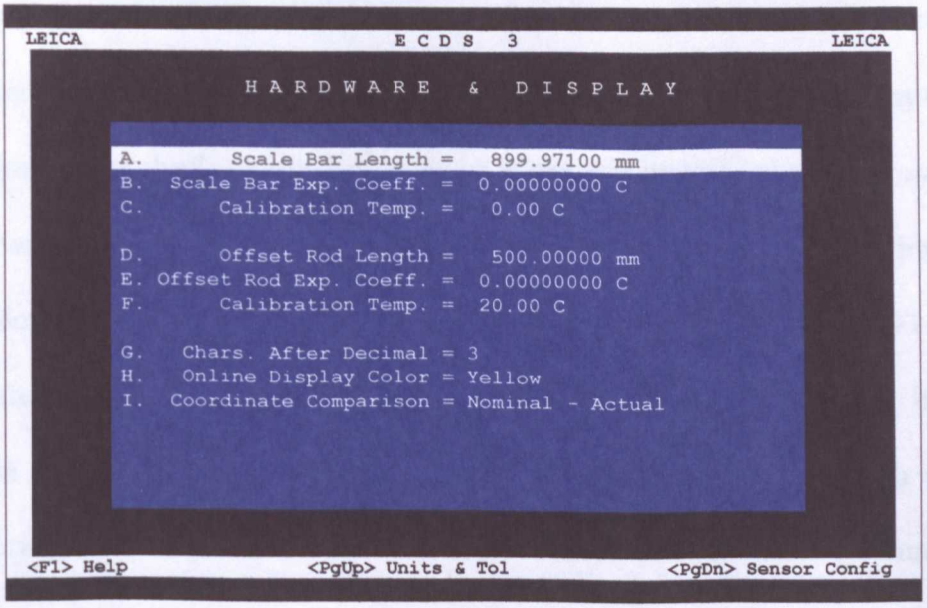

Figure 5.9 *Hardware and Display settings used in glulam project*

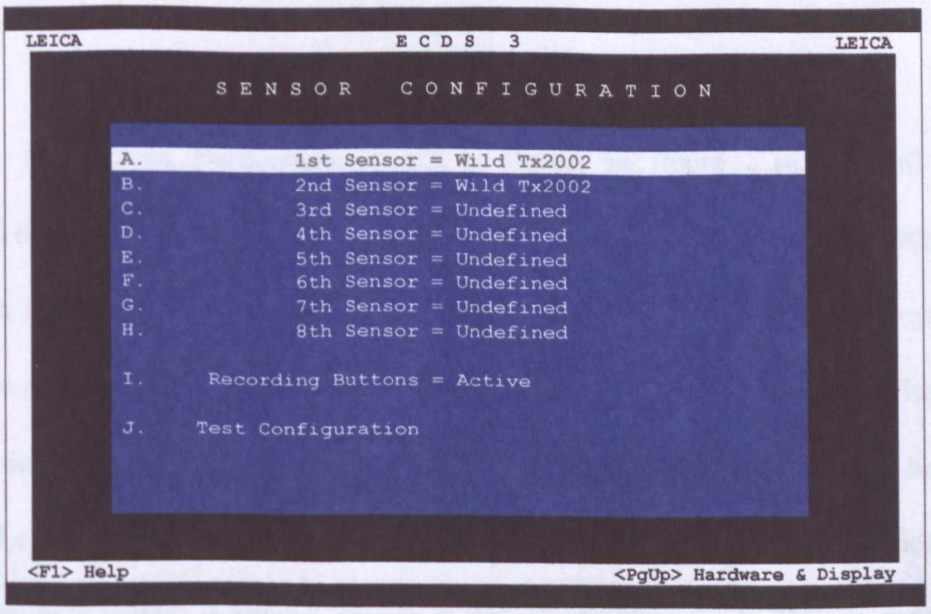

Figure 5.10 *Sensor Configurations for glulam project*

sequence. The *Job Description* screen for a typical visit to Wokingham Baptist Church is shown in figure 5.12. On line *E*, the user level `Novice` is selected rather than the other option of `Expert`. This means that the ECDS3 system keeps a better check on how it is being used and will issue more error messages to warn the operators if any entry is wrong. In *File Names*, all that is required to be done is to enter a sub-directory name for all the data files that ECDS3 will create for the current job. In figure 5.13, these are shown to be stored on drive C in the system computer in a data directory called C:\ECDS3 with sub-directory WOKHAM43 in this case. As soon as the sub-directory name is entered, the program automatically creates all the remaining system files, some of which are shown in figure 5.13, and this menu is completed. A description of these files is given in table 5.1 and Appendix B contains an example print-out of each file for a completed survey.

The *Orientation Parameters* screen is shown in figure 5.14. For all the different glulam sites monitored, the entries to this program are very similar each time ECDS3 is used, but care has been taken to ensure they are correct. Line *A* must read `Local` to indicate a local coordinate system has been adopted for defining coordinates with the centre of one of the theodolites as the origin of the coordinate system (this is designated as sensor or theodolite 1). A default coordinate system is always chosen in line *D* and instructs ECDS3 to produce coordinates for all points in the bundle system created for the current survey and the entry in line *E* specifies that a right-handed coordinate system is to be used (see figure 4.1).

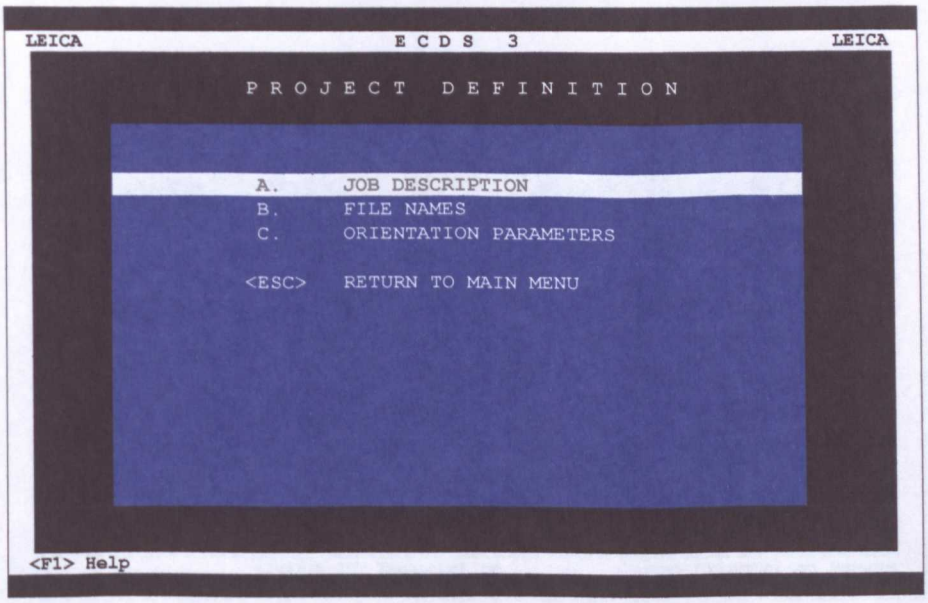

Figure 5.11 *Project Definition menu screen*

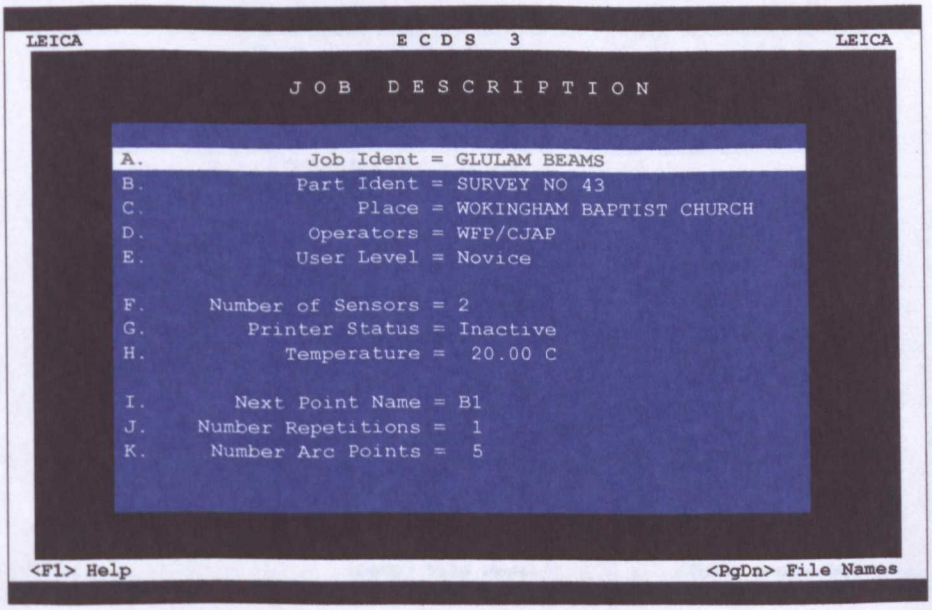

Figure 5.12 *Job Description screen for survey at Wokingham*

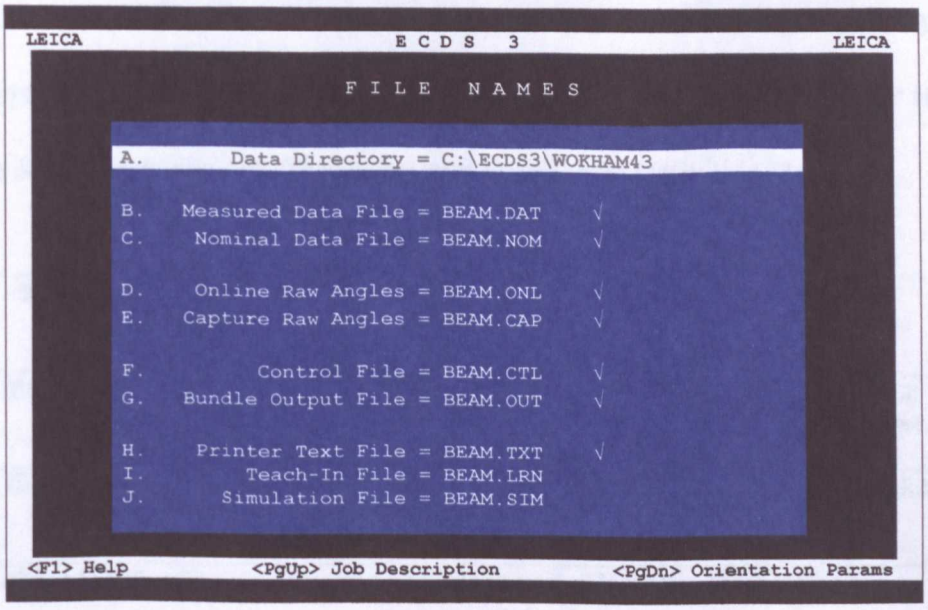

Figure 5.13 *Format for File Names used in glulam project*

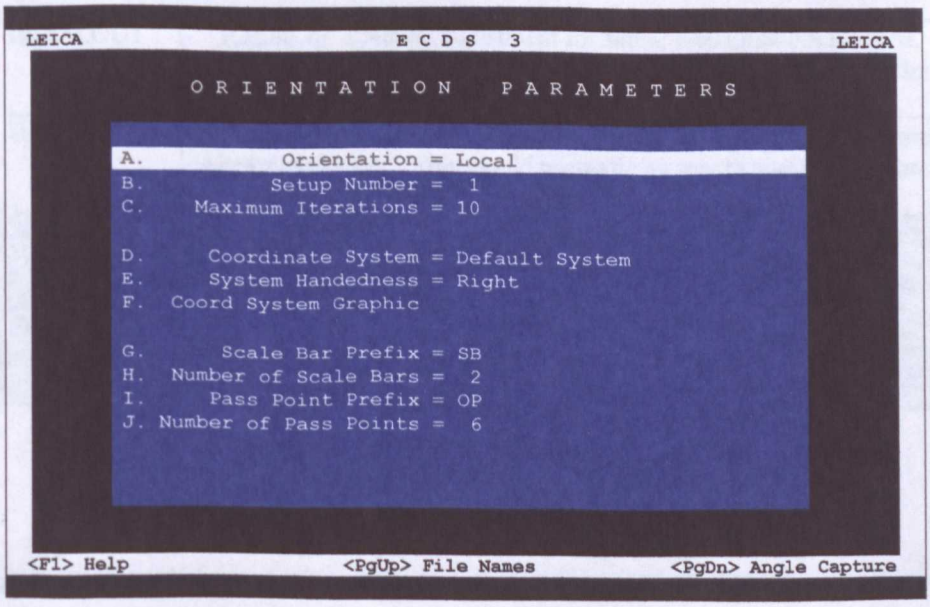

Figure 5.14 *Orientation Parameters used for glulam projects*

The only entry that usually changes in this program is the number of scale bars in line *H* and the number of pass points on line *J*. At Wokingham, six pass points (or bundle points) are chosen initially, but more are added at a later stage (see *Bundle Adjustment*). This completes the Project Definition stage.

File Name	Data content
BEAM.DAT	*XYZ* coordinates of all bundle and on-line points intersected with *RMS* values and comments. This is raw data that is processed later.
BEAM.NOM	The same as DAT files. This file is used as a source of data by other programs, eg. Local to Object and File Compare.
BEAM.ONL	Observed intersection angles from the Online program.
BEAM.CAP	All data from the Angle Capture program including observed angles and approximations required by Pre-Process.
BEAM.CTL	Information for defining the datum of the coordinate system including theodolite positions, orientations and scale constraints.
BEAM.OUT	Results of a bundle adjustment including theodolite orientations, bundle point coordinates and statistics relating to the quality of the adjustment.
BEAM.TXT	Printer text file containing output from certain programs summarising a complete project. This would normally be sent to a printer or stored to another disc.
BEAM.LRN	Teach-in information used by Capture and Online programs. Not used in this project.
BEAM.SIM	Information relating to simulation projects. Option not purchased.

Table 5.1 *ECDS3 Files*

System Orientation

The next program accessed is *System Orientation* and the programs available for this are shown in figure 5.15.

Because a local coordinate system has been chosen at all the glulam sites, there

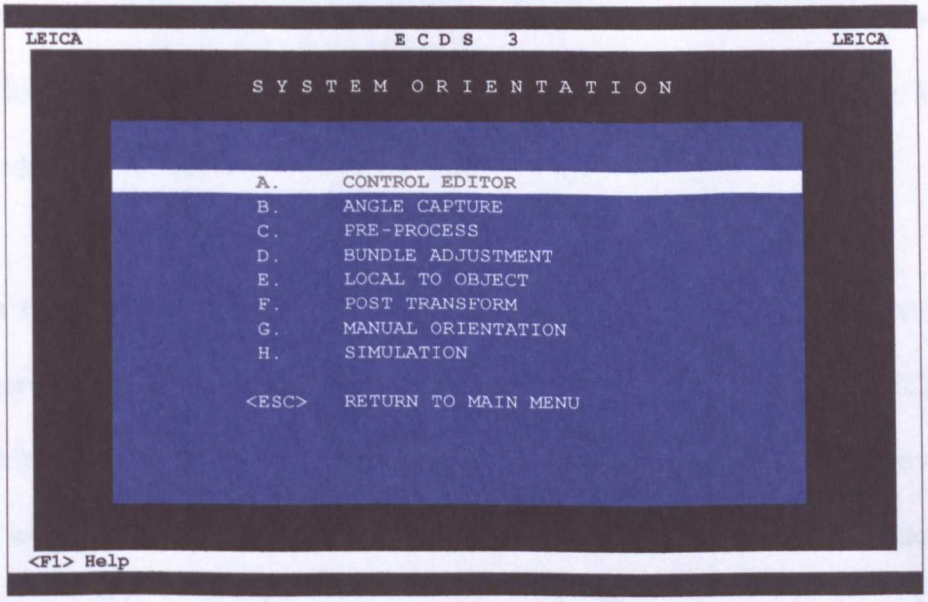

Figure 5.15 *System Orientation menu screen*

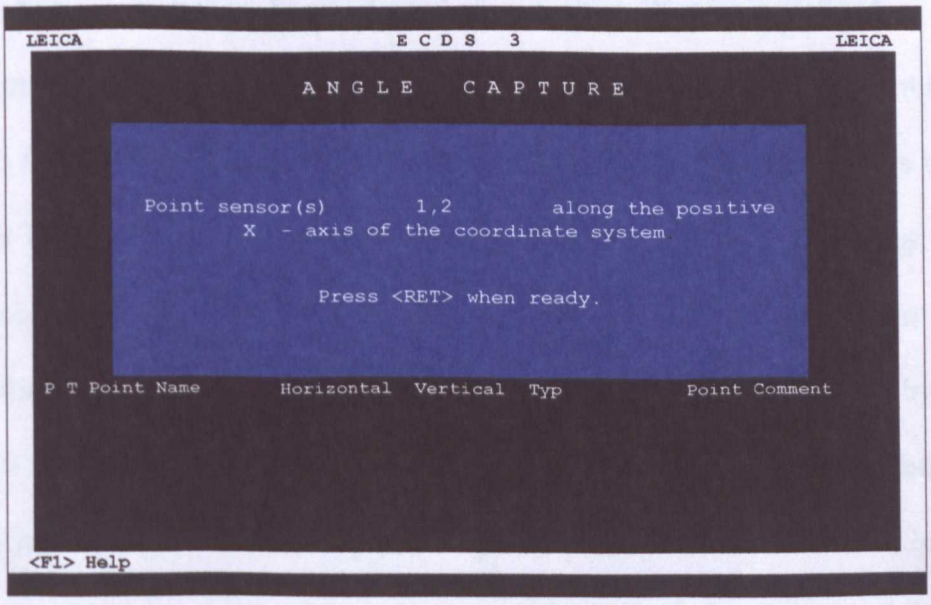

Figure 5.16 *Setting X-axis directions in Angle Capture*

has been no need to use the *Control Editor* as the purpose of this is to enable information regarding control points, theodolite orientations and scale constraints to be entered into ECDS3. These are not required for a local coordinate system.

The second program in System Orientation is *Angle Capture* which records observed orientation data. The bundle adjustment performed by ECDS3 requires estimates of the orientation and position of the theodolites relative to the axes and origin of the coordinate system adopted to be entered into the computer (this is also discussed in section 4.3). The estimates begin with the definition of the positive X-axis direction at each theodolite and the instructions for this are shown in figure 5.16. Since two theodolites are used and a local coordinate system has been adopted, the positive X-axis is defined as the direction of the baseline from theodolite 1 to theodolite 2 and to define this at both theodolites, all that is required to be done is to turn both telescopes until their objectives point along this direction. No attempt is made to align the telescopes exactly from the centre of one theodolite to the other. In this position, the horizontal circles of both theodolites are automatically set by the software to zero and for a right-handed coordinate system, the Y-axis is defined for each theodolite as a reading of 300 gon. These can be seen recorded in the lower half of the Angle Capture screen in Figure 5.17. The second phase of Angle Capture involves estimating the position of the theodolites. In a local coordinate system, theodolite 1 is assumed to be at the origin of the coordinate system and its position is known. The prompt for carrying out the estimation of

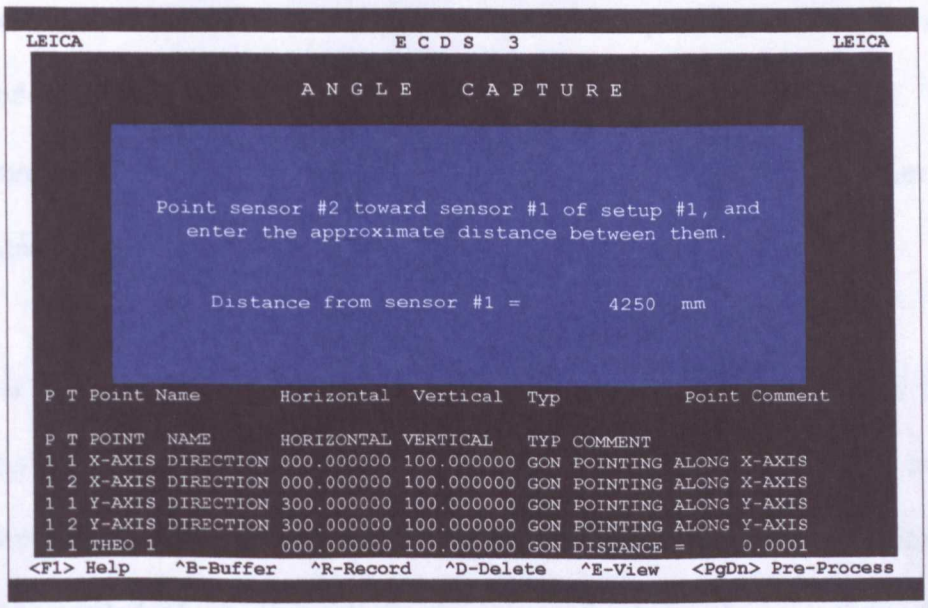

Figure 5.17 *Estimating second theodolite position in Angle Capture*

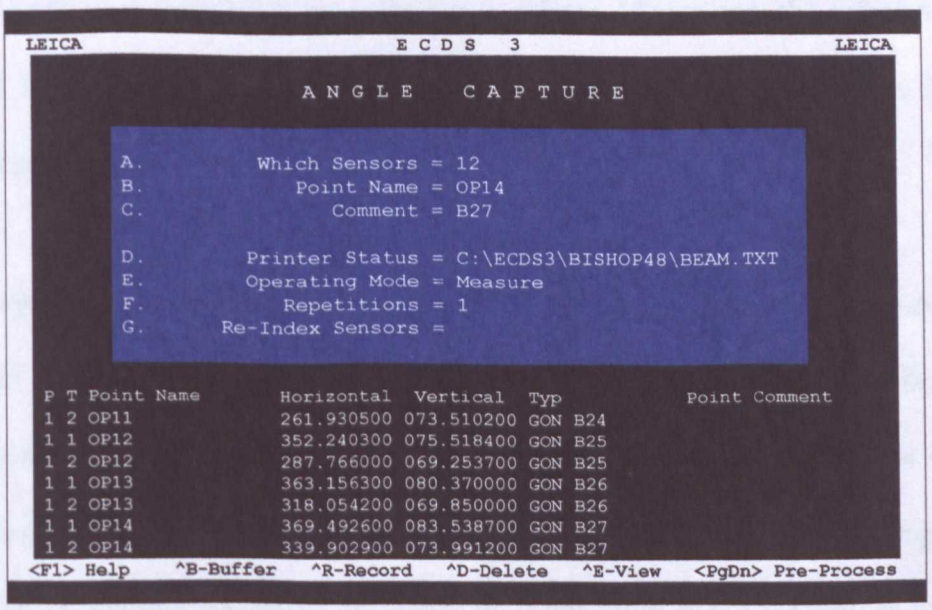

Figure 5.18 *Angle Capture during survey at Bishop Hannington*

the position of theodolite 2 is shown in the second Angle Capture screen of figure 5.17. Theodolite 2 is turned, an approximate pointing is made towards theodolite 1 and the distance between them is estimated and entered. This distance does not have to be exact but the better the guess, the sooner the bundle adjustment will converge.

After the procedure to estimate the orientation of the theodolites has been completed, all the scale bars and pass points (bundle points) defined in the Orientation Parameters are intersected and horizontal and vertical directions to these recorded. The main Angle Capture screen for this is shown in figure 5.18. On this, the printer status on line *D* shows, for the example given, that all data will be routed to a text file C:\ECDS3\BISHOP48\BEAM.TXT specified during Project Definition rather than to a printer. If required, the information sent to any text file can be printed at a later time. An example of a fully observed Angle Capture file (BEAM.CAP) is shown in Appendix B.

Following Angle Capture, a bundle adjustment is performed and commences with *Pre-Process.* This program computes the fictitious photo coordinates required for each observation (see section 4.3) and this normally takes very little time. Assuming Pre-Process is successful, the *Bundle Adjustment* program is started and this eventually computes the orientation of the theodolites in the local coordinate system using the observations taken to the scale bar and bundle points. For the surveys carried out at each glulam site, the results of the bundle are the orientation parameters of theodolite 2 (ω_2, ϕ_2, κ_2, X_{T2}, Y_{T2}, Z_{T2}) and the local *XYZ* coordinates of all the scale bar and bundle points sighted.

Using an estimated position for theodolite 2 based on the axis and position approximations carried out during Angle Capture, Bundle Adjustment first computes initial values for the coordinates of all the bundle points observed. The display obtained for this is shown in figure 5.19 and the program stops to show this screen for each point in the bundle. On the same line as the point intersected is identified, an *RMS* error is displayed which shows the difference between the *Z*-coordinates for that point computed from each theodolite: these are used as a guide to the quality of the observations made to the bundle points. Since the intersection of each bundle point is based on an estimated position for theodolite 2, a large *RMS* value does not necessarily mean that the observations to that point are bad and the way in which these have been interpreted is to compare the magnitude of each one in relation to all the others obtained. If these are similar, then the observations are assumed to be good although systematic errors are present that will be expected to be removed once theodolite 2 is accurately positioned. If one or more values are very different to all the others, the observations to these bundle points may be poor. So, from a practical point of view, the magnitude of the *RMS* errors obtained for the approximations is not important, but consistency of their magnitude is. In practice, comparing the *RMS* errors for each point observed in a bundle in this way has not always highlighted poor sightings as these are not only a function of sighting errors but also a function of the distance to a bundle point from the theodolite baseline. Even though ECDS3 provides the *RMS* values for the bundle approximations, a better check on the quality of the observations made to the bundle points can be done after Bundle Adjustment is finished in the Online Measurement program.

Assuming the *RMS* values are accepted for the observations, ECDS3 will use the initial estimates for the bundle coordinates and theodolite positions to check how well these fit the condition equations that describe the network observed. As described in section 4.3, a set of corrections to the initial estimates is computed based on the principle of least squares and the computation starts all over again with the updated estimates. This iterative process is repeated until the corrections become small enough to ignore and the final corrected estimates give the exact position for theodolite 2 and all the bundle point coordinates.

When the Bundle Adjustment program is selected, the iterations run quickly past on the screen and when the solution converges, the display shown in figure 5.20 is obtained. ECDS3 produces an assessment of the accuracy of a bundle adjustment when it is completed in the form of two *RMS* values called the total *RMS* and the maximum *RMS* for the adjustment. The total *RMS* is a measure of the amount by which the lines of sight in the bundle miss one another as a distance from each line of sight to the best fit points and is computed as an 'average error' for all the bundle points. The maximum *RMS* indicates the greatest sighting error in the adjustment. The size of these depends on many factors but mostly the number of theodolites used, the number of bundle points sighted, how well these have been sighted and the quality of the targets. Arbitrary limits of 0.1 mm were set for these *RMS* values when using ECDS3 as a means of flagging any large errors that might occur.

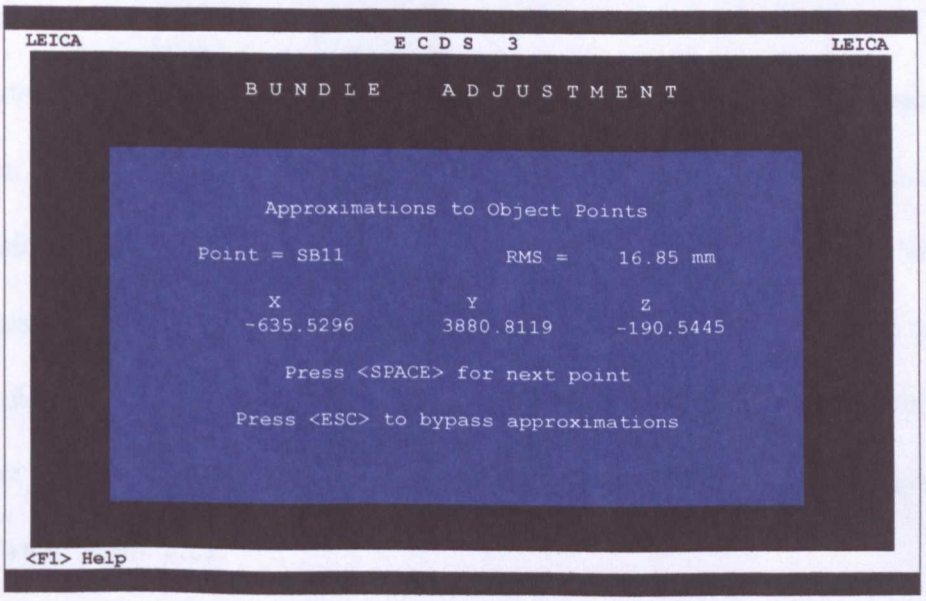

Figure 5.19 *Bundle approximation screen*

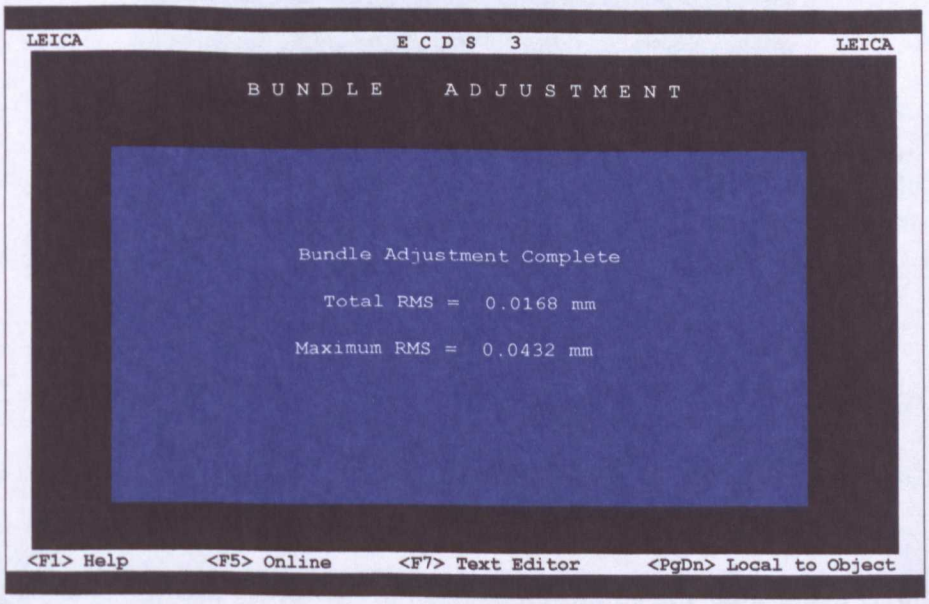

Figure 5.20 *Successful bundle adjustment*

The *RMS* values obtained in any adjustment were not taken to represent the actual errors produced but were taken as a measure of the reliability of the bundle adjustment only. In this sense, the *RMS* values were useful for detecting gross errors and in assessing whether a converged bundle had been achieved satisfactorily. This was done by observing bundles with a small number of points to start with (say 5 or 6), performing the adjustment, adding two more bundle points, repeating the adjustment and so on until the *RMS* errors stabilise. A set of maximum *RMS* bundle errors obtained in this way at Wokingham is shown in figure 5.21.

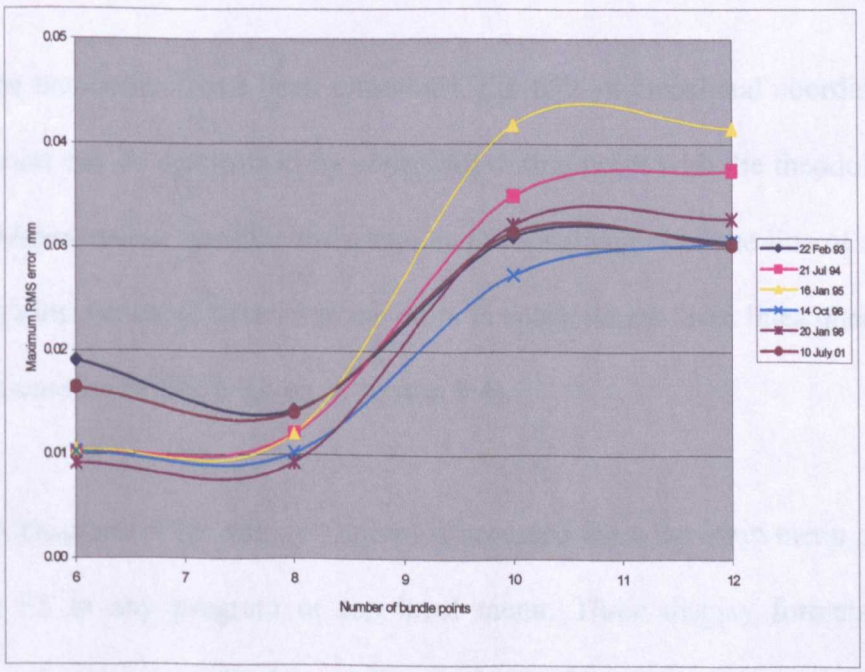

Figure 5.21 *Typical Variations of maximum RMS bundle adjustment errors at Wokingham. The increase between 8 and 10 points is caused by sighting targets towards the ends of Beams 3 and 8.*

On some occasions, a bundle adjustment has failed. This was usually due to a gross sighting error such as one operator observing the wrong point. Once identified, the incorrect observation was immediately re-observed and the

bundle repeated. Sometimes, a bundle adjustment would not converge, or the *RMS* values could not be reduced within tolerance and there was no obvious reason for this. When this happens, the bundle is abandoned and the whole procedure starts again from the Project Definition stage with new file names.

An example bundle output (BEAM.OUT) file is shown in Appendix B.

None of the other programs in System Orientation shown in figure 5.15 have been used.

Online Measurement

When the theodolites have been orientated, the three-dimensional coordinates of any point can be determined by observing to that point with the theodolites. *Online Measurement* uses the horizontal and vertical angles of the line of sight from each instrument to determine the point in space where these lines intersect (a full discussion of this is given in section 4.4).

Online Measurement (or simply Online) is accessed from the main menu or by pressing F5 in any program or top level menu. Three display formats are possible: the primary display which is used for most applications, the coordinate display in which only the intersection coordinates are shown and the angle display in which only the theodolite angles are shown. The display that has been used for the glulam monitoring has been the primary display and this is shown, for a typical pair of observations at Bishop Hannington, in figure 5.22.

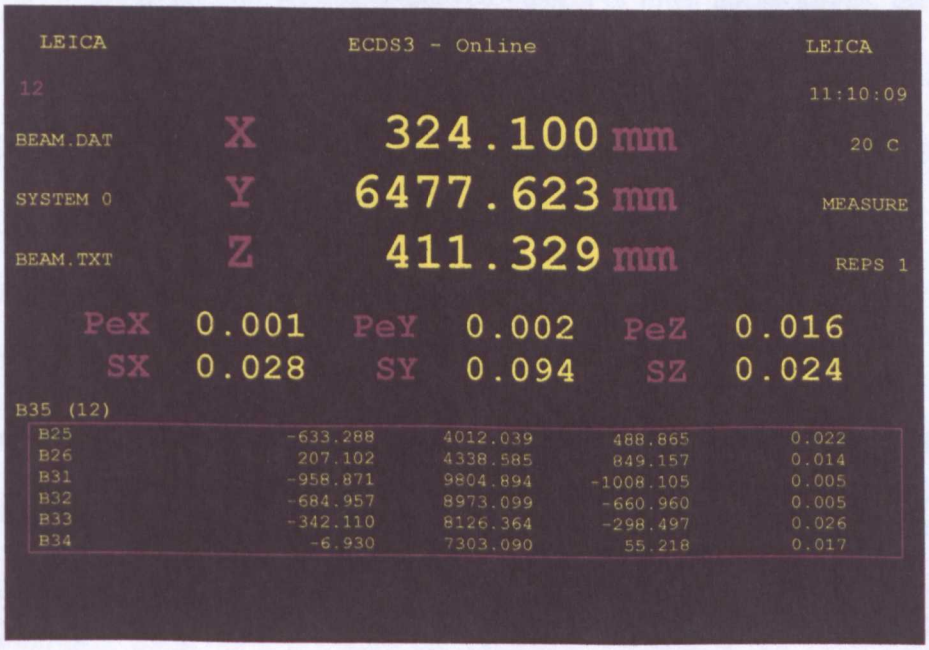

Figure 5.22 *ECDS3 Online screen*

The *XYZ* coordinates of the most recent intersection computation are displayed, with the statistics of the intersection shown below these. The top set of statistics, *PeX*, *PeY* and *PeZ* are the axial components of the *RMS* sighting errors for the intersection (these are defined in more detail in section 4.4) which describe how well the lines of sight intersect and they are used to assess the quality of an intersection. A tolerance of 0.05 mm was set arbitrarily for these: anything bigger would be highlighted on-screen as it was observed and the reasons for this could be investigated. As with the bundle adjustment, these numbers were only used as a measure of quality and not as the actual errors present in coordinates. A second set of numbers, *SX*, *SY* and *SZ* are also displayed and these are the a posteriori estimates of the standard deviations of the intersection coordinates on display but computed assuming a fixed accuracy of 1″ for angular measurement. Consequently, the *SX*, *SY* and *SZ* values are merely shown for information only and have nothing to do with how well the

lines of sight of the intersection displayed meet. For most intersections, the *SX* and *SY* values have been found to be much larger than the *PeX* and *PeY* values obtained but the *SZ* and *PeZ* values are often much closer. The reason for this is the low redundancy in a two-theodolite intersection.

Ignoring the low values of *PeX* and *PeY* usually obtained, the *PeZ* value has been found to be the critical statistic. A value of less than 0.05 mm is normally obtained at the first sighting of a target but if larger, the intersection is re-observed on-line until a satisfactory value results. At first with ECDS3, some resistance was experienced using software to improve theodolite pointings in this way but this was soon overcome when it was realised how effective ECDS3 is when managing online intersections. However, despite the advantages of software control on observations, the final results have always ultimately relied on the integrity of the observers and sometimes poorer results than desired (those with *P* values exceeding 0.05 mm) have been recorded.

At the bottom of the Online screen is a rectangular box. This is used to display the six most recently measured points and is a window into the DAT file created by ECDS3. A complete example of one of these files is shown in Appendix B and it is the data in these that is transferred to Excel files for further processing (see section 8.1).

Special Functions

This option in ECDS3 consists of a number of programs analysing various geometric functions. The only one used during any glulam monitoring has been

the *Lines* option which has been used, at the start of Online Measurements, to compute the length of a scale bar that has been observed in a check position. This use of a scale bar for checking the accuracy of an ECDS3 set up is discussed further in sections 7.5 and 7.6.

Text File Editor

The text editor allows any ECDS3 file to be viewed and altered. This has only been used occasionally during the glulam project to edit items such as point names when these have been incorrectly entered and spelling mistakes that were unnoticed before being recorded.

6

MONITORING OF GLULAM SITES

As already discussed in chapter 2, in order to assess the correlation between creep data from laboratory tests and those from full-scale structures, a measurement programme to monitor glulam beams at several sites was initiated by STRU in 1992.

Before any work started it was evident that, compared to laboratory tests, measurement of the deflections of glulam sections in situ with a theodolite intersection system from the time of construction could cause substantial problems. For example, the theodolites would have to be set up in stable positions without being disturbed whilst taking measurements and it was expected that site conditions would not be well suited to this. Furthermore, it was considered important that monitoring should start with each structure unloaded and should continue as decking and a roof covering in the form of tiles or slates was applied: it was expected that this might be difficult to accomplish. As well as this, it was desirable to monitor buildings comprising simply supported beams where possible and it might be difficult to locate and gain access to appropriate sites for this.

In spite of all these potential problems, the method proposed of using a theodolite intersection system to determine *XYZ* coordinates at selected points on glulam rafters and to determine deflections from these was thought

appropriate. At present, monitoring has been carried out in three new buildings and one older building. The first two buildings to be monitored were more complicated than was desired and are an extension to Wokingham Baptist Church in Berkshire and a new swimming pool at Shoreham in West Sussex. These were the only suitable buildings found to be available during the summer of 1992 and have already been briefly described in section 2.7.

6.1 Church Hall, Wokingham

Permission to monitor at Wokingham Baptist Church was obtained from Alastair Watson, the architect for the project, Luff Contractors and the Church Authorities in September 1992. Technical Timber Services Ltd, who designed and built the glulam frame also offered their support to the project.

The front of the extension to the existing church at Wokingham is shown as proposed and under construction in figure 6.1. Within this, the exposed glulam rafters situated above the second floor are monitored and these form a complex, asymmetric pitched roof supported by masonry walls having a plan area of 16 x 11 m as shown in figure 6.2. The hip rafters are of typical size 115 x 450 mm spanning approximately 5 m on plan at a pitch of 22.2°, interconnected by members of smaller section. All connections are made by bolted steel plates which, together with the three-dimensional shape, produce a structure of considerable rigidity. No special surface protection was applied to the glulam beams during construction apart from the initial coat of varnish which was applied off-site before delivery of the beams.

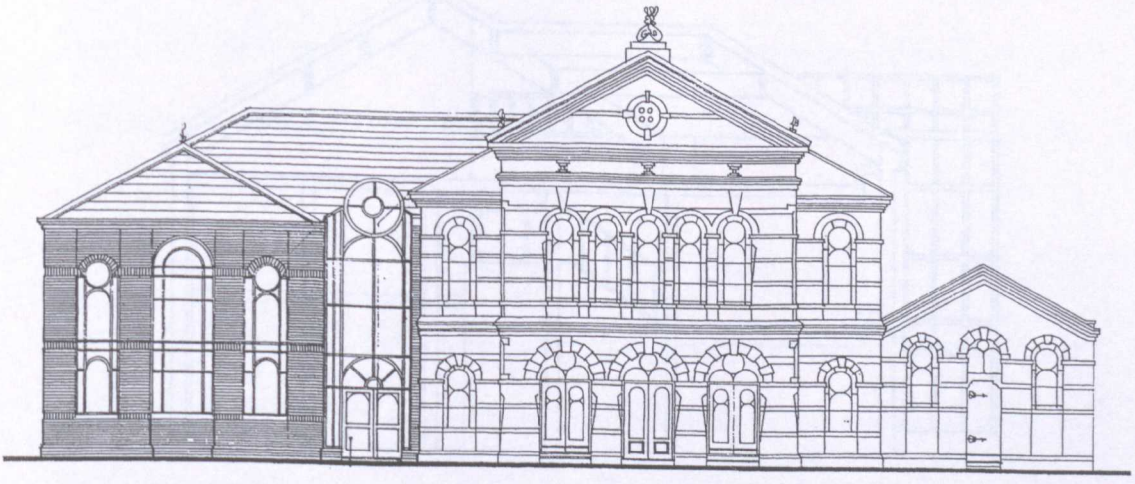

Figure 6.1 *Extension to Wokingham Baptist Church*

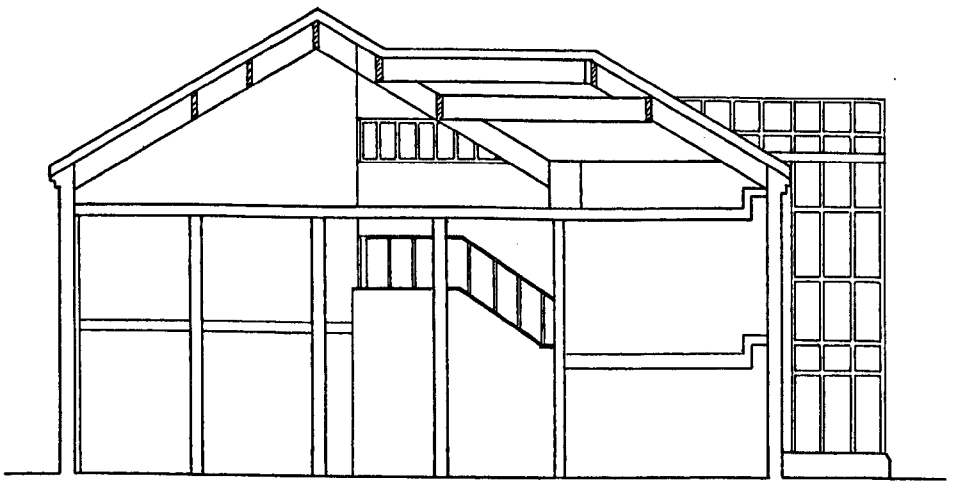

Sectional view of extension
(the glulam beams monitored are shown located in the roof space)

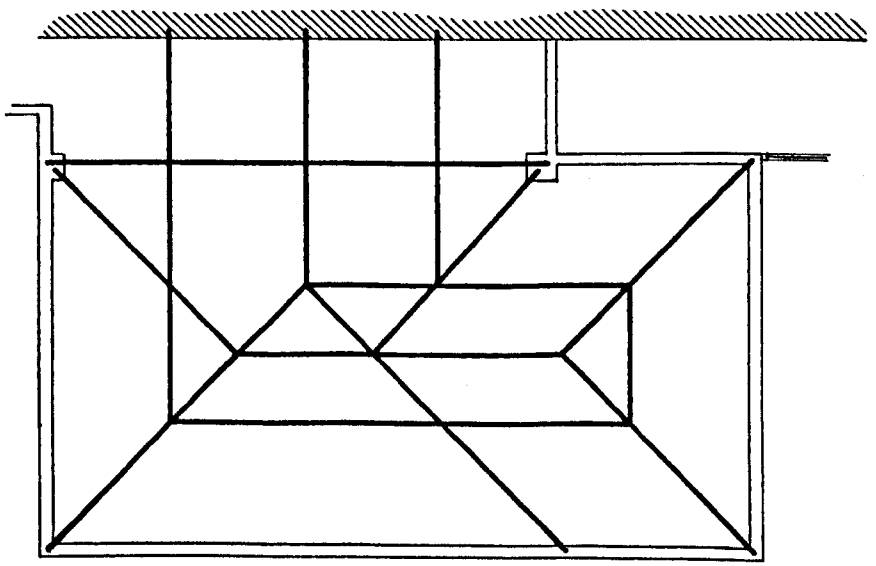

Plan view of 16 m x 11 m roof structure

Figure 6.2 *Details of extension to Wokingham Baptist Church*

The glulam frame was erected and the tongue and groove decking applied in mid-October 1992. No monitoring of the frame before and after initial loading with the decking was possible for the following reasons. First, there was no suitable access to the second floor because the concrete stairs had not been cast and second, access was denied for safety reasons until the decking was attached.

During October 1992, the measurement programme was planned and several practical issues had to be resolved before observations commenced. The first of these was to decide which rafters were to be monitored: this choice was governed by a number of factors but primarily the need to observe a selection of different (large preferably) beams in as short a period of time as possible whilst on site. This dictates the positions the theodolites were to occupy in relation to the beams which in turn establishes the geometry of the intersections and the accuracy expected for three-dimensional coordinates. All of these in relation to the site at Wokingham are discussed in sections 7.2 and 7.3.

For any monitoring scheme based on optical methods, the type of target that is to be used has to be considered in some detail. For theodolite intersection, the need for clear, unambiguous and precise targets is vital if accurate observations are to be achieved and a number of different types were available at the time. These included (see Mulder, 1989)

- a selection of obvious points (for example bolt heads, punch marks)
- plane self adhesive targets with a pattern superimposed

- solid (mechanical) targets with conical or spherical shapes for omni-directional observation
- a laser light source (independent of the theodolites)
- a laser eyepiece fitted to one of the theodolites

At Wokingham, Alastair Watson, the architect responsible for the contract was adamant that nothing should be attached to the structure that was considered to be permanent or obtrusive in any way: this meant that the use of solid targets was unacceptable. Laser light sources were also of no use because the same target positions had to be intersected each time a survey was carried out. After some discussion, it was agreed that self adhesive targets provided by Leica could be used (see figure 6.3) but with the proviso that the architect or

Figure 6.3 *Leica 'stick-on' target*

contractor could, for whatever reason, remove them at any time. With hindsight, it can be said that these have proved to be a good choice of target as they have withstood, over a long period of time, a wide range of environmental conditions without deteriorating in any way.

Having decided on the type of target to be used and which rafters to monitor, the number of targets to be placed on the rafters had to be chosen. The critical

points to be monitored are both ends and the centre of each beam but it was thought that additional measurements should be taken at points in between these, the number of extra targets depending on the length of a beam. This would provide a complete picture of the behaviour of each beam monitored, if required, and taking readings to more than the minimum number of targets would not involve a great deal more fieldwork. Five targets were placed along the full length of the shorter beams and seven on the longer giving a target separation of about 1 m (see figure 6.4). Most of the targets were easily attached by standing at floor level, but the higher beams had to be accessed by ladder (see figure 6.5).

Of equal importance as the targets is their illumination and this has been provided very effectively (at all sites) by a stand-mounted 500 W halogen lamp. Without this, taking observations would not have been possible to some targets: the lamp can be seen in the various photographs of the sites shown throughout this chapter.

Monitoring started at Wokingham on the 10 November 1992. At this time, the decking had been attached to the roof frame and it was partially covered with slates making it possible to take some observations to the rafters before all of the initial loading was applied. A complete list of all the surveys carried out to date at Wokingham Baptist Church is given in Appendix C which shows that the roof was finished between the 17 and 23 November 1992. From this, it is assumed that the initial elastic load had been fully applied at the time of the survey on the 23 November 1992.

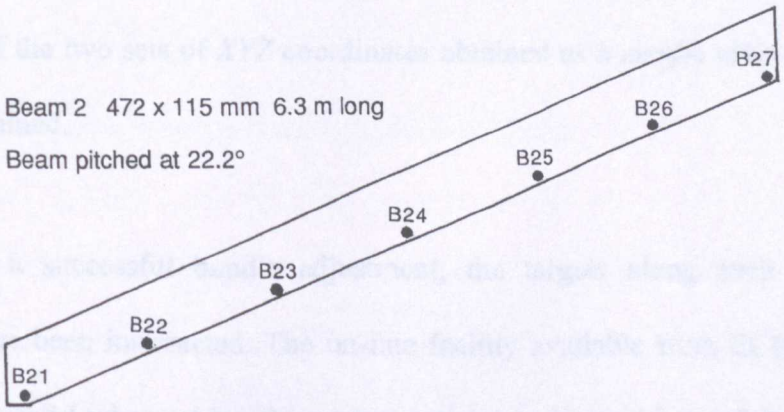

Figure 6.4 *Layout of targets for Beam 2 at Wokingham*

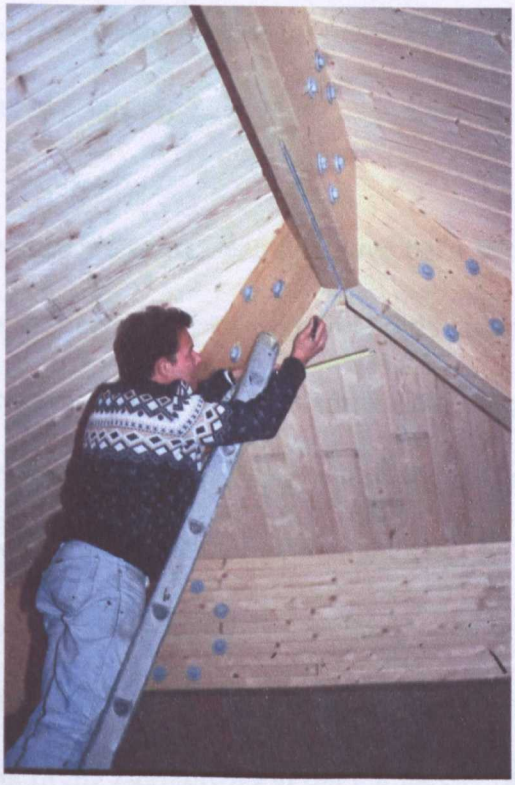

Figure 6.5 *Attaching targets to elevated beams at Wokingham*

For each survey at Wokingham, a bundle adjustment has been performed using a scale bar and up to 10 or 12 selected beam targets. The bundle points have been chosen so as to 'box in' and spread through all of the rafters and have been kept at the same locations throughout the monitoring programme. These

are points already targeted on the beams and, because they are observed a second time after the bundle adjustment has been completed, a comparison can be made of the two sets of *XYZ* coordinates obtained as a simple check on the results obtained.

Following a successful bundle adjustment, the targets along each glulam section have been intersected. The on-line facility available from ECDS3 has been very useful when taking these observations as it provides real-time *XYZ* coordinates with an indication of their precision. This has enabled any gross errors to be removed (for example, one observer sighting the wrong target) and has also enabled poor sightings to be redone.

In addition to these measurements, readings have been taken with a resistance type moisture meter to a series of stainless steel pins inserted into Beam 6. As well as this, a relative humidity/temperature data logger is permanently installed in the room in a discreet position out of sight. This is changed every six months for downloading of environmental data. To calibrate this data, further measurements are taken of relative humidity and temperature whilst on site with a dual-purpose Protimeter and all this data is in turn calibrated against reference meters kept in the laboratories at the University of Brighton.

During construction, many difficulties were experienced on site attempting observation of the rafters. Generally, some building work was usually being carried out on the second floor of the extension or close by. This tended to distract the observers and often led to poor results being obtained which had to

be repeated. Sometimes, when a major part of the construction work was in progress, the floor or the roof of the extension would vibrate. In such circumstances, it was not possible to take observations and some bundle adjustments became unstable and had to be abandoned.

At the start of the measurement programme at Wokingham, the theodolites were mounted on industrial stands (see section 7.1 under *Stability*). Without any doubt, these provided the best platforms possible for the instruments when on site but their weight and size made them very difficult to transport. At Wokingham, the stands had to be carried through the entrance to the site and then up two flights of stairs which sometimes had obstructions in front of or across them, as shown in figure 6.6.

On one occasion, having managed to install the stands on the upper floor and take the required observations, when it was time to leave the site, it was

Figure 6.6 *Obstructions to entrance at Wokingham*

discovered that a trench had been dug across the exit (see figure 6.7). No amount of forward planning could have avoided this and the stands had to be manhandled across the trench and spoil to be loaded for transportation back to Brighton.

Figure 6.7 *Extreme difficulties removing stands from Wokingham*

The problems associated with the industrial stands at Wokingham were initially overcome by having permission to leave them permanently on site on the second floor and another pair of stands was purchased to use at other sites. At present, industrial stands are not used and have been replaced with industrial tripods (see section 7.1 under *Stability*). These are extremely robust, are easy to transport and set up and have never, in several years use, ever shown any tendency to become unstable and lead to poor results being obtained. Looking back, these might have been purchased at the start of the project and their use is strongly recommended with any theodolite intersection system where moving and placing industrial stands is a problem.

Following completion of construction and hand over of the extension in March 1993, observations have proceeded with little difficulty at Wokingham. Currently, four visits are done each year: in January, April, July and September. At present, the room is never occupied at the time readings are taken and there are no problems with access or with obstructions in the room. Two contrasting views in figure 6.8 show ECDS3 set up in the same positions on the second floor of the extension at Wokingham both during and after construction.

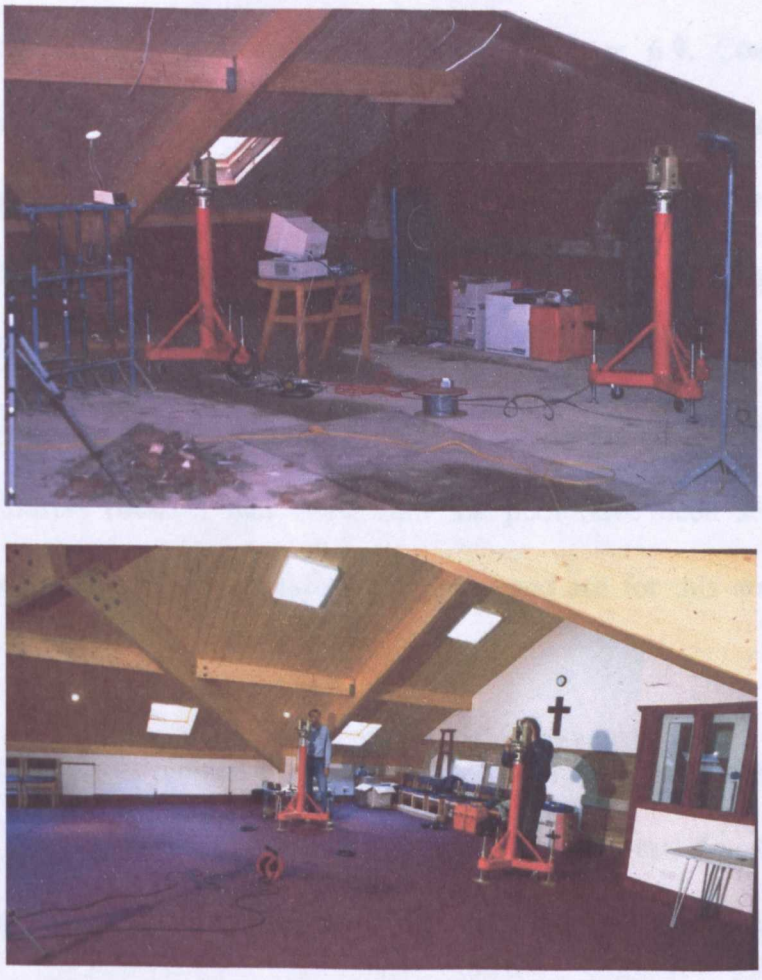

Figure 6.8 *ECDS3 at Wokingham during and after construction*

This site is referred to as *Wokingham* or *Wokingham Baptist Church* in the following chapters.

6.2 Wadurs Swimming Pool, Shoreham

Permission to monitor at Shoreham was obtained from WyncoteDevelopments, Adur District Council and the contractor, Hall and Tawse Southern Ltd, in December 1992. The designers and constructors of the roof, the Gyoury-Self Partnership and Technical Timber Services Ltd respectively, also offered their support to the project.

This building is shown in plan and section in figure 6.9. Compared to Wokingham, this is a simpler but larger structure, consisting of masonry walls supporting a double pitched roof, the rafter layout being symmetrical. The loadings, though, are asymmetrical owing to the presence of the upper plant room bearing onto the rafters at about midpoint on one side. The rafter size is 140 x 405 mm, spanning approximately 6 m in plan at a pitch of 30°. Eight of the main rafters (beams) that cover half the pool have been selected for monitoring: details of the theodolite positions used are for this are given in sections 7.2 and 7.3.

The glulam roof was erected during December 1992. Attaching targets to this proved to be very difficult because of its size. Realising that this might be a problem, an attempt was made at the time of construction to attach targets to the glulam sections whilst they were stacked on site before they were lifted in place and fixed to the roof. Figure 6.10 shows this taking place. As at Wokingham, self adhesive targets were to be used and attached to the beams but at approximately 1.5 m separations in this case. When delivered to site, each glulam section was covered in black plastic and inside this they were

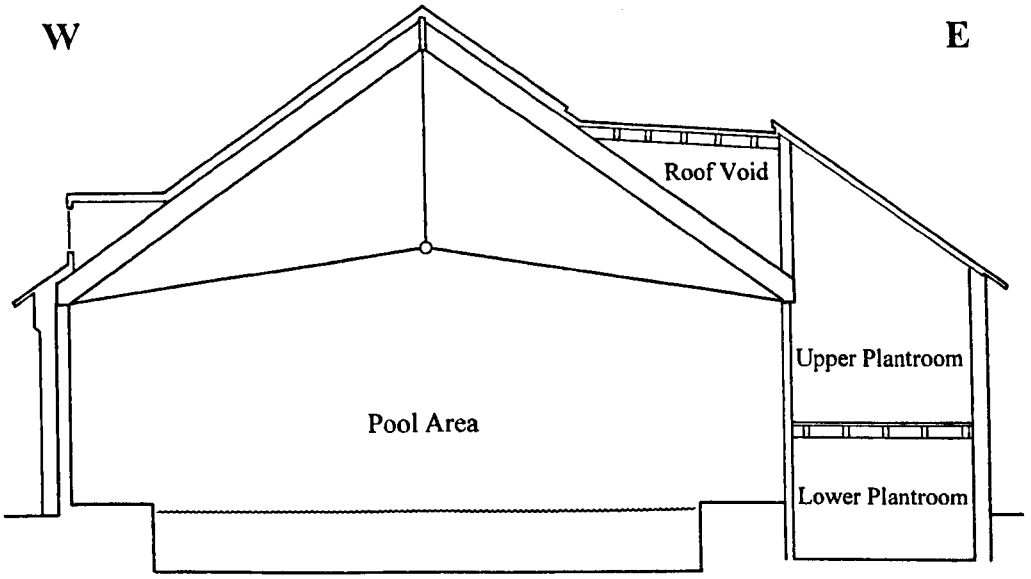

Sectional view

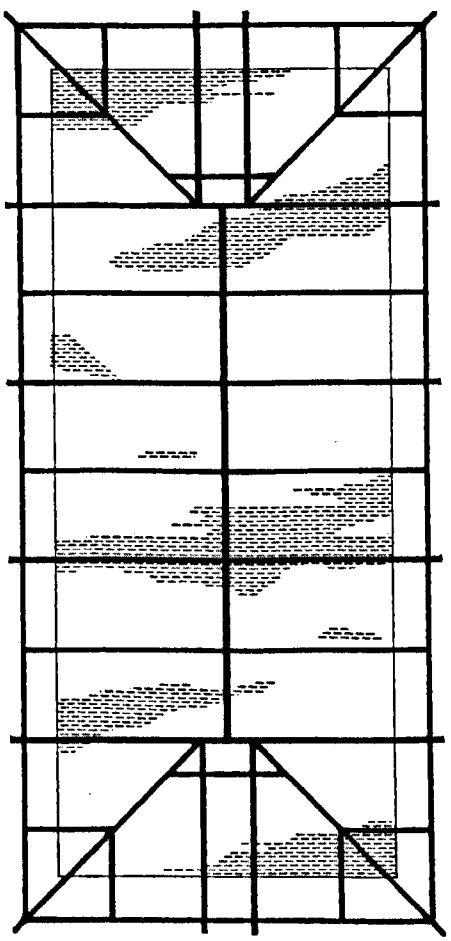

Plan view of roof structure over 25 m x 10 m pool
(not at same scale as section)

Figure 6.9 *Wadurs Pool Shoreham*

quite damp. This made attaching the targets difficult but not impossible and slowed down the speed at which they could be placed on individual sections to the extent that this was holding up the construction crew. Consequently, this had to be abandoned after only about three or four sections had been lifted and fixed in place. This meant that the remainder of the targets had to be attached to the rafters after the roof had been fully erected and scaffolding placed around it. This was a much more difficult task as shown in figure 6.11 but in spite of this, a full set of five targets was attached to eight rafters at one end of the finished frame.

Figure 6.10 *First attempts attaching targets at Shoreham*

Figure 6.11 *Attaching targets at Shoreham after roof frame erected*

Unfortunately, immediately after the roof had been erected and for safety reasons, it was not possible to have access to the building and to take observations of the unloaded structure. Just prior to Christmas 1992, the decking was added to the rafters as shown in figure 6.12 but access to the site was only eventually allowed in the New Year and monitoring started in January 1993. All surveys carried out at Shoreham to date are listed in Appendix C.

At the commencement of monitoring, no further load had been added to the roof which was completed and fully loaded between January and March. During this period, five surveys were carried out on the roof. For those surveys up to the 1 February, the scaffolding erected in the pool area made observations to the top target on each rafter impossible (see figure 6.13) and these had to be omitted from the observation programme. With the scaffolding in place in the pool, the exact positioning of the theodolites was quite awkward and several attempts were often needed to obtain unobstructed lines of sight to all of the targets. When the survey of the 11 February was carried out, the scaffolding had been removed and all targets were visible (see figure 6.14).

Similar to Wokingham, a relative humidity/temperature data logger has been permanently installed at Shoreham and moisture readings are taken with a resistance meter each survey to a set of stainless steel pins in one of the beams. Throughout the early observation period at Shoreham, similar problems to those at Wokingham were experienced with transportation of the industrial stands to and from the site. However, these difficulties have been overcome by using industrial tripods instead of the very cumbersome stands.

Figure 6.12 *Decking attached to roof at Shoreham*

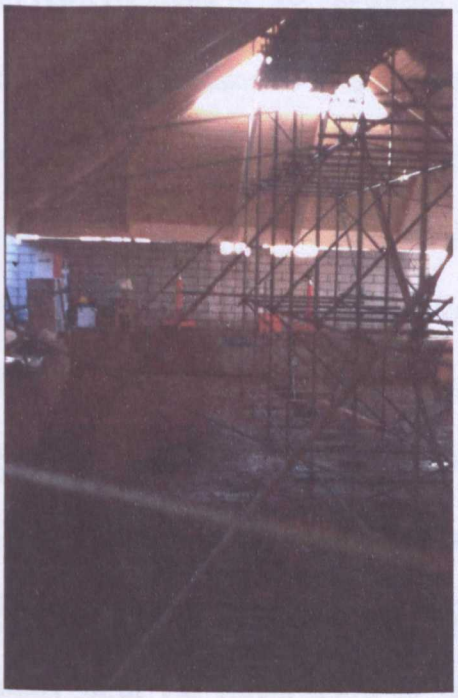

Figure 6.13 *Scaffolding obstructing lines of sight*

Figure 6.14 *View of Shoreham during construction*

Unfortunately, no further surveys were carried out from March until May 1993. During the gap since March, all the targets attached to the rafters in the previous December had been removed by the contractor prior to varnishing. If monitoring was to be continued at Shoreham, these had to be replaced. By chance during May, a temporary scaffolding was in place in the empty pool (see figure 6.15) and with the aid of this, all of the targets were replaced on the eight rafters monitored. Following this, surveys were completed in May and June at which time the pool was officially handed over by Hall and Tawse Southern to Adur District Council. During the next few months, difficulties were experienced obtaining permission from Adur District Council to continue monitoring in the (now) operational pool. This was finally agreed and monitoring has continued from November 1993 to date uninterrupted. At present, two surveys are done each year in January and July. Monitoring with ECDS3 in the finished pool is shown in figure 6.16.

Figure 6.15 *Temporary scaffolding used for attaching new targets*

Figure 6.16 *Monitoring at Shoreham after construction*

This site is referred to as *Shoreham* or *Wadurs Pool Shoreham* in the following chapters.

6.3 Community Health Centre, Moulsecoomb, Brighton

Permission to monitor at this site was obtained from Michael Blee Design, the architect for the Centre, Wiltshier Construction Specialists Ltd, the contractor and South Downs Health NHS Trust in March 1994. The designer of the glulam structure, Chatco Ltd, also offered their support for the project.

This structure consists of a quadrangle of timber panelled rooms with a square open courtyard in the middle. A corridor 2.4 m wide runs alongside the rooms next to the courtyard and the main timber roof over the rooms is pitched (see figure 6.17). The roof rafters are supported by vertical posts which transmit the roof load to horizontal paired beams that are continuous over and simply supported by a number of timber columns, as shown in figure 6.18. Next to the courtyard, a short span of 2.4 m of the paired beams covers the corridor, the roof is flat (see figure 6.19) and the heavy uniformly distributed load provides a partial counterbalance to the concentrated load from the main roof.

Four identical paired beams, two in each of the main rooms, have been selected for monitoring. The glulam sections are made up of two 65 x 270 mm paired beams of approximately 4.5 m span. Five Leica self adhesive targets have been attached to each set of paired beams monitored at about 1 m spacing. A relative humidity/temperature data logger has also been installed together with moisture content contact pins.

Figure 6.17 *Roof over rooms monitored at Moulsecoomb*

Figure 6.18 *Loading arrangement of Beams 3 and 4*

Figure 6.19 *Extension of Beams 3 and 4 into courtyard*

Monitoring started at this site on the 6 May 1994 and the procedures used for this are described in sections 7.2 and 7.3.

The first measurements were taken with the beams completely unloaded, see figure 6.20, which also shows some of the survey equipment in place. Conventional survey tripods were used at first since it was not possible to use industrial stands at this site but these have now been replaced by industrial tripods. The use of conventional tripods was justified on the grounds that each observation period was only 30 minutes. From the 6 May 1994, surveys were taken with the roof load applied in various stages (see figure 6.21) until it was completed in June (see figure 6.22).

The Health Centre was finished and handed over to the South Downs Health NHS Trust in October 1994 and uninterrupted measurements took place in Rooms 4 and 5 until December 1998. Immediately following this, some interior building alterations were completed and Room 4 was divided into two rooms with the result that Beams 1 and 2 were boxed in and it was no longer possible to monitor these. Measurements have continued in Room 5 only (Beams 3 and 4) since January 1999 with four visits a year in January, April, July and September. All surveys carried out at to date at Moulsecoomb are listed in Appendix C.

This site is referred to as *Moulsecoomb* or the *Moulsecoomb Health Centre* in the following chapters.

Figure 6.20 *Set-up for first measurements at Moulsecoomb*

Figure 6.21 *Measurements with intermediate roof load*

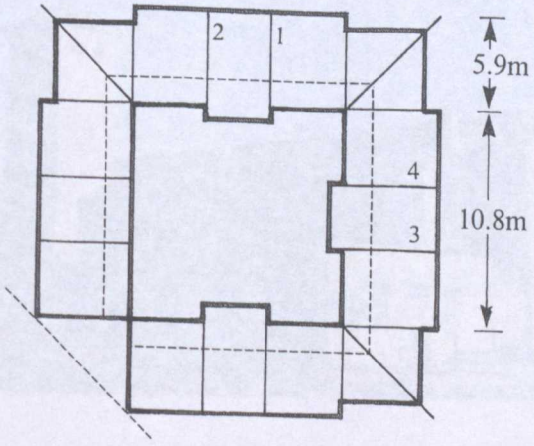

Figure 6.22 *Layout of rooms and glulam beams at Moulsecoomb*

6.4 Bishop Hannington Church Hall, Hove

The meeting hall at Bishop Hannington Church was constructed in 1982 and was chosen for monitoring to determine how older structures are subjected to continuing creep, whether due to the effect of load or environmental (mechano-sorptive) behaviour. Compared to the previous sites, obtaining permission to take measurements at Bishop Hannington Church was relatively easy and all that was necessary was to explain to the Church Warden the nature of the work that would be done, what would be attached to the beams in the hall and how frequently surveys would take place. All of these proved to be acceptable and consent was given to commence monitoring after a single visit to the Church.

The single storey hall is approximately 23 m x 12 m in outside dimensions with masonry walls and columns supporting a flat timber roof, as shown in figure 6.23. Glulam beams with section 130 x 480 mm act as the main structural members and they are simply supported with a span of 10.0 m.

Figure 6.23 *Bishop Hannington Church with the hall in the foreground*

Any number of beams could have been monitored in the hall and two were chosen as shown in figure 6.24. Seven self adhesive targets have been attached to each beam at about 1.5 m centres and the usual relative humidity/temperature data logger and moisture pins have been installed.

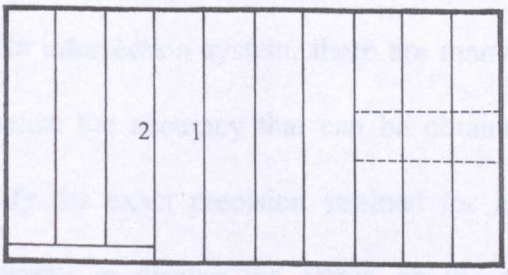

Figure 6.24 *Positions of beams monitored at Bishop Hannington*

Observations started at this site on the 5 July 1995 and have proceeded uninterrupted with little difficulty. All of the surveys completed to date are listed in Appendix C from which it is seen that four surveys are carried out each year: usually in January, April, July and September. The ECDS3 equipment is shown set up at Bishop Hannington Church in figure 6.25.

Figure 6.25 *ECDS3 at Bishop Hannington*

This site is referred to as *Bishop Hannington* or *Bishop Hannington Church* in the following chapters.

7

ASSESSMENT OF THE ACCURACY OF THEODOLITE INTERSECTION SYSTEMS

For any theodolite intersection system, there are many interdependent factors which will influence the accuracy that can be obtained and it is often very difficult to specify the exact precision attained for intersection coordinates. This chapter attempts to discuss the effect, on the monitoring done at the glulam sites described, of all the sources of potential error in theodolite intersection and an estimate of the accuracy that has been achieved with ECDS3 is given.

In Chapter 2, a standard deviation of 0.1 mm was specified for the determination of vertical deflections derived from coordinates. If the standard error of each *Z*-coordinate obtained from ECDS3 is assumed to have a maximum value of σ_V and if a vertical deflection, given by the difference of two of these coordinates, is to have a standard error of 0.1 mm this is related to σ_V as $0.1^2 = \sigma_V^2 + \sigma_V^2$ mm^2 or $\sigma_V = 0.07$ mm. So the precision required for *Z*-coordinates in the glulam project has to be slightly better than the 0.1 mm quoted for vertical deflections.

7.1 The practical nature of accuracy

The way in which a theodolite intersection system is set up and used can vary considerably in practice. The effect of this on the accuracy obtained is

discussed in this section together with the practical measures that have been taken to obtain optimum results.

Choice of theodolite

For any theodolite intersection system, this is one of the most important factors affecting the accuracy of the results obtained and must be chosen carefully. An electronic theodolite with a sub-second accuracy and dual-axis compensation was considered to be essential for the glulam project. The Wild T2002 has been chosen which has a quoted accuracy (for a direction measured once on both faces) of 0.5″ for the measurement of horizontal and vertical angles (see section 5.5). This was, in 1992, one of the highest specifications available for an electronic theodolite.

Pointing accuracy

A manual theodolite intersection system such as ECDS3 requires each operator to point and centre the reticle of the theodolites onto a series of targets. How well this is done correlates strongly with the accuracy achieved for intersection coordinates. Grist (1991) states that 'Tests have shown that under good conditions, it is possible to achieve a sighting precision of 1″ with a single pointing of a theodolite'. Similarly, Hölting (1995) quotes 'The standard deviation of a single measured angle [for ECDS3] is 0.5 mgon (1.5″) on average'. These figures are dependent on a number of factors including the precision of the theodolite used, the type of target intersected and the experience of the operators. In analyses of the accuracy of ECDS3, a figure of

1″ for the precision of a pointing is used by Leica and the ECDS3 software computes *SX*, *SY* and *SZ* using this pointing accuracy to indicate the precision expected for real-time coordinates (see section 5.6 under *Online Measurement*).

By increasing the number of pointings taken to each bundle and unknown point in a survey, the precision of a theodolite intersection system can be improved as a result of increasing the redundancy of measurement. An increase in the number of pointings can be realised in two ways: by taking more observations from a given number of theodolites or by using more than two theodolites.

If multiple pointings are to be included in an intersection survey, the extra fieldwork will usually involve taking repeated observations to all points on both faces of the theodolites. Taking observations to all points from three or more theodolites is a better way of increasing the redundancy and hence improving the quality of the results from theodolite intersection. As might be expected, both of these can be time consuming and can only be accomplished if there is sufficient time available whilst on site. In addition, few organisations can justify the expense of purchasing three or four theodolites and most employ two, as is the case here.

For all observations taken for the monitoring of the glulam sites described in chapter 6, time has been an important factor and, as discussed in section 2.5, the budget for the glulam monitoring only allowed two theodolites to be purchased. Consequently, observations have been limited to single pointings taken from single baselines with Wild T2002 theodolites.

Theodolite systematic errors

The *horizontal collimation error* in a theodolite is caused by a displaced vertical cross hair such that the line of collimation is not perpendicular with the trunnion axis. Industrial measurement creates particular problems because the magnitude of this error can vary as the focus is changed. High precision industrial theodolites are designed to minimise this variation but this error, for the Wild T2002, can increase at short distances of less than 2–3 m (Bayly, 1991). This can be a problem for close range measurement surveys and occurs when the focussing lens of the theodolite is not moved exactly along the optical axis, as might be the case at short focussing distances.

A *trunnion axis error* can occur in a theodolite when this is not perpendicular to the vertical axis and will cause errors in horizontal circle readings even when the theodolite is properly levelled.

Modern theodolites incorporate vertical axis compensators to ensure that all measured zenith angles are referenced to the local gravity vector (the vertical). In the T2002, a liquid compensator is used to achieve this and a *vertical circle index error* can arise when the compensator is not in exact adjustment. Again for the T2002, this has been shown to have a tendency to increase at short sighting distances of less than 2–3 m (Bayly, 1991).

All of these errors are eliminated by taking the mean of face left and face right circle readings.

A major source of error in theodolite observations is caused by not levelling the

instrument properly. This causes an *inclination of the vertical (or standing) axis* and will cause incorrect horizontal and vertical circle readings to be recorded that are not eliminated by taking readings on both faces of the theodolite. Using a theodolite with dual-axis compensation such as the Wild T2002 eliminates these errors since a dual-axis compensator will measure the vertical axis tilt in the longitudinal and transverse directions and will automatically correct horizontal and vertical circle readings for this. An outline of the principles of dual-axis compensation is given by Uren and Price (1994) and a detailed description of the Kern liquid compensator is given by Münch (1986).

Two more sources of error inherent in theodolites are *circle eccentricity and graduation errors*. Because the T2002 uses a dynamic angle measuring system, the circles are fully rotated during measurement and readings are taken at opposite sides of each circle and around the circumference of each circle thereby minimising to a negligible amount these sources of error (see Katowski and Saltzmann, 1983).

Is there a problem with single face readings?

For all work carried out with a theodolite intersection system, the possible systematic errors present in the theodolite observations need to be assessed and avoided where possible. As indicated, time constraints limited all of the measurements taken with ECDS3 for this project to single face even though the system can accommodate multiple observations on both faces of the theodolites. This gives rise to an interesting question: how is it possible to achieve precise results even when observations are only taken on one face and

collimation, trunnion axis and index errors are not accounted for?

For the T2002, values for these errors can be measured and programmed into the instrument which will then automatically apply corrections to every circle reading even if these are only taken on one face. However, it can be difficult to measure all of these parameters exactly and on a regular basis so the problem of long term drift or unexpected change in systematic errors still remains. For theodolite intersection systems using a bundle adjustment, it is claimed by Bayly (1991) and Staiger (1995) that the deviations in theodolite observations caused by systematic instrumental errors are absorbed into the bundle adjustment as random errors in the orientation procedure. In other words, the bundle adjustment biases the orientation parameters to account for collimation, trunnion axis and index errors and when single pointings are taken to intersected points, the effect of these errors are reduced. Staiger performs a number of tests with ECDS3 to confirm this by comparing so-called 'error-free' surveys with all instrumental errors removed to the same surveys carried out with theodolites which have known errors present. Another interesting outcome of this work is that Staiger also claims that theodolite instrumental errors for single face observations have much less influence on the accuracy obtained for intersection coordinates if the object is measured by two theodolites from one side of the baseline only. This is also confirmed by Leica (1993d), but this document stipulates that the theodolites used should have dual-axis compensation if this is to be done.

Since the work of Bayly and Staiger together with Leica confirm single face pointings are acceptable for ECDS3 in accounting for collimation, trunnion

axis and index errors and the T2002 theodolite has been used throughout, it has been assumed that theodolite systematic errors have had a negligible effect on the results obtained for intersection coordinates. In addition, it is also assumed that any small errors caused by instrumental effects are further reduced by taking the difference of two *Z*-coordinates to obtain deflections.

Targets

The accurate sighting of points on an object to be monitored or measured is essential if good quality results are to be obtained for theodolite intersection surveys and the choice of target can have a considerable effect on the accuracy of pointing.

Descriptions of the various targets possible are given in many publications, the most comprehensive being by Mulder (1989).

The importance of targets should not be underestimated and they have to be chosen to ensure that their size and type match the application. Section 6.1 gives details of the type of target chosen for the monitoring carried out at all the sites in the glulam project and also discusses its placement on the various structures involved.

Lighting

The illumination of targets for a theodolite intersection survey is as important as the choice and location of the targets themselves, mainly because most of the observations are taken indoors where the ambient light levels are low compared

to outdoors. For all observations carried out, a 500 W halogen lamp has always been used without which, some of the observations taken would have undoubtedly been of poor quality or it may not have been possible to take observations at all in some cases. It is always surprising how much light is required to be able to sight an indoor target even when the room lighting appears to be good. Although a stand mounted halogen lamp has been very effective and is recommended, other forms of lighting are possible and it cannot be overemphasised that indifferent or poor illumination of targets will have a considerable effect on the accuracy of the results obtained from theodolite intersection.

Stability

For any monitoring survey, it is always desirable to place theodolites and other instruments in stable positions whilst measurements are taken. This is even more important for a theodolite intersection system, where a high precision is expected. In order to ensure stable observing conditions are achieved, both the platform on which the theodolites are mounted and the surface on which these are placed must be stable.

The platforms used in close range and industrial surveying are permanent monuments, industrial stands, industrial tripods and conventional survey tripods.

Permanent monuments are the best type of platform but for the monitoring in this project, the use of these was completely out of the question because of site

conditions.

Leica supplied the University of Brighton with two *industrial stands* (see figure 7.1) as part of the ECDS3 package when this was delivered in 1992. Since all initial surveys were to be done whilst building work was in progress, it was decided to use the stands at Wokingham and Shoreham, the first two sites identified for monitoring. Not only would the stands provide a good platform for the theodolites, they would not slide on concrete floors and could not be knocked over accidentally in a busy work area. As reported in section 6.1, the stands were very effective in providing extremely stable observing platforms, but were very difficult to transport to all the different sites involved. The stands have been designed for use in factories where they can be wheeled easily from one workshop to another, but the author's experience was somewhat different having to move these around and across construction sites. Purchasing a second set of used stands helped ease this problem as one pair could then be left permanently on site at Wokingham and the other at Shoreham.

Figure 7.1 *Industrial stands at Shoreham*

For the initial observations at Moulsecoomb and Bishop Hannington, *conventional survey tripods* were used. The main reason for this was the difficulty in removing a pair of stands from either Wokingham or Shoreham and transporting them to the other locations. Before any monitoring was carried using conventional survey tripods, laboratory tests were carried out to check the stability of these under similar observing conditions to those expected on site. In the laboratory, a normal ECDS3 set-up was carried out but with the theodolites set on conventional tripods and a number of targets were intersected. After about 30-40 minutes, it was found that the pointing errors started to increase and eventually the set up became unstable. No such problems were encountered when the same tests were carried out using the industrial stands, even when these were tested over longer periods.

At both Moulsecoomb and Bishop Hannington, a small number of targets have been intersected compared to Wokingham and Shoreham, and the use of conventional tripods was assumed to be acceptable for the short observing times of about 30 minutes.

All of the problems associated with either industrial stands or conventional tripods have been eliminated by using *industrial tripods* (see figure 7.2). As discussed in section 6.1, these has been found to be the best solution as an observing platform, both from the point of view of stability and portability and they are currently used at all sites.

There is usually no choice of surface on which to place the theodolites for an engineering survey as this is restricted to site conditions. For Wokingham,

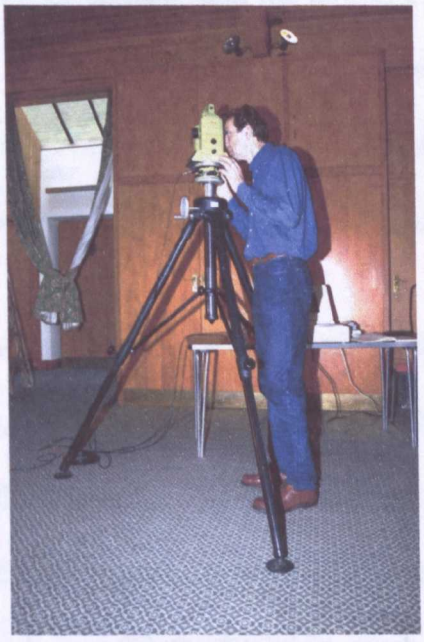

Figure 7.2 *Industrial tripod*

Shoreham and Bishop Hannington, work has been carried out directly on concrete floors or carpeted/tiled concrete floors and no problems have been experienced with these surfaces regarding stability. At Moulsecoomb, the rooms occupied for monitoring have suspended wooden floors and caution is required when working here. The practice followed, given that observing has to take place, is for the operators to stand in the same position throughout the measurement period once this has started: this is usually about 30 minutes and has overcome this problem.

Operators/ Observers

These play a significant role in the use of a manual theodolite intersection system such as ECDS3. The software assists the operators to control the measurement sequence through specified tolerances but the quality of the final

results will always be reliant on how well the targets and scale bar have been sighted. As with many of the factors discussed in this section, the input of the operators to the final accuracy of real-time intersection coordinates is very difficult to quantify. However, as before, good practice can be suggested.

The operators main function is to centre the theodolite reticule on to a series of targets. In certain cases, some careful interpretation of the centre of the target is required, especially with plane targets which can appear elliptical in the field of view of the telescope. Plane targets have been used throughout this project and particular attention has been paid to obtaining good quality observations to these when viewed at awkward angles.

ECDS3 operators need to concentrate for long periods and fatigue can become a factor in accuracy: long set-ups should be avoided and have been limited to about 90 minutes for this project. Distraction of the operators sometimes had a major influence on the results obtained and working with ECDS3 on a congested construction site often led to unacceptable results being obtained. Although this is not always possible, quiet and calm observing conditions are desirable for a high precision close range survey.

Environmental

Although most measurements taken with theodolite intersection systems are indoors, environmental factors can still have an effect on accuracy. For example, vibration of nearby plant and machinery on site could cause difficulties when observing, whilst wide temperature fluctuations can cause

problems with the stability of the theodolites.

Systematic errors in this category include the curvature of the Earth and refraction. Curvature c is given by

$$c = \frac{D^2}{2R} \qquad 7.1$$

where D = the sighting distance and R = a value for the radius of the Earth. At a distance of D = 15 m (the maximum for lines of sight in this project) and with R assumed to be 6380 km, the Earth curvature is calculated to be 0.018 mm and is ignored as a systematic error that cancels when coordinate differences are calculated.

Refraction r can be calculated using

$$r = \frac{k D^2}{R} \qquad 7.2$$

where k = the coefficient of atmospheric refraction and D and R are as before. The value of k is always in doubt for any survey because of uncertainties in the way in which light travels through air. If the usual value of 0.07 is used for k and D is 15 m, the refraction error r is 0.002 mm. This calculation is usually applied to outdoor work where the temperature gradient along the line of sight is fairly constant. For indoor work, it is possible to be observing in areas where the temperature gradient might be excessive, especially near to local heat sources such as machinery or near to drafts from heating and air conditioning ducts. Taking measurements under these conditions can give rise to very

unpredictable values of k and they must be avoided. For the work completed as part of this thesis, no situations have arisen where obvious refraction problems may have been encountered and no corrections have been applied to allow for this.

7.2 System geometry

Alongside the choice of theodolite and experience of the operators, another important factor in determining the accuracy of the results for a theodolite intersection system is the geometry of measurement. This is determined by the spatial relationship between the positions of the theodolites and targets intersected and depends on

- the length of the baselines between the theodolites
- the length of the lines of sight from the theodolites to the points observed
- the intersection angles subtended at each point observed

Although listed separately here, all of these are interrelated and the magnitude of the intersection angles is dependent on the geometrical relationship between the length of the baselines and the sighting distances.

For most intersection surveys, the geometry is usually established by choosing baseline positions from which to observe to targeted points of interest on an object. In an ideal world, the length of a baseline should be greater than the size of the object being measured but in a practical world, theodolites often have to

be placed closer together than is desirable. In the ideal world again, an intersection angle should be in the region of 90° but in a practical world, intersection angles will have values covering a wide range. Grist (1986) suggests that intersection angles should be restricted to the range 60-120° but angles as low as 15° have been used in this project because of the complexity of the structures monitored and the need to take observations quickly, especially during the construction phases at Wokingham, Shoreham and Moulsecoomb. Whilst on site, the theodolite intersection system team were often an inconvenience for site operatives and observations had to be completed in as short a time as possible.

At Wokingham, two baselines have been chosen for monitoring that enable a selection of twelve different beams to be monitored, as shown in figure 7.3. Although these enable the targets on twelve beams to be observed in as short a time as possible, the compromise is that both baselines involve taking sightings to the ends of some beams with small intersection angles.

For each survey carried out with these baseline positions, the results obtained have always, with a few exceptions, produced ECDS3 statistics within the tolerances specified for bundle adjustment closures and for real-time *XYZ* intersection coordinates. It is accepted that it might have been possible to set the theodolites in different positions in order to improve the accuracy but this has not been attempted for the following reasons. First, any change in baseline position would either decrease the number of beams that could be observed on one visit to the site or would increase the time spent on site to observe to the

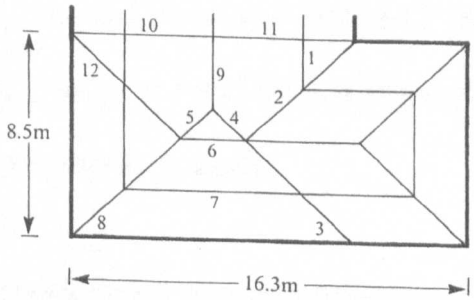

Intersection angles in range 15° – 60°
Sighting distances from 3 – 10 metres

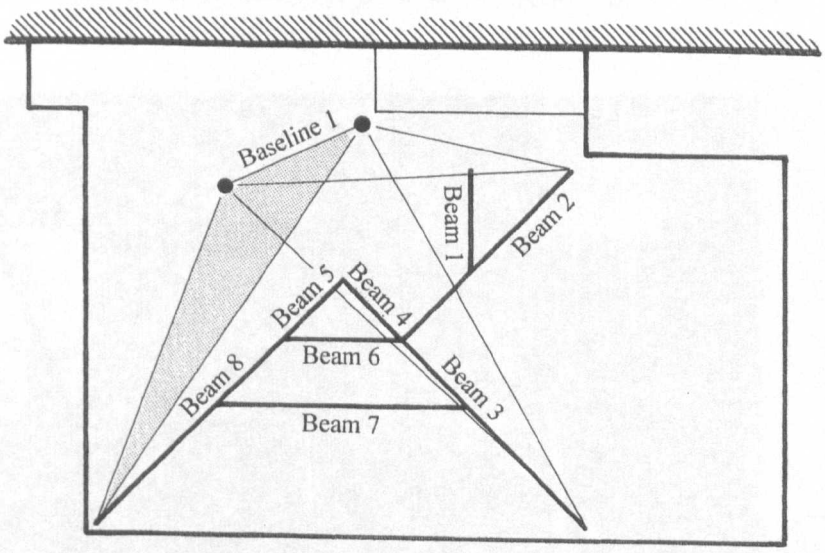

Intersection angles in range 20° – 75°
Sighting distances from 2 – 9 metres

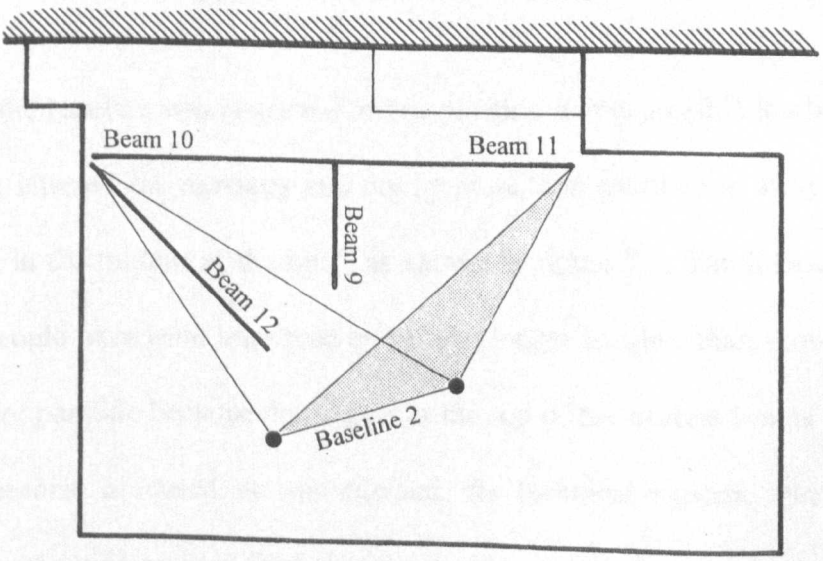

Figure 7.3 *Baseline positions at Wokingham*

same number of beams. Second, once chosen and the measurement programme had commenced, it was thought that any change in observing conditions might introduce unwanted shifts in the coordinate values obtained.

At Shoreham, the only place a baseline could be set up was at either end of the swimming pool. Figure 7.4 shows the theodolites set up on the baseline during construction on the walkway at one end of the pool (see figure 7.1 also).

Figure 7.4 *Baseline at Shoreham*

Although the baseline was restricted to this position it was possible to obtain a reasonable intersection geometry and not be more than about 15 m away from the rafters in the middle of the pool, as shown in figure 7.5. The intersection geometry could have been improved by using a longer baseline than shown but this was not possible because the targets at the top of the nearest beams to the baseline became obscured. It was decided, for technical reasons, that these beams should not be omitted from the measurement programme.

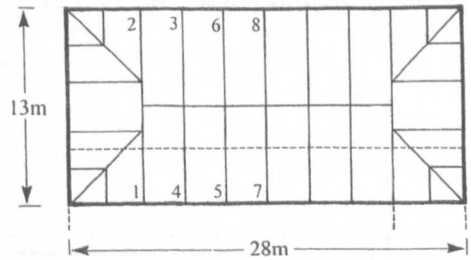

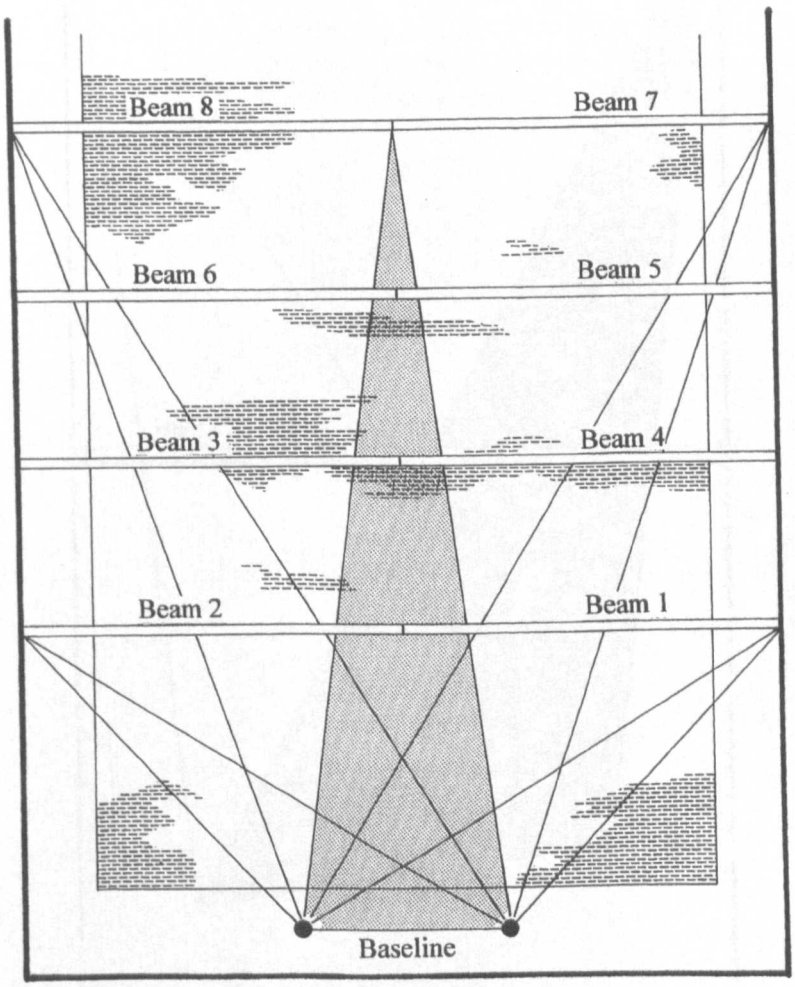

Intersection angles in range 15° - 40°
Sighting distances from 5 – 15 m

Figure 7.5 *Baseline position at Wadurs Pool Shoreham*

At Moulsecoomb, the choice of baseline was quite straightforward again and the theodolites could only be set at one end of the room containing the beams to be monitored, as shown in figure 7.6.

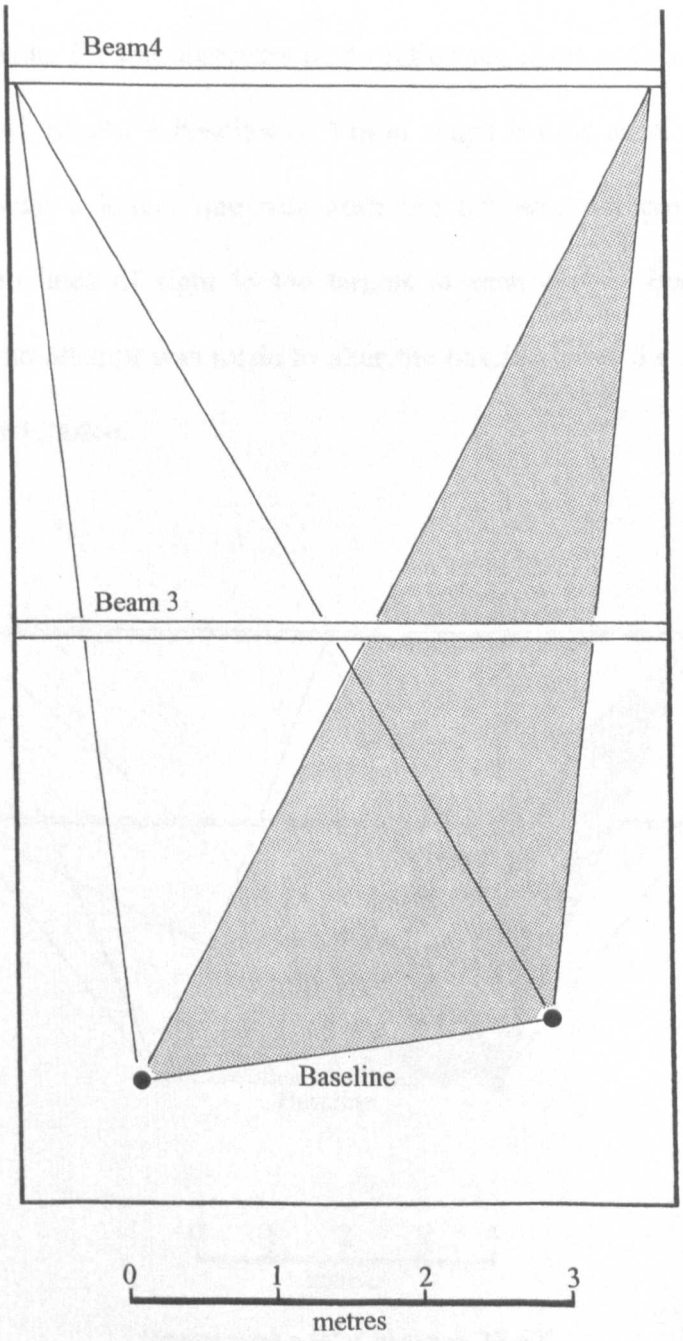

Intersection angles in range 20° – 60°
Sighting distances from 2.5 – 7. 5 metres

Figure 7.6 *Baseline position at Moulsecoomb*

At Bishop Hannington, the choice of baseline for measurements was a little less restricted compared to Shoreham and Moulsecoomb but was not completely free. The position adopted attempts to optimise intersection angles by keeping the baseline as long as possible but also ensures vertical angles are kept within comfortable limits for the observers by avoiding too short a distance between the baseline and targets. A baseline of 4 m in length is used as shown in figure 7.7 and although a longer one was desirable this was not possible due to obstructions to lines of sight to the targets at each end of Beam 1. As at Wokingham, no attempt was made to alter the baseline after the measurement programme had started.

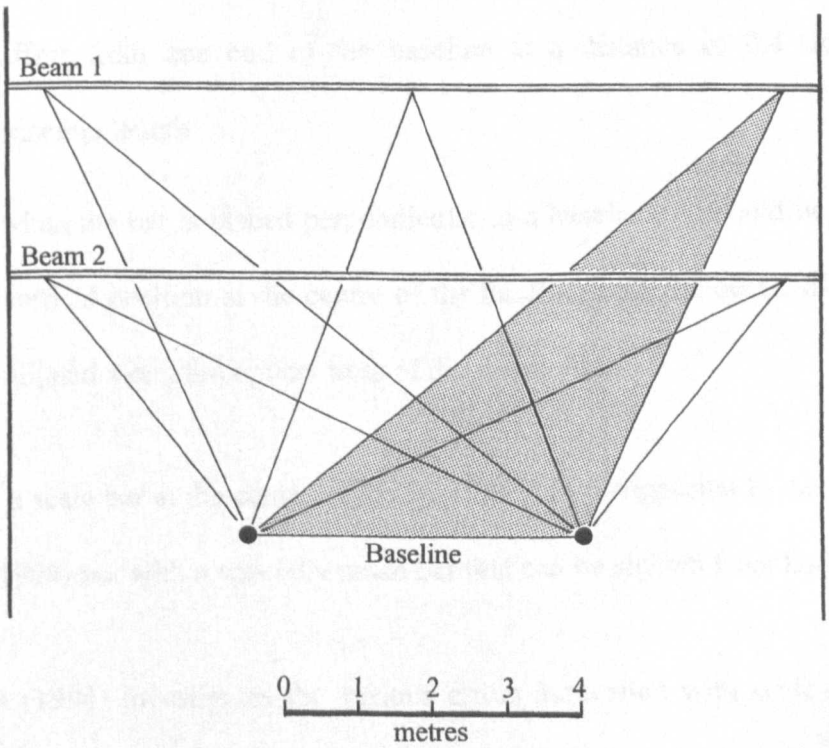

Figure 7.7 *Baseline position at Bishop Hannington*

7.3 Scale bar position

In an intersection survey, the scale bar can be placed at almost any point in the object space or anywhere near to the theodolites.

The first thing that can be said about the number and location of scale bar positions is that there is no agreed set of rules to help decide this. Leica suggest that the number of scale bar positions used should equal the number of theodolites used minus one, but at least two positions should be used (Leica, 1993e). The effect of different positions of the scale bar has been investigated by Bill, *et al.*, (1985) who give the optimum positions as the following

- when the bar is placed parallel to a theodolite baseline it should be offset from one end of the baseline at a distance of 0.4 times the baseline length
- when the bar is placed perpendicular to a baseline, it should be set in a vertical position at the centre of the baseline with the centre of the bar aligned along the optical axes of the theodolites

Setting a scale bar at the centre of the baseline is also suggested by Santala and Parm (1994) but with a specially made bar that can be sighted from both sides.

Warren (1994) investigates the various errors associated with scale bars and suggests that under ideal conditions, the scale bar should be nearly the same length as the object. A practical limit on the length of a portable scale bar is about 3 m but because there are problems with scale bar sag and in calibration of this length, the 1 m bar is more widely used. When using a 1 m bar, Warren

states that any scale errors in the length of the bar will be multiplied by the size of the bar in ratio to the size of the object measured. Long 'scale bars' are more likely to be special monuments or parts of the object to be measured itself that have been calibrated prior to measurement.

In the absence of any other guidelines for this, attempts have been made at each glulam site to place scale bars in the positions suggested by Bill.

At Wokingham, a 1m scale bar has been placed in two positions parallel to each baseline at a perpendicular distance away the same length as the baseline, as shown in figure 7.8 (two scale bar set-up).

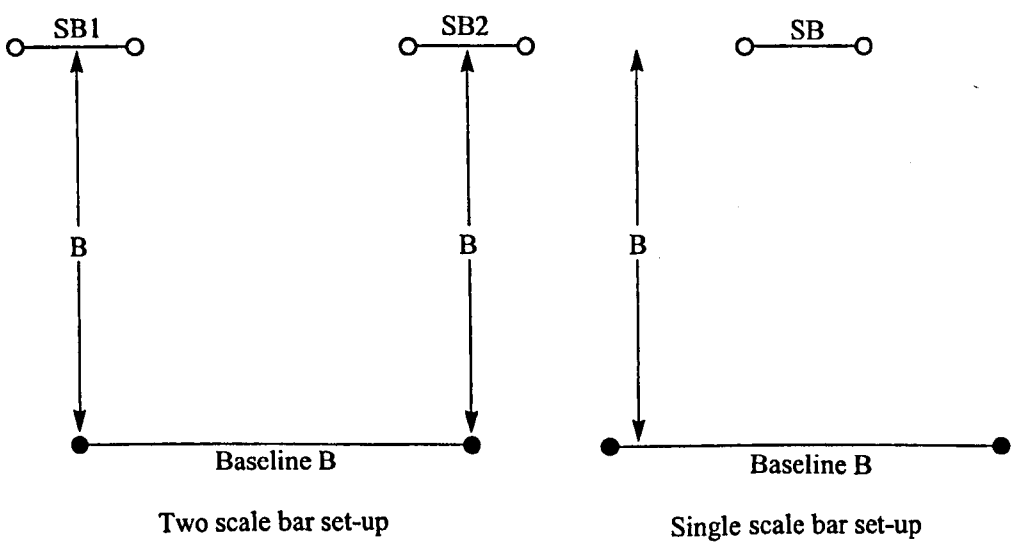

Figure 7.8 *Scale bar positions used at Wokingham*

This adopts, to some extent, the positions given by Bill but the bars are further away from the baselines as these are short (3-4 m) and the recommended 0.4 times baseline suggested for this would be less than the minimum focusing distance of the theodolites. It is not possible to observe the scale bar set up at

the centre of either baseline as the targets on this are not omni-directional and cannot be sighted from opposite sides simultaneously. The short observing distance for this would also be less than the minimum focusing distance of the theodolites. On some occasions, because of difficulties on site, only one scale bar position has been used where the bar is placed parallel to but opposite the centre of a baseline, see figure 7.8 (single scale bar set-up).

Several tests have been carried out to investigate the effect of these different scale bar positions and it has been found that there is little difference in the results obtained from either set up or baseline. Test comparisons gave a maximum difference of 0.04 mm between beam deflection values measured from the same baseline but with the scale bar positions changed in the bundle adjustment. At Wokingham then, either the one or two scale bar set-ups described has been used throughout the measurement period. It is accepted that there are many other scale bar positions that could have been used but having decided on these, they have not been varied in order to maintain consistency in the observation procedure. As with the baseline positions, it was felt that any unnecessary changes in this might cause unwanted shifts in the results obtained.

At Shoreham, the scale bar has been restricted to being placed at the sides of the swimming pool. Two positions have been chosen underneath the bottom of Beams 1 and 2, as shown in figure 7.9. If the bar is placed any further away from the baseline, the bar targets will be too small to be reliably sighted Because of the short baseline involved, it has not been possible to sight the bar if placed at the centre of the baseline. Throughout all surveys at Shoreham, the

two scale bar set-up described has been used.

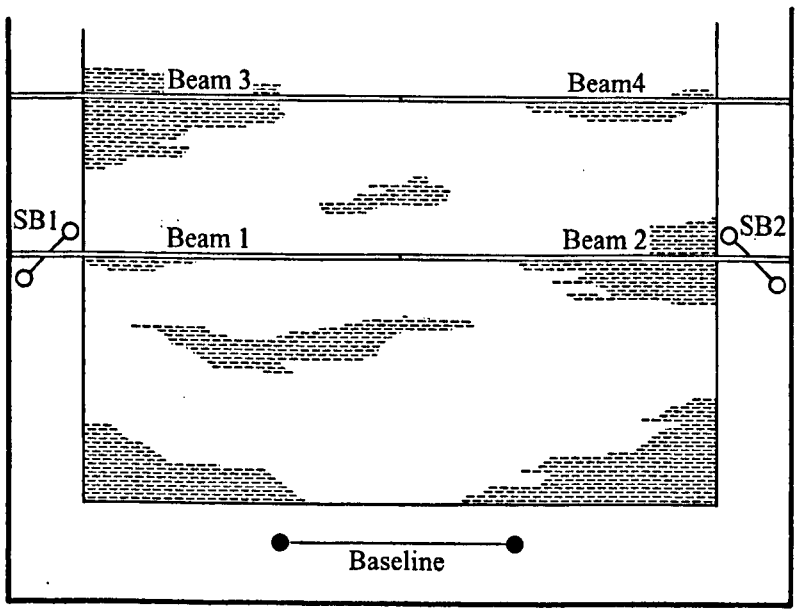

Figure 7.9 *Scale bar positions used at Shoreham*

At Moulsecoomb, a single scale bar set-up has been chosen because of the size of the room in which the monitoring has been done. The bar is positioned in the centre of the measurement space directly underneath but in between the two beams monitored and almost parallel to the baseline, as shown in figure 7.10. Some tests have been carried out with a two scale bar set-up where the bar was placed in a similar position to that given above but closer to the sides of the room. When compared with the single scale bar position, differences of less than 0.05 mm were noted in the *Z*-coordinates. Because of the awkward size of the rooms in which the observations are taken at Moulsecoomb, the small number of points observed and because of the suspended floors, it was decided that one scale bar position was a better option as it meant that the operators did not have to move once measurements has started. As at the other sites, observing the scale bar midway along the short baseline was not attempted.

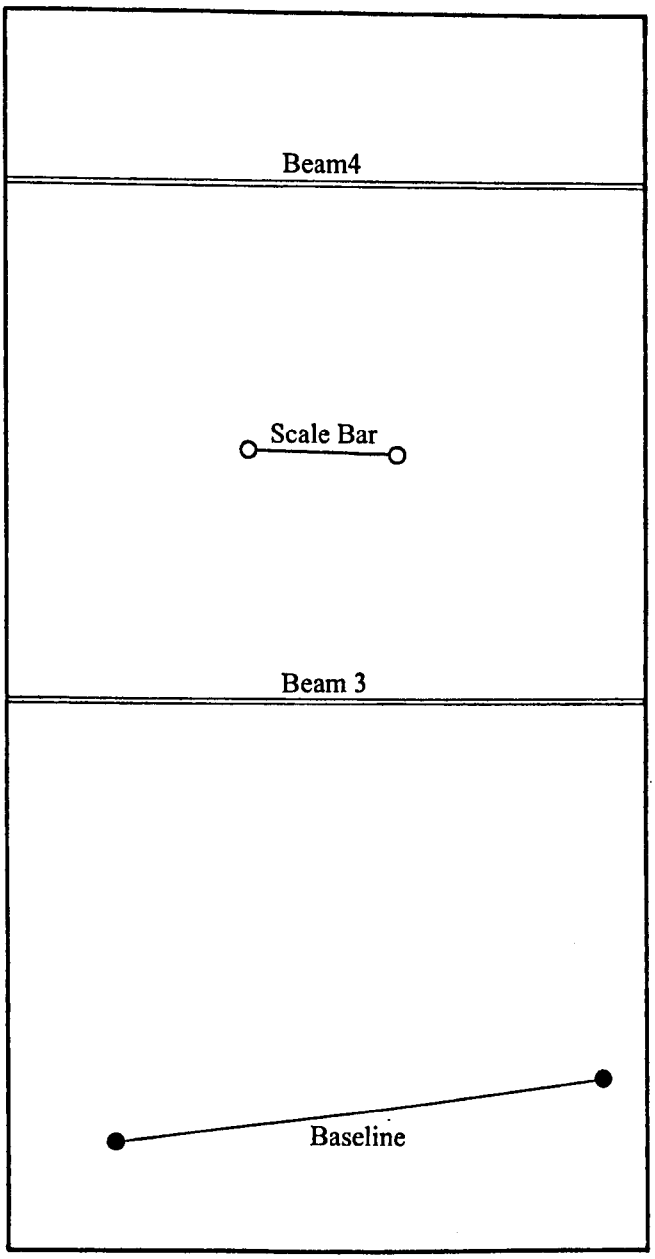

Figure 7.10 *Scale bar position used at Moulsecoomb*

At Bishop Hannington, any number of scale bar positions was possible. The set-up chosen was either to place the bar in two positions parallel to the baseline in a plan position in between the beams as shown in figure 7.11 or to use one position again in between the beams but opposite the centre of the baseline. As at Moulsecoomb, this placed the scale bar in the centre of the measurement space but at tripod not ceiling level. Again, comparisons were

made between these bar positions with little difference being apparent in the results. For consistency, and in common with all the other sites, these positions have not been varied throughout the measurement period.

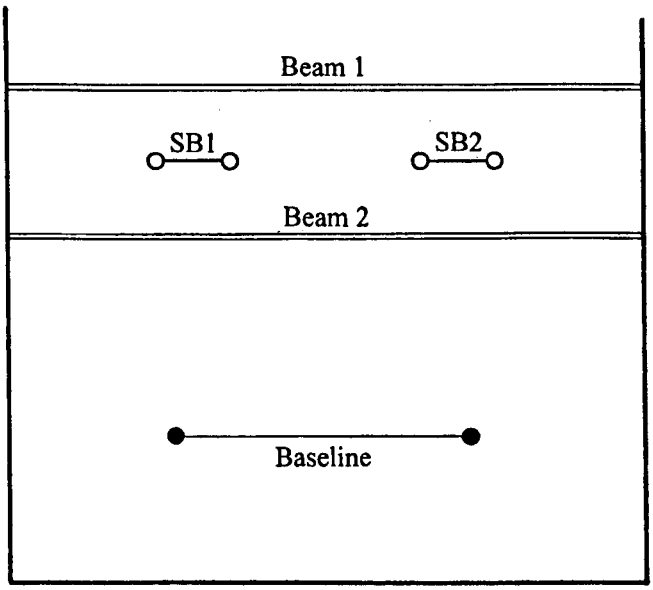

Figure 7.11 *Scale bar positions used at Bishop Hannington*

7.4 Number of bundle points

In addition to choosing baseline and scale bar positions, the number of points to be sighted in the bundle adjustment has to be chosen. Leica (1993e) suggest that the number of bundle points should be equal to the number of theodolites used times five, but that at least eight must be used. Since the minimum number required is five (see section 4.3), this will generate some redundancy in the bundle adjustment and give some meaning to the quality figures which are produced by the ECDS3 software when processing is complete.

The best configuration for these points is that they surround the object or structure to be measured and, in effect, 'box it in'. The eight minimum points

stipulated by Leica represent the corners of a cube that might be fitted around an object. However, it is also good practice to include bundle points throughout the object to be measured in addition to those surrounding it and it has been the practice here to do this as well as enclose each glulam structure with bundle points.

At Wokingham and Shoreham, many variations were possible for the bundle point distribution and 12 or more bundle points have been used as much in the box configuration described as site conditions allow. Since the original distributions chosen have always produced bundle adjustments with acceptable closures of less than 0.1 mm, no attempt has been made to vary this complicated and almost endless variable. Again, this was thought to be best practice in keeping the measurement program consistent.

At Moulsecoomb and Bishop Hannington, a small number of targets are intersected (10 and 14 respectively) and all of these are treated as bundle points. Occasionally, the targets have been re-observed on-line as a check and the two sets of *z*-coordinates obtained have been compared to see if they are within 0.1 mm of each other. Generally, this has been the case and the mean coordinate has been used in deflection calculations.

7.5 Some published results for accuracy

Another means of attempting an accuracy assessment for theodolite intersection is to examine both theoretical and experimental work published by others. A number of papers are given below accompanied by a discussion of their relevance to this project.

Bill, *et al.*, (1985) were the first to investigate the accuracy of ECDS1 and they provide a fairly comprehensive treatment of the accuracy of this theodolite intersection system. This reference includes diagrams such as those in figure 7.12 which shows theoretical relationships between intersected point accuracy, baseline length between theodolites and object size for a given angular precision of the observations. For example, if the desired precision required for real-time coordinates is 0.1 mm and the angular error of pointing with the theodolites is 3″, the baseline should be about 7.5 m long. At this baseline distance, the positional error will be 2 x 0.1 mm if the object length is 10 m. As discussed in section 7.2, the length of baselines chosen for the glulam project have been dictated mostly by site conditions and it has not been possible to follow the recommendations given here. Suggestions as to where to place the scale bar for optimum results are also included in this paper and have been discussed in section 7.3. Further graphs are included for predicting accuracy but the treatment is general and is only useful as a guide to what accuracy might be expected if certain configurations are used.

Allan (1988) describes some research carried out at University College, London in which an in-house theodolite intersection system was used to coordinate a series of targets in a room measuring 20 x 12 m. Intersection calculations are based on the formal 3*D* model given in section 4.4. The significance of the work carried out here is that the geometry of the set-up tested resembles, quite closely, some of that used at the glulam sites. For points with small intersection angles of less than 15°, the reported standard ellipsoidal errors obtained for X and Y coordinates are relatively large and deteriorate from

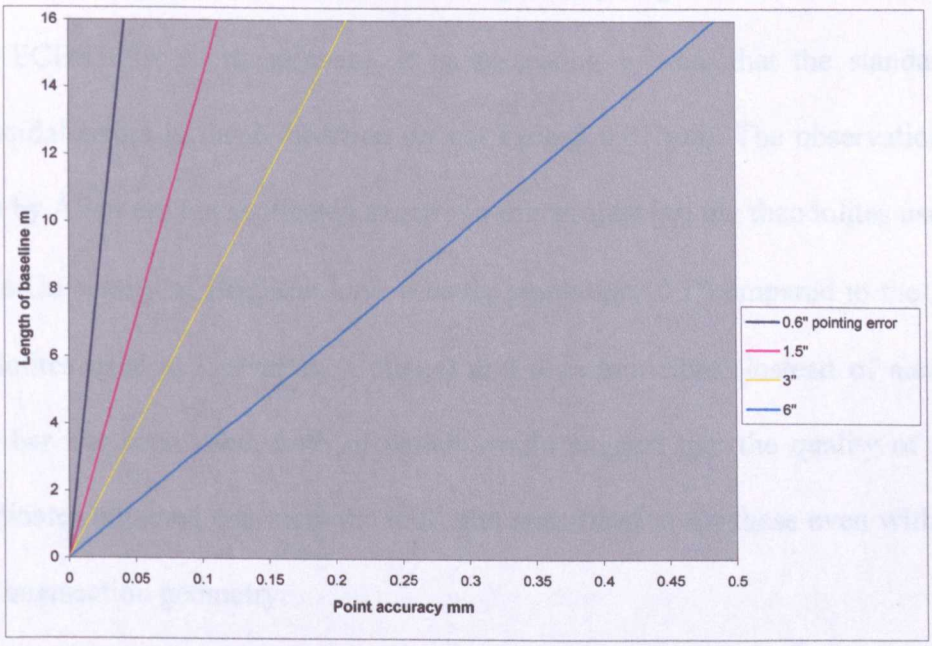

Figure 7.12a *Relationship between pointing error, point accuracy and length of baseline for ECDS1 (Bill, 1985)*

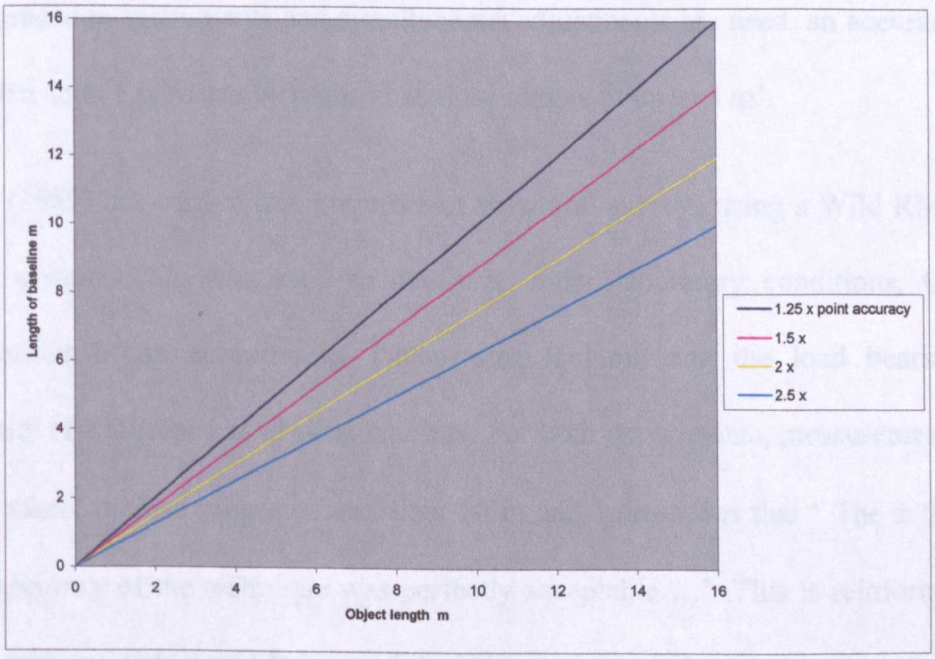

Figure 7.12b *Relationship between object length and baseline for ECDS1 (Bill, 1985)*

values less than 0.05 mm with good geometry to 0.25 mm for poor geometry and in one instance to over 2 mm, and exceptionally large *Pe* value if obtained from ECDS3. In all these cases, it is interesting to note that the standard ellipsoidal errors in the *Z*-direction do not exceed 0.05 mm. The observations made by Allan are not replicated exactly in this project but the theodolites used by the University of Brighton have a better resolution (0.1"compared to the 1" theodolites used at University College) and a carbon fibre (instead of steel) scale bar has been used, both of which would suggest that the quality of *Z*-coordinates obtained can meet the 0.07 mm specification for these even with a poor intersection geometry.

Mulder (1989) simply states that a theodolite intersection system can achieve sub-millimetre accuracy at distances less than 50 m and states 'If multiple set-ups, precision instruments and simultaneous adjustments are used, an accuracy of better than 1 ppm can be realised at close ranges of up to 5 m'.

Uren (1989) has carried out a number of structural surveys using a Wild RMS 2000 system. This was used to measure, under laboratory conditions, the deflections of an eccentrically loaded steel column and the load bearing capacity of a stiffened steel plate and box. For both experiments, measurements were taken at close ranges of less than 10 m and Uren states that ' The ± 0.1 mm accuracy of the technique was perfectly acceptable ...'. This is reinforced by a previous statement ' Prior work had shown the technique to be accurate to 0.1 mm at the sighting distances involved'. No details are given as to how the accuracy was assessed for this work but the figures quoted are equivalent to an accuracy of 1 in 100 000.

Bingley (1990) reports the results of some surveys carried out with a University of Nottingham in-house theodolite intersection system. The first of these was to help calibrate some production robots. In this survey, it was possible to obtain a good geometry with intersection angles in the range 80-105° and sight lengths were less than 3.5 m. This resulted in a mean ellipsoid of error of 0.016 mm for the points observed. The second survey involved measuring height differences as a part of a subsidence monitoring scheme. A series of points were levelled and the results of this were compared to height differences derived from coordinates determined by theodolite intersection. For most of the observations, a good geometry of measurement is reported where intersection angles are in the range 70-95° and sight lengths vary from 2.5-4 m. However, measurements were also taken when a poor geometry was unavoidable and intersection angles in the range 7-10° and sighting distances of up to 22 m were used. Bingley notes from the measurements taken in this survey that with good geometric conditions, theodolite intersection is capable of determining relative height differences to an accuracy of 0.05 mm and with poor geometrical conditions, level differences can be determined with an accuracy of 0.15 mm. The significance of these results is that height differences have been measured at each glulam site for this project using field methods similar to those used by Bingley. Also, a wide ranging geometry has been used but with intersection angles not less than 15° and sighting distances in the range 2-15 m. All of this would suggest that vertical deflections have been measured at each glulam site within the specified tolerance of 0.07 mm with a good intersection geometry but that some measurements with a poor geometry have not met this

specification. The mathematical model used for the orientation of the University of Nottingham theodolite intersection system is a $2D + 1D$ model in which horizontal coordinates of the theodolites are calculated first and then the Z-coordinates, see section 4.4. A least squares $3D$ vector solution is used to compute the coordinates of target positions.

Bayly (1991) in his doctoral thesis describes the use of theodolite intersection systems in aligning machinery. The equipment used here was two Wild T2002 theodolites and software developed in-house. Bayly compares different traditional alignment methods to theodolite intersection and quotes such as '... the displacement computed with the electronic theodolite system agreed within 0.03-0.17 mm [with results from other instrumentation] ...' are included.

Another method for assessing the accuracy achievable from a theodolite intersection system is given by Grist (1991) who includes figure 7.13 but without a reference. For the ECDS monitoring completed at each of the glulam sites described in Chapter 6, the range of object distances encountered varies from 2 to 15 m which would produce, according to figure 7.13, a range of accuracies from 0.02 mm to 0.10 mm, which are figures close to a global accuracy of 1 in 100 000. This figure is often quoted for the accuracy of a theodolite intersection system (see Leica, 1993a also) which corresponds to 0.10 mm at a measuring distance of 10 m. This figure is, of course, a rule of thumb and does depend greatly on the precision of the theodolites used and other factors, but does give some idea of the accuracy that might be expected from theodolite intersection.

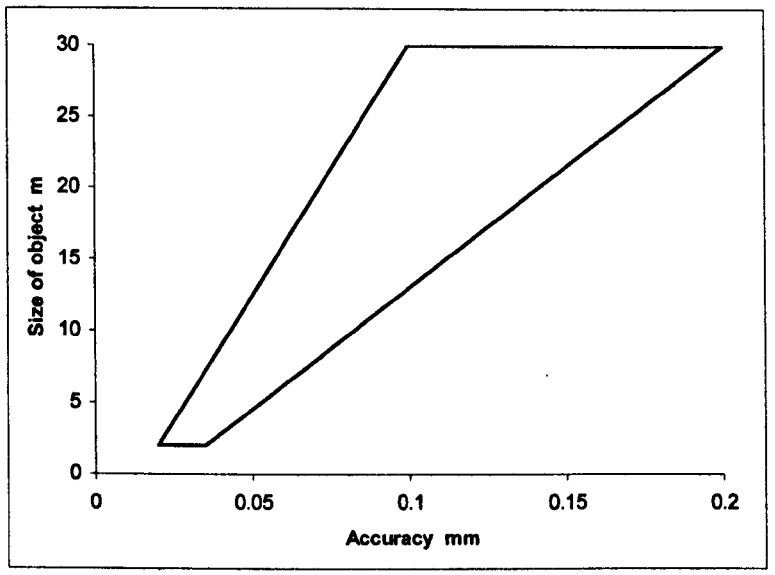

Figure 7.13 *Envelope of accuracy achievable with a theodolite intersection system (Grist 1991)*

Santala and Parm (1994) and Santala (1995) state that the precision of a theodolite intersection system can be evaluated by taking observations to the same reference points but from different baselines they state that the accuracy can be assessed by observing scale bars with different lengths situated in different positions. A number of tests have been performed with a Kern ECDS (version not given but assumed to be ECDS2) and with a Wild TMS with targets spread across a room approximately 15 x 8 x 3 m. The precision of ECDS and TMS are quoted as a three-dimensional point standard error of 0.207 mm and the accuracy is given as a scale error of 174 ± 33.2 ppm where the standard error of one scale bar length check was 0.063 mm. Santala and Parm claim that the type of model used to orientate the theodolites and compute intersections has an effect on the results obtained and that the 3*D* model of computation and the (2*D* + 1*D*) model give different coordinate results especially in a poor geometry of measurement. This is also confirmed by Cooper (1986) who states that a 3*D* model is preferred. How the work of

Santala and Parm can be related to the monitoring at the glulam sites is not entirely clear but their results seem to be pessimistic compared to the others given in this section. However, it is worth noting at this point that ECDS3 is based on a bundle adjustment orientation and *3D* spatial intersection.

The JET (Joint European Torus) project has been set up to investigate nuclear fusion as a viable energy source (European Commission, 1994) and is based at Abingdon in Oxfordshire where the experimental fusion reactors and associated equipment are being built. These have to be assembled to very precise tolerances and to assist with this, the JET project has purchased three ECDS3 coordinate measuring systems. The surveying carried out to control the construction of the fusion reactors is described by Macklin, *et al.,* (1994 and 1995). The reactor includes many different parts but it is estimated that the measurement space at JET rarely exceeds 10 m as a cube or in diameter. Their assessments of the accuracy obtained with ECDS3 are ± 0.2 mm when comparing coordinates of the same points with one another from different surveys, ± 0.05 mm / m (1 in 20 000) scale accuracy when checks are carried out by surveying reactor parts with known dimensions and ± 0.3 mm when components are being installed in the reactor. As with Santala and Parm, these are given for three-dimensional positioning with no mention of separate precisions for horizontal and vertical coordinates.

Beyer, *et al.,* (1995) discuss the quality control of digital photogrammetry where ECDS3 was used to measure a reference frame with a relative accuracy of 1 in 98 000.

Hölting (1995) describes an assessment of the accuracy of ECDS3 that was carried out for quality control purposes in aircraft manufacturing. A series of targets was placed on a Diamler-Benz Aerospace Airbus in order to inspect the overall geometry of the fully assembled aircraft. The size of the Airbus is approximately 34 x 34 x 12 m and an elaborate measurement procedure was used involving two set ups with six theodolites on-line in each set-up. This ensured that each target was sighted by at least three theodolites with an intersection angle close to 90°. A 2.5 m scale bar was used in six positions and the whole set up took five hours to observe. When computed, a special adaptation of the ECDS3 software was used to adjust both set-ups simultaneously. All of this produced standard deviations for measured coordinates of σ_X = 0.13 mm, σ_Y = 0.14 mm and σ_Z = 0.07 mm. In his conclusions, Hölting claims that ECDS3 measured to an accuracy of 1 in 250 000 of the object size.

Staiger (1995) quotes a repeatability of 0.01-0.02 mm for distances obtained with ECDS3 but only up to 6 m which are similar to the accuracies predicted by Grist.

Wu, *et al.*, (1996) have attempted to predict the theoretical accuracy of theodolite intersection systems and although not made clear in their paper, it is assumed some tests were performed to compare scale bar lengths obtained by producing coordinates with the calibrated length of scale bar. This was done for an orientation carried out by collimation and by using a bundle adjustment. The relative scale errors quoted for the scale bar comparisons range from 27-92 ppm for a collimation orientation and 7-33 ppm for a bundle orientation and

Wu *et al.*, conclude that a theodolite intersection system orientated by a bundle adjustment will produce better results than one orientated by collimation. This contradicts Zhang, *et al.*, (1997) who have investigated the accuracies of theodolite intersection systems that have been orientated by what they call the geodetic method (autocollimation) and the photogrammetric method (bundle adjustment). The system tested is not specified but uses two theodolites: a Wild T2000S and T3000. The size of the object tested is not given. The error obtained for the repeated measurement to a single point is quoted as the ratio of the length of the error vector obtained to the length of the vector to the single point. For a bundle adjustment, these are given as 26 ppm. In other words, the combined accuracy from all three coordinate axis directions is expected to be 0.26 mm at a distance of 10 m. If the standard error along each coordinate axis is assumed to be the same, then these results suggest that the error for X, Y and Z coordinates should be 0.15 mm at 10 m from the theodolite baseline.

Bas (2000) has published a theoretical prediction of the accuracy expected for point coordinates produced by a theodolite intersection system. The results suggest that the rate of increase of errors in XYZ coordinates is slow for both observed horizontal and vertical angles less than 45°, but is fast for angles greater than 45°. How horizontal angles are defined is unclear but they are assumed to be measured relative to a baseline. To control the accuracy, Bas states the optimum baseline-object distance ratio should be 2:1. This, it is suggested, would be impractical for many close range intersection surveys.

A wide ranging set of assessments of the accuracy that might be expected for a theodolite intersection system are given above. The question that arises from all

of these is how they apply to the monitoring done for the glulam project.

A figure that seems to be quoted more than others is an accuracy close to 1 in 100 000. Whether this relates to the size of the object or the sighting distance is not always clear but taking a maximum sighting distance of 15 m for the glulam project, the worst measurement accuracy for ECDS3 should be 0.15 mm. For an average sight length of between 5 and 10 m, the accuracy will be 0.05 mm and 0.1 mm respectively. These figures are close to the magnitude of error specified for the glulam project.

Of the authors referenced above, the work of Allan and Bingley are most relevant as their work was carried out using equipment and methods very similar to those used at the various glulam sites. Allan confirms that sub-0.1 millimetre accuracies are obtained for *Z*-coordinates even when the system geometry is poor, as is the case for work in this thesis. Bingley is even more to the point and quotes accuracies of 0.05 mm for height differences determined from theodolite intersection with a good geometry and 0.15 mm with a poor intersection geometry up to distances of 20 m. Hölting also gives a standard error for *Z*-coordinates of 0.07 mm but for a very elaborate configuration. None of the other papers mentioned quote accuracies as specific as Allan and Bingley to the glulam project but most of the values given do not differ greatly from the global value of 1 in 100 000.

All of these suggest that, for the monitoring carried out in this research that it is possible to measure *Z*-coordinates and to determine height differences from these with an accuracy of 0.07 mm and 0.1 mm respectively. For some beams,

though, these will deteriorate to accuracies of 0.1 and 0.15 mm with poor intersection geometry. Bearing in mind all the restrictions imposed by the site conditions described in Chapter 6, the loss of accuracy for some beams is accepted.

7.6 Evaluation of system accuracy

Once a theodolite intersection system has been set up and orientated, there is a need to check the measurement accuracy of the system for a given configuration in order to give confidence and ensure that the set-up meets expectations. This can be done by a number of different methods.

The simplest and quickest check is to measure the length of a scale bar in various positions throughout the object or measuring space. A single position is not sufficient because the bar is usually short compared to the object being measured and the precision of a set-up can vary across the measurement space. As well as varying the position of the scale bar, a different bar to the one used in the orientation procedure should be used for checking purposes. A scale bar check produces values for what is often called the scale error for a theodolite intersection system and this is given as a relative error proportional to the length of the bar under test. Sometimes, this check is quoted simply as the difference of the scale bar and check lengths obtained from intersection coordinates.

Repeated measurements taken of an object from different theodolite positions is also a method used to check the accuracy of a theodolite intersection system as it is assumed that consistent results could not be obtained if errors were

present. This check can be performed directly on the different sets of coordinates obtained or coordinate differences can be compared. If coordinates are used, these have to be transformed to the same local or object coordinate system for comparison since different baselines are used to obtain them. The check result is quoted as a direct comparison of coordinates or coordinate differences, as a standard error along each coordinate axis, as a point standard error or as a scale error.

A check on the absolute accuracy of a theodolite intersection system can be accomplished by taking measurements to a test object where the coordinates of the reference targets are known to an accuracy at least as good as the expected system accuracy.

Another check proposed by Kyle (1993) is the need to check the software of a theodolite intersection system which, it is claimed, is as important as checking the hardware and set-up. The essential requirement for this is to have an independent reference software package designed to much stricter standards than the package under test. This reference software would be used to generate coordinates from the same system configuration and observations under test and if the two sets of results agree within acceptable limits, the test software is assumed to have performed favourably. Any reference software should be capable of checking a bundle adjustment and intersection coordinates and should be able to verify error estimates provided by the test software. During the period of research covered by this thesis, no such software has been produced.

7.6 Verifying the accuracy at Brighton

To check that the accuracies so far discussed are realistic and obtainable by the author, some tests were carried out both on-site and under laboratory conditions.

On site, the check most often completed is to measure the length of a second scale bar in a number of different positions throughout the measurement space varying from two at Moulsecoomb to five at Wokingham. The difference between the calibrated length of the scale bar and that obtained from intersection coordinates has rarely exceeded 0.1 mm. Any difference larger than 0.1 mm has been investigated and sometimes this has resulted in bundle points being re-observed and the bundle adjustment re-run. On some occasions, the whole orientation has been abandoned and a new one started.

In addition to scale bar checks, repeat surveys have been carried out at all sites, but not on a regular basis as these take a long time to complete. These start with a normal set-up in which a bundle adjustment is performed followed by on-line observations. This is then repeated but with the theodolites in different positions and, if time permits, on consecutive days. The coordinate differences obtained from each set of tests have been compared and on no occasion have they differed by more than 0.1 mm.

As well as regular scale bar checks and repeat measurements, the statistics produced by the ECDS3 software have been analysed each time a survey is carried out: this has already been discussed in section 5.6. According to the *RMS* values obtained for real-time ECDS3 *XYZ* coordinates, the 'accuracy' for

local z-coordinates in this project have been better than 0.1 mm with the exception of some beams at Shoreham. The S (or sighting) statistics produced by ECDS3 also show that, despite some poor horizontal geometric conditions, the expected standard deviations for local z-coordinates is still within acceptable limits. For example, at Wokingham, the predicted horizontal S values for target 31 are SX = 0.064 mm and SY = 0.216 mm but SZ is 0.042 mm. At target 87, SX = 0.176 mm, SY = 0.148 mm but SZ = 0.042 mm again. However, at Shoreham, the SZ value for targets 75 and 85 is 0.188 mm but it is worth noting that the RMS errors reported by ECDS3 for these intersections are usually less than 0.05 mm and occasionally in excess of 0.1 mm.

The first laboratory test carried out at Brighton was by Conheady (1993). A small steel cube had six self adhesive Leica targets placed on it and the distances between these were calculated from the coordinates of the targets which were measured with a coordinate measuring machine in the mechanical engineering laboratory. Targets 1 and 3 on the cube defined an horizontal distance and 2-4 and 5-6 defined two vertical distances. Taking the coordinate measuring machine distances as reference, Conheady tested how well ECDS3 could match these, via measurement of intersected target coordinates on the cube. ECDS3 was set up in the surveying laboratory at the University and the cube was placed in eight different plan positions, as shown in figure 7.14, in an attempt to simulate conditions at some of the glulam sites. In positions A to F, the cube was placed at three different heights, approximately 1 m below the theodolite collimation, at the same level as the theodolites and approximately 1 m above. In positions G and H, the cube was set 1 m below the theodolites.

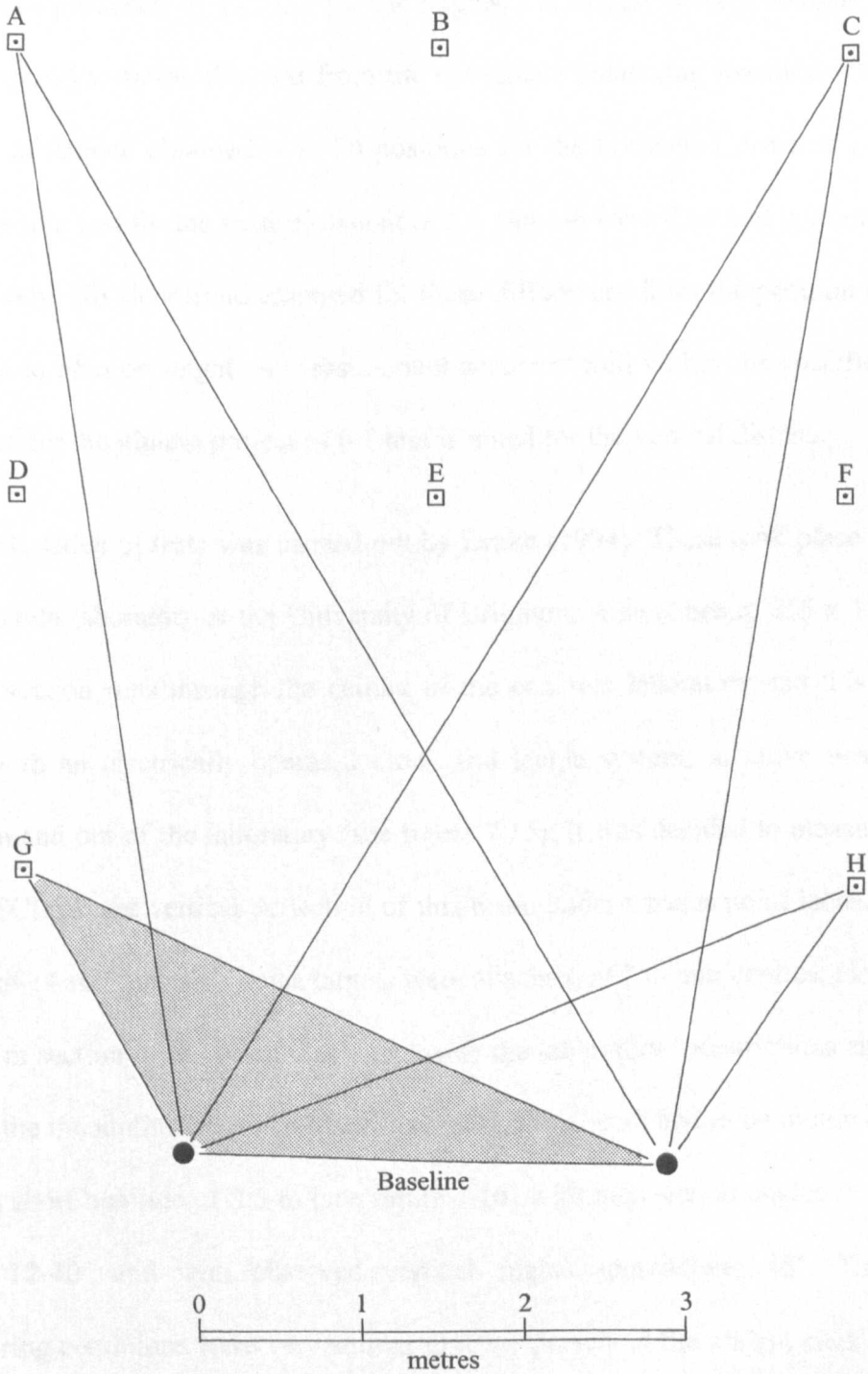

Figure 7.14 *Measuring positions for ECDS3 checks (Conheady, 1993)*

This gives rise to 20 different measuring positions for the cube. From the coordinates produced by ECDS3 for the targets, the distances were computed and compared to those obtained from the coordinate measuring machine. The average difference obtained over 20 positions for the horizontal distance 1-3 was 0.09 mm and for the vertical distances 2-4 and 5-6 were 0.04 and 0.03 mm respectively. No clear trend emerged for these differences from the position of the cube in plan or height. A measurement accuracy well within the specified tolerance for the glulam project of 0.1 mm is noted for the vertical distances.

A second series of tests was carried out by Drake (1994). These took place in the concrete laboratory at the University of Brighton. A steel beam, 255 x 133 mm in section runs through the ceiling of the concrete laboratory and this is used, with an electrically operated block and tackle system, to move heavy loads in and out of the laboratory (see figure 7.15). It was decided to measure, using ECDS3, the vertical deflection of this beam under various point loads. A series of 14 self adhesive Leica targets were attached, at 750 mm centres, along the 10 m section of the beam that runs inside the laboratory. Restrictions as to where the theodolites could be placed meant that the beam had to be monitored from a short baseline of 3.5 m (see figure 7.16) with intersection angles in the range 12-40° and with observed vertical angles approaching 45°. These measuring conditions were very similar to those present at the glulam sites and the objective of these tests was not to test the accuracy but the response of the system to measuring vertical deflections.

At the start of fieldwork, the targets along the beam were intersected to give the

Figure 7.15 *Concrete laboratory showing steel loading beam (top) and 1.5 tonne block being positioned on this (bottom)*

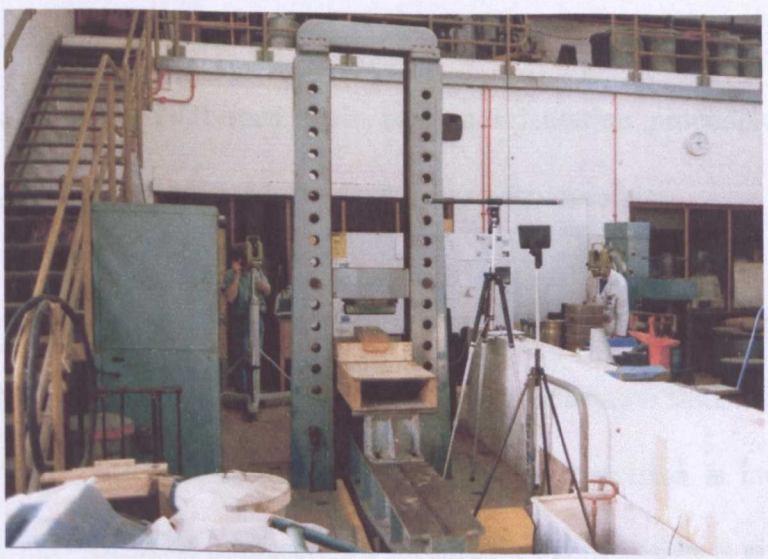

Figure 7.16 *Baseline for monitoring in concrete laboratory*

initial position of the beam. A 1.5 tonne load was then applied under target 6, the targets were re-intersected and with the load removed, the targets intersected again. The results for this loading of the beam are shown in figure 7.17. The vertical deflection produced by ECDS3 clearly matches the load conditions and points where the beam is fixed at target 2 and close to target 12. A structural analysis of the beam and load was carried out using the OASYS program and this produced a similar curve to the one in figure 7.17 but the maximum deflection predicted at target 6 was 3.1 mm compared to 3.3 mm obtained from ECDS3. Since further tests have produced similar results to these, it is clear that ECDS3 is capable of measuring vertical deflections through the comparison of *z*-intersection coordinate distances.

7.7 Summary

Data quality for theodolite intersection is related to accuracy, precision and reliability.

For this project, an attempt has been made to maintain *accuracy* in *XYZ* coordinates by using T2002 theodolites with their sub-second angle measuring capability, by using calibrated scale bars in orientation procedures and by optimising the system geometry where this has been possible.

Precision is a function of the random errors in observed angles and derived coordinates and is related to the orientation and intersection statistics provided by the ECDS3 software. For a bundle adjustment, precision is indicated by *RMS* values and for *XYZ* intersection coordinates, the precision is given by the *Pe* and *S* values in the Online program.

Figure 7.17 *Vertical deflection of loaded steel beam measured with ECDS3 (Drake, 1994)*

The *reliability* of *XYZ* coordinates is indicated by the presence or otherwise of gross errors in the system. The detection of these is through the many check measurements taken but they are mainly observed through the statistics produced by the ECDS3 software. The most common error is that of an operator sighting the wrong target. If this occurs during System Orientation, the bundle adjustment program will compute large *RMS* values and will issue an error message. When measuring in the Online program, the *Pe* values will be very large if a gross error has occurred. These can be investigated and the source of error removed.

Taking account of all that has been covered in this chapter, it is evident that assessing the accuracy of ECDS3 can be very difficult. As can be seen, the accuracy possible is a function of the system specification, the way in which it is set up and is different for each application. A variety of published results are presented but with no positive trend emerging regarding accuracy and with many of these not distinguishing between the accuracy of horizontal or vertical coordinates. However, an attempt has been made to show, from the tests at Brighton and elsewhere, that ECDS3 can measure vertical deflections with an accuracy approaching 0.1 mm at the various glulam sites despite the short baselines used and poor geometry sometimes encountered. Consequently, it is assumed that the specification of 0.1 mm for the measurement of vertical deflections is met by ECDS3 and the measurement system.

8

RESULTS OBTAINED AND CREEP ANALYSIS

Although much research has been done to predict the long-term magnitude of creep, most of this has been carried out for wood and timber specimens other than glulam and this is the reason why the Structural Timber Research Unit at the University of Brighton commenced, in 1988, its research programme to monitor creep in structural glulam under laboratory conditions. Following this, the monitoring of full-scale structures commenced in 1992 and it is the analysis of these rather than the laboratory specimens that is given in this chapter.

8.1 Processing beam deflections

The methods used on site with ECDS3 to measure the coordinates at discrete points along individual glulam beams at different locations throughout a structure is described in chapters 5 and 6. For each survey carried out, all the three-dimensional coordinates of beam targets are obtained in a local coordinate system and the values are listed in ECDS3 DAT files, an example of which is shown in Appendix B. However, because each survey is based on a different local system, the coordinates produced do not have a common origin and orientation with the exception of the z-axes which are aligned with the local gravity vector since the theodolites are levelled. Assuming that the z-coordinates are always referenced in the same direction, vertical deflection along a beam at different times is obtained by comparing z-coordinates for a

beam from survey to survey. This is the basis of the measurement technique developed to monitor the glulam structures and has the advantage that no control points are required for transforming coordinates into an object (or structure) based coordinate system and there is no need to set up over the same points each time measurements are taken.

Although the calculation of vertical deflection is quite straightforward, the problem of how to reference these, even in a local system, still remains. In an ideal world, one or more points at each site should have been chosen as reference points and their heights recorded during each survey and all *z*-coordinates could have been referenced to these. Since three of the structures in the measurement programme were monitored whilst building was in progress, it was very difficult to identify any reliable reference points stable enough to be considered fixed throughout the construction period and beyond. So, the conventional procedure of relating movement to some reference points was abandoned and each beam was analysed in isolation. To do this, one end (the lowest with pitched beams) was arbitrarily chosen to be the reference point for deriving vertical deflection even though this point was almost certainly moving itself. This would enable the creep behaviour of an individual beam to be evaluated but would not enable any overall structural movement at any site to be evaluated. After discussions with STRU, this proposed method of working was agreed.

The calculations for deriving vertical deflections of glulam beams are as follows. Taking the example of a pitched beam shown in figure 8.1, the *z*-

coordinate differences for the beam $(z_2 - z_1)$, $(z_3 - z_1)$ and so on are calculated using one end of the beam as an arbitrary reference to give the vertical distances to each target along a beam resulting from a particular survey. The first set of *z*-coordinate differences obtained in this way are taken to be the 'reference' target positions for a beam and all subsequent deflections are related to these.

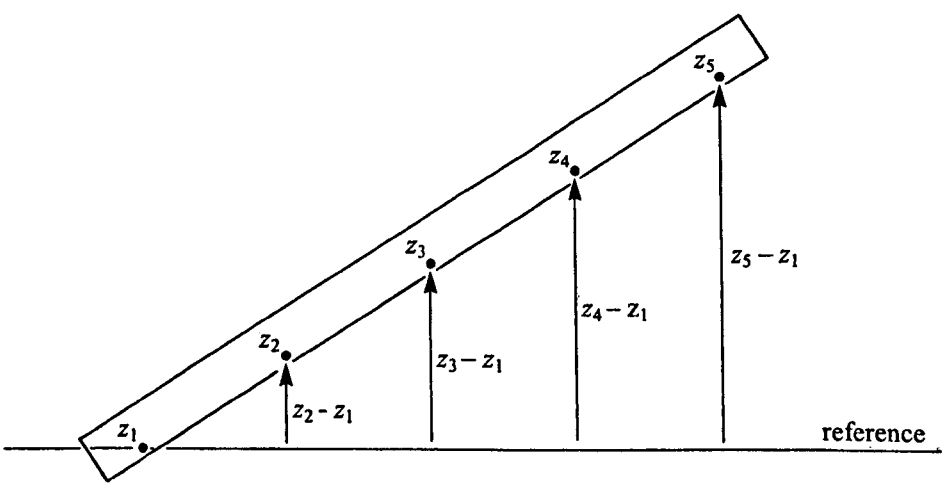

Figure 8.1 *Calculation of z-coordinate differences along a beam*

For each survey after the first, a characteristic deflection curve is usually obtained as shown in figure 8.2. On this diagram, the position of the beam at the start of monitoring (the reference position defined above) is represented by the straight line joining the $z_{1,1}$ to $z_{1,5}$ targets where the suffix 1,1 indicates the first survey, target point 1. Assuming the top end of the beam moves downwards relative to the reference in subsequent surveys, the area enclosed by the straight line joining $z_{n,1}$ to $z_{n,5}$ for the n^{th} survey and the reference represents the amount of structural movement that the beam has been subjected to in between the two surveys, which has not been measured. The area enclosed by the deflection curve and the $z_{n,1}$ to $z_{n,5}$ line represents the deflection

or creep of the beam. This can be obtained by comparing the z-coordinate differences for each survey to the first (reference) values. The relative deflection or creep at the centre of the beam is equivalent to its maximum bending deflection relative to the original profile and this value is calculated and used for later analysis.

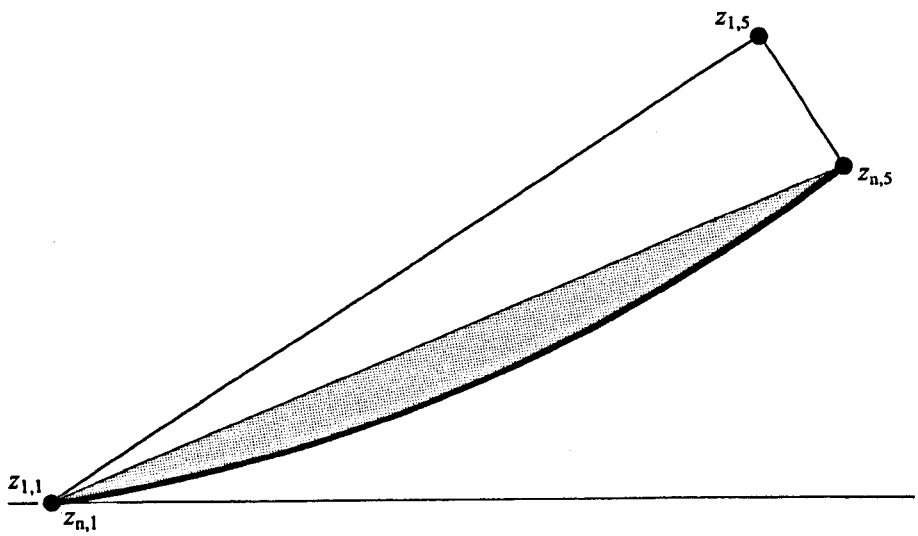

Figure 8.2 *Graphical representation of the deflection of a beam*

All data processing has been performed in Microsoft Excel 97. As an example, the first page of the workbook for Beam 2 at Wokingham is shown in table 8.1. On this, the row and columns have been added to assist with the description of the page.

The date of each survey is given in row 10 and the z-coordinates, imported from ECDS3 DAT files, are in rows 12 to 18. The computed z-coordinate differences for each survey are in rows 22 to 27 and the beam deflections are in rows 32 to 38. The first of these recorded on the 10 November 1992 in column C are the reference deflections and are all zero. In column D, showing data for the survey of the 16 November 1992, the beam deflections are obtained by

	A	B	C	D	E	F	G	H
1								
2	WOKBEAM2.XLS							
3								
4	DISPLACEMENT OF GLULAM BEAMS							
5	WOKINGHAM BAPTIST CHURCH							
6								
7	BEAM No 2 Page 1							
8								
9	MEASURED COORDINATES							
10	TARGET		10 NOV 92	16 NOV 92	23 NOV 92	24 NOV 92	30 NOV 92	14 DEC 92
11								
12	21		-895.40	-878.79	-884.84	-879.26	-995.29	-956.78
13	22		-529.62	-513.49	-519.71	-514.09	-630.17	-591.68
14	23		-166.17	-150.31	-156.68	-151.00	-267.16	-228.61
15	24		197.06	212.77	206.30	212.02	95.87	134.45
16	25		561.98	577.73	571.13	576.91	460.73	499.44
17	26		923.45	939.35	932.73	938.55	822.50	861.28
18	27		1255.93	1271.95	1265.21	1271.08	1154.94	1193.86
19								
20								
21	COORDINATE DIFFERENCES							
22	22-21		365.78	365.30	365.13	365.17	365.12	365.10
23	23-21		729.23	728.49	728.16	728.27	728.13	728.17
24	24-21		1092.46	1091.56	1091.14	1091.28	1091.16	1091.23
25	25-21		1457.38	1456.52	1455.97	1456.17	1456.02	1456.23
26	26-21		1818.85	1818.14	1817.56	1817.81	1817.79	1818.07
27	27-21		2151.33	2150.74	2150.05	2150.34	2150.23	2150.64
28								
29								
30	BEAM DEFLECTIONS RELATIVE TO 10 NOV 92							
31		*						
32	21	0	0.00	0.00	0.00	0.00	0.00	0.00
33	22	974	0.00	-0.48	-0.65	-0.61	-0.66	-0.68
34	23	1946	0.00	-0.74	-1.07	-0.96	-1.10	-1.05
35	24	2927	0.00	-0.90	-1.32	-1.17	-1.30	-1.23
36	25	3901	0.00	-0.86	-1.41	-1.20	-1.36	-1.15
37	26	4872	0.00	-0.71	-1.29	-1.04	-1.06	-0.79
38	27	5772	0.00	-0.59	-1.28	-0.99	-1.09	-0.69
39								
40								
41	RELATIVE DEFLECTION AT CENTRE OF BEAM FROM 10 NOV 92							
42	DAYS		0	6	13	14	20	34
43	24 (Deflection)		0.00	0.60	0.68	0.68	0.75	0.88
44								
45	BEAM 2 472x115mm SECTION 6.3m LONG							
46								
47	* Horizontal lengths along beam mm							
48								
49								

Table 8.1 *Page 1 of Excel workbook for Beam 2 at Wokingham (all coordinates are in mm)*

comparing the coordinate difference values in columns *C* and *D*. The deflection at target 21, the reference target, is always zero. The beam deflection at target 22 shown in cell *D*33 is obtained by comparing the coordinate difference (22-21) on the 16 November 1992 with the same reference difference on the 10 November 1992 or the entry in cell $D33 = (D22 - C22) = (365.30 - 365.78) = -0.48$ mm. Similarly, cell $D34 = (D23 - C23) = (728.49 - 729.23) = -0.74$ mm and so on to cell *D*38. For the survey of the 23 November 1992 in Column *E*, the corresponding beam deflections are cell $E33 = (E22 - C22)$ and cell $E34 = (E23 - C23)$ which repeats to cell *E*38.

The relative deflection at the centre of the beam for the 16 November 1992 in cell *D*43 is given by $\left[\frac{D38}{2} - D35\right] = \left[\frac{-0.59}{2} - (-0.90)\right] = 0.60$ mm and for the 23 November 1992 is given by $\left[\frac{E38}{2} - E35\right] = \left[\frac{-1.28}{2} - (-1.32)\right] = 0.68$ mm. This is computed for each survey.

All of the calculations are repeated throughout the workbook, the full version of which is given in Appendix D. This attempts to show the extent of the data collected for Beam 2 at Wokingham, where a total of twelve beams have been continuously monitored through 55 surveys since November 1992.

Similar workbooks have been prepared for Shoreham (31 Surveys from January 1993), Moulsecoomb (43 surveys from May 1994) and Bishop Hannington (35 surveys from July 1995).

8.2 Modelling deflection and creep behaviour

Deflection and creep in timber and glulam subjected to sustained stress is a time-dependent phenomenon and the relationship between deflection, creep and time has been expressed mathematically using a wide range of equations (see Morlier, 1994 and Dinwoodie, 2000). In general, these expressions are divided into two categories: those which tend to a limiting value (exponential and hyperbolic functions) and those which increase indefinitely (power and logarithmic functions) (Neville, *et al.*, 1993). Although the former are more common, there is no justification for acceptance of an ultimate value of creep. It is also noted that such expressions are all purely empirical and are not based on a generally agreed theoretical basis at this time. When one method is said to be better than another, this merely reflects on how easily their constants can be determined and how well they fit experimental results.

This thesis is concerned with the application of coordinate measurement (by surveying methods) to determine the deflection of various glulam sections under differing conditions. The main aim is not to process the results obtained by all possible means and reach a conclusion or proposal on the long-term behaviour of glulam in differing environments but to demonstrate that the measurement method implemented is of some value in timber research. To this end, and given the complexity and amount of work carried out in this field, the results obtained here will only be analysed to see how they agree with two versions of the most widely used creep models, the power law and exponential models. This approach to modelling is recommended by Le Govic (1994b) for experimental work following his extensive review of current practice.

The *power law model* is one of the most successful mathematical descriptions of creep and it is also used extensively in the study of other materials such as polymers and concrete. This law exists in many forms but the most basic version is

$$\mu(t) = \mu_{inst} + at^b \qquad 8.1$$

where

$\mu(t)$ = total deflection at time t

μ_{inst} = instantaneous or initial deflection

at^b = time-dependent creep (or beam deflection in this project)

a and b are material specific constants to be determined experimentally

t = the elapsed time

Equation 8.1 gives the expected deflection for a structural element as a function of time. For the beams monitored, the relative deflection or creep = $\mu(t) - \mu_{inst} = at^b$ and this can be expressed in logarithmic form as (choosing base 10 for logarithms)

$$\log_{10}(\textit{relative deflection}) = \log_{10}(a) + b\log_{10}(t) \qquad 8.2$$

which is equivalent to the linear relationship $y = c + mx$. If measured deflections are plotted as $y = \log_{10}$ (*deflection*) against $x = \log_{10}(t)$ and a linear regression is performed on the result, values for the constants a and b can be obtained. This rather straightforward way of determining the power law

constants explains its popularity for modelling creep.

An alternative mathematical expression used to model deflections and creep in timber is the *exponential model* of the form

$$\mu(t) = \mu_{inst} + a(1 - e^{-bt}) \qquad 8.3$$

where a and b again signify material parameters which are required to be determined experimentally.

As with the power law, it is convenient to reduce this to some linear form for modelling purposes. In this case, the creep component of deflection as a function of time is given as relative deflection = $a(1-e^{-bt})$. The rate of change of relative deflection is given by

$$\frac{\mathrm{d}(deflection)}{\mathrm{d}t} = abe^{-bt} = ab - b(a - ae^{-bt})$$

$$= ab - b(deflection) \qquad 8.4$$

If the deflection data is plotted as $x = deflection$ and $y = \frac{\mathrm{d}(deflection)}{\mathrm{d}t}$, the linear form is again realised with b given by the slope of a linear regression line fitted to the plot and with a given by $\left[\frac{\text{y intercept}}{\text{b}}\right]$.

8.3 Creep results

In this section, the creep behaviour of the beams in the four structures monitored is described and an attempt is made to model this. A reminder is

given that only the centre deflections with respect to the ends of the targeted lengths in each beam have been considered when deriving beam deflections. As might be expected, the deflection pattern of each beam at each site is made up of components resulting from applied loads together with a creep response, the latter including mechano-sorptive effects. Consequently, a brief history of the environmental conditions at the four sites monitored is given together with the discussion of the results obtained.

Wokingham Baptist Church

At Wokingham, a glulam roof frame continues to be monitored which was constructed in mid-October 1992 and monitoring of twelve selected beams (rafters) on this structure commenced on the 10 November 1992. A detailed description of this site and the monitoring procedures used can be found in section 6.1.

For the first 100 days this building was unheated and often subject to cold and damp winter conditions whilst construction was in progress. Temperatures during this period averaged about 8°C while humidities were very high (80-100%). After commissioning in March 1993, heating has been applied intermittently in the room during the autumn-winter-spring period each year, resulting in temperatures generally in the range 10-20°C. Humidities have reduced gradually from the initial high values to a range of 40-70% since then.

Once the initial drying period was completed, the relative humidity of the surrounding air has only exceeded 65% for a few weeks each year which

classifies Wokingham as a Eurocode 5 Service Class 1 building (see section 2.4).

As monitoring has proceeded, the deflection curves observed along the length of all beams have been plotted after each survey has been completed and examples of some of these are given in figure 8.3 for Beam 3. The reason for producing these curves is to compare results from the latest survey to previous surveys in order to highlight any unusual changes. Any abnormalities in a set of beam deflection curves could be caused by measurement errors, the targets being interfered with or could be due to some peculiar behavioural pattern in a beam. If any unusual results have been obtained, these have been investigated by a repeat survey but for nearly all measurements, no such problems have normally been encountered.

However, on occasions, targets have been accidentally removed or damaged in between site visits and to reinstate these at the same point with a sub-millimetre accuracy would be very difficult if not impossible to do. To overcome this problem, no attempt is made to replace a missing or disturbed target in the same place and a new one is fixed to the beam as close as possible to its original position. On site, observations are then taken to this target in the normal way. When processing data, a theoretical value for the z-coordinate for the replaced target is obtained by first producing a best-fit polynomial function through the other observed targets along the beam that gives a similar shaped beam deflection curve to that obtained in previous surveys: a value for the missing z-coordinate is then either interpolated or extrapolated from this. The value derived is then compared to the latest measured coordinate and the

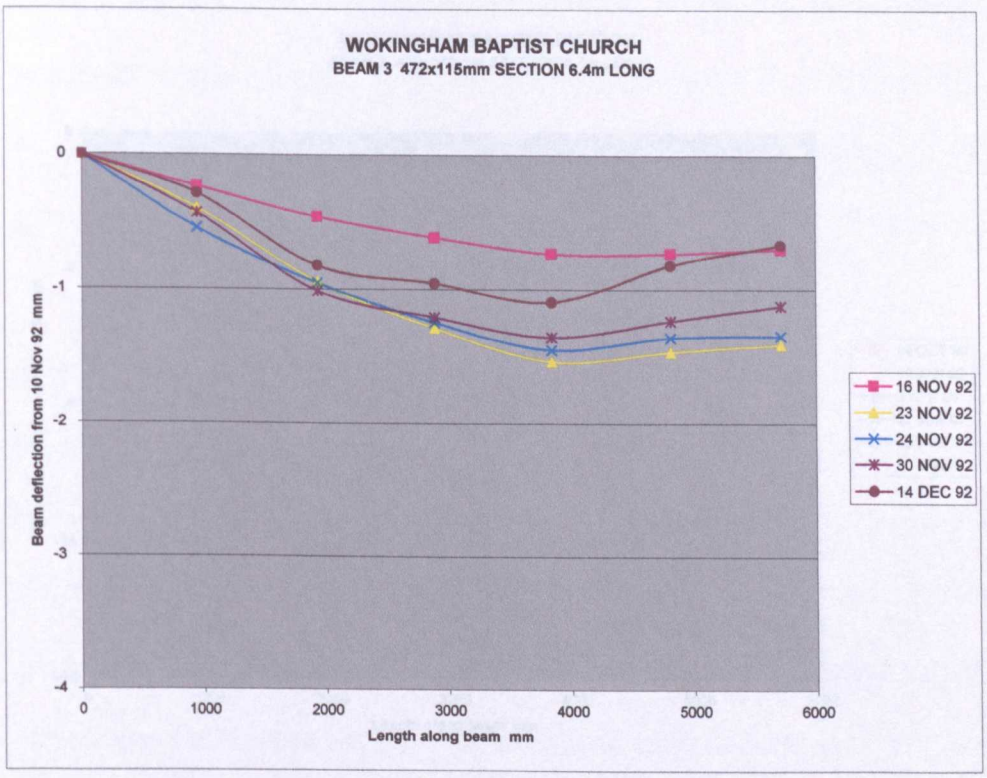

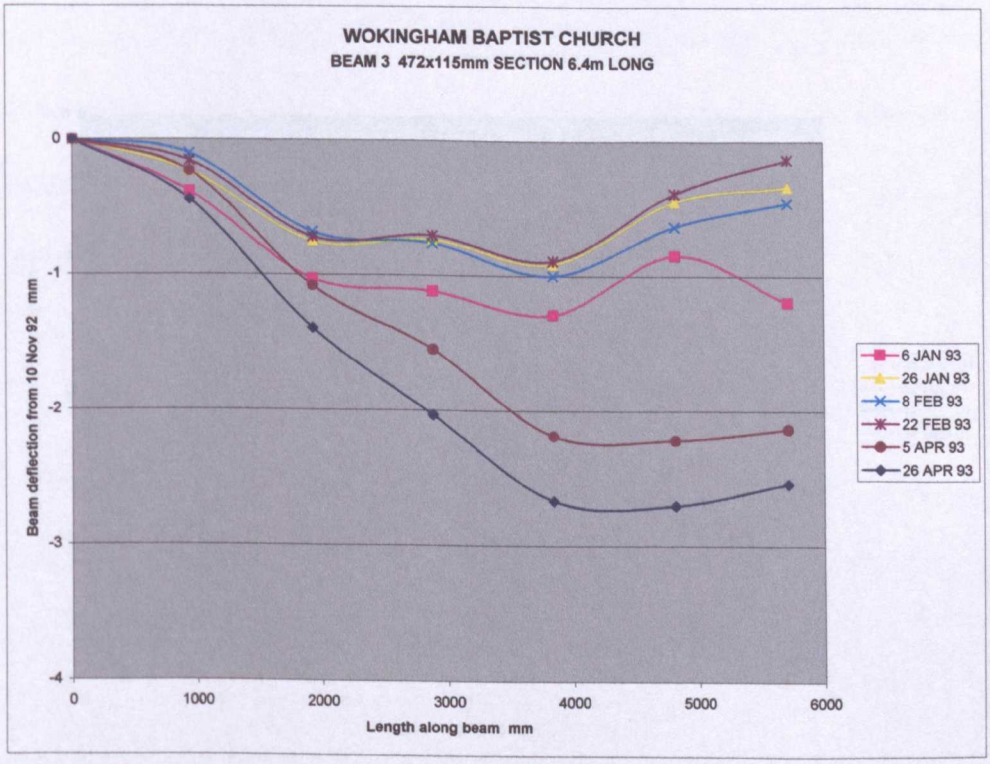

Figure 8.3(a) *First deflections for Beam 3 at Wokingham*

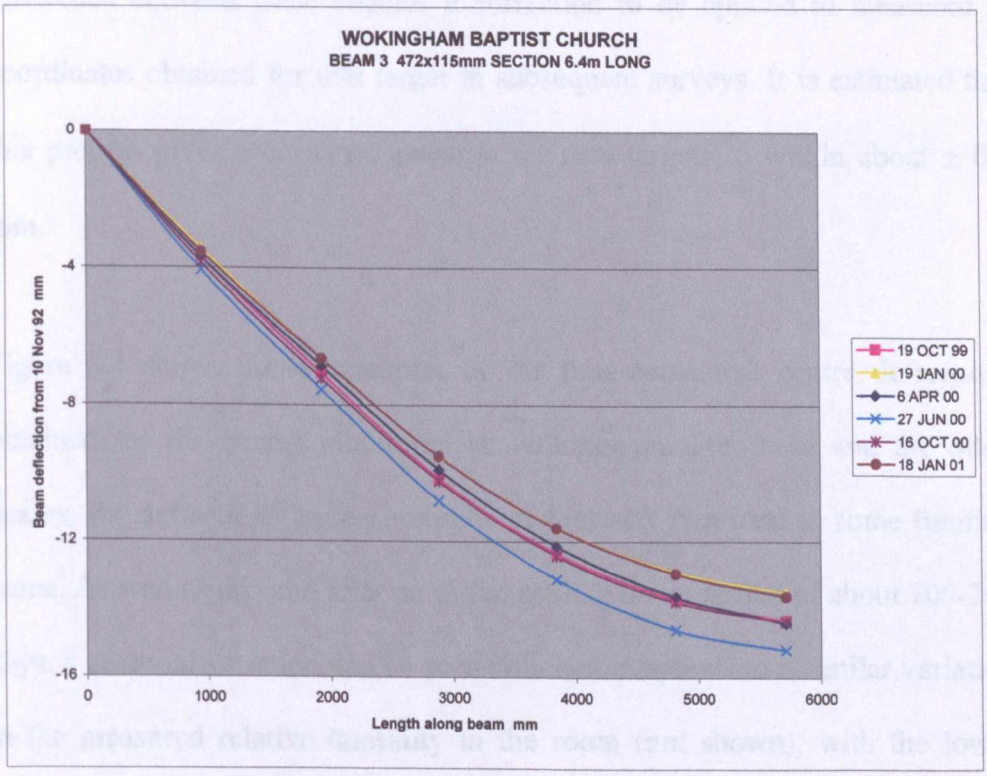

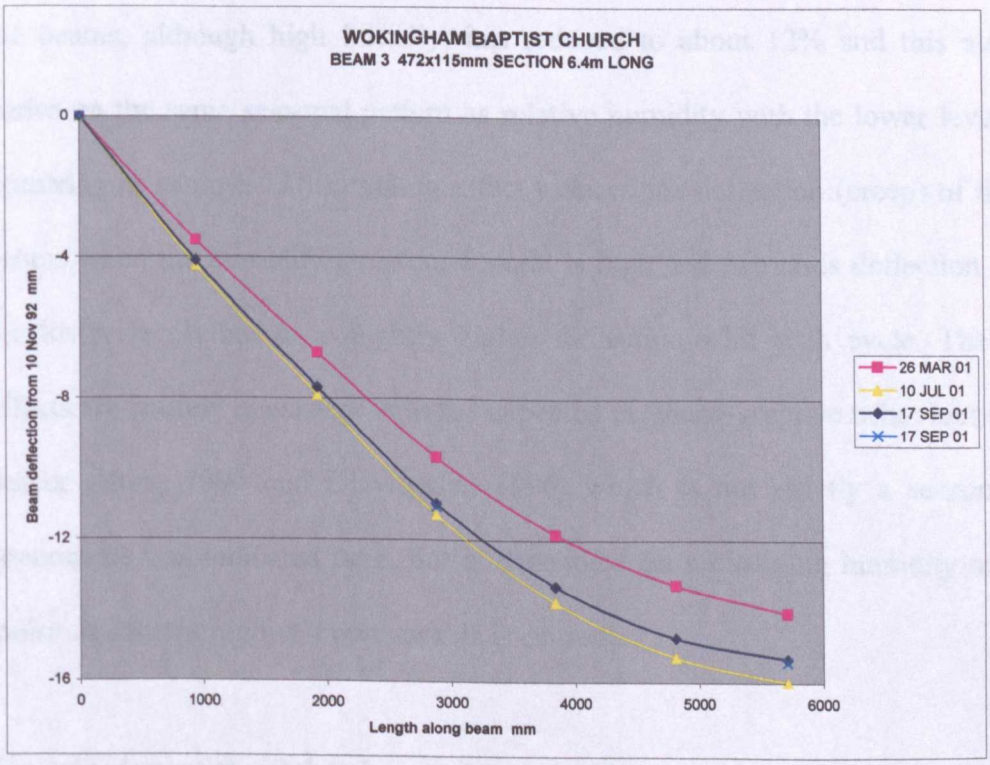

Figure 8.3(b) *Latest deflections for Beam 3 at Wokinhgam*

difference between these enables a correction to be applied to measured *z*-coordinates obtained for that target in subsequent surveys. It is estimated that this process gives a corrected position for new targets to within about ± 0.1 mm.

Figure 8.4 shows some examples of the time-dependent centre deflections obtained for the beams monitored at Wokingham. For these and the other beams, the deflections increase rapidly at first and then tend to some limiting value. As well as this and after an initial settling down period of about 100-200 days, a seasonal variation can be seen which corresponds to a similar variation in the measured relative humidity in the room (not shown), with the lower values of humidity occurring in the summer months. The moisture content of the beams, although high initially, has reduced to about 12% and this also varies on the same seasonal pattern as relative humidity with the lower levels occurring in summer. This cycling effect reduces the deflection (creep) of the beams when the humidity/moisture content is high and increases deflection at the lower levels but to a slightly higher deflection with each cycle. These effects are entirely consistent with the expected mechano-sorptive behaviour of timber (Hunt, 1994 and Dinwoodie, 1996) which is not strictly a seasonal phenomenon as indicated here, but is dependent on a changing humidity and moisture content regime, however this is caused.

The behaviour of the glulam beams shows that the magnitude of the deflections (or creep) obtained due to load is approximately constant after a given time but that the mechano-sorptive component is much more variable, being dependent

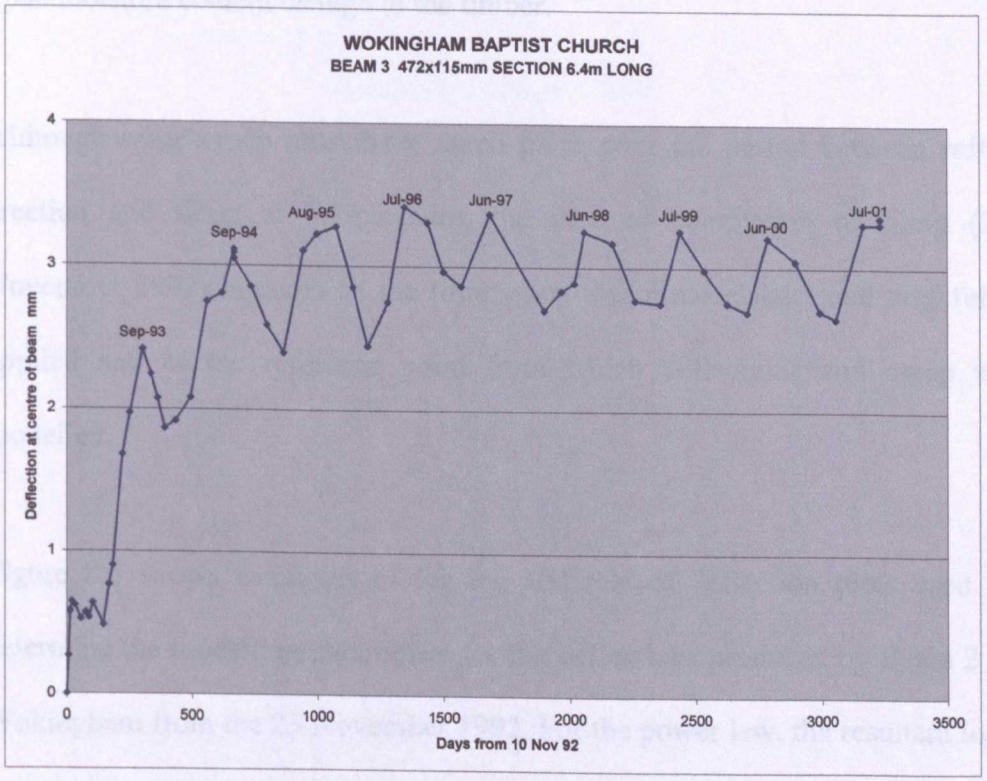

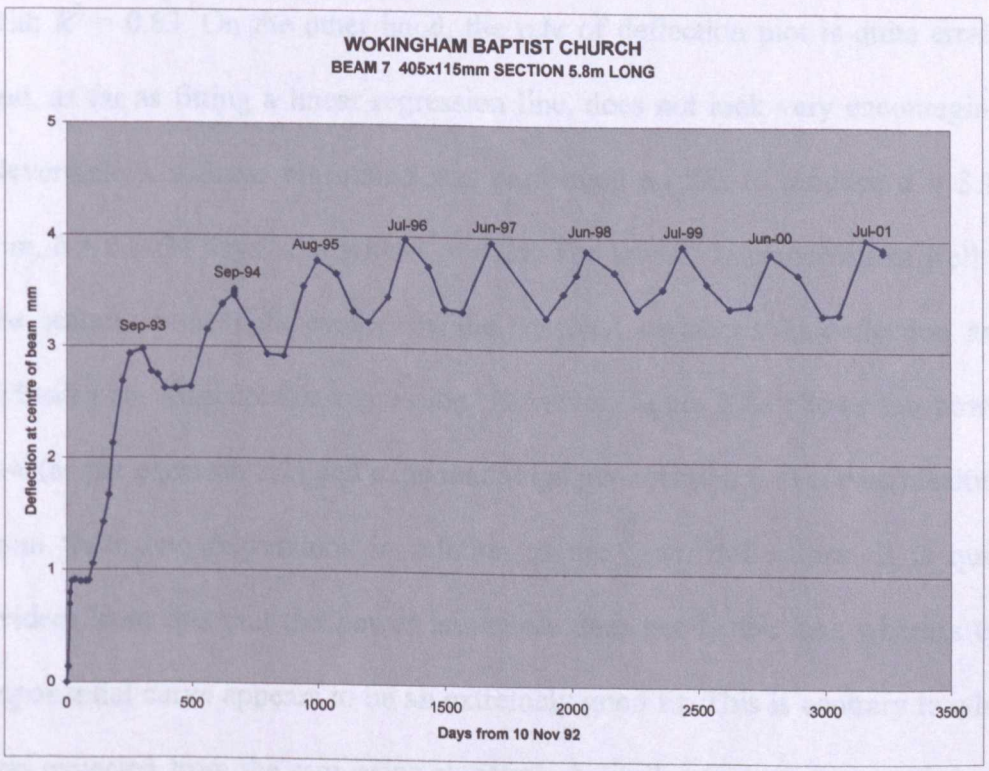

Figure 8.4 *Examples of centre deflections at Wokingham*

upon moisture content change in the timber.

Although some creep must have taken place over the period between rafter erection and tiling at Wokingham, the date of completion of tiling (23 November 1992) is taken as the time when the initial elastic load was fully applied and as the reference point from which deflections and creep are modelled.

Figure 8.5 shows examples of log-log and rate of deflection plots used to determine the modelling parameters for the deflections produced by Beam 2 at Wokingham from the 23 November 1992. For the power law, the resultant log-log plot and linear regression line (from Excel 97) $a = 0.025$ and $b = 0.6593$ with $R^2 = 0.83$. On the other hand, the rate of deflection plot is quite erratic and, as far as fitting a linear regression line, does not look very encouraging. Nevertheless, a linear regression was performed on this to produce $a = 3.16$ mm, $b = 0.0024$ days^{-1} but with $R^2 = 0.25$. The low R^2 value correlates well to the scatter in the data caused by the seasonal variations in deflection and indicates an unacceptable regression. However, figure 8.6a shows the power law (as per equation 8.1) and exponential (as per equation 8.3) curves resulting from these two regressions in relation to the beam deflections. It is quite evident from this that the power law curve does not fit the data whereas the exponential curve appears to be an extremely good fit. This is contrary to what was expected from the regression statistics. A similar analysis was carried out on the deflections produced by Beam 7 and the results from this are shown in figure 8.6b. For the power law in this case, $a = 0.0765$, $b = 0.4907$ (R^2 high)

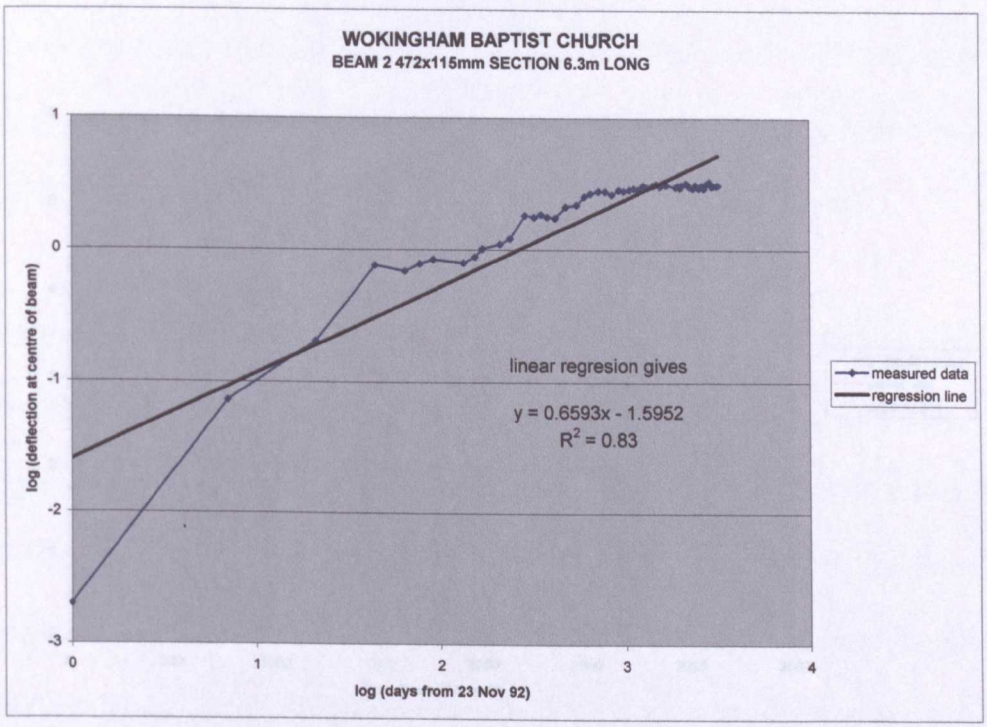

Log-log plot for power law constants

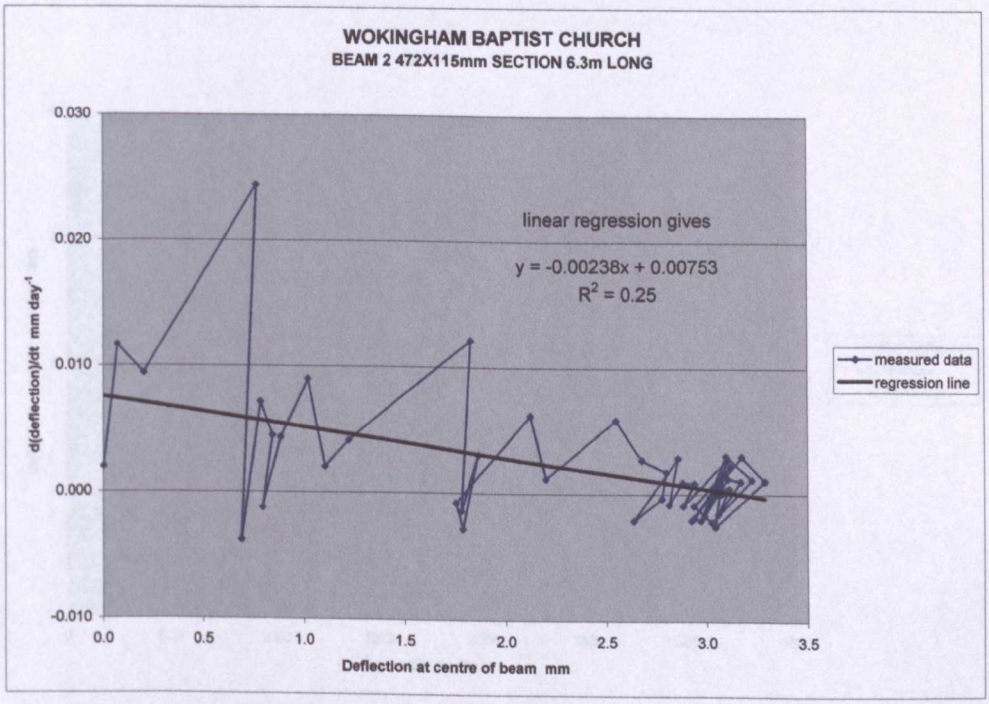

Rate of deflection plot for exponential constants

Figure 8.5 *Linear regression results for Beam 2 at Wokingham*

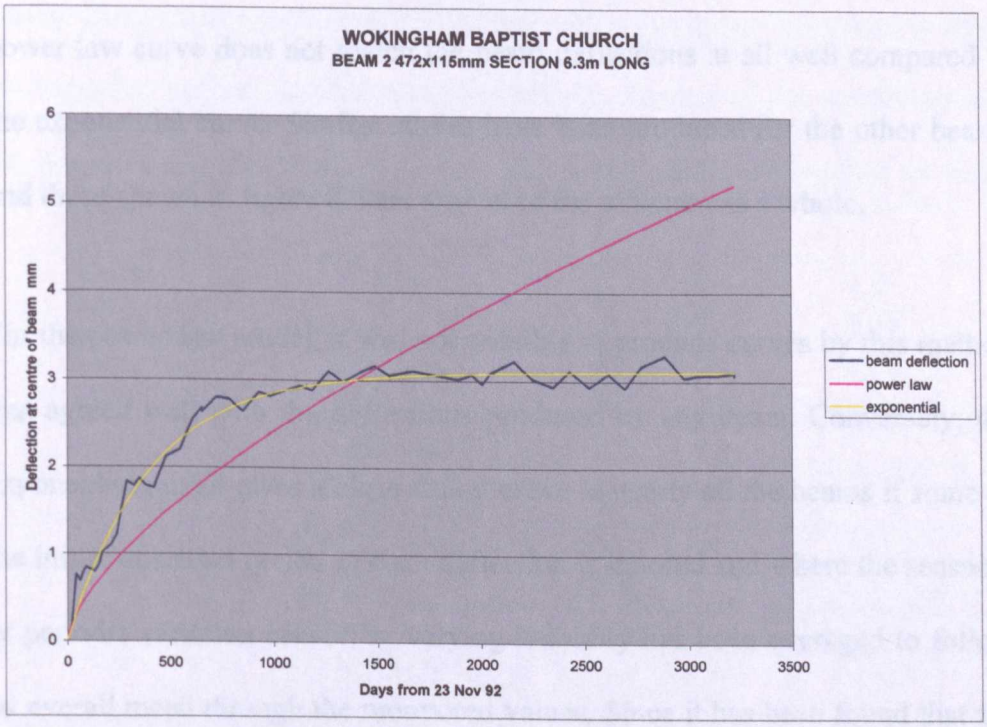

(a) Beam 2

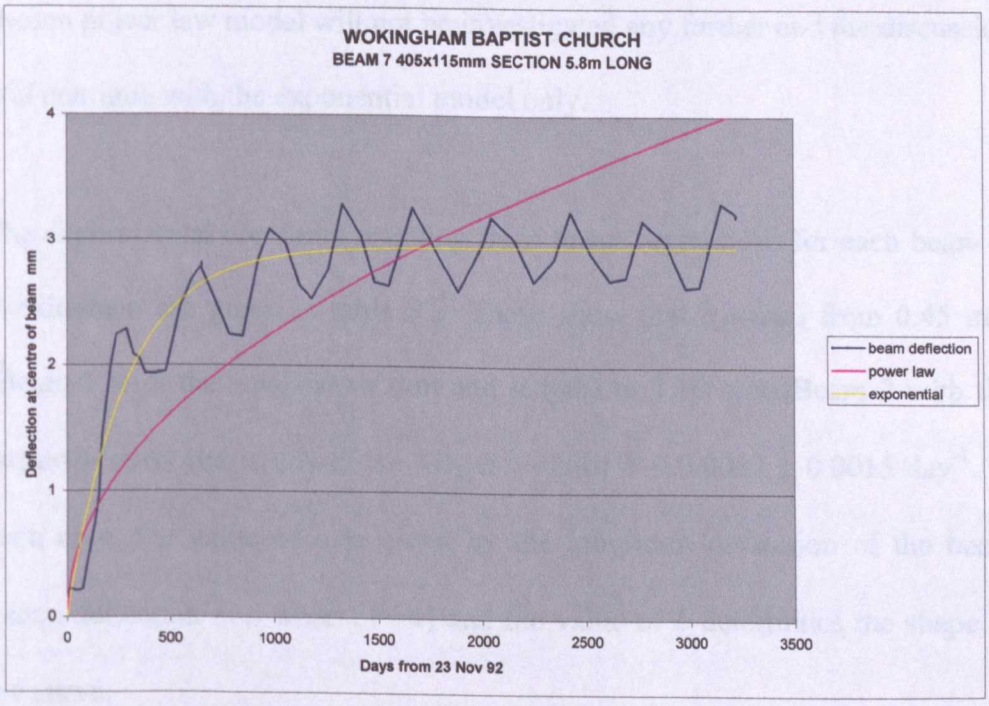

(b) Beam 7

Figure 8.6 *Theoretical power law and exponential curves*

and for the exponential $a = 2.95$ mm, $b = 0.0040$ day^{-1} (R^2 low). As before, the power law curve does not match the beam deflections at all well compared to the exponential curve. Similar curves have been produced for the other beams and those shown in figure 8.6 are typical of the structure as a whole.

For the power law model, it was not possible to produce curves by this method that agreed well with the deflections produced by any beam. Conversely, the exponential model gives a close-fitting curve to nearly all the beams if some of the initial unsettled period of each deflection is ignored and where the seasonal or periodic variation caused by varying humidity has been averaged to follow an overall mean through the monitored values. Since it has been found that the exponential model at Wokingham gives a much better fit to the data, the chosen power law model will not be investigated any further and the discussion will continue with the exponential model only.

The experimental constants resulting from linear regressions for each beam at Wokingham are given in table 8.2. These show that a varies from 0.45 mm (Beam 1 with the smallest section and length) to 3.16 mm (Beam 2 with the largest section and is one of the longest) whilst $b = 0.0032 \pm 0.0015$ day^{-1}. In each case, the value of a is given by the long-term deflection of the beam (since deflection = a when $t = \infty$) and the value of b determines the shape of the curve.

In the analysis of beam deflections discussed so far, the value of the a constant obtained depends on the sizes of the beams and their loading. In order to

compare the response of each beam on a common datum it is necessary to change the y-axis of each centre deflection curve to a creep factor and to show the values of k_{def} for each beam. Unfortunately, because of site conditions and the practical difficulties of measuring true initial elastic deflections as loads

Beam	Size	a mm	b days^{-1}
1	270x 90mm SECTION 2.5m LONG	0.45	0.0060
2	472x115mm SECTION 6.3m LONG	3.16	0.0024
3	472x115mm SECTION 6.4m LONG	2.40	0.0030
4	450x115mm SECTION 2.3m LONG	1.60	0.0035
5	450x115mm SECTION 2.3m LONG	not possible to fit exponential curve to data	
6	495x115mm SECTION 2.9m LONG	0.65	0.0020
7	405x115mm SECTION 5.8m LONG	2.95	0.0040
8	450x115mm SECTION 6.4m LONG	2.75	0.0020
9	495x115mm SECTION 2.7m LONG	2.05	0.0055
10	405x90mm SECTION 6.6m LONG	1.15	0.0015
11	405x90mm SECTION 6.6m LONG	0.45	0.0035
12	472x115mm SECTION 6.4m LONG	0.50	0.0015

Table 8.2 *Exponential constants for beams at Wokingham*

were applied in stages, it is not possible to determine, with absolute certainty, the creep factors for each beam. Even the early deflections shown in figure 8.3a do not help in this as they were measured after the roof had been partially loaded and no obvious change in deflection can be seen during tiling. However, a full set of design drawings and specifications for the building have been obtained and it has been possible to calculate values for initial elastic deflections for some of the beams at Wokingham based on estimated total

loads and the beam sizes/spans. These are listed in table 8.3 and are used to convert deflections into k_{def} values using the definition given in equation 2.1.

Using the calculated initial deflections for beams *B*2, *B*3, *B*7 and *B*8 (four of the largest section and length rafters), figure 8.7 shows the creep factors for

Beam	2	3	7	8
calculated initial deflection	5.75 mm	5.46 mm	6.66 mm	6.24 mm
k_{def} = measured beam deflection/calculated initial deflection				

Table 8.3 *Calculated initial deflections at Wokingham (Abdul-Wahab, et al., 1998)*

these beams from 23 November 1992. They show a variation of about 0.20 in magnitude and are the largest creep factors obtained at Wokingham. Also shown on figure 8.7 is an exponential curve where the creep factor $k_{def}(t)$ as a function of the elapsed time t (with t in days) is given by $k_{def}(t) = 0.50(1-e^{-0.0032t})$. Following on from this and despite the varying creep responses, the results shown at Wokingham for the larger beams could satisfy an equation of the form

$$k_{def}(t) = k_{def}(1-e^{-0.0032t}) \qquad 8.5$$

where, after almost 10 years, the k_{def} value does not exceed 0.60.

For a Service Class 1 building in the long-term (up to 10 years), the k_{def} value given by Eurocode 5 in table 2.1 is 0.50 and for a permanent load (more than 10 years) is 0.60. Taking account that the creep factors derived from measured deflection curves are estimated on the basis of assumed initial deflections, the

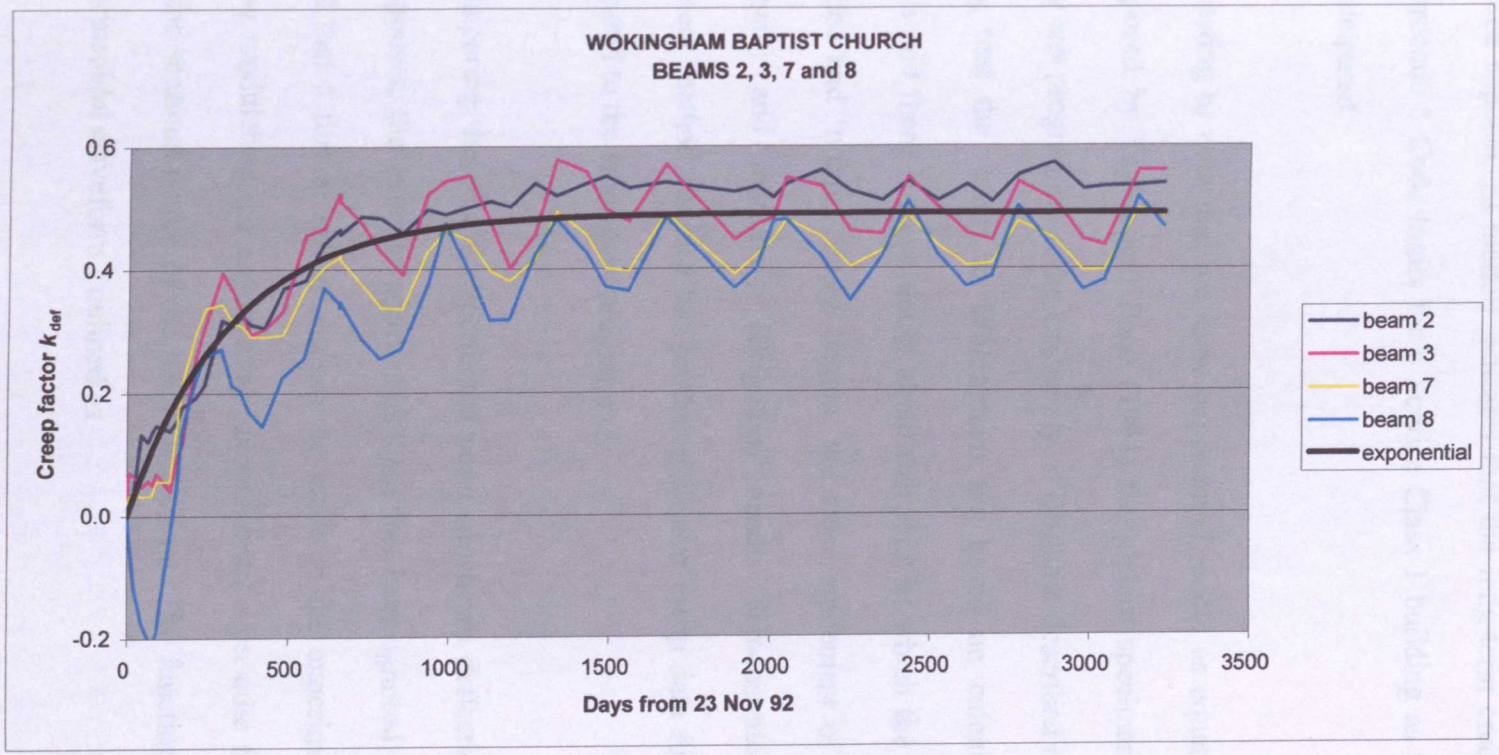

Figure 8.7 *Creep factors for Beams 2, 3, 7 and 8 at Wokingham*

creep response obtained for some of the larger beams at Wokingham (based on the proposed exponential model) indicates that the long-term creep just falls within Eurocode 5 Code limits for a Service Class 1 building as the original design anticipated.

It is interesting to note that the same exponential model as equation 8.5 has been proposed by Taylor and Pope (1994) for glulam specimens from the laboratory test programme at the University of Brighton described in chapter 2. Accepting that the results at Wokingham are based on calculated initial deflections and there is some doubt about the point at which the structure is fully loaded and 'normal' creep begins, the close agreement of the on-site (Wokingham) and laboratory (Brighton) results demonstrates that the measurement method adopted has produced similar creep data for glulam in situ compared to the laboratory programme.

When comparing theoretical exponential curves to beam deflections and the creep responses, the annual variation in these has been ignored so far. It is suggested that a further refinement can be made to the experimental model derived by modulating the exponential function with a periodic function that matches the seasonal nature of the beam deflections. The function chosen for this is a sinusoidal waveform s defined as

$$s = c\sin\left[\frac{2\pi}{T}(t+\Delta t)\right] \qquad 8.6$$

where

s = sinusoidal periodic function

c = amplitude of sinusoidal function

T = period of the sinusoidal function

t = elapsed time in days

Δt = a phase angle

Combined with the exponential model, this gives

$$\mu(t) = \mu_{inst} + a(1 - e^{-bt}) + c\sin\left[\frac{2\pi}{T}(t + \Delta t)\right] \qquad 8.7$$

The effect of modulating the exponential models for Beams 7 and 9 is shown in figure 8.8. For these analyses, the value of T was assumed to be 365 days and optimum values for c and Δt were obtained by minimising the sum of squares of the residuals produced by each variable in turn. From this, it is evident that the deflection (and the creep response) of these two beams does follow a predictable (exponential + sinusoidal) model. All of the beams at Wokingham have been analysed in this way and all show similar results. The value of c varies from 0.1 mm (small beams) to 0.45 mm (large beams) and $\Delta t = 200 \pm 15$ days.

This result highlights an interesting response of glulam to a seasonal variation in environmental conditions that warrants a further investigation that is outside the scope of this thesis. It would be useful if some means could be devised for assigning values in advance to c and Δt in order that the creep response of a structure could be predicted more closely at the design stage.

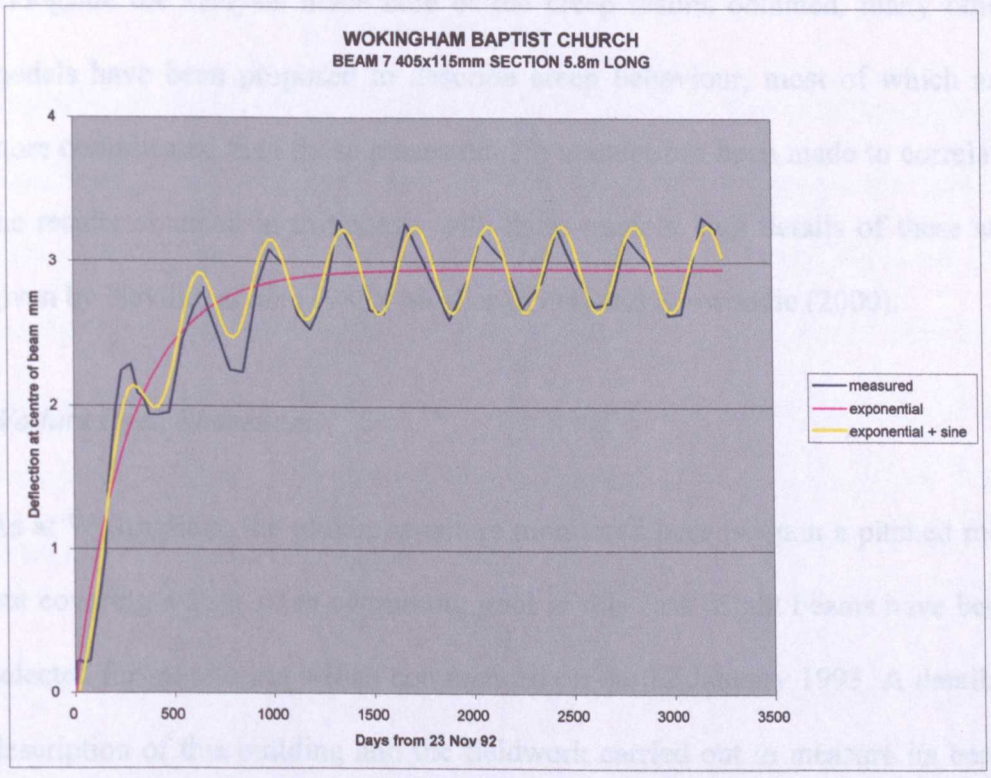

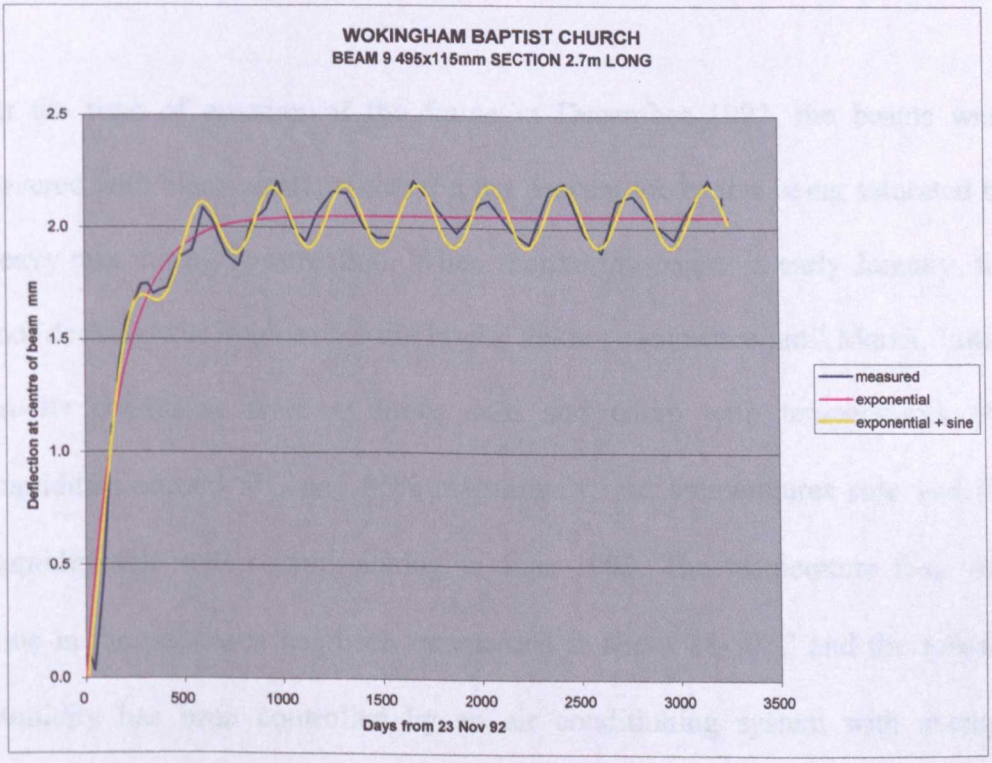

Figure 8.8 *Modulated deflections for Beams 7 and 9 at Wokingham*

Alongside the analysis made here of the creep results obtained, many other models have been proposed to describe creep behaviour, most of which are more complicated than those presented. No attempt has been made to correlate the results obtained in this thesis with these models. Full details of these are given by Neville, *et al.*, (1983), Morlier (1994) and Dinwoodie (2000).

Wadurs Pool, Shoreham

As at Wokingham, the glulam structure monitored here is again a pitched roof but covering a 25 x 10 m swimming pool in this case. Eight beams have been selected for monitoring which commenced on the 12 January 1993. A detailed description of this building and the fieldwork carried out to measure its beam deflections is given in section 6.2.

At the time of erection of the frame in December 1992, the beams were covered with black plastic which did not prevent the beams being saturated by heavy rain during construction. When monitoring began in early January, the roof decking was in place but tile laying did not commence until March. Initial on-site conditions were at times cold and damp with temperatures and humidities around 5°C and 85% respectively, but temperatures rose and the humidity fell until commissioning in June 1993. The temperature from this time in the pool area has been maintained at about 28-30°C and the relative humidity has been controlled by an air conditioning system with average values of 40-70% being recorded. These tend to be slightly higher in the summer but vary considerably from day-to-day and where sudden increases (sometimes up to 100%) can occur for a few hours during the night when the

system is switched off.

According to the Eurocode 5 definition of Service Class, this building might be considered as Service Class 3 because the relative humidity of the air exceeds 85% (each night) for more than just a few weeks per annum. However, the moisture contents developed in the glulam beams have not exceeded 16% after construction and on this basis and bearing in mind the short duration of the high humidity pulses, the nearest equivalent service class of Eurocode 5 for Wadurs Pool should be Service Class 2.

To provide an initial check on results, the deflection curves measured along the beams have been plotted following completion of each survey and any unusual behaviour investigated. Figure 8.9 shows some of these curves for the first monitoring period which took place during construction from the 12 January-1 March 1993. These curves are typical of those obtained for all eight beams at Shoreham. In section 6.2, it was noted that the top targets on each beam were not visible at Shoreham at the start of monitoring in January because of obstructions caused by scaffolding that had been erected in the pool area since the targets were put in place in December. As shown in figure 8.9, this only affects the surveys of the 18 January and the 1 February. No obvious early trend in deflection (or creep) is noted for the beams in figure 8.9 until the change in deflection patterns corresponding to the roof being partially tiled between the surveys of the 11 February and the 1 March 1993. Although this change in deflections has been recorded, it does not provide enough information to determine the magnitude of the effect of applying all the initial load to the roof but it does show how the measurement system responded to the

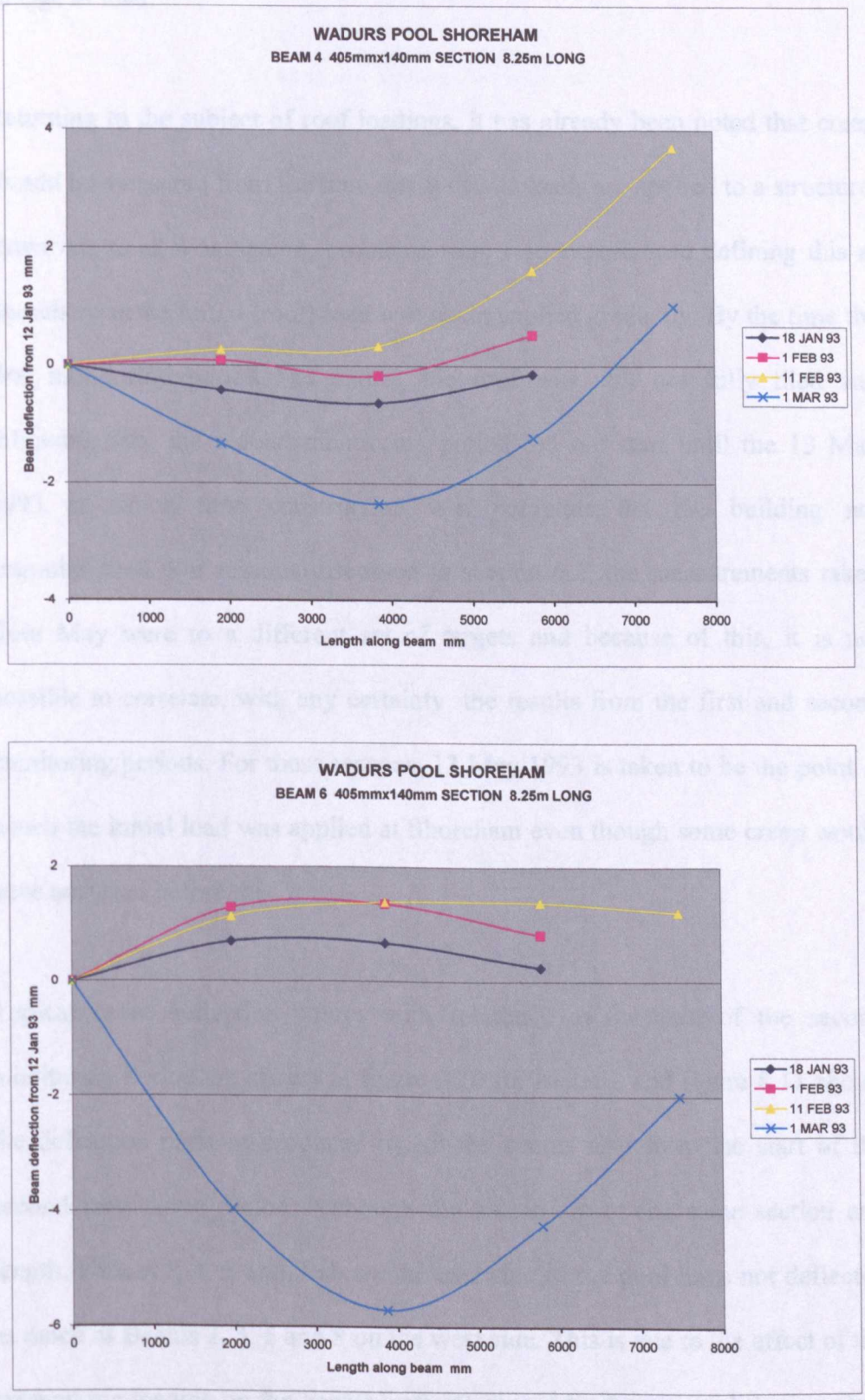

Figure 8.9 *Typical beam deflections for first monitoring period at Shoreham*

change in load.

Returning to the subject of roof loadings, it has already been noted that creep should be measured from the time initial elastic loads are applied to a structure. However, as at Wokingham, problems were also experienced defining this at Shoreham as the initial (roof) load was again applied gradually. By the time the first monitoring period had ended, the roof was still not fully tiled and following this, the second monitoring period did not start until the 13 May 1993 at which time construction was complete but the building not commissioned. For reasons discussed in section 6.2, the measurements taken from May were to a different set of targets and because of this, it is not possible to correlate, with any certainty, the results from the first and second monitoring periods. For these reasons, 13 May 1993 is taken to be the point at which the initial load was applied at Shoreham even though some creep would have occurred before this.

Typical beam deflection curves with reference to the start of the second monitoring period are shown in figure 8.10 for Beam 2 and figure 8.11 shows the deflection patterns produced by all the beams also from the start of the second monitoring period. Although the beams are of the same section and length, Beams 1, 4, 5 and 7 above the east side of the pool have not deflected as much as Beams 2, 3, 6 and 8 on the west side. This is due to the effect of the asymmetric loading on the beams (rafters) caused by the air conditioning plant room which has been built over the east side of the roof (see figure 6.9).

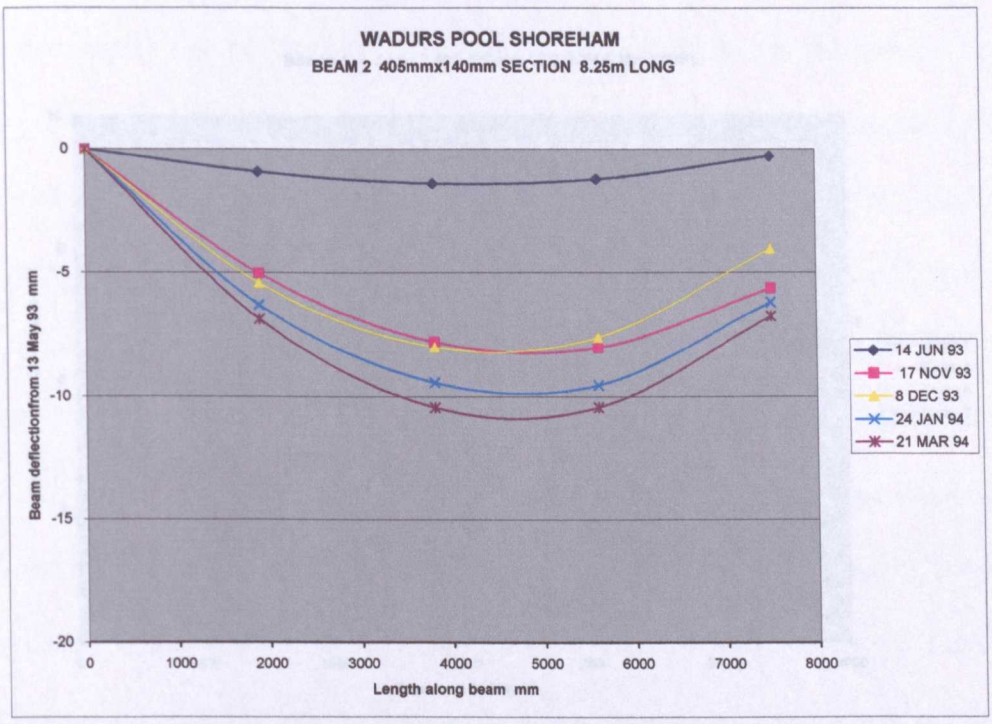

(a) Initial results

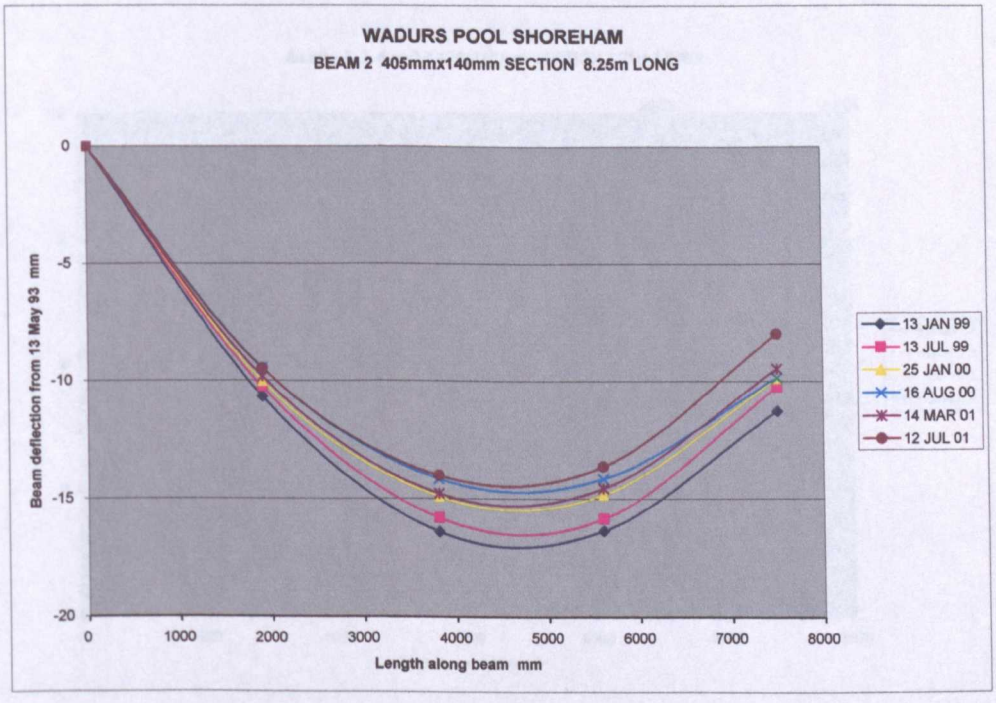

(b) Latest results

Figure 8.10 *Beam 2 deflections at Shoreham for second monitoring period*

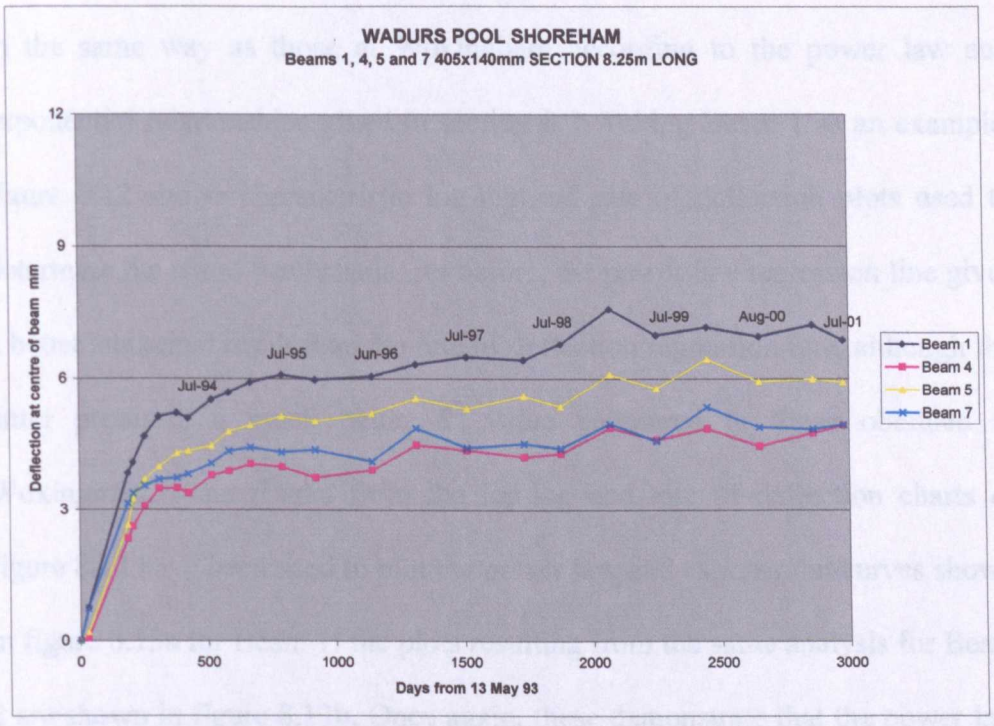

(a) Deflections for beams along east side of pool

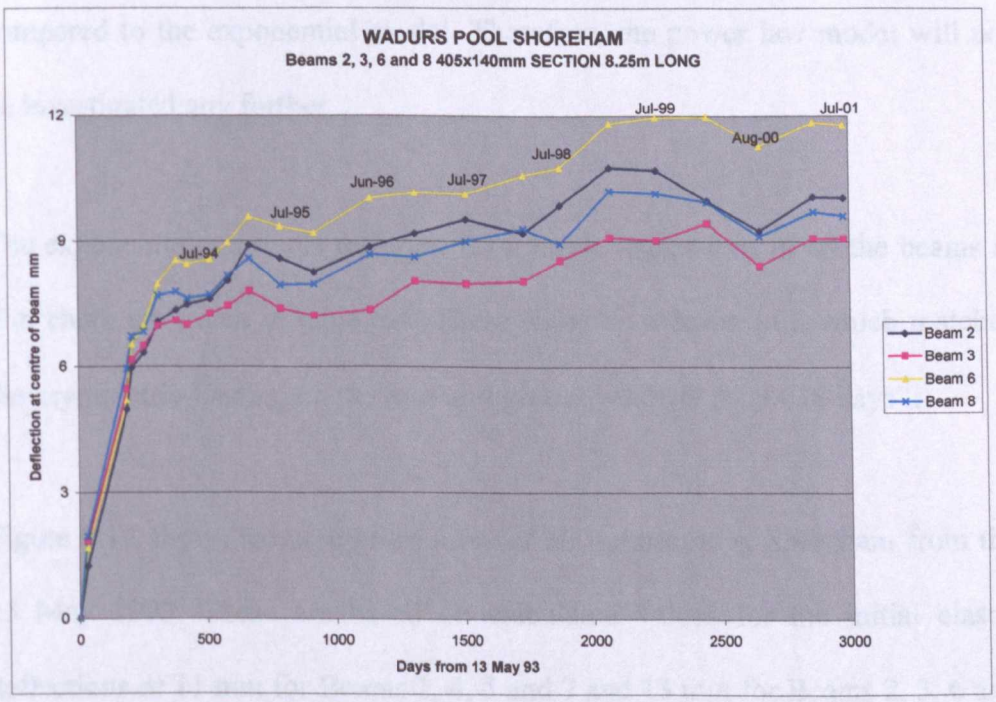

(b) Deflections for beams along west side of pool

Figure 8.11 *Beam deflections at Shoreham*

The deflections produced by all of the beams at Shoreham have been modelled in the same way as those at Wokingham according to the power law and exponential relationships given in section 8.2. Taking Beam 1 as an example, figure 8.12 shows characteristic log-log and rate of deflection plots used to determine the a and b constants. As before, the power law regression line gives a better statistical result than the rate of deflection regression line, although the latter produces a much better R^2 value compared to those obtained at Wokingham. The results from the log-log and rate of deflection charts of figure 8.12 have been used to plot the power law and exponential curves shown in figure 8.13a for Beam 1: the plots resulting from the same analysis for Beam 2 are shown in figure 8.13b. Once again, these demonstrate that the power law model is not capable of producing a very good fit to the measured deflections compared to the exponential model. Therefore, the power law model will not be investigated any further.

The exponential constants resulting from linear regressions of all the beams at Shoreham are given in table 8.4. These show a variation in a which matches the asymmetric loading on the roof and give $b = 0.0047 \pm 0.0018$ days^{-1}.

Figure 8.14 shows the creep responses of all the beams at Shoreham from the 13 May 1993. These are based on calculated values for the initial elastic deflections of 11 mm for Beams 1, 4, 5 and 7 and 13 mm for Beams 2, 3, 6 and 8 as calculated by Abdul-Wahab, *et al.*, (1998).

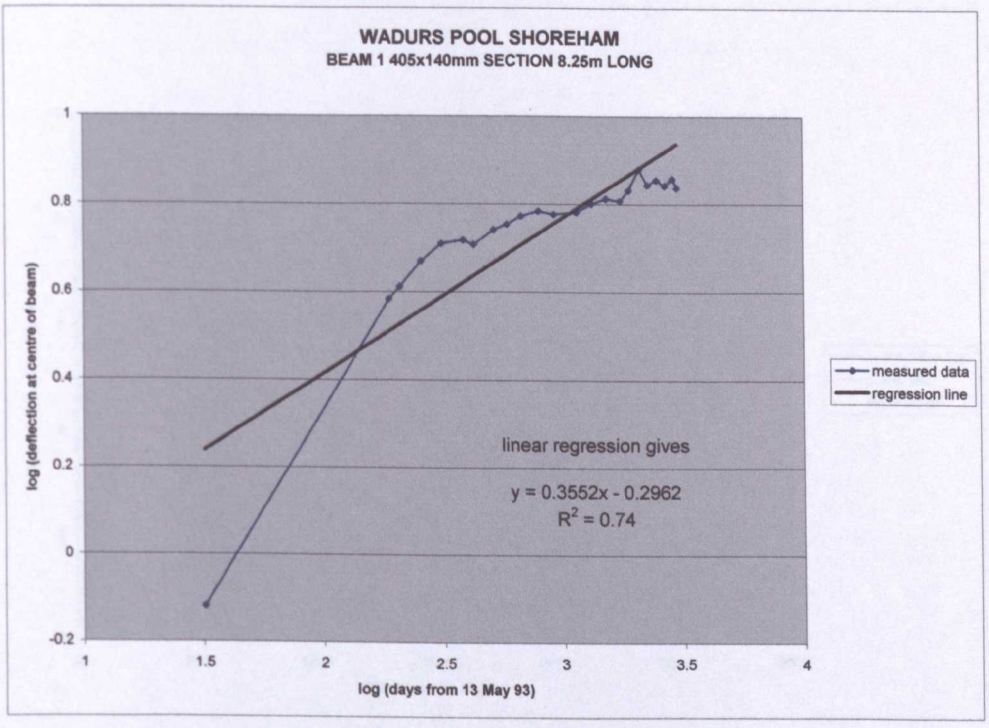

Log-log plot for power law constants

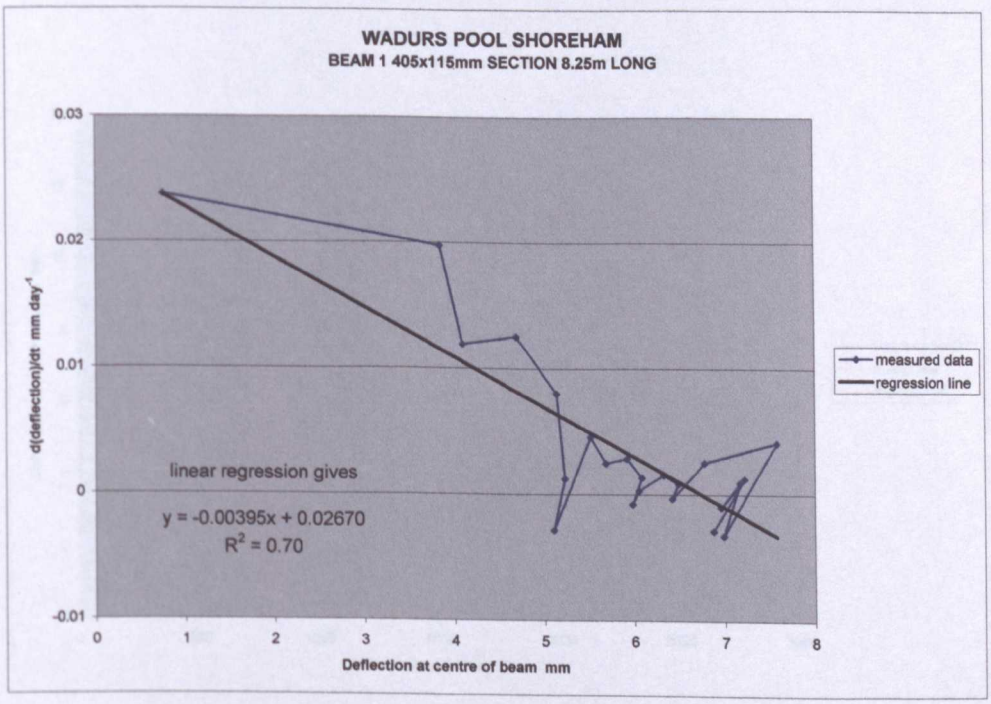

Rate of deflection plot for exponential constants

Figure 8.12 *Linear regression results for Beam 1 at Shoreham*

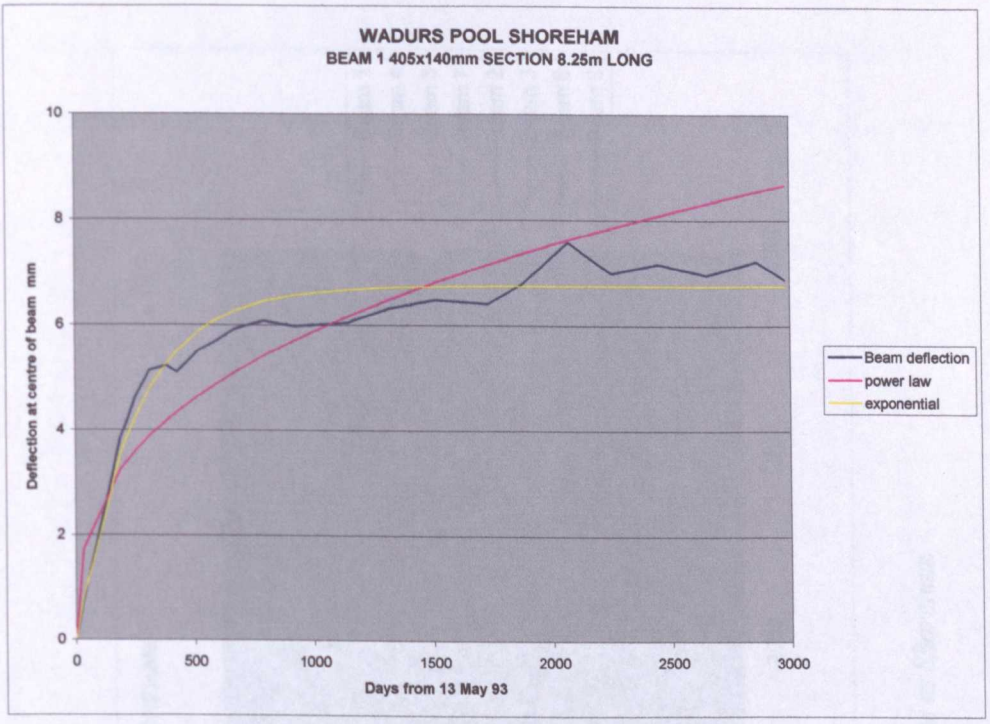

(a) Beam 1

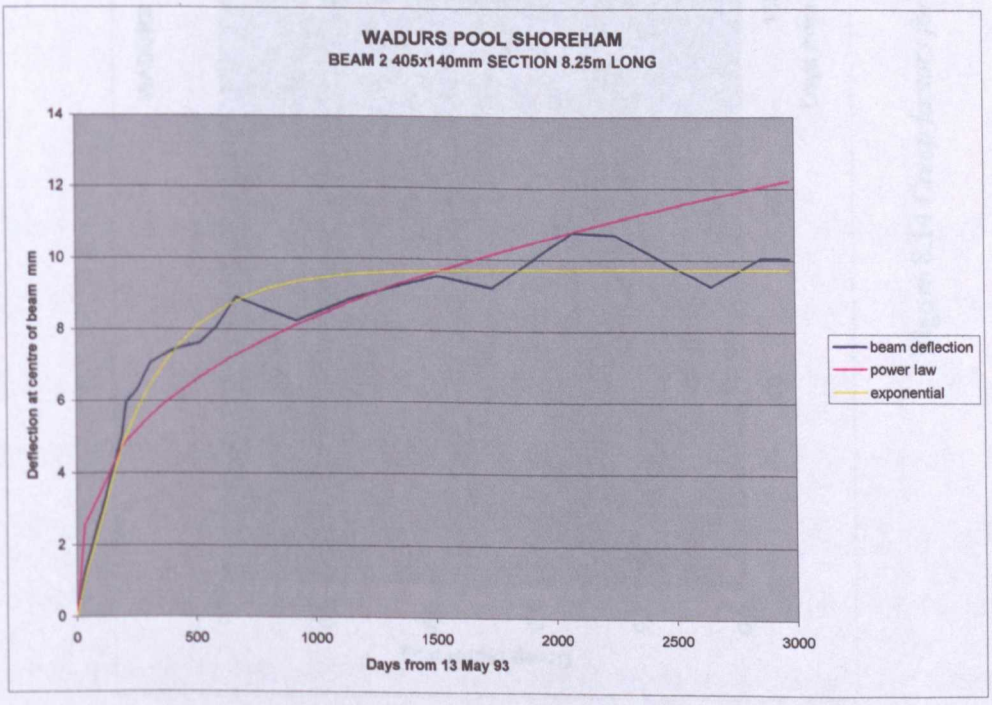

(b) Beam 2

Figure 8.13 *Theoretical power law and exponential curves at Shoreham*

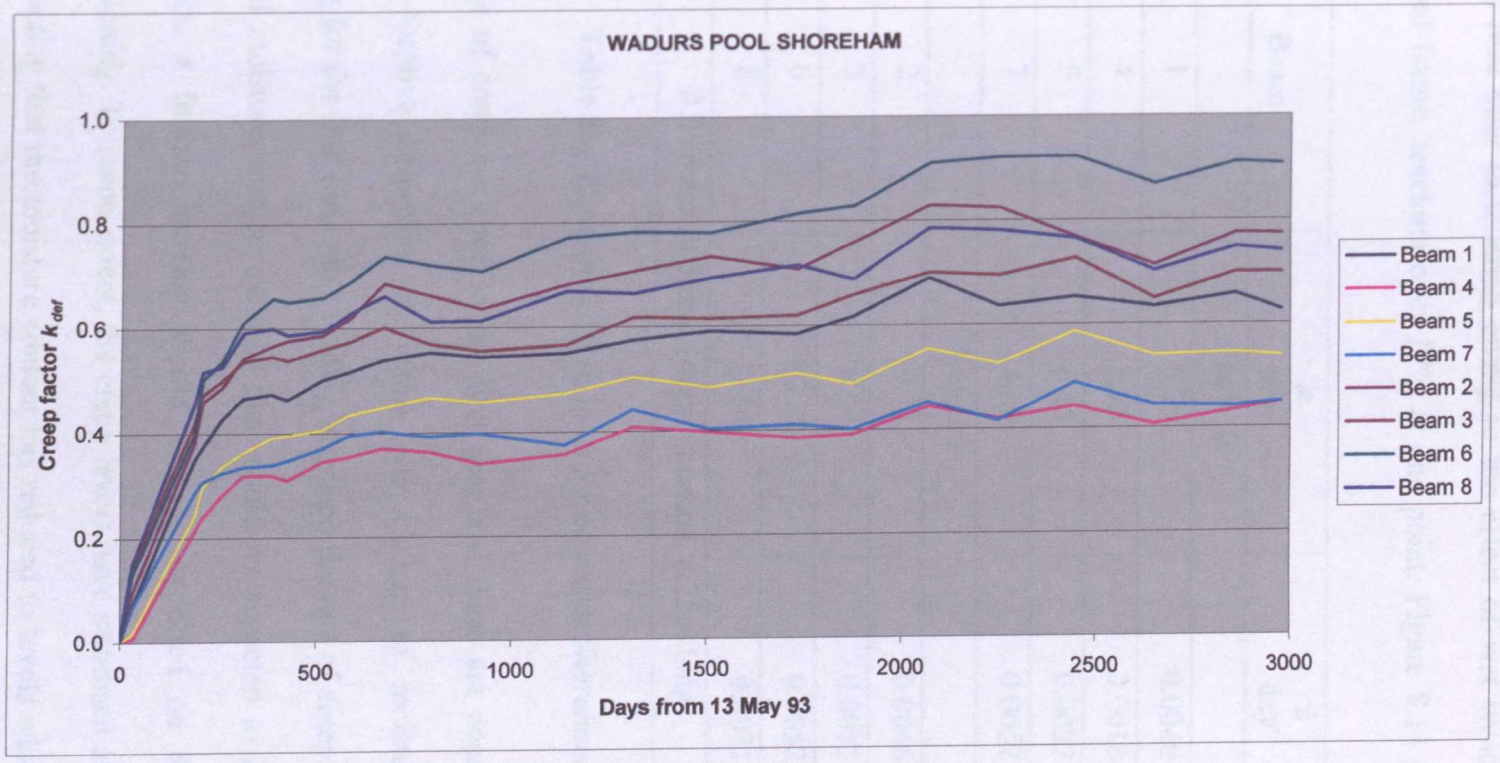

Figure 8.14 *Creep factors for all beams at Shoreham*

Environmental measurements show that the moisture content of the glulam at Shoreham rose after installation owing to the effect of wet weather on the unprotected frame, reaching over 17% at one point. Figure 8.14 shows that

Beam	*a* mm	*b* day^{-1}
East side		
1	6.75	0.0040
4	5.16	0.0018
5	6.15	0.0027
7	4.69	0.0052
West side		
2	9.73	0.0046
3	8.36	0.0073
6	10.83	0.0052
8	9.14	0.0071
All beams 405mmx140mm section 8.25m long		

Table 8.4 *Exponential constants for beams at Shoreham*

high rates of creep occurred in the first year and these are consistent with mechano-sorptive behaviour in which any change of moisture content occurring for the first time after loading increases the rate of creep. As well as the initial moisture content increase that would be expected to increase the creep rate, a further increase would also be expected on drying after commissioning. To some extent, the creep levels have stabilised after the first year reflecting that the moisture content has reduced to levels which fluctuate from 12-16% with the higher values being measured in summer. However, unlike Wokingham, there is no obvious seasonal variation in the creep responses despite small annual changes in humidity and moisture content. This

is due to the controlled environment in the pool area. Consequently, the creep produced by the beams in the long-term in this case is mostly due to loading.

As commented earlier, the environment at Shoreham does not readily fit into any of the Eurocode 5 Service Classes but it has been suggested that Service Class 2 might be appropriate. According to table 2.1, figure 8.14 indicates that most of the creep responses at Shoreham are Service Class 3 at present (long-term load category) but could be stabilising to Service Class 2 in the permanent load category. This reflects the difficulty experienced earlier in deciding which Eurocode 5 Service Class in which to place Shoreham. The higher rate of deflection in the first year resulting in the Class 3 response was due to the wetting/drying cycle described above increasing mechano-sorptive creep levels. Since then, automatic control of the environment has resulted in lower permanent creep levels in spite of the daily fluctuations which may be of insufficient duration to affect creep levels significantly.

Combining the exponential results in table 8.4 with figure 8.14 gives a possible model for creep at Shoreham as a function of time in the form $k_{def}(t) = k_{def}(1-e^{-0.0047t})$ where k_{def} is less than 0.80 for nearly all beams. Based on this, the expected permanent creep just falls within Eurocode 5 limits for a Service Class 2 building and the recommended k_{def} value of 0.80 could be used to predict the maximum creep deflection expected for any beam in this structure using $k_{def}(t) = 0.80(1-e^{-0.0047t})$.

At this point, it is emphasised once again that the values of the creep factors presented above for Shoreham can vary from those shown according to the date

the initial deflection was assumed to take place and according to the value assumed for the magnitude of that deflection.

Moulsecoomb Health Centre

Construction of the Health Centre at Moulsecoomb commenced in April 1994 and the building was completed and handed over to the client in October 1994. Monitoring of the selected beams at this site coincided with the start of construction and surveying began on the 6 May 1994. A full description of this site is given in section 6.3.

Since commissioning, this building is heated throughout the winter, with temperatures varying between about 18 and 25°C throughout the year. The relative humidity now lies between about 30 and 60% rising beyond this occasionally in the summer. The structure can be considered to be of Service Class 1.

Beam deflection curves have been plotted at Moulsecoomb following each survey and figure 8.15 shows some of these for Beam 3 where curves with similar shapes to those measured at Wokingham and Shoreham have been obtained. The effect of the roof being gradually loaded is recorded in figure 8.15a as the 6 May reference was taken with no load applied to Beam 3, the surveys of the 19 and 27 May correspond to an increasing load and the 7 June to the roof being fully loaded. However, although these deflection curves show some response to the changing roof load, the results are inconsistent for the first surveys. The same difficulty trying to identify early trends in beam

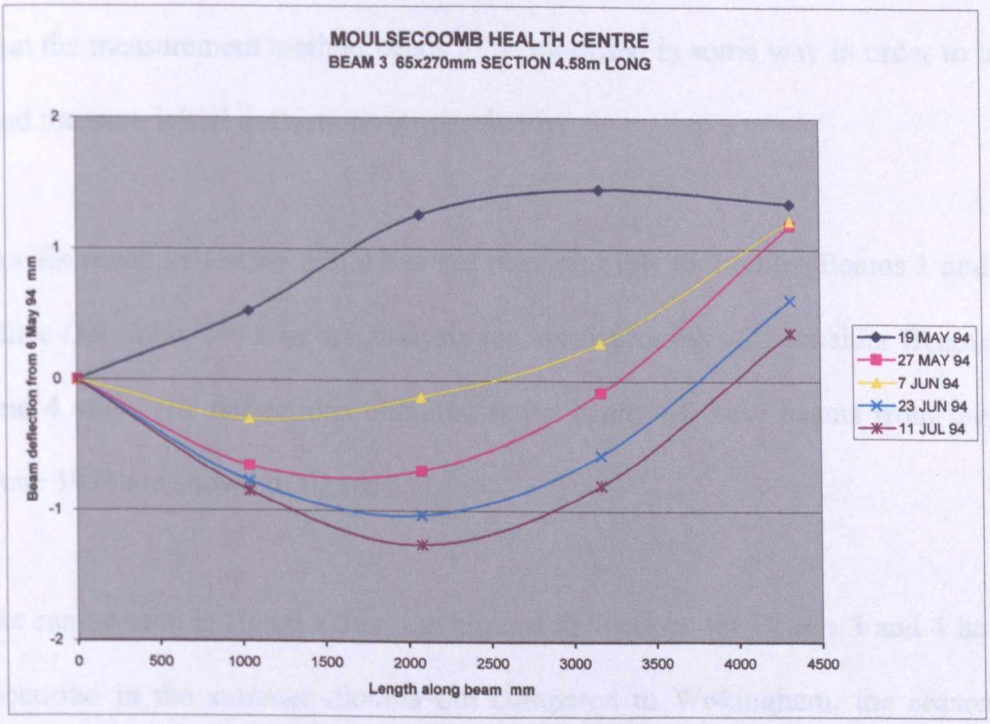

(a) Initial results

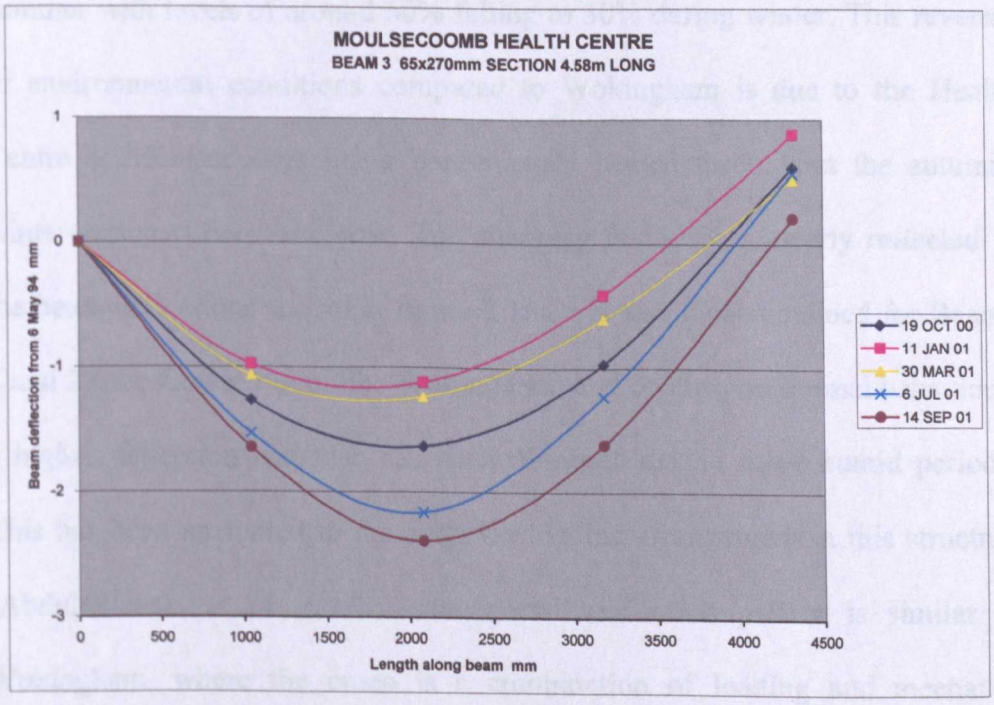

(b) Latest results

Figure 8.15 *Beam 3 deflections at Moulsecoomb*

deflections has been experienced at Wokingham and Shoreham and it seems that the measurement method needs to be modified in some way in order to try and measure initial deflections more reliably.

As discussed in section 6.3, it has not been possible to monitor Beams 1 and 2 since December 1998 so the analysis for Moulsecoomb will consider Beams 3 and 4 only. The deflections obtained at the centre of these beams from the 7 June 1994 are shown in figure 8.16.

As can be seen in figure 8.16a, the highest deflections for Beams 3 and 4 have occurred in the summer months but compared to Wokingham, the seasonal variation in the humidity in the room containing the beams is also higher in the summer with levels of around 60% falling to 30% during winter. This reversal of environmental conditions compared to Wokingham is due to the Health Centre at Moulsecoomb being continuously heated throughout the autumn-winter-spring period each year. The changing humidity is clearly reflected in the beam deflections shown in figure 8.16a and also those obtained for Beams 1 and 2 (not shown) but unlike Wokingham, and contrary to normal behaviour, a higher deflection response has been observed during more humid periods. This has been attributed to the complex loading arrangement in this structure (Abdul-Wahab, *et al.*, 1998). The overall deflection pattern is similar to Wokingham, where the creep is a combination of loading and mechano-sorptive effects.

An attempt has been made to model the deflections produced by Beams 3 and 4

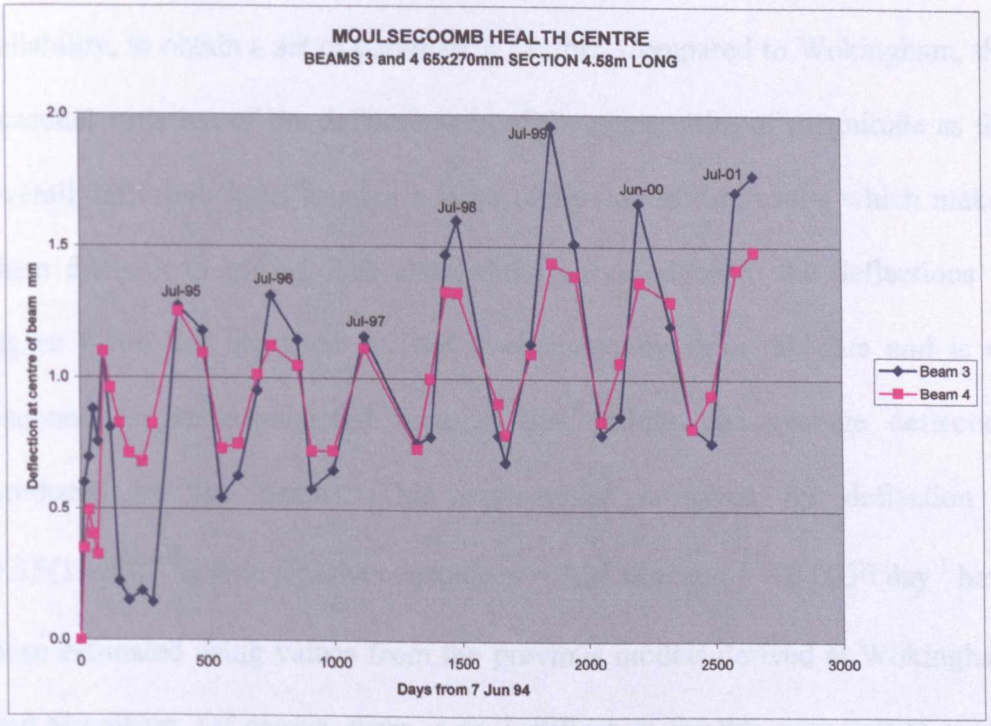

(a) Deflections for Beams 3 and 4

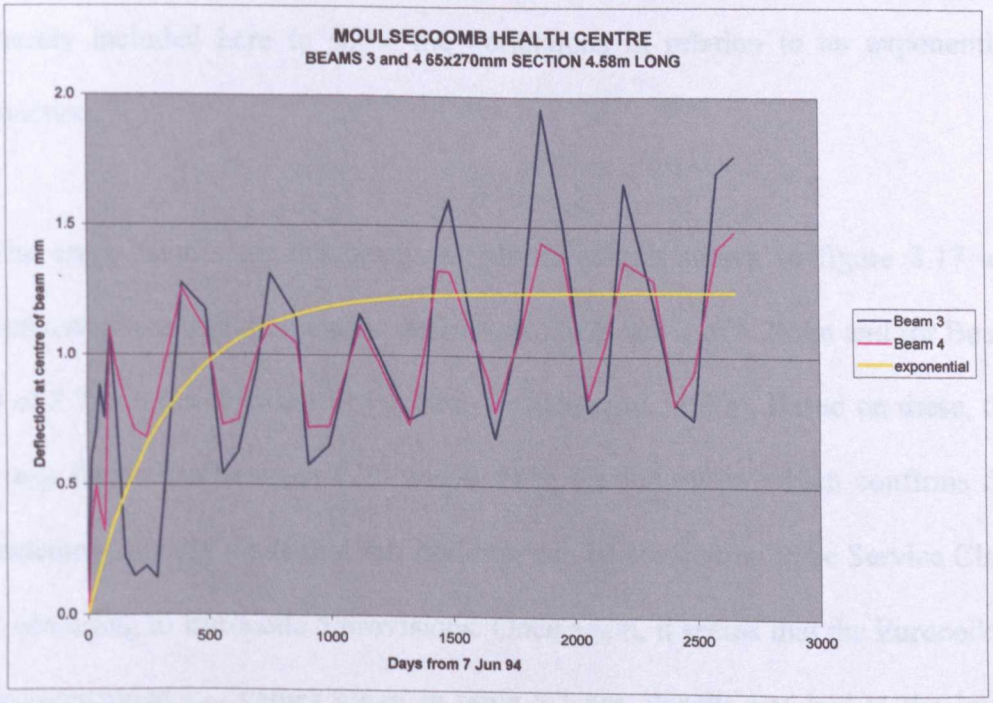

(b) Exponential function in relation to deflections

Figure 8.16 *Moulsecoomb beam deflections*

with an exponential function but it was not possible, with any statistical reliability, to obtain a set of parameters for this. Compared to Wokingham, the seasonal variation of the deflections is of the same order of magnitude as the overall deflection itself causing a large dispersion of the results which makes them difficult to model. The exponential curve added to the deflections in figure 8.16b has not been derived mathematically from the data and is an estimate for an exponential function that follows the average deflection produced by the beams. This exponential is given by deflection = $1.25(1-e^{-0.0030t})$ mm and the constants $a = 1.25$ mm and $b = 0.0030$ day^{-1} have been estimated using values from the previous models derived at Wokingham and Shoreham. Of course, there is no justification for this exponential model other than it is based on the results obtained at Wokingham and Shoreham: it is merely included here to show the deflections in relation to an exponential function.

The creep factors for the beams at Moulsecoomb shown in figure 8.17 are derived assuming initial elastic deflections for Beam 3 of 4.2 mm and for Beam 4 of 3.7 mm (as calculated by Abdul-Wahab, *et al.*, 1998). Based on these, the creep factor lies between 0.20 and 0.40 in the long-term which confirms the statement already made that this building can be considered to be Service Class 1 according to Eurocode 5 provisions. Once again, it seems that the Eurocode 5 recommended k_{def} values given in table 2.1 are closely matched to the long-term creep factors obtained.

To complete the analysis of Beams 3 and 4, figure 8.18 shows a sinusoidal

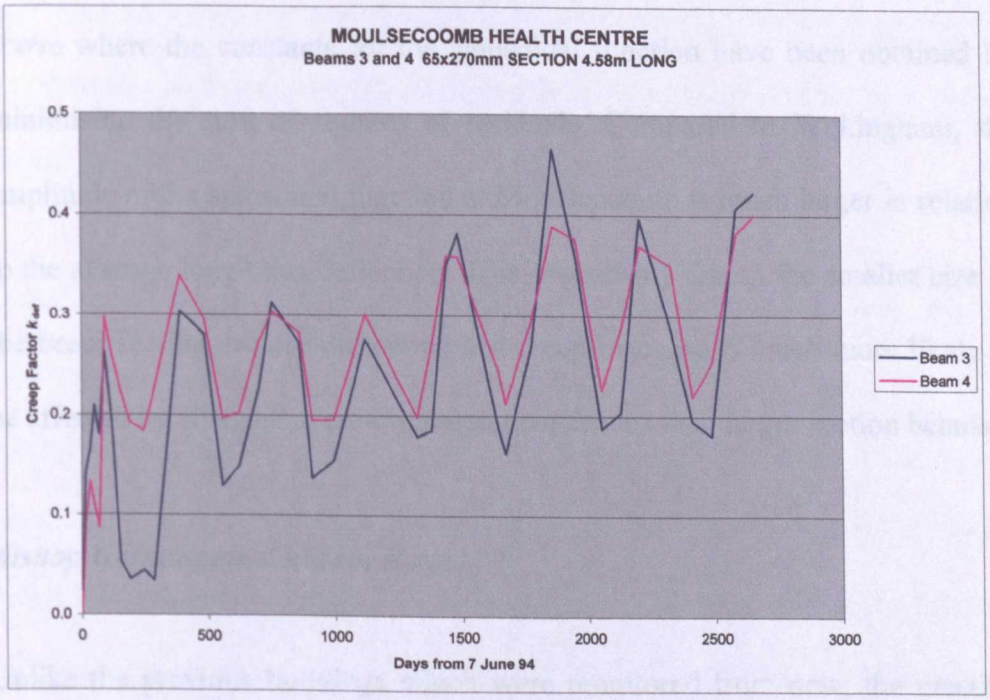

Figure 8.17 *Creep factors for Beams 3 and 4 at Moulsecoomb*

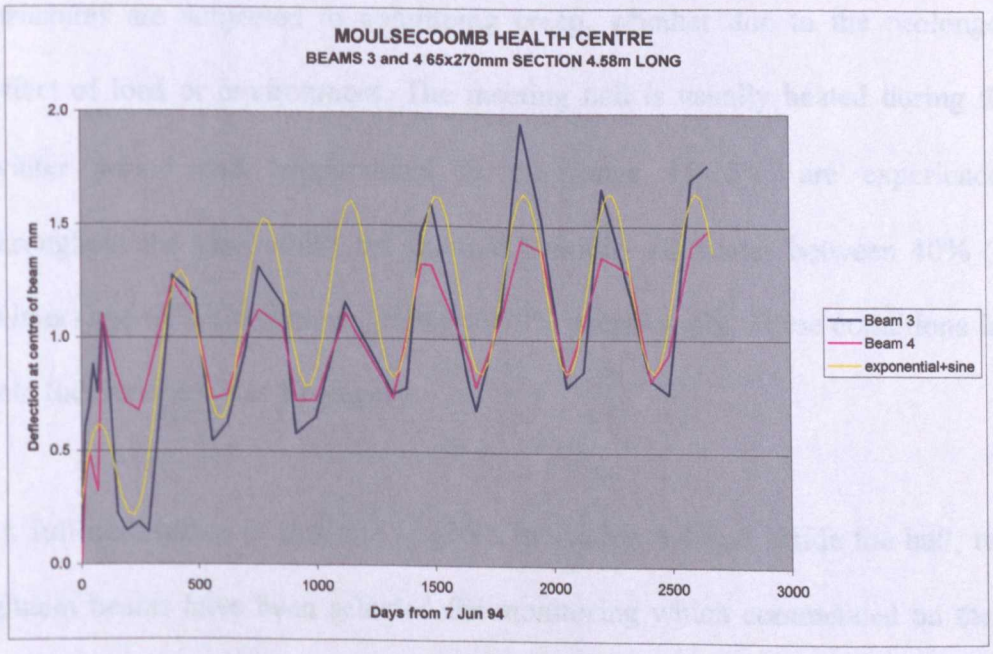

Figure 8.18 *Modulated deflections for Beams 3 and 4 at Moulsecoomb*

function (see equations 8.6 and 8.7) added to the exponential function proposed above where the constants for the sinusoidal function have been obtained by minimising the sum of squares of residuals. Compared to Wokingham, the amplitude of the sinusoidal function at Moulsecoomb is much larger in relation to the average long-term deflection. This is probably due to the smaller size of the beam sections whose deflection and creep response is much more likely to be affected by changes in environmental conditions than larger section beams.

Bishop Hannington Church, Hove

Unlike the previous buildings which were monitored from new, the meeting hall at Bishop Hannington Church was constructed in 1982. This was included in the monitoring programme in order to determine the extent to what older structures are subjected to continuing creep, whether due to the prolonged effect of load or environment. The meeting hall is usually heated during the winter period and temperatures in the range 15-25°C are experienced throughout the year whilst the relative humidity fluctuates between 40% (in winter) and 60% (in summer) rising to 70% occasionally. These conditions fall into the Service Class 1 category.

A full description of this site is given in section 6.4 and inside the hall, two glulam beams have been selected for monitoring which commenced on the 5 July 1995 and continued, every three months, until the 26 June 1997. Unfortunately, the site was not visited again until the 26 January 1998 and in the intervening period, all of the beam targets were removed when the hall was

redecorated. To continue monitoring, a new set of targets had to be installed and, because it was not possible to correlate the results from these to the first set of targets, a second set of beam deflections had to be referenced from the 26 January 1998.

In common with the previous sites, beam deflection curves have been plotted following each survey and the initial results for Beam 1 from the 5 July 1995 are shown in figure 8.19a and an intermediate set for Beam 2 referenced fromthe 26 January 1998 are shown in figure 8.19b. The results for these beam deflections are quite different to those obtained at the other sites: they do not follow any predictable pattern and the magnitude of the measured deflections are small for large beams. This is probably due to the difference in age of the meeting hall compared to the other buildings monitored and shows that deflection due to load has stabilised.

Figure 8.20 shows the centre deflections produced by Beams 1 and 2 from the 26 January 1998. During the period shown, both beams exhibit creep behaviour that mirrors environmental conditions in the hall as during the summer when the humidity in the hall is at its highest, the beam deflection is always at its lowest. Both responses are referenced to zero at the start and have not moved more than 0.8 mm from this. The regression line shown on each chart is linear and this shows that the average deflection (creep) due to load is still increasing but only by about 0.3 mm over four years for Beam 1 and by about 0.4 mm for Beam 2. At the start of the monitoring period shown in figure 8.20, 16 years after construction, a theoretical exponential response would show a negligible increase in the average deflection. However, it is evident that this is not the

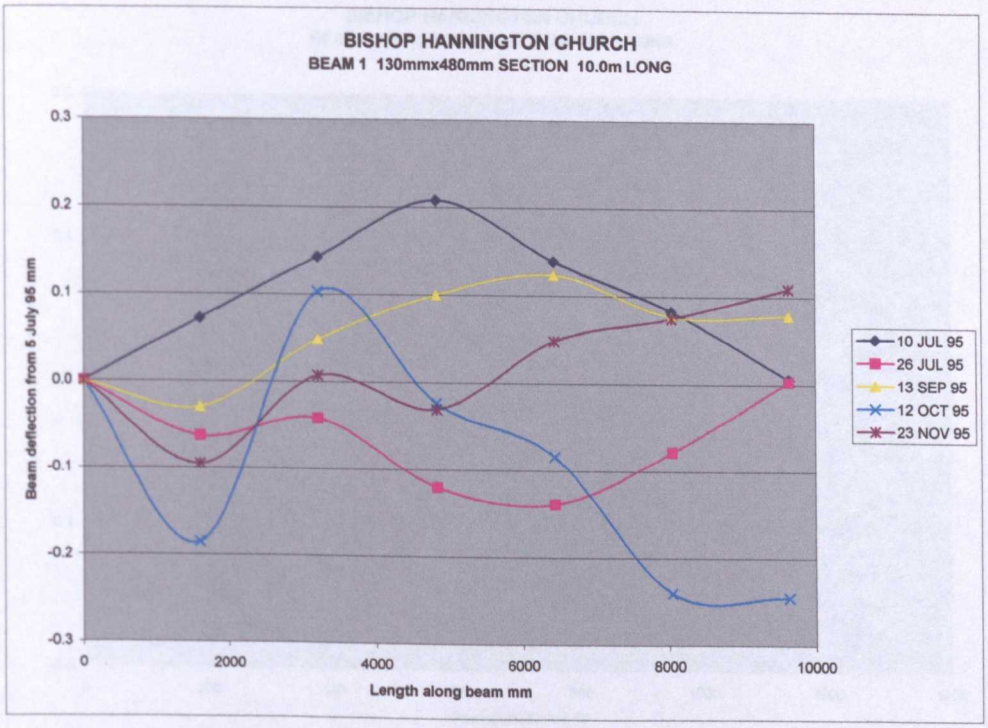

(a) Initial deflections for Beam 1

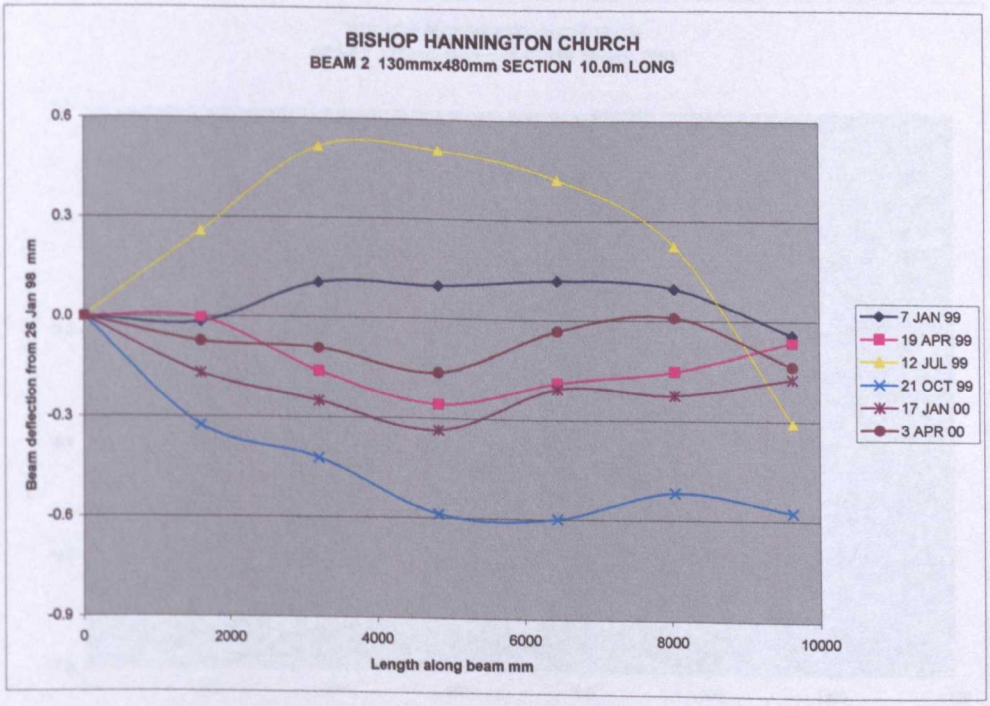

(b) Interim deflections for Beam 2

Figure 8.19 *Deflections for beams at Bishop Hannington*

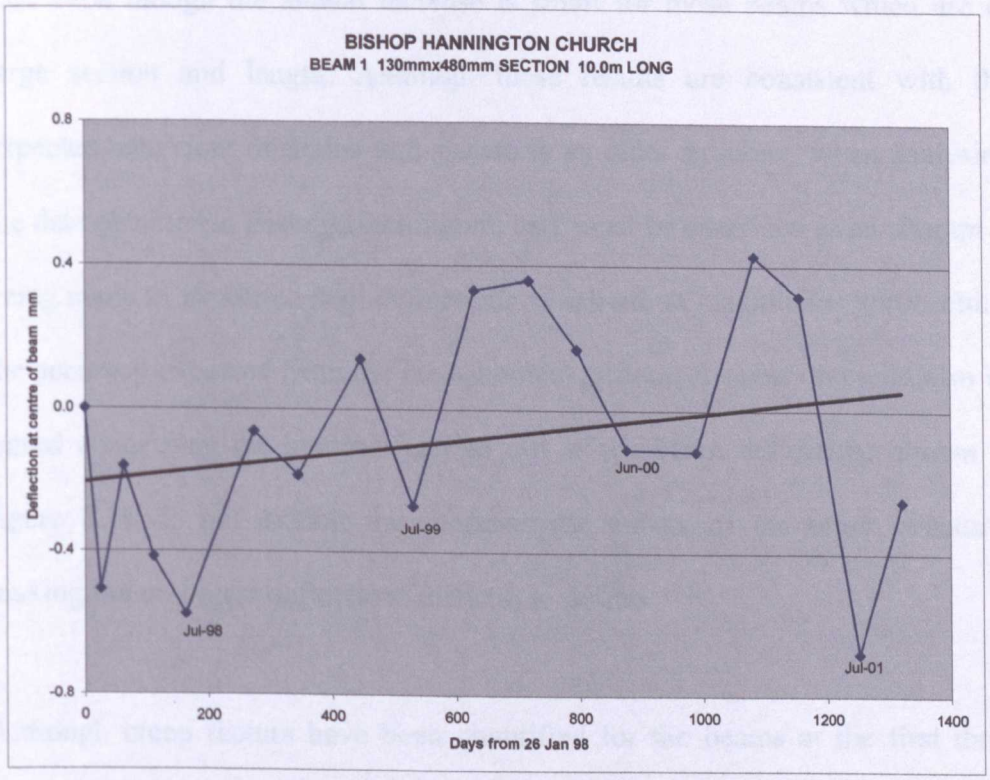

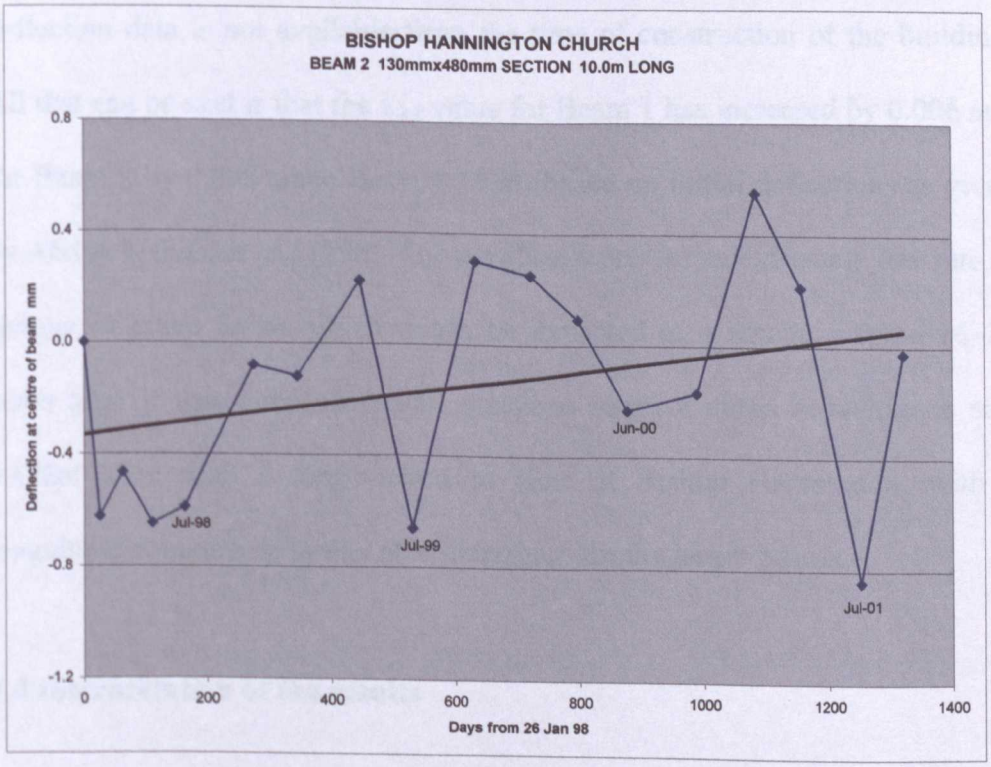

Figure 8.20 *Centre deflections at Bishop Hannington*

case even though the annual increase is small for these beams which are of large section and length. Although these results are consistent with the expected behaviour of timber and glulam in an older structure, when analysing the data obtained at Bishop Hannington, care must be exercised as an attempt is being made to measure small deflections which are at magnitudes approaching the accuracy expected from the measurement system. A question could also be raised concerning the analysis carried out as the beam deflections shown in figure 8.19 do not exhibit the characteristic curves of the other structures making the mid-span deflections difficult to define.

Although creep factors have been quantified for the beams at the first three sites, it is not possible to do this for the two beams at Bishop Hannington as deflection data is not available from the time of construction of the building. All that can be said is that the k_{def} value for Beam 1 has increased by 0.006 and for Beam 2 by 0.008 since January 1998 (based on initial deflections as given by Abdul-Wahab, *et al.*, 1998). These values represent an extremely low rate of change of creep factor which might be expected in a structure some 16–20 years after it was built. However, mechano-sorptive creep behaviour is still evident after such a long period of time at Bishop Hannington, with a magnitude comparable to that at Wokingham for the larger beams.

8.4 Interpretation of the results

From the *surveying* point of view, and despite many practical difficulties, it is claimed that all of the objectives set out in section 2.6 have been met and the measurement system as a whole has produced the results required by STRU to

obtain creep data for a number of structures, the first known buildings to be monitored in this way.

ECDS3 has demonstrated its ability to measure three-dimensional coordinates at sub-millimetre levels and the method employed to convert these into deflections and to quantify creep has produced sets of results consistent with the known behaviour of glulam. The complete measurement system has withstood the test of time, having now been in place for almost ten years at Wokingham. However, the problem of defining the exact accuracy of the system remains but the resolution seems to have matched the application as shown by figure 8.16 at Moulsecoomb and figure 8.21 at Wokingham where relatively small but clearly recognisable trends in results have been obtained at the limit of the accuracy thought possible from ECDS3 and the way in which it has been used to monitor glulam.

At each of the new sites monitored, measurement of the initial deflection of the beams has not been successful as monitoring started too late or produced confusing results during the construction period. If creep factors are to be properly analysed for a full-scale structure, it is essential that the initial deflections are precisely measured in some way. It is expected that this will be very difficult to realise during the construction of any building since roof and other loads are usually applied gradually and site conditions at the time of erection are often not suitable for monitoring with surveying or other precise equipment. One possible way of overcoming this problem might be to have a 'controlled' site of some form: this could be a building erected solely for the purpose of monitoring creep or one where the measurement process takes

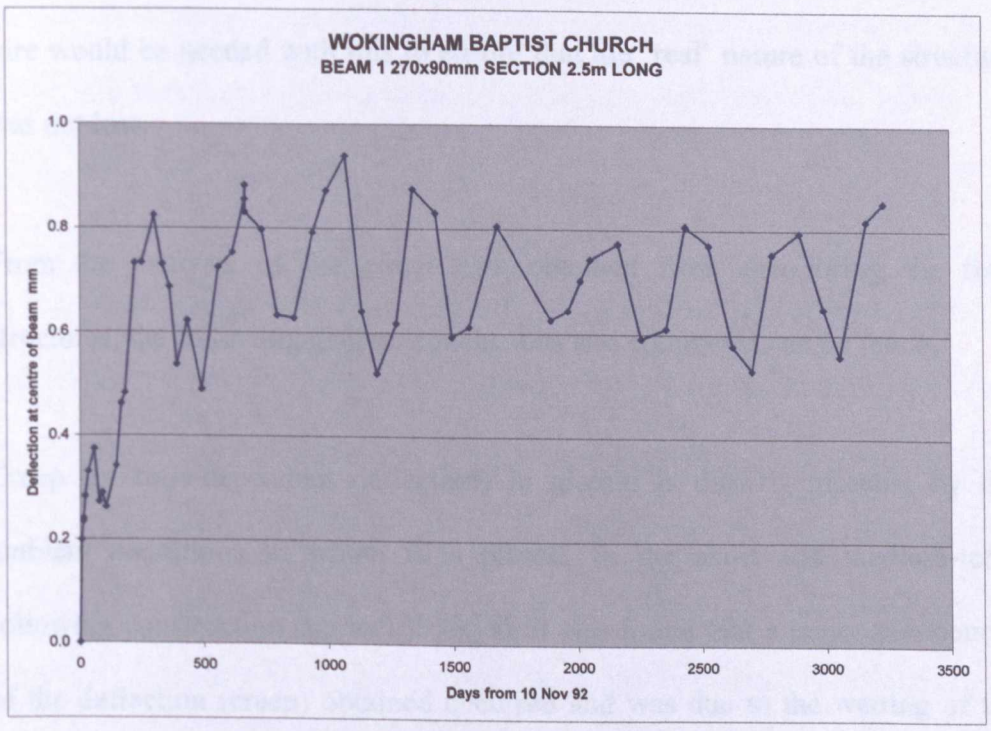

Centre deflections for Beam 1 (the smallest at Wokingham)

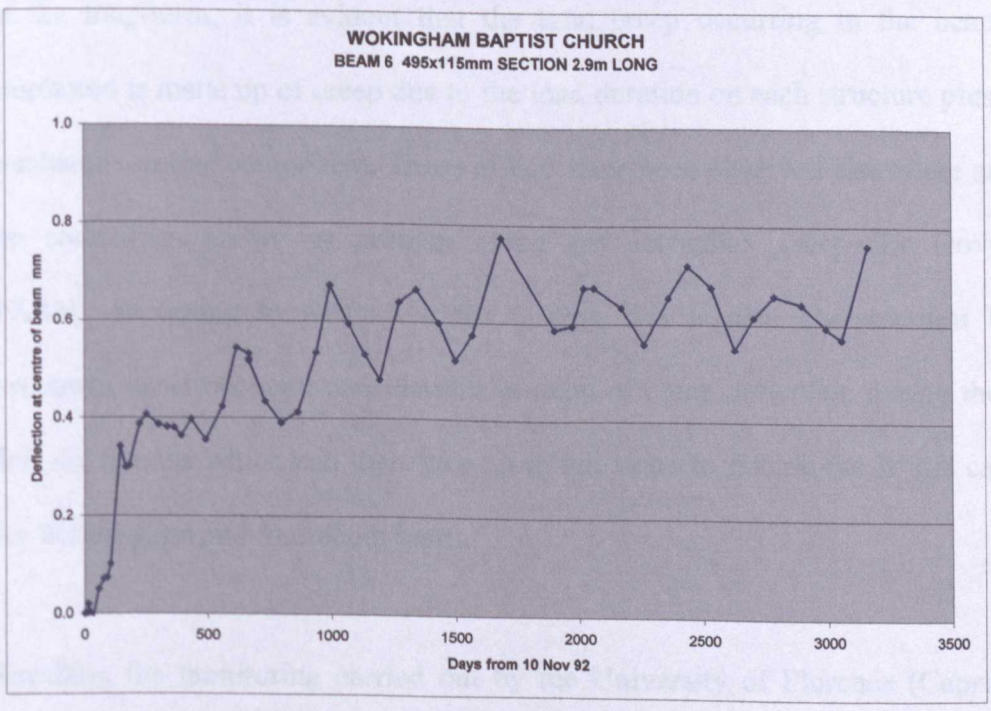

Centre deflections for Beam 6 (one of the shortest at Wokingham)

Figure 8.21 *Examples of small deflections at Wokingham*

precedence over construction at critical times during loading. However, some care would be needed with this to ensure that the 'real' nature of the structure was not lost.

From the analysis of the *creep data* obtained from monitoring the four structures, the following general conclusions and comments can be made.

Creep (or time-dependent deflection) in glulam is directly affected by the ambient conditions in which it is placed. In the short and medium-term following construction (up to 180 days), it was found that a major component of the deflection (creep) obtained occurred and was due to the wetting of the glulam prior to completion of each roof followed by drying on commissioning. In the long-term, it is evident that the total creep occurring in the beams monitored is made up of creep due to the load duration on each structure plus a mechano-sorptive component. These effects have been observed elsewhere and are sometimes known as primary creep and secondary creep (Le Govic, 1994b). According to Ranta-Maunus (1996), this is also characterised by structures experiencing a considerable amount of creep deflection during their first six months which can then take up to ten years to double (as is this case for Wokingham and Shoreham here).

Recalling the monitoring carried out by the University of Florence (Capretti and Ceccotti, 1996), their limited study of three composite concrete/glulam beams shows similar responses to those obtained here where seasonal variations have been observed that follow changes in humidity. However, they

have not taken readings at the same time of the year throughout the measurement programme which is essential for long-term measurements in timber research (see Ranta-Maunus, 1996) and no modelling of the results has been carried out.

In this study, the typical creep/time behaviour for the internal environments monitored can be described by a simple exponential function. In addition, mechano-sorptive creep has been found to be dependent on the time scale of relative humidity changes in each of the buildings and the section size of the timber where there is a greater relative variation in mechano-sorptive behaviour in beams with smaller sections (eg. Moulsecoomb) compared to larger beams (eg. Wokingham). The response of the beams at Shoreham also demonstrates that changes of environment of short duration have little effect on the structural behaviour of glulam beams of large section which confirms the same conclusion made by Therlandersson (1994b).

There seems to be some confirmatory evidence that creep depends on the service environment of a building defined by Eurocode 5 and that the creep allowances indicated in Eurocode 5 for internal environments (see table 2.1) can be considered to be realistic.

9

MONITORING SYSTEMS TODAY

In chapter 3, a lengthy discussion is given on the various methods available, in 1992, for monitoring structures at the sub-millimetre level. The outcome of this was to choose a manually operated theodolite system for monitoring the movement of glulam structures, the decision being based largely on the accuracy attainable with these and costs.

Some ten years on, monitoring at the various structures in this project still continues with the theodolite intersection system and an interesting question arises – how would this be done if the research were to be started today. There have been many developments in the way in which monitoring can be done compared to ten years ago and some of the systems and methods included in chapter 3 have progressed and changed considerably whilst others have not. Some new equipment continues to be introduced, but the emphasis seems to be on improving and automating existing techniques.

Recalling the specifications given in section 2.5 for the measurement of creep, all of these are still considered valid, especially the accuracy requirement and any re-examination of the methods used to measure creep still need to satisfy these. In this chapter, then, a review of current practice in high accuracy close range monitoring and measurement is presented and concentrates on how this might impact on the glulam project. The review is also limited to off-the-shelf

instruments and systems that are available now and those that are capable of measuring with a point accuracy of better than 1 mm.

An overview of some of the techniques currently used for monitoring structures is given by Armer (2001). This provides practical advice on the latest methods available for the in-service assessment of buildings and other structures.

9.1 Monitoring with theodolite systems

The early development of theodolite intersection systems has been discussed in section 3.2 and chapter 5. What can be said about these through the 1990s is that their development has slowed considerably and the applications they tend to be used for have not changed a great deal. Typical examples of their continuing use for industrial measurement are given by Mulder and Smith (1997) and by Greenwood (1997).

In a manually operated system, at least two operators are required to identify each passive target and then accurately align the theodolite reticule with the centre of the target. Today, this is considered to be labour intensive and is not as efficient, user friendly or reliable as other techniques now available. Despite these drawbacks, it is estimated there may be several hundreds of industrial measuring and monitoring systems still in use today based on manually operated theodolites (Shortis and Fraser, 1998). The most common application for these now is any measuring or monitoring survey involving a small number of points – this would, of course, include the glulam sites in this project.

Equipment currently available in this category of monitoring system includes the Leica TM5005 industrial theodolite (see figure 9.1). In many respects, this is similar to the T2002 theodolites (angles measured with a standard deviation of 0.5″) but it has enhanced features such as motorised drives and the installation of microswitches on the slow motion controls so that recording can be initiated whilst sighting targets. The TM5100 with panfocal telescope and TM5100A with autocollimation device are also available.

Figure 9.1 *Leica TM5005 theodolite (left) and TDM5005 total station (right) (courtesy Leica Geosystems)*

The software currently available from Leica for use with the TM theodolites is known as Axyz (see Leica, 1999, Möser and Höper, 1998 and Kyle, 1997). This is modular in nature and the Core Data Module (CDM) contains the software where a project is administered and where data is analysed and presented. It also includes the orientation software and program for computing real-time coordinates. The Multiple Theodolite Module (MTM) contains the relevant communications software to connect the theodolites to the system

computer. Recognising that much of the processing carried out by the CDM can be used by other measuring systems, Leica have developed the Single Theodolite Module (STM) which allows a total station to take measurements but use the same data management software as the MTM. As well as this, there is a Laser Tracker Module (LTM). This configuration of Axyz, it is claimed by Leica, offers a much greater flexibility in the way in which a number of different measuring systems can operate. It is also possible to process different jobs simultaneously with Axyz and share instruments provided all the necessary orientation measurements have been taken.

Despite all these innovations, it is clear that the manually operated theodolite system has reached its maximum potential and no major developments or increase of use are expected in the future. The current cost (March 2002) of a manually operated theodolite intersection system consisting of two TM5005s and the Axyz software is about £50 000.

Also included in the category of theodolite monitoring system are polar (or bearing/distance) three-dimensional methods of monitoring again previously discussed in section 3.2. but, in a modern setting, discussed at length by Cook (2001).

The MONMOS system is still available from Sokkia and currently uses the NET2100 total station and SDR4E control terminal. The measuring specification for the NET2100 is 2″ for angles and 0.8 mm for distances at close ranges using plane self-adhesive reflecting targets. Holmes (1996) advocates the use of MONMOS for dimensional control in shipbuilding

construction and repair where point accuracies of 0.8 mm were obtained.

Leica have introduced the TDM5005 industrial total station (shown in figure 9.1) which has the same specification for measuring angles as the TM5005 but has a distance measuring facility added. Using Axyz, this would require the STM to be installed in the system computer. According to Leica, the point accuracy obtainable from the TDM5005 is 0.3 mm within a 20 m measuring volume. At this accuracy level, the TDM5005 would be a contender for the glulam project if measurements were to be started today. The cost of a polar measuring system is about half that of a theodolite intersection system and only one operator is needed. However, the 0.3 mm point accuracy is only possible using a corner cube reflector of some type which would not be practicable at the glulam sites monitored. It is possible to use targets in the form of special reflector tape (see figure 9.2), but the accuracy obtainable for distances with these is, under ideal viewing conditions, 0.5 mm and would not meet specifications in the glulam project.

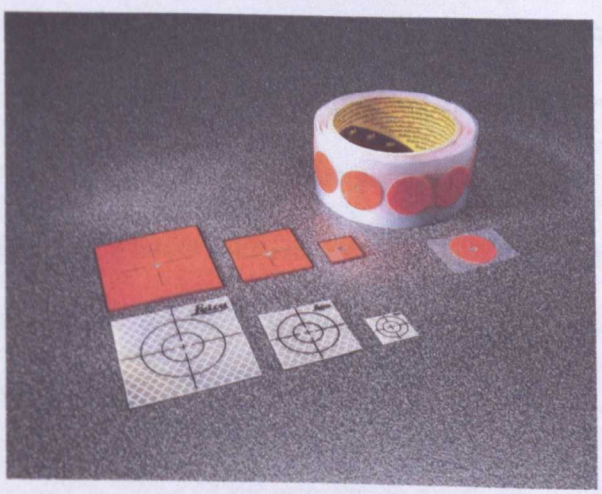

Figure 9.2 *Plane reflecting targets for use with TDM5005 (courtesy Leica Geosystems)*

If it were possible to accept the accuracy expected from the TDM5005 and MONMOS when measuring with reflective tape targets, the polar method would be considered for use in place of a theodolite intersection system to monitor each glulam site because of the cost savings that could be made when purchasing hardware. It is not certain at this time if the development of a high specification total station with an improved distance measuring capability (especially to plane reflective targets) is under consideration by any of the leading manufacturers. Until this is the case, theodolite intersection would still be preferred to guarantee that the accuracy required is obtained.

9.2 Automation of theodolite systems

Motorised theodolites and total stations are currently available from all of the principal survey instrument manufacturers.

At a low level of automation, the capability to drive a theodolite to a particular direction allow measurements at pre-determined locations to be repeated more efficiently as the theodolites would carry out the coarse pointing and the operators would simply adjust the fine pointing. This could be carried out at the glulam sites since all the targets are in the same positions for each survey but this would require the system software to be able to compute coordinate positions with respect to a local theodolite orientation to allow automated pointing to predicated locations.

A high level of automation with a theodolite requires the complete elimination of manual operation. The Kern SPACE and Wild ATMS based on video

theodolites appeared in the late 1980s and had similar features. These were very expensive fully automated theodolite intersection systems based on CCD technology and motorised theodolites. Unlike manually operated theodolite systems, the number of targets which can be measured with these is not limited to small sets by operator fatigue, particular if the target locations can be predicted. Whilst this may be suitable at Wokingham, SPACE and ATMS would not be economical at the other sites. All of this has been discussed in section 3.2 where the use of the systems, even if they still available today, would be rejected because of costs.

Relatively few of these highly automated measuring systems are in use today and the lack of success of this type of system has forced instrument manufacturers to pursue other measurement solutions. One of these is the motorised total station with automatic target recognition based on the intensity maximum pointing method which uses the return beam of the distance measuring signal to locate the centre of a corner cube prism. Both Trimble and Leica produce an instrument with these features and the Trimble Total Station 5601 and Leica TDA5005 have independent automatic target recognition and can lock onto a prism and follow it as it is moved from target to target. This may have advantages for monitoring in some industrial applications but would offer no real advantage at the glulam sites where this would not be possible to those targets that are inaccessible once installed. The increasing use of motorised total stations is likely to reduce the cost of manufacture of these which in turn may make the use of them on a project such as the glulam structures more attractive in the future provided the problems of accuracy and

using reflective tape as targets can be overcome.

9.3 Laser trackers

Although available in 1992 at the start of the glulam project, laser trackers were only in their infancy at that time. Since then, and especially in the late 1990s, they have gained in popularity for industrial measurement and are now considered to be more accurate than theodolite intersection systems for many applications. The Leica SMART 310 described in section 3.2 has now been replaced by the LT series of trackers and when used with Axyz, the LTM is required. Other trackers currently available include the SMX Laser Tracker produced by the SMX Corporation (figure 9.3) and the API Tracker II manufactured by Automated Precision Incorporated.

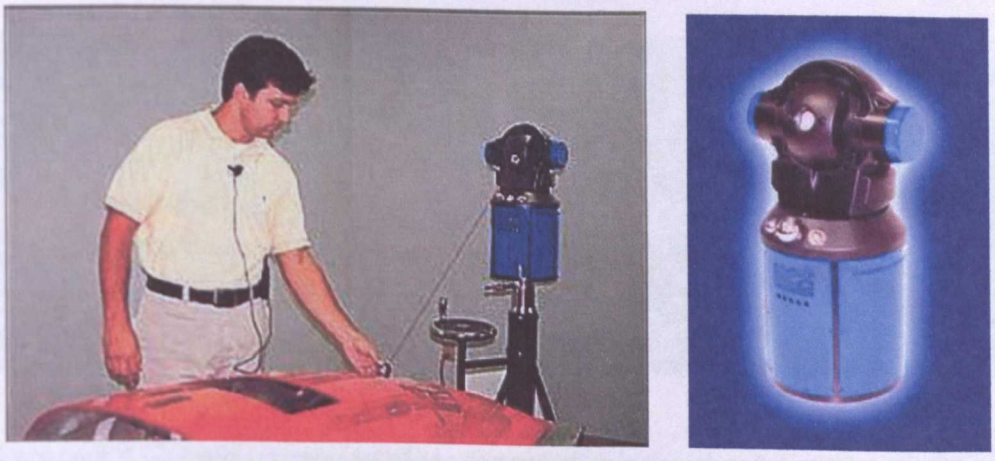

Figure 9.3 *SMX Laser Tracker (SMX Corporation, 2002)*

All of these trackers have overcome the disadvantages of the earlier ones and they are now considered to be more portable and are easier to set up than before due to advances made in miniaturisation, in optics and in computer technology. Where these instruments excel is still in the calibration of

industrial robots and coordinate measuring machines but they are now used for more general applications and are seen as an industrial solution to many measurement problems. Today, the popularity of these is attributed to their ease of operation in a single instrument, the fact that no sightings have to be taken, the high level of automation possible and the user-friendliness of the software. A discussion of the expected use of laser trackers in the aerospace industry is given by Clarke (1998), Gooch (1998) and by Shortis and Fraser (1998).

Despite all of these improvements, the problem for many non-contact monitoring schemes that might use a laser tracker (and total station) is getting a corner cube reflector to the points to be measured (as shown in figure 9.4) and tracking this through a measurement.

Figure 9.4 *Getting a prism in place for monitoring with total station (left) and laser tracker (right) (courtesy Leica Geosystems)*

For the sites monitored in this project, this would either be impractical or impossible and laser trackers cannot be used because of this. At present, most laser trackers still cost about twice as much as a theodolite intersection system and this extra cost is only justified for a high volume of work which does not suit the relatively small number of points observed at each of the glulam sites.

For industrial users, it is expected that the use of laser trackers will increase in the near future and they show no sign of the lack of development currently affecting theodolite-based systems.

9.4 Photogrammetric systems

The development of close range photogrammetric systems to the late 1980s/early 1990s has been discussed in section 3.2. Most off-the-shelf systems at this time were film-based and a comprehensive review of these is given by Fraser (1988). Through the 1990s, the majority of developments for industrial measurements and monitoring based on photogrammetry have been associated with the introduction of digital cameras (see figure 9.5) giving rise to digital photogrammetry.

Figure 9.5 *INCA digital camera (courtesy Leica Geosystems)*

As stated in section 3.2, photogrammetry in all its forms is well published and this is especially true for close range digital photogrammetry. Consequently, this section is only a brief overview of the state of the art in relation to the monitoring that might be carried out with it for this project.

Although digital methods now dominate for monitoring and industrial measurements with photogrammetry, the best possible accuracies obtainable for three-dimensional measurement with photogrammetry (say better than 1 in 100 000) are still only possible with large format film cameras. However, for the accuracy required for most monitoring tasks, photogrammetric systems based on the use of high resolution digital still cameras are now used. The application of digital close range photogrammetry to precise measurement in industry is sometimes called vision metrology, videometrics or videogrammetry. Another term used is machine vision although this strictly refers to the ability of a computer to perform tasks normally performed by a human such as the inspection of parts: this may or may not include a three-dimensional measurement of that part.

The development and current status of high precision close range photogrammetry over the last few years is described in many publications of which those listed below are a representative sample. The discussion of photogrammetric measuring systems in this chapter is based on these. The papers with a brief summary include

Brown and Dold (1995): introduction to V-STARS with applications.

Fraser and Shortis (1995): description of camera technology in relation to some industrial projects.

Shortis and Fraser (1995): the development of vision metrology for industrial use.

Ganci and Shortis (1996): description of some detailed tests to compare digital photogrammetry with theodolite intersection where accuracies of the order of 1 in 50 000 were achieved.

Antilla (1997): a comparison of photogrammetry and theodolite intersection regarding accuracy.

Fraser (1996): a complete overview of close range photogrammetry.

Fraser (1997): a discussion of the latest developments in automation in phtotgrammetry.

Fraser (1998): a discussion of the emergence of digital close range photogrammetry.

Gruen (1997): full coverage of the fundamentals of videogrammetry.

Maas (1997): an update on real-time photogrammetry.

Clarke (1998): discussion of the advantages and disadvantages of monitoring and measuring by photogrammetry in the aerospace industry.

Shortis and Fraser (1998): an overview of all close range measuring systems.

Leica (2000): description of the V-STARS system.

Stirling (2001): a complete overview of the application of photogrammetry to the monitoring of structures.

Geodetic Services Incorporated (2002): In-house publication 'Basics of Photogrammetry'.

Most off-the-shelf digital photogrammetric measuring systems currently available are capable of operating in offline or online modes. In the *offline mode*, a single camera is used to take pictures of the object to be measured but from several different locations, as shown in figure 9.6.

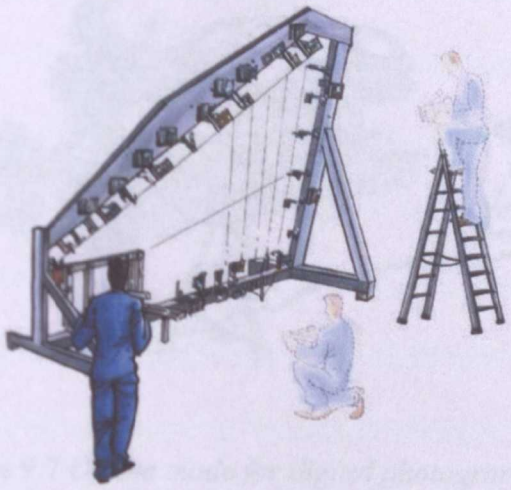

Figure 9.6 *Offline mode for digital photogrammetry (courtesy Leica Geosystems)*

The different camera locations are needed to ensure that all the points to be measured are seen from enough geometrically different locations to get good intersection angles. The camera can be connected directly to the system computer or the images taken can be stored on a removable disc for subsequent processing. In either case, the computation of three-dimensional coordinates on the object starts after all images from all viewing directions have been acquired. These systems are usually extremely portable and the entire system (including notebook computer, camera and accessories) is easily transported from site to site. For an industrial measurement, the limitation of the offline mode is a delay between measurements and results (measurements are not real-time).

In the *online mode*, the object is photographed using two or more cameras from different viewing locations (see figure 9.7). The images are processed instantly by the system computer, which is connected directly to the cameras.

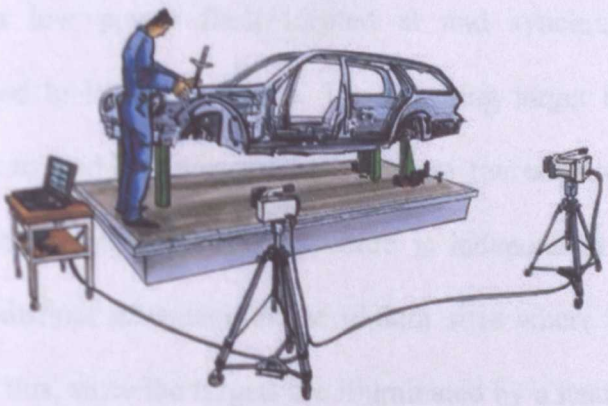

Figure 9.7 *Online mode for digital photogrammetry (courtesy Leica Geosystems)*

The accuracy of photogrammetric measurement by these methods can vary significantly but depends primarily on

- the resolution and quality of the camera(s) used
- the size of the object measured
- the number of photographs taken
- the geometric layout of the cameras relative to the object

and these accuracies can be of the order of 1 in 100 000 of the object size offline and 1 in 50 000 online.

As with any monitoring system, the object to be measured has to have targets

attached to it at points of interest. Although a variety of these are available, the most commonly used are retro-reflective targets. These are very similar to the self-adhesive targets currently used at each glulam site and they reflect light very efficiently back to a light source when illuminated. During a measurement, a low power flash located at and synchronised with the camera(s) is used to light the targets. The resulting target images are very bright and easy to find and measure and because the targets are illuminated completely by the flash, the target exposure is independent of the ambient illumination, a distinct advantage at the glulam sites where this is generally low. As well as this, since the targets are illuminated by a nearly instantaneous flash, the camera(s) do not have to be steady during a measurement. This means that in the offline mode, the camera can be hand-held and no tripods are necessary and in the online mode, measurements are immune to vibrations. A disadvantage of retro-reflective targets is their loss of reflectivity if viewed at acute angles (rather like reflective distance measuring targets). This requires careful planning of photogrammetric surveys using these to ensure this does not happen.

In the online mode, small hand held probes can be used to measure points on an object without targets. The tip of the probe is positioned over a point, the measurement is triggered by the operator and three-dimensional coordinates are computed for that point. Some examples of these probes are shown in figure 9.8.

Similar to theodolite intersection, it is not necessary to know the position of the camera(s) during a photogrammetric measurement as a bundle adjustment

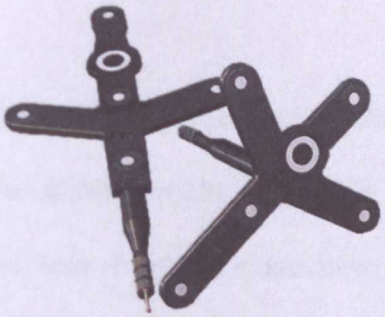

Figure 9.8 *Probes for use in online digital photogrammetry (courtesy Leica Geosystems)*

takes care of this. Another important feature of photogrammetric measurements is the calibration of the camera: this can also be carried out by the bundle adjustment software in a process known as self-calibration. In order to do this, it is necessary to take a minimum number of photographs from a minimum number of locations when measuring an object. This may involve taking more photographs than required and if this is not possible, the cameras have to be pre-calibrated, which is not recommended. Referring once again to a theodolite intersection system and comparing this to close range photogrammetry, scale has to be introduced into a measurement and is achieved by similar methods. The coordinates of some targeted points or a scale bar can be used and the bundle adjustment software will include measurements to these when computing orientation parameters for the cameras.

Regarding costs at present, an off-the-shelf digital photogrammetric measuring system with single camera (offline mode) capable of achieving the accuracies required for the glulam project would now cost about the same as a theodolite intersection system (in March 2002, about £50 000). As the most expensive item is the digital camera, online systems with two cameras cost about twice as

much as this amount.

If the project were started today, for the type of measurement taken in the glulam project, an offline system would be chosen both from the cost and accuracy points of view. Several systems are currently available including Geodetic Services Incorporated V-STARS/S which is also marketed in collaboration with Leica, the Metronor System, together with products from AICON and Imetric. There is no doubt that all of these compete with and would probably be used instead of theodolite intersection for taking the measurements in the glulam project. They would be easier to transport to the various sites, the system software is as user friendly as ECDS3, measurements can be taken with a hand-held camera to retro-reflective self-adhesive targets attached to each structure and, as already mentioned, the accuracy and cost meet specifications.

In addition to the glulam project, the use of digital photogrammetry in industry is also recommended and Clarke and Gooch (1999) state that a survey recently undertaken of 200 non-contact metrology products concluded that photogrammetry is the most practical method for taking high accuracy measurements of multiple points simultaneously in manufacturing.

9.5 Application of electrolevel systems

Over the last decade the electrolevel has become an accepted measuring instrument in structural and geotechnical engineering. In general terms, its advantages are seen to be its simplicity, robustness, small size, and high

accuracy if installed, calibrated and interpreted carefully.

They have been successfully installed in a wide range of structures (see Price, *et al.*, 1996) and all recent major UK tunnelling projects in or around London have specified comprehensive and extensive instrumentation systems which use electrolevels as sensing elements. Some of the more publicised applications for electrolevel monitoring systems include the Mansion House in London where tunnelling to extend the Docklands Light Railway caused concern (Price, *et al.*, 1994). Forbes, *et al.*, (1994) describe in detail the installation of an electrolevel monitoring system installed for the Heathrow Express Rail Link where, in October 1994, the collapse of three adjoining tunnels was predicted and the area evacuated without any casualties occurring (Penman, 1995). Various prominent sites along the Jubilee Line Extension, such as Westminster Bridge and Big Ben have also had electrolevel monitoring systems installed.

For all of these installations, improvements have been made in the way in which electrolevels are attached to a structure and as these electrolevel monitoring systems have become larger and more complex, computerised data retrieval logging and display systems have also become more sophisticated. An example of this is the Bassett Convergence System for use in tunnels (see Bassett, *et al.*, (1999).

A number of companies based in the UK now offer a measurement service for the installation of electrolevel monitoring systems and the cost of these, when installed at all four glulam sites, would be comparable with a theodolite intersection system. With an accuracy similar to theodolite intersection, the

huge advantage of an electrolevel monitoring system, once installed, would be the automatic logging of the movement of the glulam beams at whatever rate desirable. This could be downloaded, via a modem and telephone connection, to a computer located in Brighton.

Despite all the developments in electrolevel monitoring systems over the last few years, installation of these on the four glulam structures in this project is still seen as problematical. The most obvious difficulty with their use is the appearance of the electrolevel beams, cables and data loggers once installed. Although there have been many advances in electrolevel technology, miniaturisation has not come about and a beam is required to enable movement to be determined. Some installations with currently available standard 2 m beams are shown in figure 9.9 and, as in 1992, it cannot be envisaged how the installation of these would be permitted on structures where appearance is a sensitive issue. If some means of disguising the electrolevel beams and associated equipment could be devised, this would be a step forward.

Another potential problem with electrolevels applied to the glulam project are recent doubts expressed about their temperature sensitivity and long-term stability, which is the least researched area and the most difficult characteristic of an electrolevel to assess. The debate currently in progress is clearly relevant for a project that is expected to last five or more years and, in the specific case of Wadurs Pool at Shoreham in this project, the performance of electrolevels in a high humidity would be questionable. The concerns over electrolevels have been expressed in papers published by Glennie (1998) and Chan, *et al.*, (1995) where their temperature stability is questioned, Spalton (1995) who has doubts

Installation of electrolevel beams

Complete system of horizontal and vertical beams in Hurley Tunnel

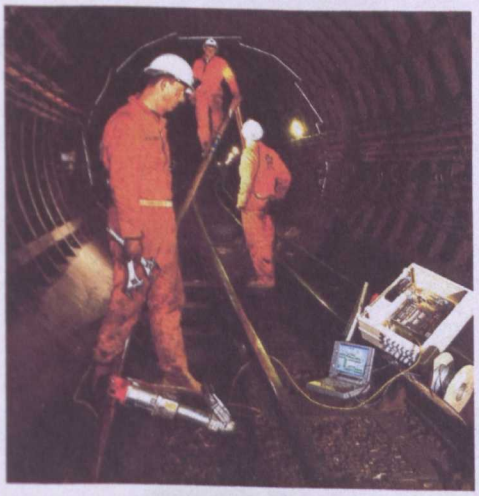

Installation of Bassett electrolevel tunnelling monitoring system
(circular beams in tunnel lining lit in background)

Figure 9.9 *Examples of modern electrolevel systems (courtesy of Monitoring Systems Ltd and ITM Ltd)*

about the long-term stability of electrolevels and Green (2000) with concerns about both. These doubts are refuted by two leading exponents of electrolevel technology, Price (1996) and Rasmussen (2001).

As in 1992, although their use would be ideal for the glulam project in many respects, electrolevel monitoring systems would not be chosen today because of their appearance and because of doubts over their long-term stability. In addition, although this would be of interest, it is not necessary to take (almost) continuous measurements of the behaviour of the glulam beams, as demonstrated in chapter 8.

9.6 Scanning systems

Leica, in association with MetricVision in the USA, introduced the laser radar LR200 (see figure 9.10) in 2001.

Figure 9.10 *Leica LR 200 (courtesy Leica Geosystems)*

This is marketed as a non-contact measurement device that scans any surface without the need for reflectors to an accuracy of 0.1 mm at a range of 10 m (1 in 100 000). If this instrument could be adapted to the monitoring of glulam structures, it would overcome the problems associated with such instruments as laser trackers and total stations with regard to reflectors and it would create a number of interesting measurement solutions. Unfortunately, the cost of the LR200 at present (£300 000 in March 2002) is prohibitive.

As well as this, the much less expensive Cyrax 2500 laser scanner is available but with an accuracy of 6 mm for position, this is not intended for high precision measurement.

9.7 Summary and recommendation

Taking account of all the close range measurement systems described in the previous sections, it is recommended that, for measuring deflection in glulam and similar indoor structures at the 0.1 – 0.2 mm level

- a theodolite intersection system could still be used but is too slow and labour intensive compared to other methods
- a polar system, even though this is the most cost effective method, is not accurate enough because of the need to use plane retro-reflecting targets
- laser trackers, although extremely accurate and versatile, could not be used because of the need to use a corner cube prism of some sort

on the structure and because of high costs

- an electrolevel monitoring system should not be used because of problems with their appearance and their long-term performance
- an offline digital photogrammetric system would offer great flexibility and would probably be the best measurement solution regarding accuracy, cost and ease of use.

10

CONCLUSION

What can be said about close range measurement today, whether based on surveying or geotechnical instrumentation, is that many different techniques are available and it is in demand from a variety of sources. For example, city and town centre construction projects routinely specify that monitoring of movement in adjacent buildings is carried out, high precision measurement for industry continues to develop and monitoring by survey methods is expanding into other areas, as exemplified by the work described in this thesis.

Although the topics covered here include high precision close range measurement, the thesis has concentrated on the application of theodolite intersection to the monitoring of full-size glulam structures. Theodolite intersection is still in use nowadays despite the lack of development it has suffered from in recent years and it is still often used as a reference system for calibrating other monitoring instruments although this position is now being challenged by the latest generation of laser trackers.

10.1 Discussion of aims and objectives

The first question arising from the work completed here concerns the choice of theodolite intersection for the measurement of deflection at discrete points on a variety of structures. With hindsight, was the correct measurement system

chosen and how would this change today? Based on the monitoring carried out, the unequivocal answer is that the most appropriate measurement system has been used, it has withstood the test of time and it has produced the results required by STRU for *Project 3: The effect of fluctuating moisture conditions upon the creep behaviour of glulam beams*. This was the first aim of the work in this thesis: the objectives set for this are given below (see section 1.1 also) with comments arising from the work completed during the period of the thesis.

- *to establish a specification for the measurements [required by STRU]*

This is discussed and presented in section 2.6.

- *to investigate the choice, availability and suitability of instrumentation for measurement of deflection in large-scale structures*

In chapters 3 and 9, all of the close range measurement systems currently available for monitoring surveys have been compared and contrasted, but mostly by reviewing published articles and the brochures produced by the various manufacturers. From the 1992 review (chapter 3), it was decided to use theodolite intersection as the measurement method for monitoring glulam.

Although theodolite intersection was chosen as the measurement method, if the project were to be started today, it is very likely that this would be replaced by close range digital photogrammetry.

For the type of monitoring carried out here, it appears that no investigations have been done to compare all the systems at one site. This would be a strong

recommendation for further work: to establish a test site where theodolite intersection, polar methods, digital photogrammetry and an electrolevel system could be compared directly, and in the long-term.

- *to establish a measurement procedure and to comment on its performance*

Having decided on theodolite intersection, the implementation of this on site is described in chapters 5, 6 and 7 with additional comments in the conclusions to chapter 8 (section 8.4) all of which show that non-contact measurement using large-scale survey methods can monitor the creep response of timber structures.

For the measurement procedures adopted, choices made with regard to which glulam beams to measure and where, the accuracy required and the frequency of measurement would probably remain unchanged. Some difficulties with the measurement of full-scale buildings to be borne in mind for any future work would be access, can the monitoring equipment be put in the right place and are the observing conditions satisfactory? The latter is especially relevant to site work. In addition, targeting can be a problem on larger structures and some thought is needed as to which type of target is to be used and where to place these.

- *to assess the accuracy obtained from the chosen measurement system*

Another issue of some concern with regard to the measurement system used has been the accuracy obtained. This has been discussed at length in Chapter 7 and it is claimed that the accuracy of the measurement of vertical deflection is nominally 0.1 mm, as originally specified.

The second aim of the work carried out here was to show that survey techniques are capable of producing results that can be useful in timber research. The objectives given for this in section 1.1 are listed below with concluding remarks.

- *to devise a method of converting survey data into beam deflections*

The method devised to convert *Z*-coordinates produced by theodolite intersection into vertical beam deflections is described in section 8.1. This has concentrated on calculating mid-span deflections of the glulam beams monitored as this is standard practice when assessing the behaviour of structural members.

- *to model the beam deflections obtained and to compare these model(s) with those proposed by others engaged in timber research*

In this timber-related project, beam deflections have been recorded over a long time and this was one of the requirements of the measurement system originally specified by STRU. From the responses shown in chapter 8, the behaviour of the in-situ glulam beams monitored can be expressed as a modulated exponential function. Variations of the exponential function have been observed by others, but the seasonal modulation has not been modelled elsewhere.

One of the original aims of this research programme set by STRU was to provide a better understanding of glulam. Certainly, more data on the behaviour of glulam has been collected and the author has attempted some analysis of the results to illustrate they are of some value in wood mechanics.

In addition to this, Taylor and Pope (1994), Taylor, Price and Pope (1996) and Abdul-Wahab, *et al.*, (1998) have also attempted partial analyses of the data collected for *Project 3* in the glulam programme at Brighton.

Taylor and Pope (1994) concluded that the behaviour of glulam specimens tested under laboratory conditions at Brighton gave rise to the following creep response

$$k_{def}(t) = k_{def}(1 - e^{-ct}) \qquad 10.1$$

where

$k_{def}(t)$ = relative creep at time t (days)

k_{def} = long-term relative creep defined by Eurocode 5 (see table 2.1)

c = a constant = 0.0032 day^{-1}

The value of k_{def} obtained from the laboratory specimens varied from 0.7 to 2 depending on the specimen under test.

Although Taylor, Price and Pope (1996) attempted an analysis of the data acquired at Wokingham and Shoreham, the conclusion made was that it was too early to carry out a proper investigation of these results until further data became available.

Abdul-Wahab, *et al.*, (1998) completed an investigation of the results obtained at all four sites monitored in this project using a power law model of the form

$$k_{def}(t) = k_{def}\left[\frac{t^a}{b + t^a}\right]K \qquad 10.2$$

where

a = a constant = 0.7

b = a constant = 55

K is a correction factor linked to the type of beam under test

For the analysis carried out in this thesis, an exponential function of the form given by equation 10.1 has been derived for glulam creep responses (ignoring the seasonal modulation) where k_{def} = 0.50 on average and c = 0.0032 day^{-1} at Wokingham and where k_{def} has a maximum value of 0.80 and c = 0.0047 day^{-1} at Shoreham.

The results presented by Taylor and Pope show a close agreement with those obtained by the author but those of Abdul-Wahab, *et al.*, do not. The reasons for this are that a deliberate attempt was made by Abdul-Wahab, *et al.*, to model a power law but that this was only based on measurements taken at the full-scale structures from 1993-1997. Since 1997, beam deflections and creep have not increased at the same rates initially observed and the slower long-term response is better modelled by an exponential function.

As noted in chapter 8, many other models have been proposed to describe the long-term behaviour of wood and glulam and no attempt was made to model the results obtained here other than using the most basic power law and exponential function. However, what the project needs at this time is a full analysis of all the data in the fourteen year programme in relation to the work of others referenced in chapters 3 and 8. This would advance the knowledge of glulam considerably.

- *to discuss the correlation between laboratory and full-scale measurements*

In chapter 8, it was also noted that the exponential response of glulam measured on the full-scale structures was very similar to that obtained from the laboratory test programme at Brighton as demonstrated by Taylor and Pope (1994) compared to the results obtained here. Although not quantified in any way, the fact that an exponential response has been obtained and that it closely matches laboratory results demonstrates that there is a correlation between measurements taken in the laboratory and on full-scale structures for glulam: providing evidence for this was another of STRU's objectives for this research programme. However, one study is not conclusive and further work is required to establish the degree of correlation between laboratory and real structure.

- *to determine the relationship of the results obtained with Eurocode 5*

Questions relating to the validity of the creep factors given in Eurocode 5 have also been raised in this thesis in connection with the measurements taken on the full-scale structures. Despite the debate that exists, it does seem from the results obtained here that the k_{def} values incorporated into Eurocode 5 are valid but this analysis was based on initial elastic deflections that were calculated for each beam monitored. The difficulties associated with measuring initial beam deflections have already been described in chapter 8 and further work is required in this area so that k_{def} values in real structures can be properly assessed.

10.2 General comments

A considerable amount of data has been generated by this project and only vertical movement in glulam structures has been fully analysed so far, as required by STRU. No three-dimensional analysis has been carried out on the data to date which seems to ignore the other half of the results that describe any horizontal movement occurring in the measured beams. A recommendation for any further work for this project would be the analysis of the horizontal and three-dimensional behaviour of the structures monitored. However, this may only be of interest to surveyors as it seems that wood mechanics researchers are mostly interested in vertical deflections in timber produced by static loading of some sort.

Additional funding to continue *Project 3* in the glulam programme at Brighton has been sought but has proved difficult to obtain. The reasons for this are that the k_{def} values derived from research (albeit mostly laboratory based) tend to confirm those values in Eurocode 5 and the need to investigate further is not seen as a priority. However, the biggest obstacle to research into glulam in the UK lies in the British preference for steel and concrete instead of wood-based building materials, as claimed by Ansell (1999). In contrast to this, timber research in other European countries and elsewhere is encouraged. Despite this, Ansell does give some recent examples of the UK timber industry supporting research into timber but, unfortunately, none of these included glulam.

At present (April 2002), STRU is committed to the continuation of *Project 3* and measurements continue to be taken in the laboratory and at each of the four

structures described. It is hoped that some new structures will be added to the measurement programme but this is dependent on any future funding that might become available.

These days, three-dimensional monitoring is an accepted practice in civil engineering and is used at some time during the construction of most major projects. Based on the experiences gained whilst completing the work here, an effective and integrated monitoring system should be based on the following.

- From the beginning, good planning is required and starts with the definition of what is to be monitored. This may seem obvious, but needs to be discussed at length so that both the surveyor and client have a clear understanding of the project. This should be accompanied by having some knowledge of the expected behaviour of the structure, most important of which are the magnitude and rate of change of any movements. A monitoring scheme should also have clearly stated objectives and an agreed budget.

- When the need for monitoring has been identified, what to measure must be clearly specified (for example, vertical deflection, temperature and relative humidity for the glulam project), where to measure can be crucial (for example, the ends and centres of selected glulam beams to determine mid-span deflections) and when to measure has to be agreed (varying from once a week at the start to once every three months for the glulam project). A specification for a measurement system requires the accuracy to be defined and it is essential that the way in which the results obtained are to be presented is also agreed and fully understood.

- With regard to instrumentation currently available and in service, a wide range is now available as discussed in chapters 3 and 9. A careful selection from these have to be made focusing on a small range of well-understood methods where possible. The use of too many different instruments can be counter-productive on a monitoring scheme as the volume of information they produce can overload data management systems. Although this was not a problem experienced for the measurement of the glulam structures, it has been reported elsewhere (see Glennie, 1998, Clayton, *et al.*, 2000 and Cook and Adams, 2002).

APPENDIX A

Scale bar calibration certificate

Leica

QUALITÄTSPRÜF-ZERTIFIKAT
QUALITY TEST CERTIFICATE

Leica Aarau AG
CH-5001 Aarau
Schweiz
Tel +41 (0)64 26 44 44
Fax +41 (0)64 24 80 22
Telex 981 106

Norm
Standard: DIN 55 350-18-4.2.2

Lieferant
Supplier: Leica Aarau AG 5001 Aarau

Kunde
Customer:

Bestellungs-Nr. Kunde
Customer order no.:

Datum
Date:

Artikelbezeichnung
Article designation: Eichmass für ECDS

Artikel-Nr.
Article no.: 115.586.0000

Auftrags-Nr. Leica
Leica order no.:

Serie-Nr.
Serial no.: 375449

Liefermenge
Quantity supplied: 1 Stk.

Lieferschein-Nr.
Delivery note no.:

Datum
Date:

Beigefügte Prüfdokumente
Enclosed test documents:

Bemerkungen
Remarks: IST-Mass: 899,971 ±0,002 mm

Prüfmittel: SIP Längenmessmaschine Typ: Mull-1000

Wir bestätigen, dass die Lieferung geprüft worden ist und den Bestellgrundlagen entspricht.
We herewith confirm that the goods have been tested and correspond with the particulars of the order.

Leica Aarau AG
Q-Prüfung Mechanik
R. Kuhn

Ort, Datum
City, Date: Aarau 22.04.91

Stempel und Unterschrift
Stamp and signature

APPENDIX B

Example ECDS3 files

DAT File

Wadurs Pool Shoreham
13 Jan 99
C:\ECDS3\SHOHAM37\BEAM.DAT

OP1	7820.287	4830.941	775.717	0.025 B11
OP2	6247.622	4873.071	1858.504	0.001 B12
OP3	4652.986	4909.492	2958.276	0.013 B13
OP4	3166.237	4947.841	4010.996	0.008 B14
OP5	1677.100	4984.487	5045.156	0.033 B15
SB11	-4724.690	4877.213	-328.325	0.038
SB12	-4122.760	5546.253	-330.512	0.028
SB21	7081.329	5326.950	-338.421	0.015
SB22	7782.101	4762.334	-329.780	0.049
OP6	-4844.380	5103.572	777.120	0.018 B21
OP7	-3275.770	5074.642	1848.689	0.019 B22
OP8	-1702.180	5046.363	2935.322	0.022 B23
OP9	-241.944	5021.157	3958.096	0.008 B24
OP10	1305.815	4992.751	5058.744	0.016 B25
OP11	8020.211	13383.060	762.375	0.034 B71
OP12	6459.768	13417.590	1843.065	0.029 B72
OP13	4963.182	13451.150	2874.813	0.052 B73
OP14	3533.907	13485.490	3867.079	0.008 B74
OP15	1874.230	13523.180	5031.877	0.018 B75
OP16	-4667.860	13642.940	756.952	0.048 B81
OP17	-3083.040	13611.400	1841.354	0.048 B82
OP18	-1491.350	13583.160	2938.149	0.014 B83
OP19	64.416	13555.360	4021.369	0.018 B84
OP20	1489.497	13529.900	5028.630	0.035 B85
B31	-4799.420	7949.894	764.431	0.027
B32	-3229.710	7917.524	1831.931	0.015
B33	-1653.120	7885.665	2919.693	0.058
B34	-122.461	7859.668	3984.401	0.063
B35	1385.969	7835.683	5041.270	0.006
B41	7892.245	7683.390	763.954	0.013
B42	6302.234	7722.933	1854.250	0.049
B43	4738.912	7760.460	2939.569	0.065
B44	3171.079	7798.199	4028.115	0.052
B45	1740.885	7829.910	5035.157	0.052
B51	7943.336	10528.530	775.077	0.008
B52	6373.191	10566.750	1855.514	0.011
B53	4788.226	10605.100	2946.976	0.001
B54	3228.446	10644.560	4035.970	0.023
B55	1811.268	10678.520	5038.154	0.023
B61	-4735.660	10801.300	769.673	0.008
B62	-3147.600	10772.670	1846.618	0.009
B63	-1561.520	10744.140	2942.003	0.052
B64	41.551	10713.870	4058.370	0.016
B65	1440.681	10686.420	5058.570	0.001

ONL File

Wadurs Pool Shoreham
13 Jan 99
C:\ECDS3\SHOHAM37\BEAM.ONL

```
B31          265.422500 094.771400 G 248.017200 096.630300 G
B32          275.342800 086.564200 G 254.969600 089.614000 G
B33          286.844700 077.867800 G 263.476500 081.442100 G
B34          299.008200 070.134200 G 273.347000 073.031700 G
B35          311.145200 064.049000 G 284.499700 065.177700 G
B41          350.853600 095.591500 G 333.575700 095.885300 G
B42          343.573200 088.291100 G 323.196600 087.425200 G
B43          334.900300 080.094000 G 311.495600 078.679400 G
B44          324.587500 071.587500 G 298.844800 070.760400 G
B45          313.927900 064.312900 G 287.284800 064.965300 G
B51          341.147800 096.263000 G 325.412200 096.715800 G
B52          334.550800 090.498600 G 317.133300 090.419800 G
B53          326.999200 084.208700 G 308.089500 083.927800 G
B54          318.747000 077.841400 G 298.813300 077.835100 G
B55          310.696400 072.282200 G 290.382400 072.921200 G
B61          273.695200 095.851300 G 257.853900 097.149800 G
B62          281.902800 089.618200 G 264.409200 091.465300 G
B63          290.811900 083.153900 G 271.866300 085.170600 G
B64          300.246900 076.948600 G 280.280400 078.584900 G
B65          308.531100 072.075300 G 288.214200 072.943400 G
```

CAP File

Wadurs Pool Shoreham
13 Jan 99
C:\ECDS3\SHOHAM37\BEAM.CAP

```
KERN BUNDLE ADJUSTMENT DATA CAPTURE PROGRAM -- DATA FILE

 JOB NAME = GLULAM BEAMS
PART NAME = SURVEY NO24
     DATE = 13 Jan 1999

 P T POINT NAME       HORIZONTAL  VERTICAL  TYP COMMENT
 1 1 X-AXIS DIRECTION 000.000000 100.000000 GON POINTING ALONG X-AXIS
 1 2 X-AXIS DIRECTION 000.000000 100.000000 GON POINTING ALONG X-AXIS
 1 1 Y-AXIS DIRECTION 300.000000 100.000000 GON POINTING ALONG Y-AXIS
 1 2 Y-AXIS DIRECTION 300.000000 100.000000 GON POINTING ALONG Y-AXIS
 1 1 THEO 1           000.000000 100.000000 GON DISTANCE =     0.0001
 1 2 THEO 1           197.080000 102.957400 GON DISTANCE =  3000.0000
 1 1 SB11             251.011000 103.075500 GON
 1 2 SB11             233.244300 103.504300 GON
 1 1 SB12             259.305700 103.042500 GON
 1 2 SB12             239.513500 103.561500 GON
 1 1 SB21             358.941800 102.430200 GON
 1 2 SB21             339.119100 104.864700 GON
 1 1 SB22             365.039000 102.299700 GON
 1 2 SB22             347.638500 104.755800 GON
 1 1 OP1              364.771700 094.640500 GON B11
 1 2 OP1              347.435700 094.403900 GON B11
 1 1 OP2              357.829100 085.332600 GON B12
 1 2 OP2              334.925100 082.156000 GON B12
 1 1 OP3              348.292700 073.753400 GON B13
 1 2 OP3              318.158800 068.567600 GON B13
 1 1 OP4              336.240100 061.860200 GON B14
 1 2 OP4              299.590200 057.975100 GON B14
 1 1 OP5              320.662500 051.321100 GON B15
 1 2 OP5              280.904100 051.765600 GON B15
 1 1 OP6              251.658300 092.997500 GON B21
 1 2 OP6              234.113600 095.905700 GON B21
 1 1 OP7              263.507900 081.091500 GON B22
 1 2 OP7              240.678100 086.971100 GON B22
 1 1 OP8              279.289300 067.931500 GON B23
 1 2 OP8              249.635900 075.742000 GON B23
 1 1 OP9              296.934800 057.537900 GON B24
 1 2 OP9              260.896300 064.036200 GON B24
 1 1 OP10             316.285500 050.635200 GON B25
 1 2 OP10             276.586600 052.381200 GON B25
 1 1 OP11             334.370500 096.891600 GON B71
 1 2 OP11             320.306200 097.383800 GON B71
 1 1 OP12             328.564500 092.160600 GON B72
 1 2 OP12             313.521400 092.368100 GON B72
 1 1 OP13             322.503300 087.402500 GON B73
 1 2 OP13             306.678000 087.510100 GON B73
 1 1 OP14             316.315900 082.773800 GON B74
 1 2 OP14             299.966500 082.988900 GON B74
 1 1 OP15             308.767300 077.519700 GON B75
 1 2 OP15             292.154700 078.105000 GON B75
 1 1 OP16             279.013200 096.660900 GON B81
 1 2 OP16             264.829700 097.632200 GON B81
 1 1 OP17             285.819600 091.649000 GON B82
 1 2 OP17             270.673700 092.909200 GON B82
 1 1 OP18             293.038200 086.517000 GON B83
 1 2 OP18             277.103100 087.846100 GON B83
 1 1 OP19             300.302500 081.640500 GON B84
 1 2 OP19             283.859700 082.766900 GON B84
 1 1 OP20             306.980400 077.470900 GON B85
 1 2 OP20             290.363000 078.184100 GON B85
```

CTL File

Wadurs Pool Shoreham
13 Jan 99
C:\ECDS3\SHOHAM37\BEAM.CTL

```
KERN BUNDLE ADJUSTMENT V3.20 - CONTROL FILE Local
THEO                    1 1
X Y Z
0.0000 FIX              0.0000 FIX            0.0000 FIX
Omega-Phi-Kappa
0.000000 FIX            0.000000 FIX          0.000000 FIX
SCALE SB11              1    1   899.97100 FIX
SCALE SB12              1    2   899.97100 FIX
SCALE SB21              2    1   899.97100 FIX
SCALE SB22              2    2   899.97100 FIX
```

OUT File

Wadurs Pool Shoreham
13 Jan 99
C:\ECDS3\SHOHAM37\BEAM.OUT

```
13 Jan 1999   Begin @ 10:30:16

KERN BUNDLE ADJUSTMENT V3.00

FROM PROG       = PROCESS
   JOB NAME     = GLULAM BEAMS
PART NAME       = SURVEY NO24
MEAS DATE       = 13 Jan 1999

   24 - Total number of object points
   24 - Number of object points used
    2 - Number of stations

XYZ Position corrections       553.936     1219.744      324.579
XYZ Position corrections        49.072       82.536       38.013
XYZ Position corrections         8.516       16.751        5.128
XYZ Position corrections         0.005        0.013        0.003
Solution converged

Object point residuals (mm)

OP1
       1   1                 0.031
       1   2                 0.017
    RMS                      0.025
OP2
       1   1                 0.001
       1   2                 0.001
    RMS                      0.001
OP3
       1   1                 0.015
       1   2                 0.009
    RMS                      0.013
OP4
       1   1                 0.009
       1   2                 0.007
    RMS                      0.008
OP5
       1   1                 0.034
       1   2                 0.032
    RMS                      0.033
OP6
       1   1                 0.012
       1   2                 0.022
    RMS                      0.018
OP7
       1   1                 0.013
       1   2                 0.023
    RMS                      0.019
OP8
       1   1                 0.018
       1   2                 0.025
    RMS                      0.022
OP9
       1   1                 0.007
       1   2                 0.008
    RMS                      0.008
OP10
       1   1                 0.017
       1   2                 0.016
    RMS                      0.016
OP11
       1   1                 0.037
       1   2                 0.030
    RMS                      0.034
OP12
       1   1                 0.031
       1   2                 0.027
```

RMS		0.029
OP13		
1	1	0.054
1	2	0.050
RMS		0.052
OP14		
1	1	0.008
1	2	0.007
RMS		0.008
OP15		
1	1	0.018
1	2	0.018
RMS		0.018
OP16		
1	1	0.043
1	2	0.052
RMS		0.048
OP17		
1	1	0.045
1	2	0.051
RMS		0.048
OP18		
1	1	0.014
1	2	0.015
RMS		0.014
OP19		
1	1	0.018
1	2	0.018
RMS		0.018
OP20		
1	1	0.035
1	2	0.035
RMS		0.035
SB11		
1	1	0.030
1	2	0.045
RMS		0.038
SB12		
1	1	0.016
1	2	0.036
RMS		0.028
SB21		
1	1	0.011
1	2	0.018
RMS		0.015
SB22		
1	1	0.057
1	2	0.039
RMS		0.049
Total RMS		0.029

Final station parameters (Gon & mm)

1 1				
Angles :	0.000000	0.000000	0.000000	(Omega-Phi-Kappa)
Coords :	0.000	0.000	0.000	
1 2				
Angles :	0.000879	-0.000558	-2.555777	(Omega-Phi-Kappa)
Coords :	2999.725	9.089	174.731	

Final object point coords (mm)

	X	Y	Z	
OP1	7820.287	4830.941	775.717	B11
OP2	6247.622	4873.071	1858.504	B12
OP3	4652.986	4909.492	2958.276	B13
OP4	3166.237	4947.841	4010.996	B14
OP5	1677.100	4984.487	5045.156	B15
OP6	-4844.382	5103.572	777.120	B21
OP7	-3275.765	5074.642	1848.689	B22
OP8	-1702.177	5046.363	2935.322	B23
OP9	-241.944	5021.157	3958.096	B24

OP10	1305.815	4992.751	5058.744	B25
OP11	8020.211	13383.056	762.375	B71
OP12	6459.768	13417.588	1843.065	B72
OP13	4963.182	13451.146	2874.813	B73
OP14	3533.907	13485.491	3867.079	B74
OP15	1874.230	13523.184	5031.877	B75
OP16	-4667.858	13642.935	756.952	B81
OP17	-3083.040	13611.404	1841.354	B82
OP18	-1491.350	13583.164	2938.149	B83
OP19	64.416	13555.360	4021.369	B84
OP20	1489.497	13529.902	5028.630	B85
SB11	-4724.693	4877.213	-328.325	
SB12	-4122.755	5546.253	-330.512	
SB21	7081.329	5326.950	-338.421	
SB22	7782.101	4762.334	-329.780	

Completed @ 10:30:19

TXT File

Wadurs Pool Shoreham
13 Jan 99
C:\ECDS3\SHOHAM37\BEAM.TXT

```
KERN ECDS 3.21

ORIENTATION DATA CAPTURE

Job Id       : GLULAM BEAMS                          Date         : 13 Jan 1999
Part Id      : SURVEY NO24                           Time         : 9:56:42
Place        : WADURS POOL SHOREHAM
Operator(s)  : WFP/CJAP
File Name    : C:\ECDS3\SHOHAM37\BEAM.CAP

  Pos Th Point  Name      Horizontal  Vertical  Typ Comment
   1   1 X-AXIS DIRECTION 000.000000 100.000000 GON  POINTING ALONG X-AXIS
   1   2 X-AXIS DIRECTION 000.000000 100.000000 GON  POINTING ALONG X-AXIS
   1   1 Y-AXIS DIRECTION 300.000000 100.000000 GON  POINTING ALONG Y-AXIS
   1   2 Y-AXIS DIRECTION 300.000000 100.000000 GON  POINTING ALONG Y-AXIS
   1   1 THEO 1           000.000000 100.000000 GON  DISTANCE =      0.0001
   1   2 THEO 1           197.080000 102.957400 GON  DISTANCE =   3000.0000
   1   1 SB11             251.011000 103.075500 GON
   1   2 SB11             233.244300 103.504300 GON
   1   1 SB12             259.305700 103.042500 GON
   1   2 SB12             239.513500 103.561500 GON
   1   1 SB21             358.941800 102.430200 GON
   1   2 SB21             339.119100 104.864700 GON
   1   1 SB22             365.039000 102.299700 GON
   1   2 SB22             347.638500 104.755800 GON
   1   1 OP1              364.771700 094.640500 GON  B11
   1   2 OP1              347.435700 094.403900 GON  B11
   1   1 OP2              357.829100 085.332600 GON  B12
   1   2 OP2              334.925100 082.156000 GON  B12
   1   1 OP3              348.292700 073.753400 GON  B13
   1   2 OP3              318.158800 068.567600 GON  B13
   1   1 OP4              336.240100 061.860200 GON  B14
   1   2 OP4              299.590200 057.975100 GON  B14
   1   1 OP5              320.662500 051.321100 GON  B15
   1   2 OP5              280.904100 051.765600 GON  B15

END OF DATA CAPTURE


KERN ECDS 3.21

ORIENTATION DATA CAPTURE

Job Id       : GLULAM BEAMS                          Date         : 13 Jan 1999
Part Id      : SURVEY NO24                           Time         : 10:12:36
Place        : WADURS POOL SHOREHAM
Operator(s)  : WFP/CJAP
File Name    : C:\ECDS3\SHOHAM37\BEAM.CAP

  Pos Th Point Name       Horizontal  Vertical  Typ Comment
   1   1 OP6              251.658300 092.997500 GON  B21
   1   2 OP6              234.113600 095.905700 GON  B21
   1   1 OP7              263.507900 081.091500 GON  B22
   1   2 OP7              240.678100 086.971100 GON  B22
   1   1 OP8              279.289300 067.931500 GON  B23
   1   2 OP8              249.635900 075.742000 GON  B23
   1   1 OP9              296.934800 057.537900 GON  B24
   1   2 OP9              260.896300 064.036200 GON  B24
   1   1 OP10             316.285500 050.635200 GON  B25
   1   2 OP10             276.586600 052.381200 GON  B25

END OF DATA CAPTURE


KERN ECDS 3.21

ORIENTATION DATA CAPTURE
```

```
Job Id        : GLULAM BEAMS                          Date         : 13 Jan 1999
Part Id       : SURVEY NO24                           Time         : 10:18:25
Place         : WADURS POOL SHOREHAM
Operator(s)   : WFP/CJAP
File Name     : C:\ECDS3\SHOHAM37\BEAM.CAP

  Pos Th Point Name       Horizontal  Vertical  Typ Comment
   1   1 OP11             334.370500 096.891600 GON  B71
   1   2 OP11             320.306200 097.383800 GON  B71
   1   1 OP12             328.564500 092.160600 GON  B72
   1   2 OP12             313.521400 092.368100 GON  B72
   1   1 OP13             322.503300 087.402500 GON  B73
   1   2 OP13             306.678000 087.510100 GON  B73
   1   1 OP14             316.315900 082.773800 GON  B74
   1   2 OP14             299.966500 082.988900 GON  B74
   1   1 OP15             308.767300 077.519700 GON  B75
   1   2 OP15             292.154700 078.105000 GON  B75

END OF DATA CAPTURE


KERN ECDS 3.21

ORIENTATION DATA CAPTURE

Job Id        : GLULAM BEAMS                          Date         : 13 Jan 1999
Part Id       : SURVEY NO24                           Time         : 10:24:00
Place         : WADURS POOL SHOREHAM
Operator(s)   : WFP/CJAP
File Name     : C:\ECDS3\SHOHAM37\BEAM.CAP

  Pos Th Point Name       Horizontal  Vertical  Typ Comment
   1   1 OP16             279.013200 096.660900 GON  B81
   1   2 OP16             264.829700 097.632200 GON  B81
   1   1 OP17             285.819600 091.649000 GON  B82
   1   2 OP17             270.673700 092.909200 GON  B82
   1   1 OP18             293.038200 086.517000 GON  B83
   1   2 OP18             277.103100 087.846100 GON  B83
   1   1 OP19             300.302500 081.640500 GON  B84
   1   2 OP19             283.859700 082.766900 GON  B84
   1   1 OP20             306.980400 077.470900 GON  B85
   1   2 OP20             290.363000 078.184100 GON  B85

END OF DATA CAPTURE



KERN ECDS 3.21

ECDS 3 - Online

Job Id        : GLULAM BEAMS                          Date         : 13 Jan 1999
Part Id       : SURVEY NO24                           Time         : 10:31:35
Place         : WADURS POOL SHOREHAM
Operator(s)   : WFP/CJAP
File Name     : C:\ECDS3\SHOHAM37\BEAM.DAT

    Name : B31   Sensors 1,2
X        :     -4799.423 mm
Y        :      7949.894 mm
Z        :       764.431 mm
     RMS :         0.027 mm

    Name : B32   Sensors 1,2
X        :     -3229.708 mm
Y        :      7917.524 mm
Z        :      1831.931 mm
     RMS :         0.015 mm

    Name : B33   Sensors 1,2
X        :     -1653.118 mm
Y        :      7885.665 mm
Z        :      2919.693 mm
     RMS :         0.058 mm
```

	Name	: B34	Sensors 1,2
X		:	-122.461 mm
Y		:	7859.668 mm
Z		:	3984.401 mm
	RMS	:	0.063 mm
	Name	: B35	Sensors 1,2
X		:	1385.969 mm
Y		:	7835.683 mm
Z		:	5041.270 mm
	RMS	:	0.006 mm
	Name	: B41	Sensors 1,2
X		:	7892.245 mm
Y		:	7683.390 mm
Z		:	763.954 mm
	RMS	:	0.013 mm
	Name	: B42	Sensors 1,2
X		:	6302.234 mm
Y		:	7722.933 mm
Z		:	1854.250 mm
	RMS	:	0.049 mm
	Name	: B43	Sensors 1,2
X		:	4738.912 mm
Y		:	7760.460 mm
Z		:	2939.569 mm
	RMS	:	0.065 mm
	Name	: B44	Sensors 1,2
X		:	3171.079 mm
Y		:	7798.199 mm
Z		:	4028.115 mm
	RMS	:	0.052 mm
	Name	: B45	Sensors 1,2
X		:	1740.885 mm
Y		:	7829.910 mm
Z		:	5035.157 mm
	RMS	:	0.052 mm
	Name	: B51	Sensors 1,2
X		:	7943.336 mm
Y		:	10528.532 mm
Z		:	775.077 mm
	RMS	:	0.008 mm
	Name	: B52	Sensors 1,2
X		:	6373.191 mm
Y		:	10566.745 mm
Z		:	1855.514 mm
	RMS	:	0.011 mm
	Name	: B53	Sensors 1,2
X		:	4788.226 mm
Y		:	10605.101 mm
Z		:	2946.976 mm
	RMS	:	0.001 mm
	Name	: B54	Sensors 1,2
X		:	3228.446 mm
Y		:	10644.564 mm
Z		:	4035.970 mm
	RMS	:	0.023 mm
	Name	: B55	Sensors 1,2
X		:	1811.268 mm
Y		:	10678.519 mm
Z		:	5038.154 mm
	RMS	:	0.023 mm

```
    Name : B61   Sensors 1,2
X        :     -4735.664 mm
Y        :     10801.295 mm
Z        :       769.673 mm
    RMS  :         0.008 mm

    Name : B62   Sensors 1,2
X        :     -3147.595 mm
Y        :     10772.674 mm
Z        :      1846.618 mm
    RMS  :         0.009 mm

    Name : B63   Sensors 1,2
X        :     -1561.523 mm
Y        :     10744.143 mm
Z        :      2942.003 mm
    RMS  :         0.052 mm

    Name : B64   Sensors 1,2
X        :       41.551 mm
Y        :     10713.872 mm
Z        :      4058.370 mm
    RMS  :         0.016 mm

    Name : B65   Sensors 1,2
X        :      1440.681 mm
Y        :     10686.424 mm
Z        :      5058.570 mm
    RMS  :         0.001 mm

END OF ONLINE DATA CAPTURE
```

APPENDIX C

Site diaries

WOKINGHAM BAPTIST CHURCH

DATE	FILE	BEAMS	COMMENTS
Building under construction			
10 Nov 92	WOKHAM1	1-8	Survey 1 First measurements. Beams partially loaded. Points observed as bundle + online.
	WOKHAM2	9-12	
16 Nov 92	WOKHAM4	1-8	Survey 2 Beams still not fully loaded. Room very wet, humidity very high. Site very busy.
17 Nov 92	WOKHAM7	9-12	
	WOKHAM8	1-8	
23 Nov 92	WOKHAM9	1-8	Survey 3 Roof finished and fully loaded. Humidity still high in room.
24 Nov 92	WOKHAM10	9-12	
	WOKHAM12	1-8	
30 Nov 92	WOKHAM13	1-8	Survey 4 Room very damp: glulam beams very wet Lot of activity on site.
1 Dec 92	WOKHAM15	9-12	
14 Dec 92	WOKHAM18	1-8	Survey 5 Humidity continues to be high in room. New 50 mm floor screed laid in room.
	WOKHAM20	9-12	
6 Jan 93	WOKHAM21	1-8	Survey 6 Room *extremely* damp following Christmas break. Site very quiet.
7 Jan 93	WOKHAM22	9-12	
26 Jan 93	WOKHAM23	1-8	Survey 7 Humidity lower in room. Site at its busiest ever with many obstructions to overcome.
27 Jan 93	WOKHAM24	9-12	
8 Feb 93	WOKHAM25	1-8	Survey 8 Room wet again but now fully waterproof and being dried out.
9 Feb 93	WOKHAM26	9-12	
22 Feb 93	WOKHAM27	1-8	Survey 9 Room finished. Humidity much lower. No site activities to hamper work.
23 Feb 93	WOKHAM28	9-12	
End of construction period			
5 Apr 93	WOKHAM29	1-8	Survey 10 Building commissioned. Humidity decreasing. Beams 1-8 observed as bundle + online. Beams 9-12 observed as all bundle.
	WOKHAM30	9-12	
26 Apr 93	WOKHAM31	1-8	Survey 11
	WOKHAM32	9-12	
11 May 93	WOKHAM33	1-8	Survey 12
	WOKHAM34	9-12	

DATE	FILE	BEAMS	COMMENTS
21 Jun 93	WOKHAM35	1-8	Survey 13
	WOKHAM36	9-12	
19 Jul 93	WOKHAM37	1-8	Survey 14
	WOKHAM38	9-12	
7 Sep 93	WOKHAM39	1-8	Survey 15
	WOKHAM40	9-12	
11 Oct 93	WOKHAM41	1-8	Survey 16
	WOKHAM42	9-12	
8 Nov 93	WOKHAM43	1-8	Survey 17
	WOKHAM44	9-12	
6 Dec 93	WOKHAM45	1-8	Survey 18
	WOKHAM46	9-12	
17 Jan 94	WOKHAM47	1-8	Survey 19
	WOKHAM48	9-12	
17 Mar 94	WOKHAM49	1-8	Survey 20
	WOKHAM50	9-12	
23 May 94	WOKHAM51	1-8	Survey 21
	WOKHAM52	9-12	
21 Jul 94	WOKHAM53	1-8	Survey 22
	WOKHAM54	9-12	
7 Sep 94	WOKHAM55	1-8	Survey 23
	WOKHAM56	9-12	
	WOKHAM57	9-12	
8 Sep 94	WOKHAM60	1-8	
	WOKHAM61	1-8	
14 Nov 94	WOKHAM62	1-8	Survey 24
	WOKHAM63	9-12	
16 Jan 95	WOKHAM64	1-8	Survey 25
	WOKHAM65	9-12	
23 Mar 95	WOKHAM66	1-8	Survey 26
	WOKHAM67	9-12	

DATE	FILE	BEAMS	COMMENTS
7 Jun 95	WOKHAM68	1-8	Survey 27
	WOKHAM69	9-12	
2 Aug 95	WOKHAM70	1-8	Survey 28
	WOKHAM71	9-12	
16 Oct 95	WOKHAM73	1-8	Survey 29
	WOKHAM74	9-12	
21 Dec 95	WOKHAM75	1-8	Survey 30
	WOKHAM76	9-12	
19 Feb 96	WOKHAM77	1-8	Survey 31
	WOKHAM78	9-12	
8 May 96	WOKHAM80	1-8	Survey 32
	WOKHAM81	9-12	
15 Jul 96	WOKHAM82	1-8	Survey 33
	WOKHAM83	9-12	
14 Oct 96	WOKHAM84	1-8	Survey 34
	WOKHAM86	9-12	
17 Dec 96	WOKHAM87	1-8	Survey 35
	WOKHAM88	9-12	
25 Feb 97	WOKHAM89	1-8	Survey 36
	WOKHAM91	9-12	
19 Jun 97	WOKHAM92	1-8	Survey 37
	WOKHAM94	9-12	
20 Jan 98	WOKHAM95	1-8	Survey 38
	WOKHAM96	9-12	
31 Mar 98	WOKHAM97	1-8	Survey 39
	WOKHAM98	9-12	
20 May 98	WOKHAM99	1-8	Survey 40
	WKHAM100	9-12	
30 Jun 98	WKHAM101	1-8	Survey 41
	WKHAM103	9-12	

DATE	FILE	BEAMS	COMMENTS
19 Oct 98	WKHAM104	1-8	Survey 42
	WKHAM105	9-12	
18 Jan 99	WKHAM106	1-8	Survey 43
	WKHAM107	9-12	
27 Apr 99	WKHAM108	1-8	Survey 44
	WKHAM109	9-12	
15 Jul 99	WKHAM111	1-8	Survey 45
	WKHAM112	9-12	
19 Oct 99	WKHAM113	1-8	Survey 46
	WKHAM114	9-12	
19 Jan 00	WKHAM115	1-8	Survey 47
	WKHAM116	9-12	
6 Apr 00	WKHAM117	1-8	Survey 48
	WKHAM119	9-12	
27 Jun 00	WKHAM120	1-8	Survey 49
	WKHAM121	9-12	
16 Oct 00	WKHAM122	1-8	Survey 50
	WKHAM123	9-12	
18 Jan 01	WKHAM124	1-8	Survey 51
	WKHAM125	9-12	
26 Mar 01	WKHAM126	1-8	Survey 52
	WKHAM127	9-12	
10 Jul 01	WKHAM128	1-8	Survey 53
	WKHAM130	9-12	
17 Sep 01	WKHAM131	1-8	Survey 54
	WKHAM132	1-8	
18 Sep 01	WKHAM133	9-12	
	WKHAM 134	9-12	
14 Feb 02	WKHAM135	1-8	Survey 55
	WKHAM136	9-12	

Note: Files missing in the numerical sequence given above have not been used because of gross errors in a bundle adjustment that were not resolved, unwanted stand movement during measurements or other problems encountered with the system.

WADURS POOL SHOREHAM

DATE	FILE	BEAMS	COMMENTS
Building under construction			
12 Jan 93	SHOHAM2	1-8	Survey 1 Very cold on site, humidity moderate. Lot of activity on roof and in pool area. Plant room under construction. Top targets not visible.
18 Jan 93	SHOHAM4	1-8	Survey 2 Good observing conditions. Roof partially loaded. Top targets not visible.
1 Feb 93	SHOHAM6	1-8	Survey 3 Roof still not fully loaded. Humidity moderate. Top targets not visible.
11 Feb 93	SHOHAM8	1-8	Survey 4 All targets now visible. Roof still not fully loaded. Very busy in pool area.
1 Mar 93	SHOHAM10	1-8	Survey 5 Roof now fully loaded. Pool area finished and pool full of water for the first time. Humidity lower.
End of construction period			
Targets in new positions			
13 May 93	SHOHAM11	1-8	Survey 6
14 June 93	SHOHAM13	1-8	Survey 7
17 Nov 93	SHOHAM15	1-8	Survey 8 Long gap since previous survey.
8 Dec 93	SHOHAM16	1-8	Survey 9
24 Jan 94	SHOHAM18	1-8	Survey 10
21 Mar 94	SHOHAM19	1-8	Survey 11
1 Jun 94	SHOHAM20	1-8	Survey 12
13 July 94	SHOHAM21	1-8	Survey 13
11 Oct 94	SHOHAM22	1-8	Survey 14
19 Dec 94	SHOHAM23	1-8	Survey 15
14 Mar 95	SHOHAM24	1-8	Survey 16
13 Jul 95	SHOHAM26	1-8	Survey 17

DATE	FILE	BEAMS	COMMENTS
20 Nov 95	SHOHAM27	1-8	Survey 18
27 Jun 96	SHOHAM29	1-8	Survey 19
18 Dec 96	SHOHAM30	1-8	Survey 20
2 Jul 97	SHOHAM32	1-8	Survey 21
9 Feb 98	SHOHAM34	1-8	Survey 22
2 Jul 98	SHOHAM36	1-8	Survey 23
13 Jan 99	SHOHAM37	1-8	Survey 24
13 July 99	SHOHAM38	1-8	Survey 25
25 Jan 00	SHOHAM39	1-8	Survey 26
16 Aug 00	SHOHAM40	1-8	Survey 27
14 Mar 01	SHOHAM41	1-8	Survey 28
12 Jul 01	SHOHAM42	1-8	Survey 29
12 Sep 01	SHOHAM43	1-8	Survey 30

Note: Files missing in the numerical sequence given above have not been used because of gross errors in a bundle adjustment that were not resolved, unwanted stand movement during measurements or other problems encountered with the system.

MOULSECOOMB HEALTH CENTRE

DATE	FILE	BEAMS	COMMENTS
Building under construction			
6 May 94	MCOOMB1	1 & 2	Survey 1 First measurements. Beams not loaded. Very wet conditions on site.
	MCOOMB2	3 & 4	
19 May 94	MCOOMB3	1 & 2	Survey 2 Wet conditions again on site. Beams partially loaded. Very busy on site.
	MCOOMB4	3 & 4	
27 May 94	MCOOMB5	3 & 4	Survey 3 Roof almost fully loaded. Very busy on site again. Some problems with communications on new computer (Toshiba T6600C).
7 June 94	MCOOMB6	1 & 2	Survey 4 Roof fully loaded in both rooms.
	MCOOMB7	3 & 4	
23 June 94	MCOOMB8	1 & 2	Survey 5 Experiencing problems with software again. Plasterers working in rooms. Working on suspended floors in both rooms from now on.
	MCOOMB10	3 & 4	
11 Jul 94	MCOOMB11	3 & 4	Survey 6 Working with new ECDS3 software version 3.21.
	MCOOMB13	1 & 2	
28 Jul 94	MCOOMB14	1 & 2	Survey 7 Quiet on site. Some discussion with South Downs Health Authority and architect re targets in long-term. Beams have been varnished.
	MCOOMB15	3 & 4	
15 Aug 94	MCOOMB16	1 & 2	Survey 8
	MCOOMB17	3 & 4	
6 Sep 94	MCOOMB18	1 & 2	Survey 9
	MCOOMB19	3 & 4	
End of construction period			
3 Oct 94	MCOOMB20	1 & 2	Survey 10 Health Centre now finished and handed over to South Downs Health Authority but building not occupied.
	MCOOMB21	3 & 4	
9 Nov 94	MCOOMB22	1 & 2	Survey 11
	MCOOMB23	3 & 4	

DATE	FILE	BEAMS	COMMENTS
16 Dec 94	MCOOMB24	1 & 2	Survey 12
	MCOOMB25	3 & 4	
6 Feb 95	MCOOMB26	1 & 2	Survey 13
	MCOOMB29	3 & 4	
20 Mar 95	MCOOMB30	1 & 2	Survey 14
	MCOOMB31	3 & 4	
3 Jul 95	MCOOMB34	1 & 2	Survey 15
	MCOOMB35	3 & 4	
18 Sep 95	MCOOMB36	1 & 2	Survey 16
9 Oct 95	MCOOMB38	3 & 4	Survey 17
	MCOOMB40	1 & 2	
MCOOMB41-MCOOMB51 None of these files used because of software problems.			
18 Dec 95	MCOOMB52	1 & 2	Survey 18
	MCOOMB53	3 & 4	
22 Feb 96	MCOOMB55	3 & 4	Survey 19
	MCOOMB56	1 & 2	
9 May 96	MCOOMB57	1 & 2	Survey 20
	MCOOMB58	3 & 4	
3 Jul 96	MCOOMB60	1 & 2	Survey 21 Using industrial stands for first time.
	MCOOMB61	3 & 4	
15 Oct 96	MCOOMB62	1 & 2	Survey 22
	MCOOMB63	3 & 4	
5 Dec 96	MCOOMB64	3 & 4	Survey 23
	MCOOMB66	1 & 2	
28 Feb 97	MCOOMB67	3 & 4	Survey 24
	MCOOMB68	1 & 2	
4 Jul 97	MCOOMB69	1 & 2	Survey 25
	MCOOMB70	3 & 4	

DATE	FILE	BEAMS	COMMENTS
23 Jan 98	MCOOMB72	1 & 2	Survey 26
	MCOOMB73	3 & 4	
20 Mar 98	MCOOMB74	1 & 2	Survey 27
	MCOOMB75	3 & 4	
22 May 98	MCOOMB76	1 & 2	Survey 28
	MCOOMB77	3 & 4	
6 Jul 98	MCOOMB78	1 & 2	Survey 29
	MCOOMB79	3 & 4	
11 Dec 98	MCOOMB80	3 & 4	Survey 30
	MCOOMB81	1 & 2	
No more measurements possible for Beams 1 & 2 as the room has been divided and the beams boxed in as a result.			
6 Jan 99	MCOOMB82	3 & 4	Survey 31
21 Apr 99	MCOOMB83	3 & 4	Survey 32
16 Jul 99	MCOOMB84	3 & 4	Survey 33
11 Oct 99	MCOOMB85	3 & 4	Survey 34
21 Jan 00	MCOOMB86	3 & 4	Survey 35
4 Apr 00	MCOOMB87	3 & 4	Survey 36
21 Jun 00	MCOOMB88	3 & 4	Survey 37
19 Oct 00	MCOOMB89	3 & 4	Survey 38
11 Jan 01	MCOOMB90	3 & 4	Survey 39
30 Mar 01	MCOOMB91	3 & 4	Survey 40
6 Jul 01	MCOOMB92	3 & 4	Survey 41
14 Sep 01	MCOOMB94	3 & 4	Survey 42
	MCOOMB95	3 & 4	
8 Feb 02	MCOOMB96	3 & 4	Survey 43

Note: Files missing in the numerical sequence given above have not been used because of gross errors in a bundle adjustment that were not resolved, unwanted stand movement during measurements or other problems encountered with the system.

BISHOP HANNINGTON CHURCH

DATE	FILE	BEAMS	COMMENTS
5 Jul 95	BISHOP4	1 & 2	Survey 1 First measurements.
10 Jul 95	BISHOP5	1 & 2	Survey 2
	BISHOP6	1 & 2	
	BISHOP7	1 & 2	
26 Jul 95	BISHOP8	1 & 2	Survey 3
13 Sep 95	BISHOP10	1 & 2	Survey 4
12 Oct 95	BISHOP13	1 & 2	Survey 5
23 Nov 95	BISHOP14	1 & 2	Survey 6
19 Dec 95	BISHOP15	1 & 2	Survey 7
20 Feb 96	BISHOP16	1 & 2	Survey 8
17 May 96	BISHOP17	1 & 2	Survey 9
4 Jul 96	BISHOP18	1 & 2	Survey 10
26 Sep 96	BISHOP20	1 & 2	Survey 11
24 Oct 96	BISHOP21	1 & 2	Survey 12
16 Dec 96	BISHOP22	1 & 2	Survey 13
6 Mar 97	BISHOP23	1 & 2	Survey 14
26 Jun 97	BISHOP24	1 & 2	Survey 15
26 Jan 98	BISHOP25	1 & 2	Survey 16 First measurements since Jun 97. New set of targets installed as previous removed by contractor. Beams re-varnished.
20 Feb 98	BISHOP26	1 & 2	Survey 17
30 Mar 98	BISHOP27	1 & 2	Survey 18
18 May 98	BISHOP28	1 & 2	Survey 19
9 Jul 98	BISHOP29	1 & 2	Survey 20
28 Oct 98	BISHOP31	1 & 2	Survey 21
7 Jan 99	BISHOP32	1 & 2	Survey 22
19 Apr 99	BISHOP33	1 & 2	Survey 23
12 Jul 99	BISHOP35	1 & 2	Survey 24
21 Oct 99	BISHOP36	1 & 2	Survey 25
17 Jan 00	BISHOP37	1 & 2	Survey 26

DATE	FILE	BEAMS	COMMENTS
3 Apr 00	BISHOP38	1 & 2	Survey 27
22 Jun 00	BISHOP39	1 & 2	Survey 28
12 Oct 00	BISHOP40	1 & 2	Survey 29
15 Jan 01	BISHOP41	1 & 2	Survey 30
29 Mar 01	BISHOP43	1 & 2	Survey 31
2 Jul 01	BISHOP45	1 & 2	Survey 32
10 Sep 01	BISHOP48	1 & 2	Survey 33
	BISHOP50	1 & 2	
	BISHOP51	1 & 2	
26 Sep 01	BISHOP52	1 & 2	Survey 34
	BISHOP53	1 & 2	
13 Feb 02	BISHOP55	1 & 2	Survey 35

Note: Files missing in the numerical sequence given above have not been used because of gross errors in a bundle adjustment that were not resolved, unwanted stand movement during measurements or other problems encountered with the system.

APPENDIX D

Workbook for Beam 2 at Wokingham

WOKBEAM2.XLS							
DEFLECTION OF GLULAM BEAMS							
WOKINGHAM BAPTIST CHURCH							
BEAM No 2 Page 1							
MEASURED COORDINATES							
TARGET		10 NOV 92	16 NOV 92	23 NOV 92	24 NOV 92	30 NOV 92	14 DEC 92
21		-895.40	-878.79	-884.84	-879.26	-995.29	-956.78
22		-529.62	-513.49	-519.71	-514.09	-630.17	-591.68
23		-166.17	-150.31	-156.68	-151.00	-267.16	-228.61
24		197.06	212.77	206.30	212.02	95.87	134.45
25		561.98	577.73	571.13	576.91	460.73	499.44
26		923.45	939.35	932.73	938.55	822.50	861.28
27		1255.93	1271.95	1265.21	1271.08	1154.94	1193.86
COORDINATE DIFFERENCES							
22-21		365.78	365.30	365.13	365.17	365.12	365.10
23-21		729.23	728.49	728.16	728.27	728.13	728.17
24-21		1092.46	1091.56	1091.14	1091.28	1091.16	1091.23
25-21		1457.38	1456.52	1455.97	1456.17	1456.02	1456.23
26-21		1818.85	1818.14	1817.56	1817.81	1817.79	1818.07
27-21		2151.33	2150.74	2150.05	2150.34	2150.23	2150.64
BEAM DEFLECTIONS RELATIVE TO 10 NOV 92							
	*						
21	0	0.00	0.00	0.00	0.00	0.00	0.00
22	974	0.00	-0.48	-0.65	-0.61	-0.66	-0.68
23	1946	0.00	-0.74	-1.07	-0.96	-1.10	-1.05
24	2927	0.00	-0.90	-1.32	-1.17	-1.30	-1.23
25	3901	0.00	-0.86	-1.41	-1.20	-1.36	-1.15
26	4872	0.00	-0.71	-1.29	-1.04	-1.06	-0.79
27	5772	0.00	-0.59	-1.28	-0.99	-1.09	-0.69
DEFLECTION AT CENTRE OF BEAM FROM 10 NOV 92							
DAYS		0	6	13	14	20	34
24 (Deflection)		0.00	0.60	0.68	0.68	0.75	0.88
DEFLECTIONS FROM 10 NOV 92							
DAYS		0	6	13	14	20	34
24 (Centre deflection)		0.00	-0.90	-1.32	-1.17	-1.30	-1.23
27 (End deflection)		0.00	-0.59	-1.28	-0.99	-1.09	-0.69
BEAM 2 472x115mm SECTION 6.3m LONG							
* Horizontal lengths along beam mm							

WOKBEAM2.XLS							
DEFLECTION OF GLULAM BEAMS							
WOKINGHAM BAPTIST CHURCH							
BEAM No 2 Page 2							
MEASURED COORDINATES							
TARGET		6 JAN 93	26 JAN 93	8 FEB 93	22 FEB 93	5 APR 93	26 APR 93
21		-969.01	-962.00	-972.69	-959.10	-953.08	-952.82
22		-604.22	-596.98	-607.81	-594.12	-588.26	-588.01
23		-241.34	-233.99	-244.91	-231.17	-225.71	-225.63
24		121.76	129.09	118.13	131.89	136.81	136.78
25		486.96	494.25	483.26	497.09	501.50	501.34
26		849.01	856.43	845.40	859.37	863.23	863.13
27		1181.82	1189.33	1178.28	1192.35	1196.07	1195.92
COORDINATE DIFFERENCES							
22-21		364.79	365.02	364.89	364.98	364.82	364.81
23-21		727.67	728.01	727.78	727.93	727.38	727.19
24-21		1090.76	1091.09	1090.82	1090.99	1089.90	1089.60
25-21		1455.96	1456.25	1455.95	1456.19	1454.58	1454.16
26-21		1818.02	1818.44	1818.10	1818.48	1816.32	1815.95
27-21		2150.83	2151.33	2150.98	2151.45	2149.15	2148.74
BEAM DEFLECTIONS RELATIVE TO 10 NOV 92							
	*						
21	0	0.00	0.00	0.00	0.00	0.00	0.00
22	974	-0.99	-0.75	-0.89	-0.80	-0.96	-0.97
23	1946	-1.56	-1.21	-1.45	-1.30	-1.85	-2.04
24	2927	-1.69	-1.37	-1.64	-1.46	-2.56	-2.86
25	3901	-1.41	-1.13	-1.42	-1.18	-2.79	-3.21
26	4872	-0.83	-0.41	-0.76	-0.38	-2.54	-2.90
27	5772	-0.50	0.00	-0.35	0.13	-2.17	-2.59
DEFLECTION AT CENTRE OF BEAM FROM 10 NOV 92							
DAYS		57	77	90	104	146	167
24 (Deflection)		1.44	1.37	1.46	1.52	1.47	1.56
DEFLECTIONS FROM 10 NOV 92							
DAYS		57	77	90	104	146	167
24 (Centre deflection)		-1.69	-1.37	-1.64	-1.46	-2.56	-2.86
27 (End deflection)		-0.50	0.00	-0.35	0.13	-2.17	-2.59
BEAM 2 472x115mm SECTION 6.3m LONG							
* Horizontal lengths along beam mm							

WOKBEAM2.XLS							
DEFLECTION OF GLULAM BEAMS							
WOKINGHAM BAPTIST CHURCH							
BEAM No 2 Page 3							
MEASURED COORDINATES							
TARGET		11 MAY 93	21 JUNE 93	19 JULY 93	7 SEP 93	11 OCT 93	8 NOV 93
21		-948.83	-960.04	-957.47	-964.71	-955.24	-956.76
22		-584.11	-595.33	-592.97	-600.64	-591.14	-592.67
23		-221.89	-233.24	-231.06	-239.02	-229.43	-231.00
24		140.30	128.72	130.67	122.58	132.26	130.64
25		504.74	492.99	494.75	486.65	496.37	494.82
26		866.45	854.66	856.26	848.28	858.07	856.55
27		1199.25	1187.46	1189.04	1181.30	1191.09	1189.55
COORDINATE DIFFERENCES							
22-21		364.72	364.70	364.50	364.07	364.11	364.09
23-21		726.94	726.79	726.41	725.69	725.82	725.76
24-21		1089.13	1088.75	1088.15	1087.29	1087.50	1087.40
25-21		1453.56	1453.03	1452.23	1451.35	1451.61	1451.59
26-21		1815.28	1814.69	1813.73	1812.98	1813.31	1813.31
27-21		2148.07	2147.49	2146.51	2146.01	2146.33	2146.31
BEAM DEFLECTIONS RELATIVE TO 10 NOV 92							
	*						
21	0	0.00	0.00	0.00	0.00	0.00	0.00
22	974	-1.06	-1.07	-1.28	-1.71	-1.67	-1.69
23	1946	-2.29	-2.43	-2.81	-3.54	-3.41	-3.46
24	2927	-3.33	-3.70	-4.31	-5.17	-4.96	-5.05
25	3901	-3.81	-4.35	-5.15	-6.02	-5.77	-5.79
26	4872	-3.57	-4.16	-5.12	-5.87	-5.54	-5.54
27	5772	-3.26	-3.84	-4.82	-5.32	-4.99	-5.02
DEFLECTION AT CENTRE OF BEAM FROM 10 NOV 92							
DAYS		182	223	251	301	335	363
24 (Deflection)		1.70	1.78	1.90	2.51	2.46	2.54
DEFLECTIONS FROM 10 NOV 92							
DAYS		182	223	251	301	335	363
24 (Centre deflection)		-3.33	-3.70	-4.31	-5.17	-4.96	-5.05
27 (End deflection)		-3.26	-3.84	-4.82	-5.32	-4.99	-5.02
BEAM 2 472x115mm SECTION 6.3m LONG							
* Horizontal lengths along beam mm							

WOKBEAM2.XLS							
DEFLECTION OF GLULAM BEAMS							
WOKINGHAM BAPTIST CHURCH							
BEAM No 2 Page 4							
MEASURED COORDINATES							
TARGET		6 DEC 93	17 JAN 94	17 MAR 94	23 MAY 94	21 JUL 94	7 SEP 94
21		-978.33	-964.29	-1021.91	-1014.76	-978.59	-977.23
22		-614.43	-600.24	-658.39	-651.28	-615.81	-614.52
23		-252.86	-238.59	-297.07	-290.16	-255.22	-253.93
24		108.71	123.04	64.32	70.93	105.47	106.79
25		472.75	487.07	428.18	434.54	468.74	470.10
26		834.31	848.72	789.68	795.95	829.70	831.07
27		1167.11	1181.64	1122.56	1128.79	1162.40	1163.93
COORDINATE DIFFERENCES							
22-21		363.91	364.05	363.51	363.48	362.79	362.70
23-21		725.48	725.69	724.83	724.60	723.37	723.30
24-21		1087.05	1087.32	1086.23	1085.69	1084.07	1084.01
25-21		1451.08	1451.36	1450.09	1449.30	1447.33	1447.32
26-21		1812.64	1813.00	1811.58	1810.71	1808.29	1808.29
27-21		2145.44	2145.93	2144.47	2143.55	2141.00	2141.15
BEAM DEFLECTIONS RELATIVE TO 10 NOV 92							
	*						
21	0	0.00	0.00	0.00	0.00	0.00	0.00
22	974	-1.87	-1.73	-2.27	-2.30	-2.99	-3.07
23	1946	-3.75	-3.53	-4.39	-4.63	-5.85	-5.93
24	2927	-5.41	-5.13	-6.23	-6.76	-8.39	-8.44
25	3901	-6.29	-6.02	-7.29	-8.08	-10.04	-10.05
26	4872	-6.21	-5.85	-7.27	-8.14	-10.56	-10.56
27	5772	-5.89	-5.40	-6.86	-7.78	-10.33	-10.17
DEFLECTION AT CENTRE OF BEAM FROM 10 NOV 92							
DAYS		391	433	492	559	618	666
24 (Deflection)		2.47	2.43	2.80	2.88	3.22	3.36
DEFLECTIONS FROM 10 NOV 92							
DAYS		391	433	492	559	618	666
24 (Centre deflection)		-5.41	-5.13	-6.23	-6.76	-8.39	-8.44
27 (End deflection)		-5.89	-5.40	-6.86	-7.78	-10.33	-10.17
BEAM 2 472x115mm SECTION 6.3m LONG							
* Horizontal lengths along beam mm							

WOKBEAM2.XLS							
DEFLECTION OF GLULAM BEAMS							
WOKINGHAM BAPTIST CHURCH							
BEAM No 2 Page 5							
MEASURED COORDINATES							
TARGET		8 SEP 94	8 SEP 94	14 NOV 94	16 JAN 95	23 MAR 95	7 JUN 95
			repeated				
21		-976.80	-976.63	-991.73	-973.58	-987.45	-993.22
22		-614.03	-613.80	-629.07	-610.87	-624.69	-630.75
23		-253.38	-253.28	-268.33	-250.03	-263.64	-270.37
24		107.29	107.43	92.55	110.87	96.94	90.17
25		470.66	470.70	456.06	474.41	460.38	453.35
26		831.59	831.68	817.25	835.67	821.46	814.22
27		1164.47	1164.52	1150.20	1168.64	1154.37	1147.05
COORDINATE DIFFERENCES							
22-21		362.77	362.84	362.67	362.71	362.76	362.47
23-21		723.42	723.35	723.41	723.55	723.81	722.85
24-21		1084.09	1084.06	1084.28	1084.45	1084.38	1083.39
25-21		1447.46	1447.33	1447.79	1447.98	1447.83	1446.56
26-21		1808.39	1808.31	1808.98	1809.25	1808.91	1807.43
27-21		2141.27	2141.15	2141.93	2142.21	2141.82	2140.26
BEAM DEFLECTIONS RELATIVE TO 10 NOV 92							
	*						
21	0	0.00	0.00	0.00	0.00	0.00	0.00
22	974	-3.00	-2.94	-3.11	-3.07	-3.02	-3.31
23	1946	-5.81	-5.87	-5.82	-5.68	-5.42	-6.38
24	2927	-8.36	-8.40	-8.17	-8.01	-8.07	-9.07
25	3901	-9.91	-10.04	-9.58	-9.39	-9.55	-10.81
26	4872	-10.46	-10.54	-9.87	-9.60	-9.95	-11.42
27	5772	-10.05	-10.18	-9.39	-9.12	-9.51	-11.07
DEFLECTION AT CENTRE OF BEAM FROM 10 NOV 92							
DAYS		667	667	734	797	863	939
24 (Deflection)		3.34	3.31	3.47	3.45	3.32	3.54
DEFLECTIONS FROM 10 NOV 92							
DAYS		667	667	734	797	863	939
24 (Centre deflection)		-8.36	-8.40	-8.17	-8.01	-8.07	-9.07
27 (End deflection)		-10.05	-10.18	-9.39	-9.12	-9.51	-11.07
BEAM 2 472x115mm SECTION 6.3m LONG							
* Horizontal lengths along beam mm							

WOKBEAM2.XLS							
DEFLECTION OF GLULAM BEAMS							
WOKINGHAM BAPTIST CHURCH							
BEAM No 2 Page 6							
MEASURED COORDINATES							
TARGET		2 AUG 95	16 OCT 95	21 DEC 95	19 FEB 96	8 MAY 96	15 JUL 96
21		-1005.70	-1009.70	-961.85	-993.92	-980.31	-975.34
22		-643.40	-647.38	-599.48	-631.61	-618.25	-613.32
23		-283.28	-287.12	-239.06	-271.23	-258.17	-253.34
24		76.99	73.29	121.56	89.38	102.16	106.77
25		439.87	436.26	484.76	452.51	465.14	469.57
26		800.45	797.01	845.64	813.31	825.81	830.01
27		1133.07	1129.81	1178.61	1146.21	1158.61	1162.63
COORDINATE DIFFERENCES							
22-21		362.30	362.32	362.37	362.31	362.06	362.02
23-21		722.42	722.58	722.79	722.69	722.14	722.01
24-21		1082.68	1082.99	1083.41	1083.30	1082.47	1082.11
25-21		1445.57	1445.96	1446.61	1446.43	1445.45	1444.91
26-21		1806.14	1806.71	1807.50	1807.23	1806.12	1805.35
27-21		2138.76	2139.51	2140.47	2140.13	2138.92	2137.97
BEAM DEFLECTIONS RELATIVE TO 10 NOV 92							
	*						
21	0	0.00	0.00	0.00	0.00	0.00	0.00
22	974	-3.48	-3.45	-3.41	-3.47	-3.72	-3.76
23	1946	-6.81	-6.64	-6.44	-6.54	-7.08	-7.22
24	2927	-9.77	-9.47	-9.05	-9.16	-9.99	-10.35
25	3901	-11.81	-11.41	-10.76	-10.94	-11.93	-12.46
26	4872	-12.71	-12.14	-11.35	-11.63	-12.73	-13.50
27	5772	-12.57	-11.82	-10.86	-11.20	-12.41	-13.36
DEFLECTION AT CENTRE OF BEAM FROM 10 NOV 92							
DAYS		995	1070	1136	1196	1275	1343
24 (Deflection)		3.49	3.56	3.62	3.56	3.78	3.67
DEFLECTIONS FROM 10 NOV 92							
DAYS		995	1070	1136	1196	1275	1343
24 (Centre deflection)		-9.77	-9.47	-9.05	-9.16	-9.99	-10.35
27 (End deflection)		-12.57	-11.82	-10.86	-11.20	-12.41	-13.36
BEAM 2 472x115mm SECTION 6.3m LONG							
* Horizontal lengths along beam mm							

WOKBEAM2.XLS							
DEFLECTION OF GLULAM BEAMS							
WOKINGHAM BAPTIST CHURCH							
BEAM No 2 Page 7							
MEASURED COORDINATES							
TARGET		14 OCT 96	17 DEC 96	25 FEB 97	19 JUN 97	20 JAN 98	31 MAR 98
21		-957.64	-951.61	-957.49	-940.07	-960.10	-951.80
22		-595.63	-589.56	-595.46	-578.24	-598.06	-589.94
23		-235.61	-229.58	-235.27	-218.43	-237.98	-229.95
24		124.62	130.76	125.11	141.56	122.40	130.27
25		487.51	493.74	488.09	504.19	485.33	493.08
26		848.08	854.42	848.75	864.48	845.92	853.50
27		1180.85	1187.25	1181.60	1197.18	1178.71	1186.26
COORDINATE DIFFERENCES							
22-21		362.01	362.05	362.03	361.82	362.04	361.86
23-21		722.03	722.03	722.21	721.64	722.13	721.85
24-21		1082.25	1082.38	1082.60	1081.63	1082.50	1082.07
25-21		1445.15	1445.35	1445.58	1444.26	1445.43	1444.87
26-21		1805.72	1806.04	1806.24	1804.55	1806.02	1805.30
27-21		2138.48	2138.86	2139.08	2137.25	2138.81	2138.05
BEAM DEFLECTIONS RELATIVE TO 10 NOV 92							
	*						
21	0	0.00	0.00	0.00	0.00	0.00	0.00
22	974	-3.77	-3.72	-3.75	-3.95	-3.73	-3.92
23	1946	-7.20	-7.20	-7.01	-7.59	-7.10	-7.38
24	2927	-10.20	-10.08	-9.86	-10.83	-9.96	-10.39
25	3901	-12.23	-12.03	-11.80	-13.12	-11.95	-12.50
26	4872	-13.13	-12.82	-12.61	-14.31	-12.83	-13.56
27	5772	-12.85	-12.47	-12.24	-14.08	-12.52	-13.28
DEFLECTION AT CENTRE OF BEAM FROM 10 NOV 92							
DAYS		1434	1498	1568	1682	1897	1967
24 (Deflection)		3.78	3.85	3.74	3.79	3.70	3.75
DEFLECTIONS FROM 10 NOV 92							
DAYS		1434	1498	1568	1682	1897	1967
24 (Centre deflection)		-10.20	-10.08	-9.86	-10.83	-9.96	-10.39
27 (End deflection)		-12.85	-12.03	-11.80	-13.12	-11.95	-12.50
BEAM 2 472x115mm SECTION 6.3m LONG							
* Horizontal lengths along beam mm							

WOKBEAM2.XLS							
DEFLECTION OF GLULAM BEAMS							
WOKINGHAM BAPTIST CHURCH							
BEAM No 2 Page 8							
MEASURED COORDINATES							
TARGET		20 MAY 98	30 JUN 98	19 OCT 98	18 JAN 99	27 APR 99	15 JUL 99
21		-952.86	-950.60	-953.63	-942.12	-949.67	-943.28
22		-590.93	-588.82	-591.83	-579.94	-587.66	-581.56
23		-231.02	-228.96	-231.89	-219.82	-227.65	-221.78
24		129.07	131.07	128.26	140.49	132.53	138.16
25		491.77	493.75	491.04	503.47	495.28	500.74
26		852.08	854.08	851.59	864.11	855.67	860.98
27		1184.70	1186.69	1184.36	1196.92	1188.37	1193.59
COORDINATE DIFFERENCES							
22-21		361.93	361.78	361.80	362.18	362.01	361.72
23-21		721.84	721.64	721.74	722.31	722.02	721.49
24-21		1081.92	1081.67	1081.89	1082.61	1082.20	1081.43
25-21		1444.63	1444.35	1444.67	1445.59	1444.95	1444.02
26-21		1804.93	1804.68	1805.22	1806.23	1805.34	1804.26
27-21		2137.56	2137.29	2137.99	2139.04	2138.04	2136.87
BEAM DEFLECTIONS RELATIVE TO 10 NOV 92							
	*						
21	0	0.00	0.00	0.00	0.00	0.00	0.00
22	974	-3.85	-4.00	-3.98	-3.60	-3.77	-4.06
23	1946	-7.39	-7.58	-7.49	-6.92	-7.20	-7.73
24	2927	-10.53	-10.79	-10.57	-9.85	-10.26	-11.02
25	3901	-12.74	-13.03	-12.71	-11.79	-12.43	-13.35
26	4872	-13.92	-14.17	-13.63	-12.63	-13.51	-14.59
27	5772	-13.77	-14.03	-13.34	-12.29	-13.29	-14.46
DEFLECTION AT CENTRE OF BEAM FROM 10 NOV 92							
DAYS		2017	2058	2169	2260	2359	2438
24 (Deflection)		3.65	3.77	3.90	3.70	3.61	3.79
DEFLECTIONS FROM 10 NOV 92							
DAYS		2017	2058	2149	2248	2347	2426
24 (Centre deflection)		-10.53	-10.79	-10.57	-9.85	-10.26	-11.02
27 (End deflection)		-13.77	-14.03	-13.34	-12.29	-13.29	-14.46
BEAM 2 472x115mm SECTION 6.3m LONG							
* Horizontal lengths along beam mm							

WOKBEAM2.XLS							
DEFLECTION OF GLULAM BEAMS							
WOKINGHAM BAPTIST CHURCH							
BEAM No 2 Page 9							
MEASURED COORDINATES							
TARGET		19 OCT 99	19 JAN 00	6 APR 00	27 JUN 00	16 OCT 00	18 JAN 01
21		-961.43	-954.73	-957.80	-943.98	-947.95	-953.99
22		-599.34	-592.71	-595.69	-582.33	-586.32	-591.87
23		-239.30	-232.61	-235.62	-222.49	-226.22	-231.74
24		120.86	127.73	124.57	137.51	133.88	128.60
25		483.62	490.70	487.37	500.18	496.70	491.55
26		844.07	851.33	847.83	860.45	857.25	852.19
27		1176.79	1184.13	1180.55	1193.12	1190.07	1185.04
COORDINATE DIFFERENCES							
22-21		362.10	362.02	362.11	361.65	361.63	362.12
23-21		722.13	722.13	722.18	721.48	721.74	722.25
24-21		1082.29	1082.46	1082.36	1081.49	1081.83	1082.58
25-21		1445.06	1445.44	1445.17	1444.15	1444.66	1445.54
26-21		1805.51	1806.06	1805.63	1804.43	1805.20	1806.18
27-21		2138.22	2138.86	2138.35	2137.10	2138.02	2139.03
BEAM DEFLECTIONS RELATIVE TO 10 NOV 92							
	*						
21	0	0.00	0.00	0.00	0.00	0.00	0.00
22	974	-3.68	-3.76	-3.67	-4.13	-4.15	-3.66
23	1946	-7.09	-7.10	-7.05	-7.74	-7.49	-6.98
24	2927	-10.17	-10.00	-10.09	-10.97	-10.62	-9.87
25	3901	-12.32	-11.94	-12.20	-13.22	-12.72	-11.84
26	4872	-13.35	-12.80	-13.22	-14.42	-13.65	-12.68
27	5772	-13.11	-12.47	-12.98	-14.23	-13.31	-12.30
DEFLECTION AT CENTRE OF BEAM FROM 10 NOV 92							
DAYS		2534	2626	2704	2786	2897	2993
24 (Deflection)		3.62	3.76	3.60	3.85	3.97	3.72
DEFLECTIONS FROM 10 NOV 92							
DAYS		2534	2626	2704	2786	2897	2993
24 (Centre deflection)		-10.17	-10.00	-10.09	-10.97	-10.62	-9.87
27 (End deflection)		-13.11	-12.47	-12.98	-14.23	-13.31	-12.30
BEAM 2 472x115mm SECTION 6.3m LONG							
* Horizontal lengths along beam mm							

WOKBEAM2.XLS							
DEFLECTION OF GLULAM BEAMS							
WOKINGHAM BAPTIST CHURCH							
BEAM No 2 Page 10							
MEASURED COORDINATES							
TARGET		26 MAR 01	10 JUL 01	17 SEP 01			
21		-950.83	-955.80	-955.29			
22		-588.87	-594.07	-593.58			
23		-228.83	-234.36	-233.73			
24		131.37	125.53	126.26			
25		494.24	488.02	488.87			
26		854.74	848.18	849.16			
27		1187.48	1180.77	1181.77			
COORDINATE DIFFERENCES							
22-21		361.96	361.73	361.72			
23-21		722.00	721.44	721.56			
24-21		1082.20	1081.32	1081.55			
25-21		1445.07	1443.81	1444.16			
26-21		1805.57	1803.97	1804.45			
27-21		2138.31	2136.56	2137.06			
BEAM DEFLECTIONS RELATIVE TO 10 NOV 92							
	*						
21	0	0.00	0.00	0.00			
22	974	-3.81	-4.05	-4.06			
23	1946	-7.22	-7.79	-7.66			
24	2927	-10.25	-11.14	-10.91			
25	3901	-12.31	-13.56	-13.22			
26	4872	-13.28	-14.88	-14.40			
27	5772	-13.02	-14.77	-14.26			
DEFLECTION AT CENTRE OF BEAM FROM 10 NOV 92							
DAYS		3058	3164	3233			
24 (Deflection)		3.74	3.75	3.77			
DEFLECTIONS FROM 10 NOV 92							
DAYS		3058	3164	3233			
24 (Centre deflection)		-10.25	-11.14	-10.91			
27 (End deflection)		-13.02	-14.77	-14.26			
BEAM 2 472x115mm SECTION 6.3m LONG							
* Horizontal lengths along beam mm							

REFERENCES

ABDUL-WAHAB, H.M., et al., 1998. Measurement and modelling of long-term creep in glued laminated timber beams used in structural building frames. *The Structural Engineer*, **76** (14), 21 July 1998: 271-282.

AESCHLIMANN, H., 1988. Instrumentation for deformation measurement. *Civil Engineering Surveyor,* **XIII** (1): 30-33.

ALLAN, A. L., 1988. The principles of theodolite intersection systems. *Survey Review,* **29** (January): 226-234.

ANDRIAMITANTSOA, L., 1991. Influence of timber thickness on its mechanosorptive behaviour analysing and modelling. *In: COST 508 Wood Mechanics Workshop: Fundamental aspects on creep in wood, Lund University, Sweden, March 20-21, 1991.* Brussels: Commission of the European Communities, pp. 73-83.

ANON., 1992. Deformation monitoring today. *Civil Engineering Surveyor,* **XVII** (9): 21.

ANSELL, M. P., 1999. Timber research in construction and engineering. *Technology Letters*, **3** (2): 5-27.

ANTILLA, J., 1997. Video camera measurement system approaches theodolite accuracy. *Surveying Science in Finland,* **15** (1-2): 14-24.

ARMER, G. S. T., ed., 2001. *Monitoring and assessment of structures.* London: Spon Press.

ASHWORTH, I. M., 1989. *Development of a portable non-contact coordinate measuring system.* M.Eng. thesis, Portsmouth Polytechnic.

ATKINSON, K. B., ed., 1980. *Developments in close range photogrammetry – 1.* London: Applied Science Publishers Ltd.

BADSTUBE, M., RUG, W. and SCHONE, W., 1989. Long-term tests with

glued laminated timber girders. *International Council for Building Research and Documentation (CIB W18), Meeting 22, East Berlin, GDR.*, 23 pages.

BAS, H., 2000. The accuracy of using theodolite in close-range engineering measurements. *International Archives of Photogrammetry and Remote Sensing,* **XXXIII** (B5): 45-52.

BASSETT, R. H., KIMMANCE, J. P. and RASMUSSEN, C., 1999. An automated electrolevel deformation monitoring system for tunnels. *Proceedings of the Institution of Civil Engineers, Geotechnical Engineering,* **137** (July): 117-125.

BAYLY, D. A., 1991. *Machinery alignment with an electronic theodolite system.* Ph.D. thesis, University of Calgary.

BEYER, H. A., UFFENKAMP, V. and der VLUGT, G., 1995. Quality control in industry with digital photogrammetry. *In*: A. GRUEN and H. KAHMEN, eds. *Optical Measurement Techniques III, Vienna, 2-4 October, 1995.* Wichmann, pp. 29-38.

BILL, R., et al., 1985. Fehlertheoretische untersuchung des elektronischen meßund und berechnungssystems ECDS1 von KERN. *Zeitschrift für Vermessungsswesen,* **10** (9): 399-409.

BINGLEY, R. M., 1990. *Electronic theodolite intersection systems.* Ph.D. thesis, University of Nottingham.

BRITISH STANDARDS INSTITUTION, 1994. DD ENV 1995-1-1: 1994. Eurocode 5: Design of timber structures. Part 1.1 General rules and rules for buildings.

BRITISH STANDARDS INSTITUTION, 1996. BS 5268-2: 1996. Code of practice for structural use of timber.

BROWN, D. C., 1982. STARS, a turnkey system for close range photogrammetry. *International Archives of Photogrammetry,* **24** (5/1): 68-89.

BROWN, D. C., 1985. Adaptation of the bundle method for triangulation of observations made by digital theodolites. *In: Conference of Southern African Surveyors, Paper No. 43.*

BROWN, D. C., 1989. Emerging trends in non-topographic photogrammetry. *In:* H. M. KARARA, ed. *Non-Topographic Photogrammetry,* 2nd ed. Falls Chuch, Virginia: ASPRS, pp. 367-374.

BROWN, J. and DOLD, J., 1995. V-STARS – A system for digital industrial photogrammetry. *In*: A. GRUEN and H. KAHMEN, eds. *Optical Measurement Techniques III, Vienna, 2-4 October, 1995.* Wichmann, pp. 12-21.

BUILDING RESEARCH ESTABLISHMENT, 1992. *BRE Technical Consultancy: Electrolevel monitoring system.* London: HMSO.

CAPRETTI, S. and CECCOTTI, A., 1996. Service behaviour of timber – concrete composite beams: a 5-year monitoring and testing experience. *In: Proceedings of the International Wood Engineering Conference, New Orleans, Louisiana, 28-31 October, 1996.* **3**: pp. 443-449.

CHAN, C. H. F. and WEEKS, R. C., 1995. Electrolevels or servo-accelerometers? *In: Proceedings of Seminar organised by the Geotechnical Division, Hong Kong Institution of Civil Engineers: Instrumentation in Geotechnical Engineering, Hong Kong, 10 May, 1995.* Hong Kong Institution of Civil Engineers, pp. 97-105.

CHENEY, J. E., 1973. Techniques and equipment using the surveyor's level for accurate measurement of building movement. *In: BGS Symposium on Field Instrumentation, London, 30 May-1 June, 1973.* London: Butterworths, pp. 85-99.

CHENEY, J. E., 1980. Some requirements and developments in surveying instrumentation for civil engineering monitoring. *In: Industrial and Engineering Survey Conference, London, 2-4 September, 1980.* London: FIG Commission 6 and ISP Commission V, pp. 2.3/1-2.3/10.

CHRZANOWSKI, A., FRODGE, S. L. and AVELLA, S., 1993. The worldwide status of monitoring and analysis of dam deformations. *In: Seventh International FIG Symposium on Deformation Measurements, Banff, Canada, May, 1993,* pp. 77-88.

CLARKE, T., 1998. Industrial measurement into the next century. *Surveying World,* **6** (4): 36-38.

CLARKE, T. and GOOCH, R., 1999. Real-time metrology for aerospace manufacture. *Sensor Review,* **19** (2): 113-115.

CLAYTON, C. R. I., *et al.*, 2000. Instrumentation for monitoring sprayed concrete lined soft ground tunnels. *Proceedings of the Institution of Civil Engineers, Geotechnical Engineering,* **143** (July): 119-130.

COLLINS, S. J., 1989. Linear variable differential transformers-practical hints. *Strain,* **25** (1): 25-26.

CONHEADY, W., 1993. *The use of coordinate measuring systems in high precision deformation monitoring.* B.Eng. thesis, University of Brighton.

COOK, D., 2001. Surveying type monitoring and its place within a comprehensive structural monitoring system. *In:* G.S.T. ARMER, ed. *Monitoring and assessment of structures.* London: Spon Press, 2001, pp.80-116.

COOK, D. and ADAMS, T., 2002. The monitoring process – CTRL 440 – A case study [online]. Mott MacDonald and Balfour Beatty Major Projects. Available at: http://www.mottmac.com. [Accessed 13 January 2002].

COOPER, M. A. R., 1986. Spatial positioning, vector notation and coordinates. *Land and Minerals Surveying,* **4**: 623-625.

COST 508, 1992. *State of the art of wood mechanics research.* Brussels: Commission of the European Communities.

DESCH, H. E. and DINWOODIE, J. M., 1996. *Timber-Structure, properties*

conversion and use. London: Macmillan.

DILL-LANGER, G., AICHER, S. and REINHARDT, H. W., 1996. Creep of glulam in tension perpendicular to the grain at 20°C/65%RH and at sheltered outdoor climate conditions. *In: COST 508 International Wood Mechanics Conference, Stuttgart, 14-18 May, 1996.* pp. 157-173.

DING, X., REN, D., MONTGOMERY, B. and SWINDELLS, C., 2000. Automatic monitoring of slope deformations using geotechnical instruments. *Journal of Surveying Engineering,* **126** (2): 57-68.

DINWOODIE, J. M., 1989. *Wood - Nature's cellular, polymeric fibre-composite.* London: The Institute of Metals.

DINWOODIE, J. M., 1996. Recent European research on the rheological behaviour of wood based panels. *In: COST 508 Wood Mechanics Workshop: Mechanical properties of panel products, Building Research Establishment, Watford, UK, March 22-23, 1996.* Brussels: Commission of the European Communities, pp. 5-39.

DINWOODIE, J. M., (2000). *Timber-Its nature and behaviour.* London: E & F Spon, pp. 93-146.

DRAKE, S., 1994. *Use of an electronic coordinate system to monitor movements in structures.* B.Eng. thesis, University of Brighton.

EL-GOHARY, A. M., 1989. *Real-time dimensional coordinate measurement and analysis.* Ph.D. thesis. University of Newcastle-upon-Tyne.

EUROPEAN COMMISSION, 1994. *Nuclear fusion. JET Joint European Torus.* Luxembourg: Office for Official Publications of the European Communities.

FEISTAUER, E., DONATH, B. and HOFMANN, V., 1988. The ASW-101 precision water level-a modern hydrostatic measuring system. *Jena Review,* **33** (4): 170-172.

FONDELLI, M., 1990. Traditional surveying procedures and integrated systems of monitoring in the study of movements and deformation. *In: FIG XVIX International Congress, Helsinki, Finland, 10-19 June, 1990.* 604.3/1: 108-127.

FORBES, J., BASSETT, R. H. and LATHAM, M. S., 1994. Monitoring settlement on the Heathrow Express Rail Link. *In: Engineering Surveying '94, Keele University, Staffordshire, 14-16 April,1994.* Altrincham: Institution of Civil Engineering Surveyors, 13 pages.

FRASER, C. S., 1988. State of the art in industrial photogrammetry. *International Archives of Photogrammetry and Remote Sensing,* **27** (B5): 166-181.

FRASER, C. S., 1989. Optical 3D measurement techniques in the U.S. aerospace industry – Current status and future trends. *In*: A. GRUEN and H. KAHMEN, eds. *Optical Measurement Techniques, 1989.* Wichmann, pp. 199-205.

FRASER, C. S., 1992. Photogrammetric measurements to one part in a million. *Photogrammetric Engineering & Remote Sensing,* **58** (3): 305-310.

FRASER, C. S., 1996. Industrial measurement applications. *In:* K.B. ATKINSON, ed. *Close Range Photogrammetry and Machine Vision.* Caithness: Whittles Publishing, 1996, pp.329-361.

FRASER, C. S., 1997. Innovations in automation for vision metrology systems. *Photogrammetric Record,* **15** (90): 901-911.

FRASER, C. S., 1998. Some thoughts on the emergence of digital close range photogrammetry. *Photogrammetric Record,* **16** (91): 37-50.

FRASER, C. S. and SHORTIS, M. R., 1995. Metric exploitation of still video imagery. *Photogrammetric Record,* **15** (85): 107-122.

FREEMAN, S. 1987. New perspectives in 3-D theodolite based industrial measuring systems. *Quality Today,* May.

GANCHI, G. and SHORTIS, M. R., 1996. A comparison of the utility and efficiency of digital photogrammetry and industrial theodolite systems. *International Archives of Photogrammetry and Remote Sensing,* **XXXI** (B5): 182-187.

GEODETIC SERVICES INC., 2002. *Basics of photogrammetry* [online]. Available at: http://www. geodetic.com. [Accessed 11 March 2002].

GLENNIE, H., 1998. Monitoring surveying at London Bridge. *Civil Engineering Surveyor,* **XXIII** (3): 22-24.

GLUED LAMINATED TIMBER ASSOCIATION, 2002. *Glulam specifiers guide* [online]. High Wycombe: GLTA. Available at: http://www.glulam.co.uk. [Accessed 15 January 2002].

GOOCH, R., 1998. Optical metrology in manufacturing automation. *Sensor Review,* **18** (2): 81-87.

GOTTWALD, R., 1988. *SPACE-An automated non contact 3-D measuring system for industrial applications.* Kern & Co Ltd, Aarau, Switzerland.

GRANSHAW, S. I., 1980. Bundle adjustment methods in engineering photogrammetry. *Photogrammetric Record,* **10** (56): 181-207.

GREEN, G. E., 2000. Geotechnical field instrumentation – what's new in 2000. *Geotechnical News – Vancouver,* **18** (4): 26-32.

GREENWOOD, J., 1997. Use of electronic theodolite measurement systems in shipbuilding by Transfield Defence Systems (TDS). *In: Proceedings of Second Biennial International Conference on Measurement Science, Technology and Practice, Victoria, Australia, 26-29 November, 1997.* Metrology Society of Australia, pp. 215-218.

GRIST, M. W., 1986. Real-time spatial coordinate measuring systems. *Land and Minerals Surveying,* 4 (September): 458-471.

GRIST, M. W., 1991. Close range measurement using electronic theodolite

systems. *Photogrammetric Record*, **13** (77): 721-728.

GROSSMAN, P., 1976. Requirements for a model that exhibits mechano-sorptive behaviour. *Wood Science Technology*, **10**: 163-168.

GRUEN, A., 1997. Fundamentals of videogrammetry - a review. *Human Movement Science*, **16** (1997): 155-187.

HILSON, B. O., WHALE, L. R. J. and RODD, P. D., 1990. The deflection of glued laminated timber beams. *Journal of the Institute of Wood Science*, **12** (2): 67-70.

HOLMES, M. D., 1996. 3-D computerised measuring systems for increased accuracy and productivity in shipbuilding and repair. *Journal of Ship Production*, **12** (1): 67-71.

HÖLTING, R., 1995. Leica ECDS3: A solution for extended Measuring tasks in aircraft manufacturing. *In*: A. GRUEN and H. KAHMEN, eds. *Optical Measurement Techniques III, Vienna, 2-4 October, 1995.* Wichmann, pp. 22-28.

HOOPER, B., 1987. Cubic Precision: Future with promise. *Professional Surveyor*, July/August: 38-40.

HUNT, D. G., 1994. Present knowledge of mechano-sorptive creep of wood. *In:* P. MORLIER, ed. *Creep in timber structures.* London: E & F Spon, 1994, pp.73-97.

INSTITUTION OF CIVIL ENGINEERS, 1990. *Monitoring structural movement at Mansion House.* Building and Civil Engineering Research Focus, Issue no. 3, October, pp. 1. London: Thomas Telford.

JOHNSON, D. R., 1980. An angle on accuracy. *Quality*, November: 34-37.

KARARA, H. M., ed., 1979. *Handbook of non-topographic photogrammetry.* Falls Church, Virginia: ASP.

KATOWSKI, O. and SALTZMANN, W., 1983. *The angle-measurement system in the Wild THEOMAT T2000.* Wild Heerbrugg Ltd, Switzerland.

KATOWSKI, O., 1990. Instruments and systems for the surveillance of man-made structures and of areas subject to geophysical movement. *Civil Engineering Surveyor,* **XV** (2): 20-23.

KENNIE, T. J. M., (1990). Electronic angle and distance measurement. *In:* T. J. M. KENNIE and G. PETRIE, eds. *Engineering Surveying Technology.* Glasgow: Blackie A & P, 1990, pp. 7-47.

KERN, 1984. *Electronic coordinate determination system for industrial applications.* Kern & Co Ltd, Aarau, Switzerland.

KERN, 1987. *The mobile 3D measuring system ECDS2: Taking measure!* Kern & Co Ltd, Aarau, Switzerland.

KEUFFEL & ESSER COMPANY, 1981. *Analytical Industrial Measuring Systems AIMS.* Keuffel & Esser Company, Morriston, New Jersey.

KOPCZYNSKI, P., 1992. LVDTs: theory and application. *Sensors,* **9** (3): 18-22.

KYLE, S. A., 1988. *Triangulation methods in engineering measurement.* Ph.D. thesis, University of London.

KYLE, S. A., 1993. Certification of industrial theodolite systems. *Letter to Leica Theodolite Systems User's Group.*

KYLE, S., 1997. Trains and boats and planes – Axyz does it all. *Surveying World,* **5** (2): 20-25.

LARDELLI, A., 1985. *ECDS1-A mobile 3D-measuring system-The new standard for metrology and quality control.* Kern & Co Ltd, Aarau, Switzerland.

LARDELLI, A., 1988. *ECDS2-A mobile 3D-measuring system-The new standard for metrology and quality control.* Kern & Co Ltd, Aarau,

Switzerland.

Le GOVIC, C., 1994a. Creep of wooden structural components: testing methods. *In:* P. MORLIER, ed. *Creep in timber structures.* London: E & F Spon, 1994, pp.109-116.

Le GOVIC, C., 1994b. Sensitivity of creep to different constant environments. *In:* P. MORLIER, ed. *Creep in timber structures.* London: E & F Spon, 1994, pp.43-60.

LEICA, 1992a. *Product information - SMART 310.* Leica AG, Heerbrugg, Switzerland.

LEICA, 1992b. *Mobile 3-D metrology for industry.* Leica AG, Heerbrugg, Switzerland.

LEICA, 1993a. *Theodolite Measuring Systems Polar versus triangulation.* Leica AG, Unterentfelden, Switzerland.

LEICA, 1993b. *ECDS3.* Leica AG, Heerbrugg, Switzerland.

LEICA, 1993c. *Program Reference* section in ECDS3 User Manual Version 3.20 5/93 U2 243e. Leica AG, Unterentfelden, Switzerland.

LEICA, 1993d. *IMS Newsletter.* Leica UK Limited, Milton Keynes.

LEICA, 1993e. *User's Guide* section in ECDS3 User Manual Version 3.20 5/93 U2 243e. Leica AG, Unterentfelden, Switzerland.

LEICA, 1994. *Wild T2002/T3000.* Leica AG, Heerbrugg, Switzerland.

LEICA, 1999. *Axyz Integrated Industrial Measuring System.* Leica Geosystems AG, Heerbrugg, Switzerland.

LEICA, 2000. *V-STARS. Digital photogrammetry systems for industry.* Leica Geosystems AG, Heerbrugg, Switzerland.

MAAS, H-G., 1997. Concepts of real-time photogrammetry. *Human Movement*

Science, **16** (1997): 189-199.

MACKLIN, B., et al., 1994. Alignment systems for pumped divertor installation at JET. *In*: K. HERSCHBACH, W. MAURER and J.E.VETTER, eds. *Fusion Technology Conference, Volume 1.* North-Holland, 1995: pp. 279-282.

MACKLIN, B., et al., 1995. Application of 'best-fit' survey techniques throughout design, manufacturing and installation of the MkII Divertor at JET. *In: Proceedings of the Symposium of the 16th IEEE/NPSS on Fusion Engineering, Champaign, Illinois, USA, October 1-5, 1995.*

MADSEN, B. and BARRETT, J. D., 1976. Time-strength relationships for lumbar. *Structural Research Series, Report No. 13.* Vancouver: University of British Columbia, Department of Civil Engineering.

MARTENSSON, A., 1991. Experiments: What do we want to measure and how do we do it? *In: COST 508 Wood Mechanics Workshop: Fundamental aspects on creep in wood, Lund University, Sweden, March 20-21, 1991.* Brussels: Commission of the European Communities, pp. 89-98.

MIKHAIL, E. M., 1976. *Observations and Least squares.* New York: Harper and Row.

MIKHAIL, E. M., BETHEL, J. S. and McGLONE, J. C., 2001. *Introduction to modern photogrammetry.* New York: John Wiley & Sons, Inc.

MIKHAIL, E. M. and GRACIE, G., 1981. *Analysis and adjustment of survey measurements.* New York: Van Nostrand Reinhold.

MILNE, P. H., CARRUTHERS, D. and McGOWAN, A., 1992. Monitoring movements of Kingston Bridge, Glasgow, by land survey techniques. *Civil Engineering Surveyor,* **XVII** (9): 22-24.

MOORE, J., ed., 1992. *Monitoring building structures.* Glasgow and London: Blackie.

MORLIER, P., ed., 1994. *Creep in timber structures.* London: E & F Spon.

MÖSER, M. and HÖPER, D., 1998. Engineering surveying and construction measurement technology. *In: FIG XXI International Congress, Brighton, England, 23-28 July, 1998.* Commission 6 Engineering Surveys: pp. 246-255.

MULDER, J. E. V., 1989. The use of remote measurement systems for deformation monitoring. *New Zealand Surveyor,* **XXXII** (275): 467-483.

MULDER, J. and SMITH, G., 1997. Industrial measurement opportunities. *Surveying World,* **5** (2): 26-29.

MÜNCH, K. H., 1986. *The Kern E2 electronic precision theodolite.* Kern & Co Ltd, Aarau, Switzerland.

NEVILLE, A. M., DILGER, W. H. and BROOKS, J. J., 1983. *Creep of plain and structural concrete.* London: Construction Press.

OBIDOWSKI, M. R. and CHAPMAN, M. A., 1993. Processing theodolite observations with a photogrammetric bundle adjustment: an industrial survey application. *Geomatica,* **47** (3): 245-259.

PELLICANE, P. J. and HILSON, B. O., 1985. A computer model to predict the elastic response of composite beams with inhomogenous lamellae. *Brighton Polytechnic Report to TRADA.*

PELLICANE, P. J., HILSON, B. O. and SMITH, I., 1986. A critical appraisal of the prospects for the United Kingdom glulam industry. *Journal of the Institute of Wood Science,* **10** (5): 202-209.

PENMAN, A. D. M., 1995. Deformations measured by electro-levels. *Geotechnical Instrumentation News,* **13** (1): 36-37.

POOLEY, B. D., 1996. Reinforced glued laminated timber. *Civil Engineering-ASCE,* **66** (9): 50-53.

POPE, D. J. and TAYLOR, G. D., 1994. Continuous measurement of moisture

in timber. *Structural Survey*, **12** (3): 11-12.

PRICE, G., LONGWORTH, T. I. and SULLIVAN, P. J. E., 1994. Installation and performance of monitoring systems at the Mansion House. *Proceedings of the Institution of Civil Engineers, Geotechnical Engineering,* **107** (April): 77-87.

PRICE, G., 1996. Discussion: Stability of electrolevels used to monitor movements. *In:* R. J. MAIR and R. N. TAYLOR, eds. *Proceedings of the International Symposium on Geotechnical Aspects of Underground Construction in Soft Ground, London, 15-17 April, 1996.* Rotterdam: A. A. Balkema, pp. 767-768.

PRICE, G., WARDLE, I. F. and de ROSSI, N., 1996. Monitoring of tunnels, surrounding ground and adjacent structures. *In:* R. J. MAIR and R. N. TAYLOR, eds. *Proceedings of the International Symposium on Geotechnical Aspects of Underground Construction in Soft Ground, London, 15-17 April, 1996.* Rotterdam: A. A. Balkema, pp. 737-743.

PRICE, Bill, 1995. Monitoring in 3-D: 3-dimensional monitoring. *In: Engineering Showcase '95.* Hitchin: PV Publications, pp.11-14.

PRICE, W.F., 1989. Coordinate measuring systems, *Civil Engineering Surveyor, Issue 4, Electronic Surveying Supplement*, 17-19.

PRICE, W.F. and ASHWORTH, I. M., 1990a. Use of a coordinate measuring system to assess the deflection pattern of the Mary Rose Dam, Portsmouth. *Structural Survey*, **9** (2): 127-133.

PRICE, W.F. and ASHWORTH, I. M., 1990b. A coordinate measuring system at the Mary Rose Dock, Portsmouth. *Land and Minerals Surveying*, **8**(12): 8-11.

PRICE, W.F., 1994. Monitoring timber frames. *In: Engineering Surveying '94, Keele University, Staffordshire, 14-16 April,1994.* Altrincham: Institution of Civil Engineering Surveyors, 14 pages.

PRICE, W.F., 1995a. Monitoring glulam. *In: ACSM/ASPRS Annual Convention and Exposition, Charlotte, NC, 27 February- 2 March, 1995.* ACSM/ASPRS, Technical Papers, **1**: 165-174.

PRICE, W.F., 1995b. Monitoring glulam. *In:* G.M. CARLOMAGNO and C.A. BREBBIA eds. *Seventh International Conference on Computational Methods and Experimental Measurements (CMEM 95), 16-18 May, Capri, Italy, 1995.* Computational Methods and Experimental Measurements VII, pp. 49-56.

RANTA-MAUNUS, A., GOWDA, S. and KORTESMAA, M., 1996. Creep of timber during 4 years in natural environments. *In: International Wood Engineering Conference, New Orleans, 28-31 October, 1996,* **4**: 273-278.

RASMUSSEN, C., 2001. Electrolevels – A European view. *Geotechnical News,* **19** (1): 31-33.

ROBERTS, T. P. and MOFFITT, N. M., 1987. Kern system for positioning and automated coordinate evaluation-a real time system for industrial measurement. *In: ASPRS-ACSM Annual Convention, Baltimore, USA.* Pp. 57-61.

RODD, P. R., 1994. The performance of DVW reinforced moment transmitting joints in glulam under four point loading. *Final report of EU FOREST Project No MA2B-CT91-003, Department of Civil Engineering, University of Delft, The Netherlands.*

RODD, P. R. and POPE, D. J., 1994. Resin injected dowels in moment transmitting joints. *In: 3rd Pacific Timber Engineering Conference, Brisbane, Australia,* **2**: 691-700.

ROUGER, F., *et al.*, 1990. Creep behaviour of French woods. *In: International Timber Engineering Conference, Tokyo, Japan,* **2**: 330-336.

SANTALA, J. and PARM, T., 1994. On the accuracy of a theodolite based 3D measuring system. *In: FIG XX International Congress, Melbourne, Australia, 1994.* Pp. 607.2/1-607.2/18.

SANTALA, J., 1995. The calibration of the 3D theodolite measuring system. *Surveying Science in Finland,* **13** (1): 3-17.

SASAKI, H. and MAKU, T., 1963. The creep of glued laminated wood beam. *Wood Research 31, Division of Composite Wood, Wood Research Institute, Kyoto University, Japan,* pp. 41-49.

SHORTIS, M. R. and FRASER, C. S., 1991. Trends in close-range optical 3D measurement. *Survey Review,* **31** (242): 188-200.

SHORTIS, M. R. and FRASER, C. S., 1995. Dimensional inspection in manufacturing via vision metrology. *In: 6th International Conference on Manufacturing Engineering, Melbourne, Australia, 29 November-1 December, 1995.* Pp. 415-423.

SHORTIS, M. R. and FRASER, C. S., 1998. State of the art of 3D measurement systems for industrial and engineering applications. *In: FIG XXI International Congress, Brighton, England, 23-28 July, 1998.* Commission 6 Engineering Surveys: pp. 272-290.

SMX CORPORATION, 2002. The new SMX Laser Tracker: Measurably better [online]. Available at: http://www.smxcorp.com [Accessed 11 March 2002].

SPALTON, C., 1995. Electrolevels. A practical solution or numeric nightmare? *In: Proceedings of Seminar organised by the Geotechnical Division, Hong Kong Institution of Civil Engineers: Instrumentation in Geotechnical Engineering, Hong Kong, 10 May, 1995.* Hong Kong Institution of Civil Engineers, pp. 35-42.

SOKKIA, 1992a. *MONMOS-Mono mobile 3-D station.* Sokkia Co. Ltd.

SOKKIA, 1992b. *3-D measuring system MONMOS-proposal for measurement in shipbuilding.* Sokkia Co. Ltd.

SRPCIC, J. and MOODY, R.C., 1988. Creep of small glulam beams under changing relative humidity conditions. *In: Proceedings of the International*

Conference on Timber Engineering, pp. 523-530.

STAIGER, R., 1995. The influence of instrumental errors on the results of theodolite measuring systems. *In*: A. GRUEN and H. KAHMEN, eds. *Optical Measurement Techniques III, Vienna, 2-4 October, 1995.* Wichmann, pp. 222-230.

STANEK, H., STAUDINGER, M. and FRANK, A. U., 1993. Evaluation of geodetic measurement systems. *In*: A. GRUEN and H. KAHMEN, eds. *Optical Measurement Techniques II, Zurich, 4-7 October, 1993. SPIE,* **2252**: 428-435.

STIRLING, D., 2001. Photogrammetry – theory and technology. Photogrammetry – practice and applications. *In:* G.S.T. ARMER, ed. *Monitoring and assessment of structures.* London: Spon Press, 2001, pp.32-79.

TAYLOR, G. D. and WEST, D. J., 1990. Use of stainless steel pins for in-situ measurement of moisture content in the structural members of a glulam framed church. *Journal of the Institute of Wood Science,* **12** (2): 71-76.

TAYLOR, G. D., WEST, D. J. and HILSON, B. O., 1991. Creep of glued laminated timber under conditions of varying humidity. *Proceedings of the International Conference on Timber Engineering, London, Pages 4.211-4.219.*

TAYLOR, G. D. and POPE, D. J., 1994. Creep allowances for glued laminated timber used in structural frames for buildings. *Journal of the Institute of Wood Science,* **13** (4): 461-467.

TAYLOR, G.D., PRICE, W.F. and POPE, D.J., 1996. In-situ measurements of creep in glued laminated timber used in structural frames of buildings. *Journal of the Institute of Wood Science,* **14** (2), Issue 80 Winter: 95-101.

TESKEY, W. F., 1988. Special survey instrumentation for deformation measurements. *Journal of Surveying Engineering,* **114** (1): 2-12.

TESKEY, W. F., 1989. A method of precise trigonometric leveling for deformation surveys. *CISM Journal ACSGC,* **43** (4): 357-365.

TESKEY. W. F., 1992. Trigonometric leveling in precise engineering surveys. *Surveying and Land Information Systems,* **52** (1): 46-53.

THELANDERSSON, S., 1994a. The importance of deflection requirements in the design of timber structures. *In:* P. MORLIER, ed. *Creep in timber structures.* London: E & F Spon, 1994, pp.1-8.

THELANDERSSON, S., 1994b. Variation of moisture content in timber structures. *In:* P. MORLIER, ed. *Creep in timber structures.* London: E & F Spon, 1994, pp.117-127.

TOR, Y. K., 1993. MONMOS and building settlement surveys. *Civil Engineering Surveyor,* September, pp. 23-26.

TORATTI, T. and MORLIER, P., 1995. Fluage a long terme du bois flechi en grandeur structurale. *Materials and Structures,* **28**: 284-292.

UREN, J., 1989. A land surveyor in a structural world. *Civil Engineering Surveyor,* **XIV** (8): 29-33.

UREN, J., 1992. MONMOS. Sokkia's new one-instrument, high-precision system. *CES Electronic Surveying Supplement,* April 1992, pp. 26-28.

UREN, J. and PRICE, W. F., 1994. *Surveying for Engineers.* 3rd ed. Basingstoke: Palgrave.

VYNER, M. A. and HANOLD, J. H., 1982. AIMS Analytical Industrial Measuring Systems. *International Archives of Photogrammetry Commission V, York,* **24** (*V*/2): 524-532.

WARREN, D., 1994. *Scale in measurement systems.* Leica.

WHALE, L. R. J., HILSON, B. O. and RODD, P. D., 1989. The economic implications of some recent research on glued laminated timber in the United Kingdom. *In: 2nd Pacific Timber Engineering Conference, Auckland, New Zealand,* **2**: 131-136.

WHITTED, N. C., 1993. The Sokkia MONMOS system for tunnel deformation and bridge construction measurements. *In: Seventh International FIG Symposium on Deformation Measurements, Banff, Canada, May, 1993,* pp. 461-468.

WILD LEITZ, 1990. *Wild APS Automated Polar System.* Wild Leitz Ltd, Heerbrugg, Switzerland.

WINNEY, M., 1992. Measure of success. *New Civil Engineer,* 2 July, 28.

WOLF, P. R. and DEWITT, B. A., 2000. *Elements of photogrammetry with applications in GIS.* 3rd ed. McGraw-Hill Companies.

WOODWARD, 1986. Measurements by theodolites in mechanical engineering. *Chartered Mechanical Engineer,* **33** (October): 42-45.

WONG, K. W., 1980. Basic mathematics of photogrammetry. *In:* C. S. SLAMA, ed. *Manual of photogrammetry,* Fourth edition. Falls Church, Virginia: ASP.

WU, M., 1996. The model establishment and application for a movable 3-D coordinate measuring system. *SPIE,* **2868**: 458-468.

ZHANG, L., LI, G. and XU, Z., 1997. The comparison and analysis of the different orientation methods in theodolite measuring systems. *In*: A. GRUEN and H. KAHMEN, eds. *Optical Measurement Techniques IV, Zurich, 29 September-2 October, 1997.* Wichmann, pp. 61-67.

ZOU, Z-R., et al., 2001. Bundle adjustment for data processing of theodolite industrial surveying system. *Transactions of Nonferrous Metals Society of China,* **11** (2): 307-310.